The regulation of Hox genes by microRNAs during Drosophila development

Richard Kaschula

Submitted in partial fulfilment of the requirements for the degree of Doctor of Philosophy at the University of Sussex

September 2013

I hereby declare that this thesis has not been and will not be submitted in whole or in part to another University for the award of any other degree

Richard Kaschula

UNIVERSITY OF SUSSEX

Richard Kaschula, DPhil Biology

The regulation of Hox genes by microRNAs during Drosophila development

Summary

Hox genes encode a family of evolutionarily conserved transcription factors involved in the activation of diverse cell differentiation programs along the antero-posterior axis of animals. Hox gene expression is controlled by a complex set of regulatory mechanisms which are still not fully understood. Despite this, misregulation of Hox gene expression can lead to severe developmental abnormalities and various forms of disease.

This work addresses the way in which small non-coding RNAs (microRNAs, miRNAs) regulate Hox gene expression and function during development. To do this we use the Drosophila Hox gene *Ultrabithorax* (*Ubx*) as a paradigm for Hox gene function.

Using a suite of genetic methods we first uncover a novel regulatory interaction between Drosophila *Ubx* and the *miR-310C* family of miRNAs during the development of the haltere, a small dorsal appendage involved in flight control. We also show that this miRNA cluster is required to fine tune *Ubx* expression. Furthermore, our data provides insight into the role played by *Ubx* during appendage development.

Secondly, using a next generation RNA sequencing approach, we identify the full repertoire of miRNAs present in two serially homologous appendages of Drosophila – the wing and haltere. Our results show that these morphologically distinct appendages have divergent miRNA profiles, including miRNAs which display appendage-specific expression patterns. In addition, combining these profiles with available transcriptomic data enabled us to study how miRNAs are integrated into the *Ubx* gene regulatory networks that govern haltere development. This analysis suggests that haltere miRNAs reinforce the regulatory programmes installed by *Ubx* during haltere development.

Our work therefore contributes to the understanding of the regulatory function of miRNAs during development and sheds light on the ways in which Hox gene expression can contribute to the formation of complex morphological structures.

Acknowledgements

First, I must thank my supervisor, Claudio, for first getting me interested in this work, for encouraging me to think for myself and letting me find out what really inspires me in biology. I also thank our post-doc Stefan, who put up with me during my early days in the lab and all members of the Alonso group who provided a fun, relaxed environment to complete this work. Special thanks must also go out to Pedro and João for giving me a place to stay and making me feel welcome in the final months of completing this thesis.

Thanks must also go out to everyone along the corridor for continuous support, encouragement and camaraderie through the long weeks and fun Friday nights of the past few years, especially Aiden, Emile and John who were all there from the beginning.

A big thank you to all my friends from back home, who put up with their errant friend over the last few years and were never troubled to find a place for me in their homes when I needed a break.

A huge thank you to Sam, who read through the roughest drafts of this thesis, put up with my long hours in the lab, all without ever complaining. She never stopped giving me encouragement or listening to my grumblings when work was a struggle.

Finally, a massive thank you to all my family, to my brother and sister who always were there to welcome me back home and particularly my parents who never flinched in offering support in many shapes and guises to their perpetual student son. I also must not forget the hounds, who stayed by my side whilst I wrote, listening to all my complaints and frustrations.

To all of you, a very, very big thank you.

“That the fundamental aspects of heredity should have turned out to be so extraordinarily simple, supports us in the hope that nature may after all, be entirely approachable”

- Thomas Hunt Morgan

“The fight is won or lost far away from witnesses, behind the lines, in the gym and out there on the road, long before I dance under those lights”

- Muhammed Ali

Table of Contents

CHAPTER 1 1

1. Introduction 1

1.1 Preface 1
1.2 Building complexity in morphology 1
1.3 Important regulators of appendage development 2
1.4 Diversification and specialisation of appendage morphology 3
1.5 The Hox Genes 5
1.6 Hox gene function during appendage development. 8
1.7 Hox gene transcriptomics 9
1.8 Regulating Hox gene function 12
1.9 Co-factors and cross-regulatory Interactions 13
1.10 Regulating Hox gene function through the control of expression 13
1.11 The expression patterns of the Hox gene *Ultrabithorax* 13
1.12 Transcriptional activation and epigenetic regulation 15
1.13 Alternative splicing and protein isoform diversity 16
1.14 Regulating expression levels – the role of the 3'UTR 18
1.15 The relationship between correct *Ubx* expression and function 21
1.16 miRNAs are important post-transcriptional regulators of gene expression 23
1.17 The biogenesis of miRNAs 25
1.18 Characteristics of miRNA function during development 26
1.19 Integration of miRNAs into complex gene regulatory networks 28
1.20 Questions addressed in this study 29

C*HAPTER 2* 31

2. Materials & Methods 31

CHAPTER 3 53

3. Post-transcriptional regulation of the *Drosophila* hox gene *Ultrabithorax* by miRNAs during appendage formation 53

3.1 Chapter Overview 53
3.2 *Ubx* isoform distribution during post-embryonic development 54
3.3 Identification of miRNA target sites within the *Ultrabithorax* 3'UTR. 57
3.4 The *miR-310C* - sequence and expression analysis 59

3.5 *miR-310C* gain-of-function results in phenotypic changes linked to *Ultrabithorax* loss-of-function. 62
3.6 A *miR-310C* deletion leads to increased *Ubx* expression 65
3.7 Loss of the *miR-310C* leads to phenotypic changes in haltere morphology. 69
3.8 The Δ310 phenotype is sensitive to *Ubx* dosage. 72
3.9 *Ubx* ectopic expression phenocopies the Δ310 phenotype. 77
3.10 *miR-310C* regulation of *Ubx* leads to changes in sensory field architecture but not through direct specification of sensory cells 80
3.11 A role for apoptosis during haltere sensory field formation 85
3.12 DISCUSSION 90

CHAPTER 4 97

4. miRNA expression profiling of *Drosophila* wing and haltere imaginal discs using next-generation RNA sequencing technology 97
4.1 Chapter Overview 97
4.2 Small RNA profiling of *Drosophila* imaginal discs 98
4.3 The miRNA profiles of *Drosophila* wing and haltere imaginal discs. 101
4.4 Analysis of miRNA content from wing and haltere imaginal discs 105
4.5 Differential miRNA expression through the regulation of miRNA transcription 110
4.6 Analysis of miRNA cluster expression 112
4.7 Analysis of dual strand selection from miRNA hairpins 115
4.8 DISCUSSION 120

CHAPTER 5 124

5. The functional analysis of miRNAs present within the haltere imaginal disc and their relationship to *Ubx* regulation and function 124
5.1 Chapter Overview 124
5.2 Functional similarities amongst similarly expressed miRNAs 125
5.3 Targeting overlap and specificity amongst miRNA expression groups 130
5.4 miRNA groups associate with specific biological processes 133
5.5 Functional consequences of haltere miRNA expression – The Regulation of *Ultrabithorax* 139
5.6 The integration of miRNA regulation into the *Ubx* regulated transcriptome of the haltere 145
5.7 Differential miRNA expression through the regulation of RBPs 150
5.8 Genetic interactions between *Ubx* and *Dcr1* affect haltere development 154
5.9 DISCUSSION 155

CHAPTER 6 159

6. Final Discussion 159

CHAPTER 7 164

7. Bibliography 164

APPENDIX 175

Table.1 miRNAs detected in wing and haltere tissue sorted by haltere expression levels 175

Table.2 miRNAs detected in wing and haltere tissue sorted by miRNA expression group association 178

List of Figures

Fig.1.1 The haltere flight appendage of *Drosophila melanogaster*……..……05

Fig.1.2 Hox mutations lead to severe homeotic transformations……..…06

Fig.1.3 Evolution of Hox clusters……...07

Fig.1.4 Basic patterning network of wing and haltere imaginal discs ……..…11

Fig.1.5 Ubx transcripts undergo extensive RNA processing…..……...17

Fig.1.6 The process of alternative poly-adenylation occurs co-transcriptionally……...19

Fig.1.7 *Ubx* expression and activity in the haltere imaginal disc…….…..22

Fig.2.1 Crossing scheme for generating *Ubx* allelic series……..…….34

Fig.2.2 Crossing scheme to express mCherry constructs within the haltere……..35

Fig.2.3 Crossing scheme to generate *miR-310C*-GAL4 stocks……..…37

Fig.2.4 Crossing scheme to express UAS-*miR-310C* within the haltere……..39

Fig.2.5. Crossing scheme to express UAS-*miR-310C* in a *Ubx* deficient background..40

Fig.2.6 Crossing scheme to generate clones over-expressing *miR-310C* miRNAs…...41

Fig.2.7 Crossing scheme to place Δ310 mutation in *Ubx* deficient background…….42

Fig.2.8 Crossing scheme to ectopically express *Ubx* in *miR-310C* expression domains during development……..…….43

Fig.2.9 Crossing scheme to combine a 310C-mCherry reporter with SOP cell marker……..…..44

Fig.2.10 Crossing scheme to place H99 deletion in Δ310 genetic background……..45

Fig.2.11 Crossing scheme to combine Ubx^{1} and $Dcr1^{Q1147X}$ alleles……..46

Fig.3.1 Ubx 3'UTR isoform distribution and functionality during post-embryonic development……..……55

Fig.3.2 Ubx 3'UTR miRNA target predictions……..….58

Fig.3.3 The *miR-310C* sequence conservation and expression analysis…..……61

Fig.3.4 *miR-310C* gain-of-function leads to homeotic transformations……64

Fig.3.5 *miR-310C* removal results in increased *Ubx* expression levels……..……....67

Fig.3.6 Loss of the *miR-310C* miRNAs leads to changes in haltere morphology……...70

Fig.3.7 Genetic interactions between *miR-310C* and *Ubx*……....74

Fig.3.8 *Ubx* gain-of-function phenocopies the Δ310 phenotype……79

Fig.3.9 Effects of Δ310 allele on sensory cell formation during haltere development……..84

Fig. 3.10 A role for apoptosis during haltere appendage formation……..……...87

Fig.3.11 Model of *miR-310C-Ubx* interactions during haltere development……94

Fig.4.1 Small RNA profiling of Drosophila imaginal discs……..……99

Fig.4.2 miRNA profiles of Drosophila wing and haltere imaginal discs……..…...102

Fig.4.3 Differential expression of miRNAs in wing and haltere tissue……..……104

Fig.4.4 Analysis of miRNA content from wing and haltere imaginal discs……107

Fig.4.5 Individual miRNA contributions to total miRNA content in wing and haltere imaginal discs……..109

Fig.4.6 Differential miRNA expression through the regulation of miRNA transcription……..……111

Fig.4.7 Expression analysis of miRNA clusters in wing and haltere tissue……..…114

Fig.4.8 Analysis of dual strand processing from pre-miRNA hairpins……..…117

Fig.5.1 Gene target similarities amongst expression group miRNAs – Part 1……..…126

Fig.5.1 Gene target similarities amongst expression group miRNAs – Part 2……..…127

Fig.5.2 Analysis of shared targeting amongst miRNA expression groups……..…129

Fig.5.3 Target overlap and specificity amongst miRNA expression groups……..…132

Fig.5.4 microRNA groups associate with specific molecular and biological processes……...…..135

Fig.5.5 Top gene ontology categories associated with specific miRNA groups……...138

Fig.5.6 miRNA group associations and potential for *Ubx*-miRNA regulatory interactions……..…141

Fig.5.7 miRNA expression levels and the effect on potential Ubx-miRNA regulatory interactions……..…144

Fig.5.8 Integration of miRNA regulation into the Ubx directed haltere transcriptome……..…147

Fig.5.9 Top predicted miRNA regulators of the *Ubx* instructed transcriptome……..149

Fig.5.10 *Ubx* transcriptional regulation of RBP expression……..151

Fig.5.11 Analysis of *Ubx-Dcr1* genetic interactions……..…153

Fig.5.12 *Ubx*-miRNA integrated gene regulatory networks……..…158

Abbreviations

APA - Alternative Polyadenylation

RBP – RNA Binding Protein

AbdA – Abdominal A

AbdB – Abdominal B

Antp – Antennapedia

CNS – Central Nervous System

Dicer1 – Dcr1

LOF – Loss-of-function

GOF – Gain-of-Function

GRN – Gene Regulatory Network

miRNA – microRNA

miR-310C – miR-310-313 Cluster

PS – Para-segment

pri-miRNA – primary microRNA

Scr – Sex combs reduced

Ubx – Ultrabithorax

UTR – Untranslated Region

VNC – Ventral Nerve Cord

WPP – White Pre-Pupae

CHAPTER 1

1. Introduction

1.1 Preface

Throughout time, the process of evolution has led to a stunning array of morphological and behavioural complexity within the animal kingdom. This is no more apparent than when viewing the variety in shape and structure of animal appendages.

A striking example of this diversity and specialisation can be seen when simply studying our own human appendages. Over evolutionary time our legs elongated allowing for the advent of efficient bipedalism, our arms became shorter and hands more complex, capable of complicated and dextrous behaviours.

But how do these divergent morphological structures and features occur? What regulatory factors control and shape these developing appendages?

In this work we focus our attention on one of these regulatory factors, *Ultrabithorax* (*Ubx*). One of the eight Hox genes found within the invertebrate model organism *Drosophila melanogaster*, *Ubx* is a critical factor involved in the specification of animal body plans and appendage development.

In an effort to extend our understanding on how Hox genes - like *Ubx* - regulate key developmental processes such as appendage development, we first investigate potential regulatory mechanisms that control *Ubx* expression and how these interactions are important for specific morphological features to develop within the appendage.

Secondly, we investigate how the class of gene expression regulators – microRNAs (miRNA) may help regulate *Ubx* activity and function at a broader scale during appendage development.

1.2 Building complexity in morphology

Appendage development is a complex process involving the proliferation and differentiation of numerous cell-types to create the complex morphological structures seen in animals. In both mammals and insects, appendage development requires the co-ordinated regulation of cells from the epidermis, musculature and nervous system.

However, there are fundamental differences when comparing mammalian and insect appendage formation.

1.3 Important regulators of appendage development

In both mammals and insects, it is clear that high level cellular co-operation is required to produce an appendage with the correct morphological features as well as the correct wiring into the nervous system. Both of which allow the arms, legs and wings of an animal to perform many complex functions. What genetic factors are required for the correct development of each appendage? What similarities and differences exist between species? How can we envisage the evolution of different limb structures and features?

At the heart of all developmental processes is the co-ordinated regulation the genome. Within this complex library of genetic information lie the factors which are the foundations, building blocks and instructions that control the complex cellular processes which govern animal development.

Appendage development relies on the function of numerous genes encoding transcription factors and signalling molecules, which control genetic programmes involving countless genes required to build a complex morphological structure.

In mammals, the development of the limb appendages begins with the formation of the limb bud. This process results from the signalling activity of members from the *FGF* and *Wnt* cell-signalling systems (Ohuchi et al., 1997; Sekine et al., 1999). In tetrapod animals, two pairs of limb buds form – the presumptive fore- and hind-limbs of the animal. The distinction between fore- and hind-limb fate is marked by the presence of a specific transcription factor, either *Tbx4* or *Tbx5* respectively (Logan et al., 1998; Ohuchi et al., 1998; Rodriguez-Esteban et al., 1999; Takeuchi et al., 1999). Once the initial limb bud has formed, growth along the proximo-distal axis is defined by the Apical Ectodermal Ridge (AER) which develops along the most distal portion of the limb bud. The AER acts as a signalling centre for the developing limb bud, maintaining the proliferative state of the cells below it and the expression of a number of genes required for the development of limb along antero-posterior axis including the signalling molecule *sonic hedgehog* (*shh*) (Laufer et al., 1994; Niswander et al., 1994; Riddle et al., 1993). Additionally, the AER interacts with a number of genes required to specify particular cellular fates within the growing limb bud, for example members of the *Hox* gene family which encode evolutionarily conserved transcription factors. Experimental

analysis has shown that these transcription factors are required for the correct presence and specification of particular regions of vertebrate limbs along the proximo-distal axis (Davis et al., 1995).

In contrast to mammalian development, the generation of insect appendages occurs post-embryonically. In the case of holometabolous insects (insects which undergo larval and pupal developmental phases) the insect appendages form from presumptive epidermal tissue. For example, within the model organism *Drosophila melanogaster,* appendages are formed from an epithelial bilayer known as the imaginal disc. However there are still fundamental similarities to vertebrate limb development. Key components of imaginal disc development are transcription factors and signalling systems that instruct the correct genetic programmes needed within the imaginal disc. For example, the specification of dorsal cell identity is initiated by the transcription factor *Apterous* (Blair et al., 1994; Cohen et al., 1992). The division of the wing imaginal disc into discrete segments along the anterior-posterior axis is controlled by the interactions of two highly conserved cell-signalling mechanisms, the *Hedgehog* and *Decapentaplegic (Dpp)* pathways (Capdevila and Guerrero, 1994; Guillén et al., 1995; Lecuit et al., 1996; Sanicola et al., 1995; Zecca et al., 1995) . Additionally Hox genes play an important role in specifying particular cell-types in each appendage along the anterior-posterior axis, for example, the male only sex comb structures found on the first pair of legs, the sensory bristles which are absent in the third pair of legs and the general cellular morphologies within the haltere (Kaufman et al., 1980; Roch and Akam, 2000; Rozowski and Akam, 2002). At the broader scale, the development of the haltere flight appendage is entirely dependent on the function of the Hox gene *Ubx* (Bender et al., 1983; Lewis, 1978).

1.4 Diversification and specialisation of appendage morphology

Although we see that there are striking differences in mammalian and insect appendage formation, there are also clear similarities when analysing the two systems. Many species use a similar set of genetic factors to instruct appendage development. For example, many vertebrates express similar complements of Hox genes, yet develop a diverse array of appendage morphologies. If the underlying network of genetic factors controlling limb development is shared amongst species, how do we envisage the creation of these appendages with their diverse morphologies and behaviours?

One possible scenario is that over evolutionary time, additional genetic factors are expressed within the developing limb of a particular species. This added genetic influence could enhance or interfere with the existing genetic networks that function within this developing appendage. These novel factors could be another transcription factor that becomes expressed within the limb bud, competing for the transcriptional targets of other limb transcription factors or inducing the expression of new genes within the cells of the limb. Equally this new genetic factor could be a gene associated with a cell-signalling system, which could enhance or disrupt the efficiency of cell signalling thus affecting the usual patterns of genetic interactions within the developing limb bud.

Another possible scenario is that the underlying genetic factors of appendage development do not fundamentally change, however the functional capabilities of these genes evolve between species, leading to changes in morphology and behaviour. For instance, the expression of a transcription factor maybe subtly altered between similar groups of cells. This change in expression could affect the capabilities of the transcription factor to instruct the correct genetic programmes of each cell population, leading to different developmental outcomes. A second possibility could be that the activity of a fundamental transcription factor does not alter between species, however in different cell-types additional genetic factors appear that could interact with the transcription factors targets. These subtle changes in the transcription factors genetic programmes could lead to different cellular processes and thus alternative developmental outcomes.

A number of studies have looked to elucidate how different morphologies may arise in related species. In a comparative work, Warren et al (Warren et al., 1994) examined the relationship between expression of the Hox gene *Ubx* and the development of two divergent appendages – the *Drosophila* haltere and the Butterfly hind-wing. It was known that the presence of *Ubx* in the presumptive haltere tissue was a requirement for the correct haltere developmental programme. The authors showed that *Ubx* was also expressed within the developing hind-wing of the butterfly. This observation suggested that this evolutionarily conserved transcription factor was able to direct two highly divergent morphologies.

Freitas et al., investigated how increased Hox gene expression could affect appendage development in Zebrafish (Freitas et al., 2012). The authors found that increasing expression of particular, distally located Hox genes led to phenotypes resembling particular morphologies predicted to have occurred in the evolution of limb

appendages. This data provides tantalising evidence of how changing expression levels of powerful developmental regulators can disrupt existing genetic interactions and cause the development of alternative morphologies.

1.5 The Hox Genes

A common component to all appendage developmental programmes in both mammals and insects is the presence of the Hox family of homeodomain containing transcription factors. Hox genes are evolutionarily conserved across all bilaterian animals. Their main function during development is the instruction of correct positional information and identity to cells and tissues along the anterior-posterior axis of developing animal.

Fig.1.1 The haltere flight appendage of *Drosophila melanogaster*

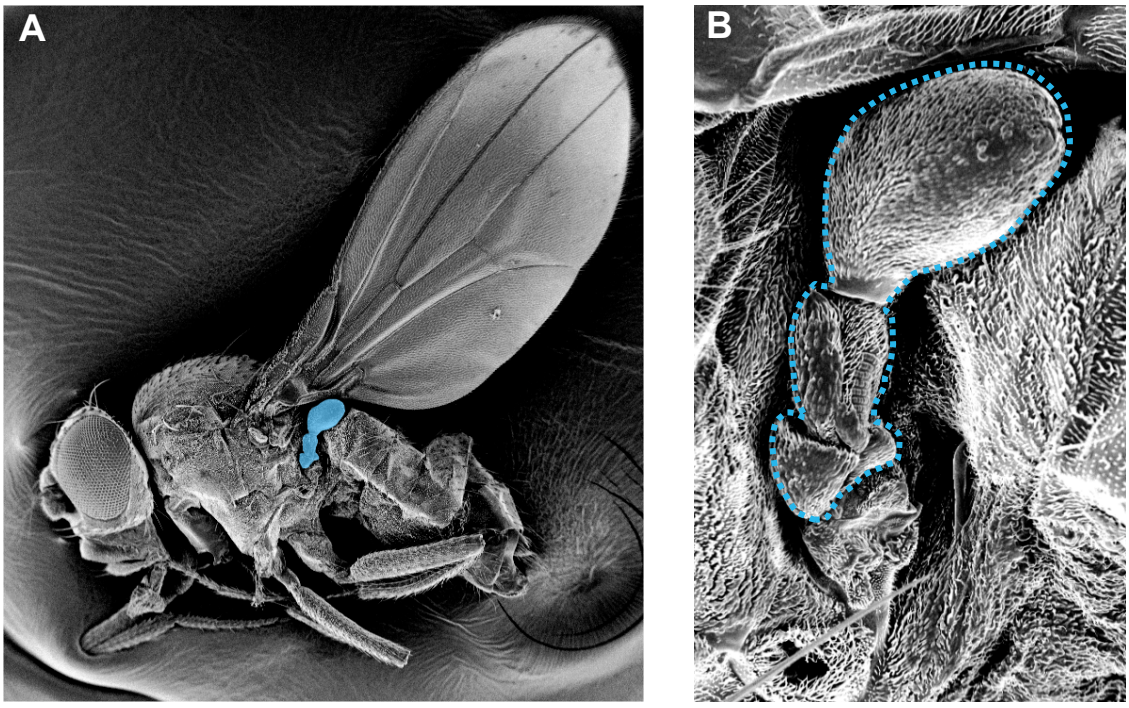

Fig.1.1 The haltere flight appendage of *Drosophila melanogaster*

(A) SEM image of an adult Drosophila highlighting the different morphologies of the wing and haltere (shaded blue). (B) Enhanced view of the adult haltere.

Members of this gene family were discovered in the early days of Drosophila genetics by Thomas Hunt Morgan and colleagues at Columbia University, New York. They were identified as mutational phenotypes that resembled examples of 'homeosis' – a transformation of one body part into the form of another. A classic example of these homeotic transformations in *Drosophila* is the transformation of the haltere appendage (Fig.1.1) into a second pair of wings (Fig.1.2).

Fig.1.2 Hox mutations lead to severe homeotic transformations

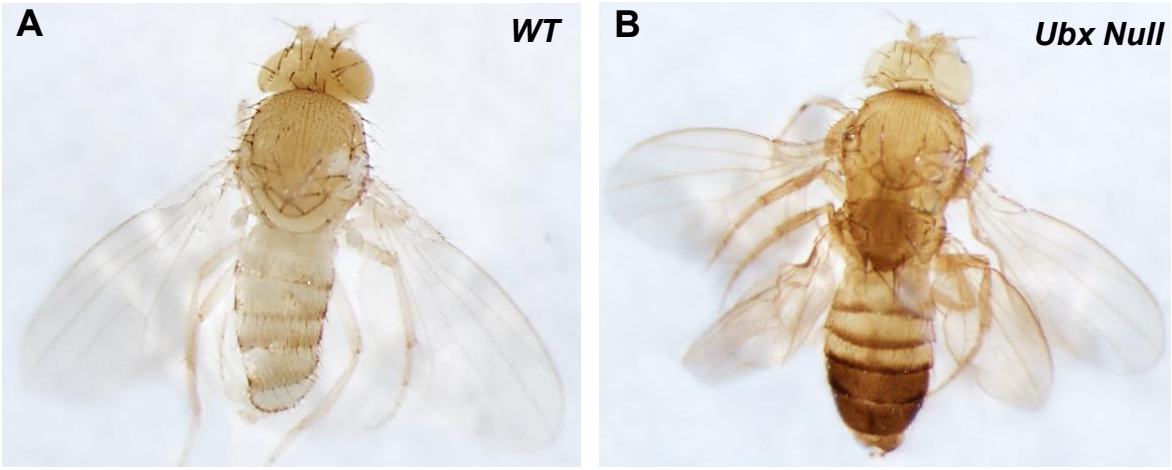

Fig.1.2 Hox mutations lead to severe homeotic transformations

(A-B) Comparison of a wild-type and Hox mutant adult Drosophila. The Hox mutant (*w;;abx^{1} bx^{3} pbx^{1}/Ubx^{1}*) animal displays a severe homeotic transformation, the duplication of the second thoracic segment generating a four-winged Drosophila.

Fig.1.3 Evolution of Hox clusters

The complement of Hox genes present in animal genomes varies. Over evolutionary time the Hox genes have duplicated and lost within many lineages. (A) The hypothetical ancestor to all bilaterian had 14 Hox genes arranged in one cluster. Hox genes are colour coded by their inferred ancestral relationship (B) The annelid *Capitella teleta* contains 11 hox genes arranged within one genomic cluster. (C) The insect *Drosophila melanogaster* has eight hox genes arranged in two genomic clusters, the Antennapedia Complex (ANTP-C) and the Bithorax Complex (BX-C). Both clusters show the loss of ancestral Hox genes. (D) The Hox clusters of *Mus musculus*. During mammalian evolution, two rounds of genome duplication led to four Hox clusters – HoxA, HoxB, HoxC, HoxD being present within the genome. Additionally each Hox cluster has lost genes. Schematics adapted from Lemons and McGinnis, 2006; Pearson et al., 2005; Simakov et al., 2013. Hox genes represented are *Labial (Lab), Proboscipedia (Pr), Deformed (Dfd), Sex combs reduced (Scr), Antennapedia (Antp), Ultrabithorax (Ubx), Abdominal A (abdA), Abdominal B (AbdB).*

Fig.1.3 Evolution of Hox clusters

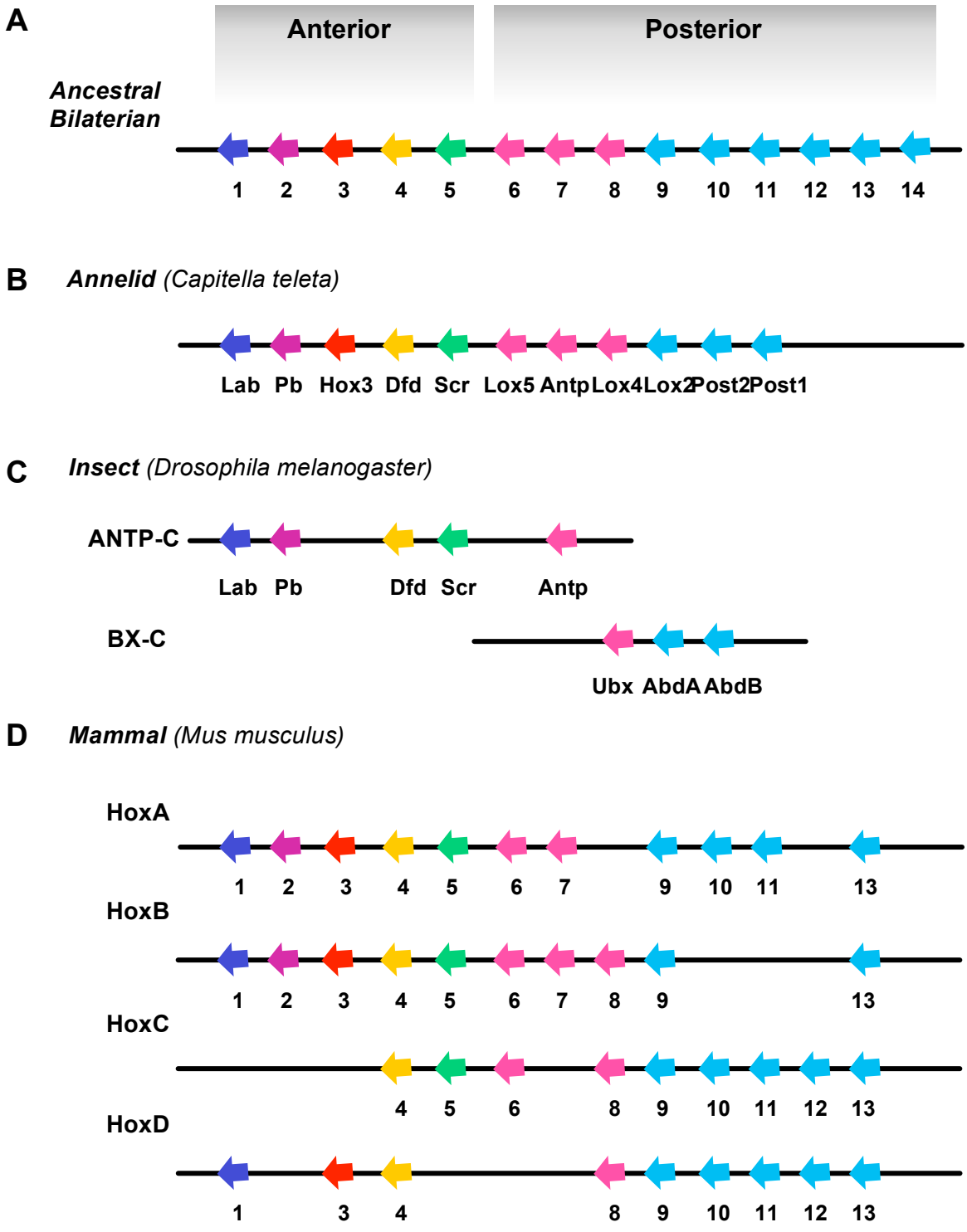

All Hox proteins contain the homeodomain DNA binding motif. This particular DNA binding structure is so called because it is shared amongst genes, that when disrupted lead to various transformations in morphology (Fjose et al., 1985; McGinnis et al., 1984). As transcription factors, each Hox gene can regulate numerous target genes leading to specific developmental programmes of cells and tissue. In this manner Hox gene function can influence the development of whole tissues or specific cells within larger tissue structures.

The number of Hox genes found within animal genome varies greatly (Fig.1.3). For example, *Drosophila* contains eight Hox genes arranged in two genomic clusters. Genomic duplication events during vertebrate evolution led to the generation of four Hox clusters, each of which has lost a number of functional genes within it thus the mouse genome contains 39 Hox genes arranged in four genomic clusters. The ancestor to all bilaterian has been hypothesised to have 14 Hox genes in a single cluster (Lemons and McGinnis, 2006; Pearson et al., 2005; Simakov et al., 2013).

As mentioned above, the primary roıe for Hox gene function during embryonic development is the instruction of tissue identity along the head-tail axis of the animal. However, it is clear that Hox genes play important roles in the cellular development of animal appendages, whether it is vertebrate limb or the *Drosophila* haltere.

1.6 Hox gene function during appendage development.

Hox genes can exert their influence over a number of different cell and tissue types during appendage development. For example, during the development of the haltere, *Ubx* not only instructs the correct developmental program of the main haltere structure-derived from epidermal tissue, it also helps guide the development of the underlying musculature and neuronal connections that innervate the appendage, allowing for the correct behavioural functions of the haltere (Burt and Palka, 1982; Fernandes et al., 1994).

Hox involvement in vertebrate appendage development is complicated by the fact that many Hox genes are expressed within one developing appendage, the *HoxA*, *HoxC* and *HoxD* complexes are prominently expressed within the developing limbs (Nelson et al., 1996). The role of Hox genes in vertebrate appendage formation is thought to be analogous to their role in body axis formation, the specification of positional identity along the proximo-distal axis of the developing appendages.

How do Hox genes impact cell/tissue development during vertebrate limb formation? Currently, the exact cellular consequences of Hox function within the developing limb bud are poorly understood. However, some of the early and essential functions have been well documented. It has been seen that an early role for Hox activity is involvement in the growth and organisation of the developing limb in relation to regulation of *Shh* signalling (Kmita et al., 2005). Others have identified more cell specific functions for some of the Hox genes present within in the limb. It has been shown that a major role for *HoxD13* in the development of the Ulna and Tibia bones is the regulation of cartilage cell proliferation. More recently, it was shown that *HoxA11* and *HoxD11* are required for the correct chondrocyte differentiation during limb development (Goff and Tabin, 1997; Gross et al., 2012).

It is becoming clear that Hox gene function can be cell specific, both in the development of appendages and other tissues within the animal. For example, during leg development in *Drosophila*, *Ubx* activity is required for the correct specification of a small number of external sensory cells within the leg appendages (Rozowski and Akam, 2002). Additionally a recent study has shown the *Drosophila* Hox gene *Antennapedia* (*Antp*) is required for the correct motoneuron innervations of the muscles within the legs (Baek et al., 2013).

A similar role has been seen for a number of vertebrate Hox genes, their expression being required for the correct motor neuron innervations along the thoracic and lumbar regions of the vertebrate body axis (Dasen et al., 2005, 2003; Jung et al., 2010).

Outside of appendage development, Hox genes play important roles in directing individual cell developmental pathways in both the invertebrate CNS development (Bello et al., 2003; Miguel-Aliaga and Thor, 2004; Rogulja-Ortmann et al., 2008) and vertebrate hindbrain development and organisation (Chen et al., 2012b; Di Bonito et al., 2013; Miguez et al., 2012).

1.7 Hox gene transcriptomics

As a means to understand how Hox genes perform their roles during animal development, uncovering which target genes are regulated by these transcription factors has interested biologists for many years. Early attempts to investigate this problem took a case by case approach to identify *Ubx* targets, often focusing on the role of *Ubx* in directing haltere development. This approach, looking for the regulation of prominent genes involved in wing/haltere development revealed many targets of *Ubx*

(Fig.1.4) (Crickmore and Mann, 2006; de Navas et al., 2006b; Galant et al., 2002; Hersh et al., 2007; Weatherbee et al., 1998).

However, this methodology does not illuminate the full picture. How many targets does one Hox gene need to regulate to ensure a particular cellular and developmental fate? How can one Hox gene enforce many different developmental pathways depending on spatial position and temporal window during development?

In order to approach these questions, many studies utilised genome-wide approaches as an un-biased method to elucidate the global transcriptome regulated by Hox genes.

Early studies comparing global gene expression levels in wing and haltere- two serially homologous dorsal appendages identified a number of genes that were alternatively expressed between the two tissues. Furthermore, through the analysis of gene expression profiles in *Ubx* mutant imaginal discs, they were able to surmise that much of this alternative gene expression was due to the presence of *Ubx* within the haltere (Hersh et al., 2007; Mohit et al., 2006). A following study took advantage of the GAL4-UAS/GAL80 temporal expression system (McGuire et al., 2003) to ectopically express *Ubx* within the wing imaginal disc at different developmental stages and monitored changes in gene expression (Pavlopoulos and Akam, 2011). The authors were able to determine that the *Ubx* gene was able to target hundreds of genes at different developmental stages. Interestingly, it appears that *Ubx* targeting was dynamic and dependant on developmental stage. Very few genes were regulated at more than one stage. In general, it was seen that the effect of *Ubx* on target gene expression levels was subtle and could be both repressive and inductive. A large majority of *Ubx* targets were components of various cell-signalling systems and transcription factors. These results suggest that *Ubx* may consistently change its targets depending on the developmental stage, and that the overall effect on gene expression is subtle.

Fig.1.4 Basic patterning network of wing and haltere imaginal discs

(A) The fundamental gene-regulatory network that leads to the axis specification and the division of the wing imaginal disc into discrete compartments. (B) Known *Ubx* regulatory interactions within the basic patterning network during haltere development. *Ubx* suppresses wing development by negatively regulating a number of fundamental genes in wing development. Scheme adapted from Weatherbee et al., 1998.

Fig.1.4 Basic patterning network of wing and haltere imaginal discs

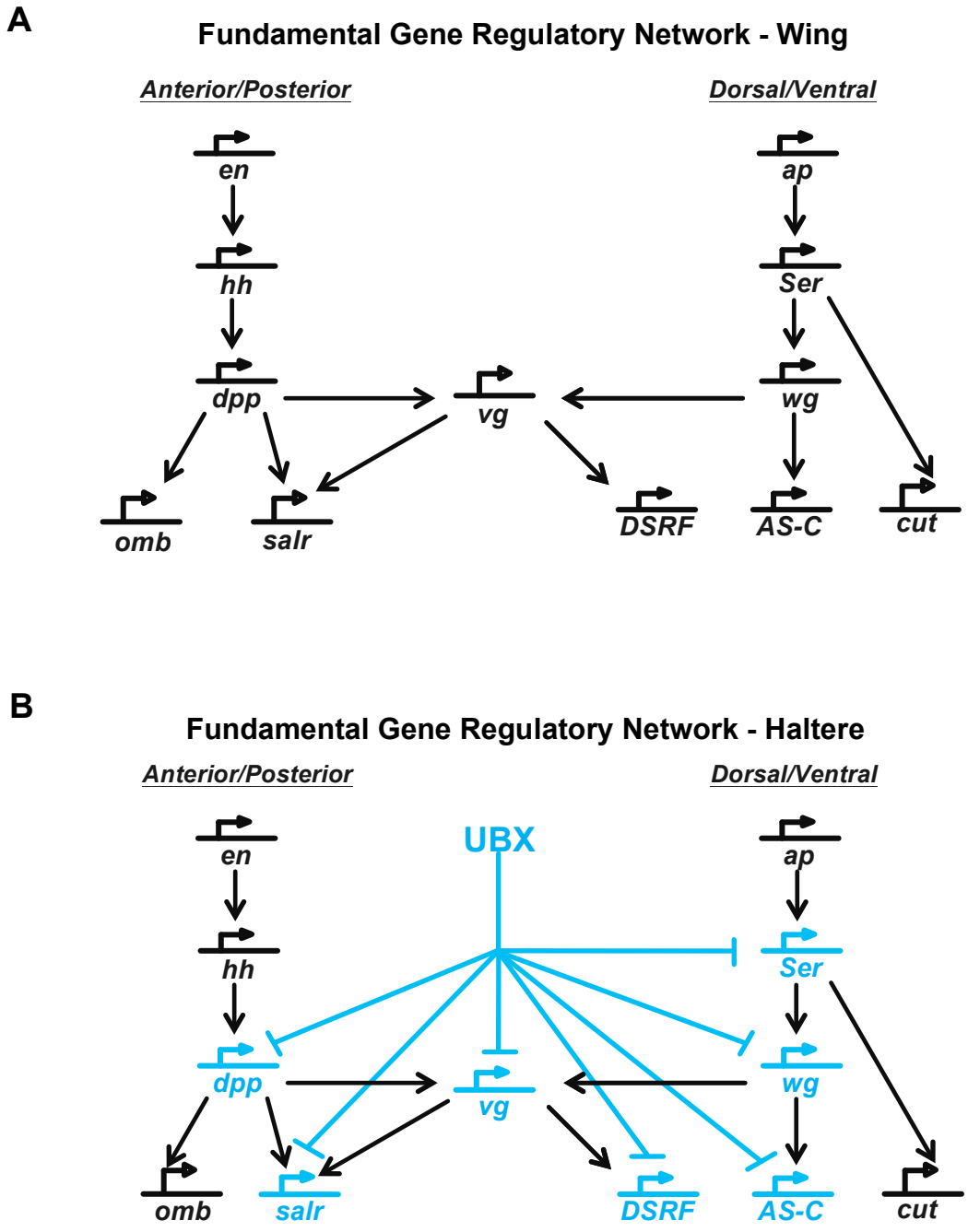

These results were in accordance with a number of comparative studies which used a ChiP-array methodology to determine where within the genome *Ubx* was bound too at a particular developmental stage (Agrawal et al., 2011; Choo et al., 2011; Slattery et al., 2011). All studies showed that *Ubx* could bind to an array of target genes associated with many different molecular functions, especially a high proportion of transcription factors or members of cell-signalling systems, for instance, the *Notch*/*Delta* or *Wingless* pathways. Integrating these ChIP-array results with available microarray gene expression data shows that a significant proportion of *Ubx* bound genes also displayed differential gene expression when compared to microarray data (Choo et al., 2011).

Overall, these results indicate that *Ubx* defines the developmental pathways of the cells within the haltere by subtly modulating the expression of many genes belong to cell-signalling systems and transcriptions factors. These expression changes lead to changes in cell proliferation and differentiation programs within the developing appendage.

1.8 Regulating Hox gene function

The clear potential for Hox gene actions to influence many cell-types and developmental pathways has meant a diverse set of regulatory mechanisms has evolved to maintain suitable control of Hox gene expression and to influence and diversify Hox gene function.

The study of the regulatory landscape governing Hox expression has provided insight into the many complex mechanisms required to accurately define and control these potent developmental regulators and other important transcription factors.

Fundamental transcriptional and post-transcriptional mechanisms contribute to the regulation of Hox expression patterns and in the generation of multiple Hox gene isoforms capable of differential transcriptional activity and function. There is a trend amongst Hox genes for cross-regulatory interactions that ensure their correct developmental expression patterns. Additionally, it is apparent that Hox proteins are capable of many protein-protein interactions with other factors within cells that can help their functional specificity in targeting the correct genes.

1.9 Co-factors and cross-regulatory Interactions

One approach to introduce functional specificity to transcription factor activity is the addition of co-factors binding to transcription factors within the nucleus. A number of co-factors have been found that function in this capacity with Hox genes. In *Drosophila*, the genes *extradenticle* (*exd*) and *homothorax* (*hth*) were initially identified because their mutant phenotypes induce homeotic-like transformations (Pai et al., 1998; Peifer and Wieschaus, 1990; Rieckhof et al., 1997). It was shown that these two factors bind to *Ubx* protein within the nucleus and affect its affinity for DNA-binding (Ryoo et al., 1999). Interestingly, homologues of *exd*/*hth* are found within vertebrates – the *Pbx*/*Meis* family of proteins which also function as co-factors for Hox gene activity.

It is known that Hox genes have an ability to cross-regulate each other's gene expression domains (Harding et al., 1985; Struhl and White, 1985; Struhl, 1983). For instance *abdominal-A (abd-A)* and *Abdominal-B (Abd-B)* restrict the posterior limits of *Ubx* expression. This mechanism, often referred to as 'posterior prevalence', ensures that the correct Hox activity is maintained within the correct cells of the developing animal (Duboule and Morata, 1994).

1.10 Regulating Hox gene function through the control of expression

Many regulatory mechanisms keep Hox gene expression and activity under control. Loss of these regulatory mechanisms can lead to many abnormal developmental and disease phenotypes (Di Pietro et al., 2012; Muragaki et al., 1996; Raman et al., 2000; Sun et al., 2013).

In this context, analysing the control of Hox gene expression during *Drosophila* development provides insight into the different types of regulatory mechanisms influencing gene expression patterns and their consequent effect on Hox gene function. In particular, understanding the regulation of *Ubx* has revealed a diverse array of regulatory mechanisms controlling this genes function.

1.11 The expression patterns of the Hox gene *Ultrabithorax*

The start of all Hox gene activity during embryonic development begins with the initial transcriptional expression of the gene. All Hox genes are initially expressed in specific patterns along the antero-posterior axis of the developing embryo – in both vertebrates

and invertebrates. Each Hox gene expression pattern follows on from the previous gene, although expression domains may overlap. The order in which the Hox genes are expressed along the animal body axis relates directly to the order in which they exist within the genome – a phenomenon known as co-linearity (Krumlauf, 1994; Lewis, 1978). In both vertebrates and invertebrates, the start of Hox gene expression is closely linked with the formation of segments within the developing embryo.

Drosophila embryogenesis is an elegant example of 'short-germ band' development. The animal body is first sub-divided into discrete sections along the antero-posterior axis by a collection of transcription factors encoded by a group of genes collectively known as the 'Gap genes'. This division of broad domains is consequently divided into 14 repeating units – the segments along the body axis. The division of the animal body can be alternatively viewed as divisions of parasegments running from the posterior of segment 1 to the anterior of segment 14, creating 'parasegmental register' running from the head to tail of the animal (Martinez-Arias and Lawrence, 1985).

Hox gene expression patterns (both transcriptional and protein) throughout the embryo are delimited at specific parasegmental (PS) borders along the antero-posterior axis. Furthermore, different tissues within the embryo maintain different regions of *Ubx* expression. For example, although we may say that *Ubx* expression occurs from PS5 through to PS13 within the embryo, expression within the epidermis is confined between PS5-6, expression in the mesoderm exists between PS6-13 and only the CNS maintains *Ubx* expression throughout all possible segmental regions, stretching from PS5-13 ((Akam and Martinez-Arias, 1985; White and Wilcox, 1985a, 1985b). An additional complexity is that *Ubx* expression levels vary depending on the tissue type and PS location within the embryo. For instance, *Ubx* expression within the epidermis and CNS peaks at PS6 and then gradually tails off towards the more posterior PSs.

Following embryogenesis, *Ubx* expression is confined to the imaginal discs corresponding to PS 5-6 (anterior T2 to T3), principally in the Haltere imaginal disc and the T2 and T3 leg imaginal discs. Expression can also be seen within the developing ventral nerve cord (VNC) of the larvae.

Overall, it is apparent that the regulation of *Ubx* expression at the transcriptional level is complex and variable, dependant on the position along the anterior-posterior axis, the cell/tissue type and the developmental stage of the animal. What mechanisms are in place to generate this complexity? How is this control of spatial and intensity of expression regulated over time during development?

1.12 Transcriptional activation and epigenetic regulation

The initial expression boundaries of *Ubx* are set by the transcriptional activities of a number of genes. Genetic interaction analyses showed that the gap genes *hunchback* (*hb*) and *tailless* (*tll*) encode transcription factors that repress *Ubx* expression outside of PS5 and PS13, setting the limits of possible *Ubx* expression and that pair-rule gene *fushi-tarazu* (*ftz*) plays an inductive role, activating the expression of *Ubx* within the developing animal (Ingham and Martinez-Arias, 1986; Reinitz and Levine, 1990; White and Lehmann, 1986). These initial studies were insightful in providing a genetic mechanism to link crucial elements of early embryogenesis, the creation of repeating sub-units – the segments within the animal, with a collection of genes that are able to give positional information to those segments along the body axis.

But how do these activating and repressive factors regulate *Ubx* expression directly? We now know that many of the classic mutant alleles associated with the Bithorax complex – *abx*, *bx*, *pbx*, *bxd* correspond to cis-regulatory regions of *Ubx*. Molecular genetics approaches showed that these genetic elements when combined with a LacZ reporter gene, could reproduce certain aspects of the endogenous *Ubx* expression pattern (Irvine et al., 1991; Simon et al., 1990). Furthermore, many groups were able to show that transcription factors encoded by *hb*, *tll*, *ftz* as well as *engrailed* (*en*) and *twist* (*tw*) were able to bind to these regulatory sequences, linking the earlier genetic studies with a molecular mechanism of action (Müller and Bienz, 1992, 1991; Qian et al., 1993, 1991; Zhang and Bienz, 1992).

The initial domains of *Ubx* expression are set up and refined through these cis-regulatory elements and regulation by the gap, pair rule and segmentation genes mentioned above. However, the expression of these factors ceases early on during the development of the embryo. How then is *Ubx* expression maintained and further regulated during the continuing development of the animal?

To continue the transcriptional activity of the *Ubx* locus throughout development, genetic and molecular analysis have identified a number of genes that act as ‘epigenetic modifiers’, binding to regulatory regions upstream of the *Ubx* transcriptional start site and repressing or sustaining transcriptional expression respectively (Chan et al., 1994; Simon et al., 1993). These genes alter the chromatin conformation of the *Ubx* genetic region, ensuring that *Ubx* can be continually transcribed within the correct cells and tissues or silenced outside the normal domains of expression. The correct expression of *Ubx* within the appropriate imaginal discs is dependent on the function of these epigenetic modifiers. A number of imaginal disc specific enhancer elements have

been identified but unlike their embryonic counterparts, they do not respond to inputs by gap/segmentation genes. A mechanism was elucidated in which the activation or suppression of these imaginal disc enhancers relied on the close proximity of the epigenetic responsive elements (Pirrotta et al., 1995; Poux et al., 1996).

The epigenetic regulators in question are the *Polycomb* (*Pc*) group of proteins, which suppress transcriptional activity, and the *trithorax* (*trx*) group of proteins, which sustain transcriptional activity. Both groups function by modifying histones, controlling chromatin conformation within the nucleus and have wide-ranging regulatory activity across animal genomes (Schuettengruber and Cavalli, 2009; Schuettengruber et al., 2011). Initially identified through classical genetics approaches, it was seen that mutant alleles of these genes would develop homeotic like phenotypes. This mechanism of regulation ensures that the correct Hox genes are available for transcription within the correct domains of expression. In vertebrates, the same mechanism has been shown to be fundamental in regulating the expression of the Hox clusters during development (Soshnikova and Duboule, 2009).

1.13 Alternative splicing and protein isoform diversity

Another mechanism to vary protein functionality is by producing transcripts with alternate exons via alternative splicing. This post-transcriptional RNA processing mechanism can result in structural changes to the protein and therefore affect protein functionality. Many of the Hox genes within *Drosophila* undergo alternative splicing to generate multiple protein isoforms.

A striking example of this phenomenon is the generation of six distinct *Ubx* transcripts during *Drosophila* development. These alternate isoforms vary in abundance during *Drosophila* development, particularly during embryogenesis (Fig.1.5). There is a general transition from isoform UbxIa, found predominantly in early embryogenesis to isoform UbxIVa, the dominant isoform expressed at later embryonic stages, particularly during the development of the CNS of the embryo (Kornfeld et al., 1989; O'Connor et al., 1988). Importantly it has been shown that each isoform has differing functional abilities (De Navas et al., 2011; Reed et al., 2010), thus the generation of alternate versions of the *Ubx* protein can lead to diverging genetic programmes instigated within developing cells and tissues. It is unclear how this change in splicing isoforms is actively regulated through development, and at the cellular scale, what composition of Ubx splicing isoforms can be found in an individual cell.

Fig.1.5 *Ubx* transcripts undergo extensive RNA processing

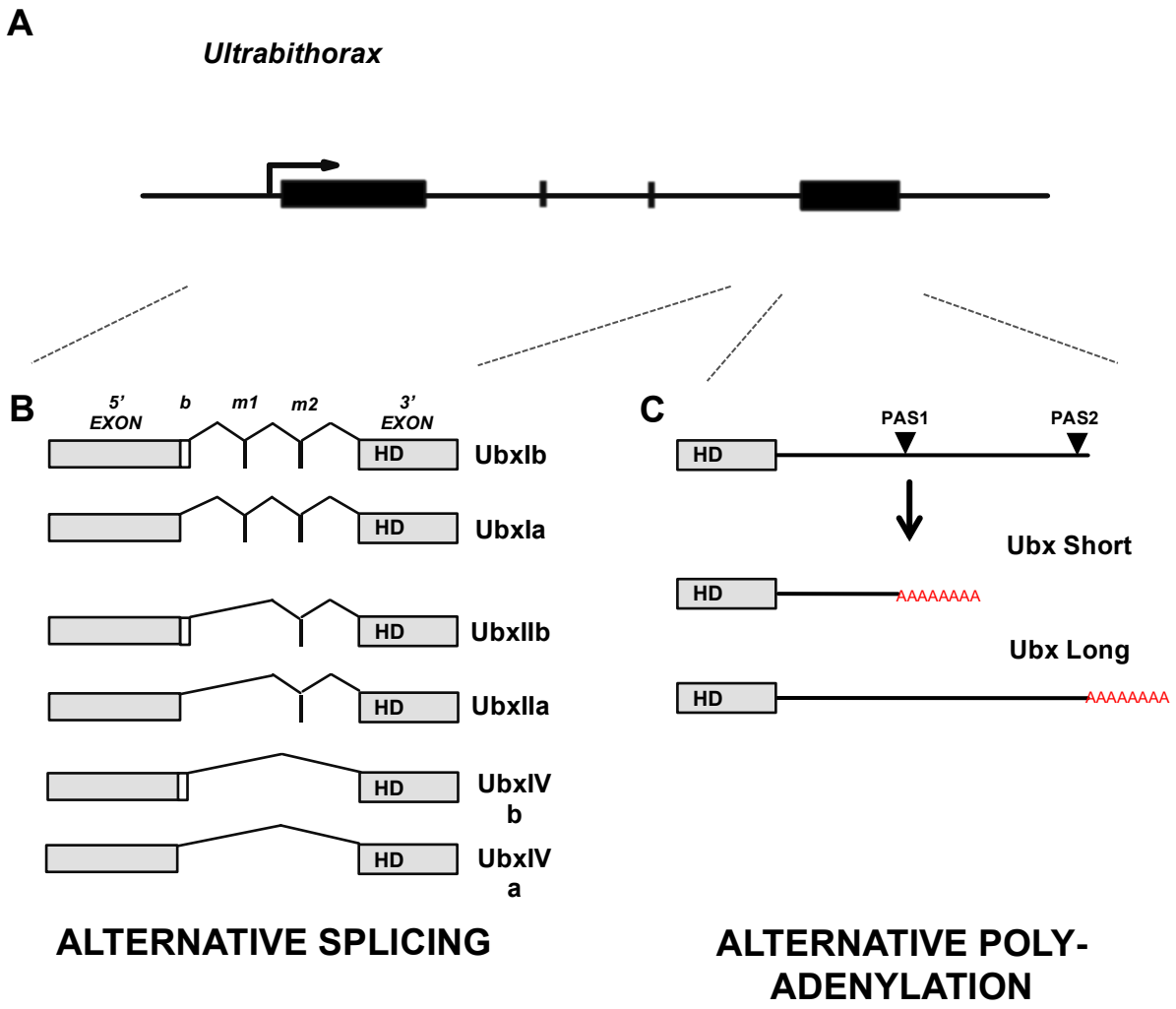

Fig.1.5 *Ubx* transcripts undergo extensive RNA processing

(A) Schematic of the Drosophila *Ubx* gene. (B) Alternative splicing leads to the generation of 6 possible isoforms. Splicing includes or excludes the *b* element, *m1* and *m2* micro-exons. (C) The *Ubx* 3'UTR contains two possible poly-adenylation sites – PAS1 and PAS2. The choice of site leads to Ubx transcripts with either a short or long 3'UTR isoform. Adding to the splicing isoform complexity, each splice variant can be paired with either the short or long 3'UTR isoform and these associations can change over the course of embryogenesis

1.14 Regulating expression levels – the role of the 3'UTR

Another addition to the canon of regulatory mechanisms controlling *Ubx* expression is the notion that the length of the *Ubx* 3' Untranslated Region (3'UTR) can be alternatively chosen during development during the post-transcriptional process of alternative poly-adenylation (APA).

In most cases the termination of the mRNA transcript involves the recognition of specific AU rich elements within the transcript by protein complexes that consequently cleave the mRNA transcript from the RNA Pol II transcriptional machinery and promote the poly-adenylation of the transcript (Fig.1.6A). The addition of these poly-A nucleotides to the gene transcript is important for the stability and translatability of each mRNA transcript within the cell. It is now apparent that the process of cleavage and poly-adenylation occurs co-transcriptionally(Bentley, 2014; Millevoi and Vagner, 2010). Indeed evidence exists that the CTD domain of the RNA Pol II complex directly interacts with and recruits cleavage/poly-A factors to the transcript (Fig.1.6B).

Alternative poly-adenylation occurs when there is more than one set of sequences present within a gene to trigger cleavage and poly-adenylation. The result is the formation of mRNAs that have alternative endings meaning, that each transcript could contain alternative exons and/or 3'UTRs (Proudfoot, 2011).

What determines which site is chosen? The main deciding factor in the decision to which site is chosen, is the relative strength of each site. Sites with high similarity to the consensus poly-adenylation sequences (including upstream and downstream sequences) will have a kinetic advantage in being able to form the cleavage complex and thus initiate transcript termination and activate poly-adenylation.

Recent evidence is emerging that suggests many factors including the relative concentration of required proteins, and the speed of RNA Pol II elongation can also affect site choice (Proudfoot, 2011). The *Ubx* locus has two possible poly-adenylation sites within its 3'UTR region, a proximal site (closest the 3' exon) and a more distal site separated by approximately 1100 nucleotides. The choice of site can lead to *Ubx* transcripts that will have either a short or long (extended) 3'UTR. It has been documented that over the course of *Drosophila* embryogenesis, the relative abundance of short and long *Ubx* 3'UTR isoforms changes so that by the time *Ubx* expression is confined to the CNS during late embryogenesis, the long 3'UTR is the dominant isoform (Kornfeld et al., 1989; O'Connor et al., 1988).

Fig.1.6 The process of alternative poly-adenylation occurs co-transcriptionally

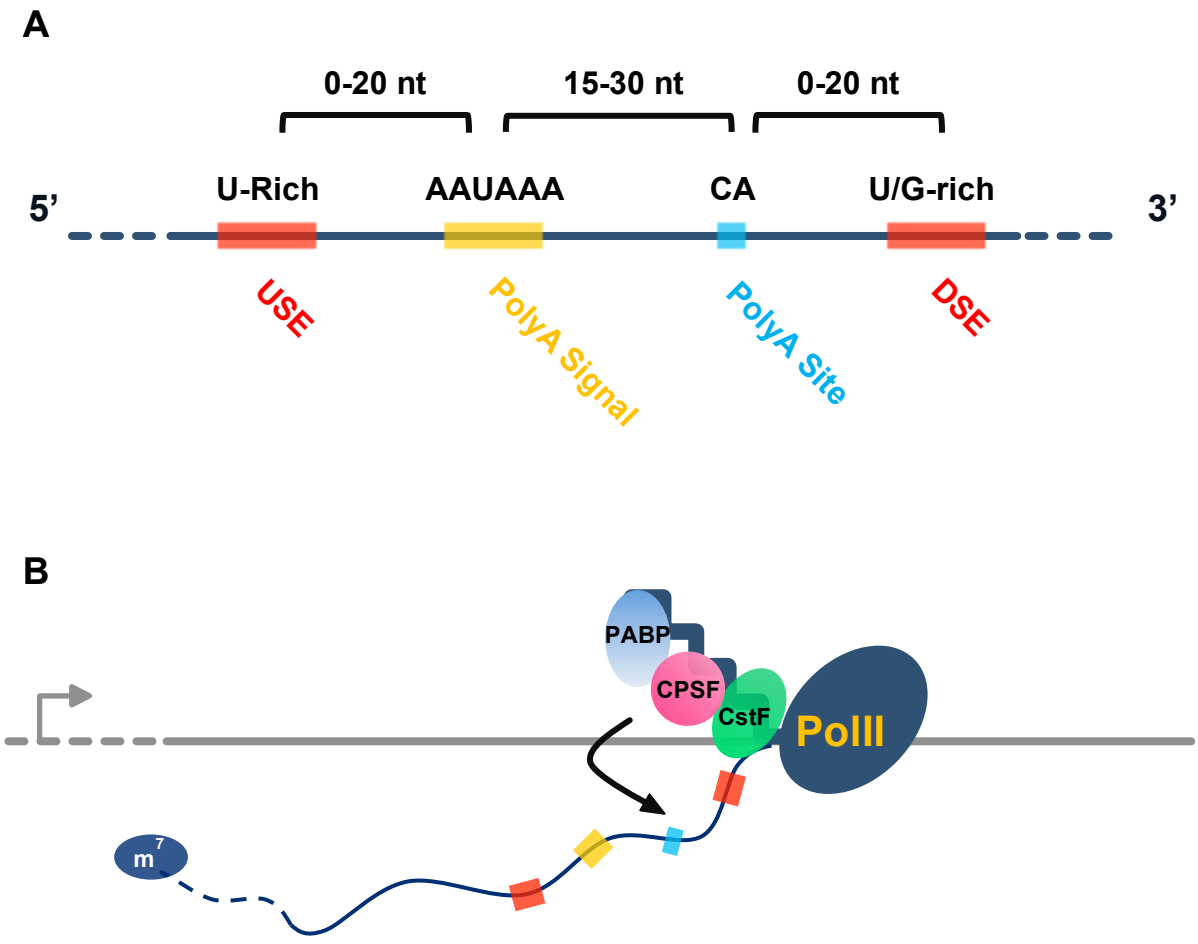

Fig.1.6 The process of alternative poly-adenylation occurs co-transcriptionally

(AB) Schematic showing the common sequence elements associated with the process of transcript cleavage and poly-adenylation site choice (B) Schematic highlighting the relationship between transcription and poly-adenylation. Three complexes/factors – CstF, CPSF and PABP are shown associated with the CTD region of the RNA Pol II machinery. These factors are heavily involved in the poly-adenylation site choice for transcript cleavage and poly-adenylation. Specific site-choice is governed by the recognition of specific sequence elements (coloured bars within transcript) by these factors. Alternative poly-adenylation occurs when more than one suitable site is present within the transcript. Alternative site choice can be affected by many factors including the speed of transcription and the relative concentration of appropriate factors required for poly-adenylation. See (Bentley, 2014; Millevoi and Vagner, 2010; Proudfoot, 2011) for detailed descriptions of these processes.

The biological relevance of this APA phenomenon has become more apparent since the discovery of microRNAs (miRNAs) - small non-coding RNAs that regulate gene expression along with a greater understanding of the role RNA-Binding Proteins (RBPs) can play in influencing gene expression during animal development. Both of these potential regulators predominantly bind to the 3'UTR of their target genes to exert their function. Thus the extension of the 3'UTRs, now seen as a common phenomenon during development can have real regulatory importance (Hilgers et al., 2011; Smibert et al., 2012).

It has been documented that the *Ubx* 3'UTR is under regulatory pressure from the miRNAs *iab-4/iab-8* during embryogenesis (Bender, 2008; Ronshaugen et al., 2005; Stark et al., 2008; Tyler et al., 2008). In a study by Thomsen et al, a correlation was made with the onset of this miRNA regulation and the transition to the extended long *Ubx* 3'UTR, showing that the extended 3'UTR isoform was required for correct *Ubx* expression patterns during late embryogenesis (Thomsen et al., 2010). The biological importance of *iab-4/iab-8* regulation of *Ubx* during CNS development is still an unresolved question.

As yet, there is no evidence linking the regulation of *Ubx* expression through RBP activity but many studies have shown the potential regulatory potential of these proteins. A well characterised example is the RBP Pumilio. This protein has been shown to regulate translation by binding to the 3'UTR of its target genes in more than one developmental context. The interaction of Pumilio and another RBP, Nanos with the 3'UTR of *hb* mRNA is essential for the posterior patterning in the embryo (Murata and Wharton, 1995; Wreden et al., 1997). Furthermore, both Pumilio and Nanos have also been implicated in the control of translation within developing neurons, affecting their morphogenesis and plasticity (Ye et al., 2004).

An intriguing relationship between RBPs and miRNAs may exist, in which the former can control the accessibility of the latter, affecting the regulatory potential of the miRNAs (Alonso, 2012). This regulatory relationship, shown by Kedde and colleagues, demonstrated that the binding of the vertebrate Pumilio homolog Pumilio-1 (PUM1) to a target 3'UTR, altered its structure, allowing miRNAs to target this gene more efficiently (Kedde et al., 2010). Other studies have implicated the regulation by *Pumilio*/miRNAs in controlling the expression of potent oncogenes (Miles et al., 2012).

Evidence suggests that the regulation of Hox gene 3'UTRs is a conserved method of fine-tuning expression and function in both vertebrates and invertebrates. An early study focusing on the transcriptional regulation of vertebrate Hox gene expression

domains using enhancer based reporter constructs found that transcriptional regulation alone was unable to reproduce the correct domains of expression. The authors reasoned that destabilisation of the Hox gene transcripts through the 3'UTR was required to maintain the correct posterior domains of expression (Brend et al., 2003).

A number of studies have shown that that *miR-196* (interestingly, the ortholog of *iab4*/*8*) targets *HoxB8* during development, controlling the posterior domains of expression along the main body axis (Hornstein et al., 2005; McGlinn et al., 2009). A further study was able to show that this miRNA regulates *HoxB8* within the neural tube and demonstrated that disruption to this regulation results in incorrect motoneuron formation (Asli and Kessel, 2010).

Regulation of gene expression through the 3'UTR is emerging as a potentially powerful method in fine-tuning the expression and consequently, the functionality of any given gene. In the case of developmental regulators like the Hox genes, transcription factors which have the potential to alter cell-states and developmental pathways, this mechanism of regulation may be very important.

1.15 The relationship between correct *Ubx* expression and function

Overall, the regulatory landscape governing Hox gene expression is complex and multi-layered. Using the analysis of *Ubx* as an example, we see that the expression of *Ubx* is regulated comprehensively at the transcriptional level by many repressor/activator inputs as well as the epigenetic silencing or sustaining of transcriptional activity.

Fig.1.7 *Ubx* expression and activity in the haltere imaginal disc

(A) *Ubx* is expressed throughout the haltere imaginal disc. There is a notable increase in expression within the pouch region of the disc. (B) Magnified section of the haltere pouch. Heterogenic expression can be seen within this region. (C) Magnified section of haltere pouch region. A group of cells are highlighted within the dash region showing dynamic expression of *Ubx* in neighbouring cells. (D) An allelic series of *Ubx* mutations increasing in phenotypic severity from left to right. Changes in phenotype correlate with gradual loss of *Ubx* expression within the haltere pouch region. The *Ubx* allelic series is made up of the following genotypes *w;;bx^{34e}/bx^{34e}, w;;Ubx^{1}/TM6b. w;;Ubx^{61d} pbx^{1} / bx34e* in increasing order of severity

Fig.1.7 *Ubx* expression and activity in the haltere imaginal disc

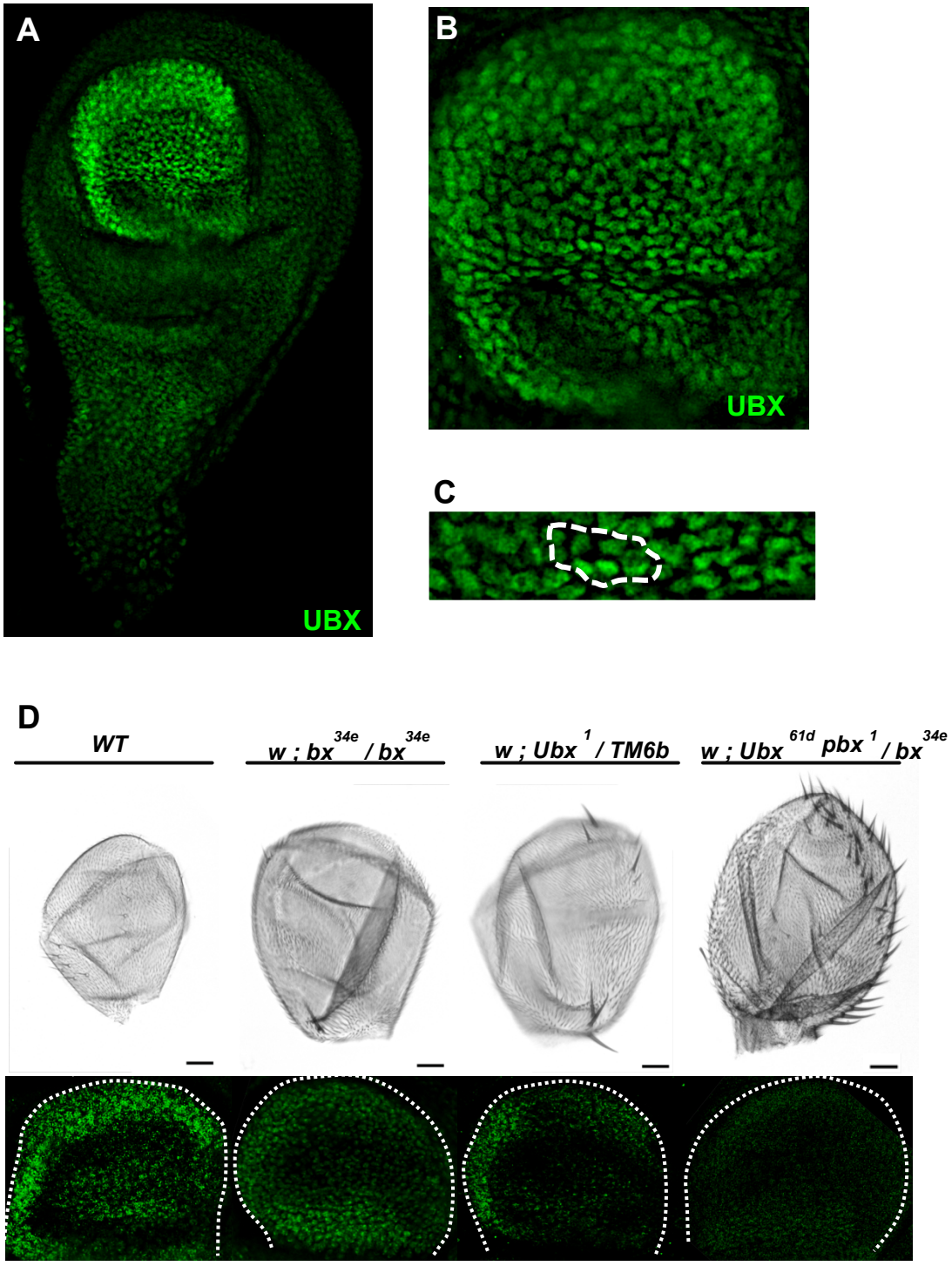

Post-transcriptionally, the *Ubx* transcript can be alternatively spliced to give multiple alternate protein isoforms and each *Ubx* transcript isoform can also be alternatively poly-adenylated leading to variable lengths of 3'UTR, the prime substrate for regulatory interactions with small non-coding RNAs and RBPs.

All of these regulatory interactions can affect the functional capabilities of the *Ubx* protein. Transcriptional regulation ensures that the appropriate cells and tissues are given the correct Hox code during development. Alternative splicing increases the functional capacity of the gene, producing specific isoforms which differ in their ability to regulate transcription within the genome. It is increasingly apparent that the generation of alternative 3'UTR isoforms through APA is an important process in development. These un-translated regions act as the regulatory substrates for potent cell and developmental regulators of gene expression such as miRNAs and RBPs.

How uniform is *Ubx* expression during development? What is the relationship between the *Ubx* expression levels and function? How are the correct levels of expression produced and maintained? Close examination of *Ubx* expression within the developing haltere imaginal disc can give light to these questions. Detailed analysis of these expression patterns reveals that *Ubx* expression is not uniform; in fact it is very heterogeneous across the disc (Fig.1.7A-C). Development of the haltere appendage is sensitive to subtle changes in *Ubx* expression, different mutant alleles of *Ubx* cause homeotic transformations with varying severity in the adult appendage (Fig.1.7D) (Bender et al., 1983).

This suggests that haltere cells are sensitive to varying levels of *Ubx* expression and that this can alter the genetic programmes instigated within these *Ubx*-sensitive cells. Evidence exists for this relationship between Hox gene expression levels and alternate developmental outcomes. For example, varying expression levels of the Hox gene *Antennapedia* (*Antp*) lead to different axonal targeting in motoneurons which innervate the legs of *Drosophila* (Baek et al., 2013).

1.16 miRNAs are important post-transcriptional regulators of gene expression

miRNAs are 18-22 nucleotide small RNAs that have been identified as key post-transcriptional regulators of gene expression (Bartel, 2009; Bushati and Cohen, 2007; Pasquinelli, 2012). They exert their function acting as guidance molecules for the RNA Induced Silencing Complex (RISC). miRNAs bind to specific regions of target transcripts through Watson-Crick base-pairing. The attachment of the RISC complex

target genes disrupts translation and can lead to the de-adenylation and degradation of the transcript (Béthune et al., 2012; Djuranovic et al., 2012; Guo et al., 2010; Meijer et al., 2013). In this manner miRNAs act as negative regulators of gene expression.

miRNAs have been implicated in the regulation of most cellular and developmental functions e.g. cell proliferation (Brennecke et al., 2003; Weng and Cohen, 2012), cell differentiation (Davis et al., 2011; Dill et al., 2012; Dore et al., 2008; Kredo-Russo et al., 2012; Xiao et al., 2007), cellular senescence (Rivetti di Val Cervo et al., 2012), stem cell function (Marson et al., 2008; Melton et al., 2010) and tissue regeneration (Eulalio et al., 2012; Williams et al., 2009; Yin et al., 2008).

A study highlighting the importance of miRNA function for developmental biology was the experimental analysis of the *Drosophila* miRNA *bantam* (*ban*) (Brennecke et al., 2003). Discovered in a screen looking for determinants of tissue growth, it was seen that this miRNA was deeply involved in the regulation of tissue growth during development. It was shown that *ban* both enhances cell proliferation and negatively regulates apoptosis.

A study by Davis and colleagues looked for the general role of miRNAs during the development of the vertebrate optic cup neuro-epithelium (Davis et al., 2011). By disrupting the production of mature miRNAs within this developing epithelium the authors found that a number of developmental processes were affected, including the disruption to many cell differentiation programs required in the developing optic cup.

The mis-regulation of these genes is also associated with the development and enhancement of many cancers (Miles et al., 2012; Png et al., 2012; Suh et al., 2012) and diseases (De Pontual et al., 2011; Haramati et al., 2010; Liu et al., 2012; Wu et al., 2010). For example, Png and colleagues showed that a *miR-126*, a miRNA silenced in a number of common human cancers, was required for the suppression of metastatic endothelial recruitment and angiogenesis. Thus this miRNA has strong anti-cancer functionality within cells and tissues (Png et al., 2012). The cellular importance of miRNAs is not necessarily restricted to developmental processes. In a ground breaking study, Liu et al., were able to show the *Drosophila* miRNA *miR-34* was required for the long term brain integrity of *Drosophila* brains. The loss of this *miR-34* leads to accelerated brain ageing, neuro-degeneration and a sharp decline in survival (Liu et al., 2012).

1.17 The biogenesis of miRNAs

The biogenesis of the 18-22 nucleotide mature miRNA is a complex multi-step process (reviewed Kim et al., 2009). miRNA genes are situated in intergenic regions of the genome (canonical intergenic miRNA) or found within intronic regions of protein-coding transcripts (mirtron) (Okamura et al., 2007; Ruby et al., 2007a). The first step in the biogenesis pathway is the transcription of a primary-miRNA (pri-miRNA) transcript from the genome. This primary transcript is capped and poly-adenylated, forming a stable secondary structure. The first biochemical processing step is endonucleolytic cleavage of the pri-miRNA by the RNAse III enzyme *Drosha*. The enzyme is partnered by the protein *DGCR8* (named *Pasha* in *Drosophila*) which contains RNA binding domains. This initial cleavage produces a single stranded RNA approximately 80-100 nucleotides in length which forms a stable stem-loop structure termed the pre-miRNA or miRNA hairpin. The pre-miRNA is exported from the nucleus by the *Exportin-5/RAN-GTP* complex. The initial processing of mirtrons differs slightly. Following transcription, genes containing intronic miRNAs undergo splicing. A by-product of this RNA processing step is the release of small intronic sequences that have structural features mimicking *Drosha* processed pre-miRNA stem-loops. These intronic miRNAs are then exported from the nucleus in the same fashion as canonical pre-miRNAs.

Once in the cytoplasm the pre-miRNA stem-loop is bound to the *RLC* (RISC Loading Complex) which contains *Ago2*, *TRBP*/*Loquacious (Loqs)* and another RNAase III enzyme *Dicer1*. The *Dicer1* enzyme endonucleolytically cleaves the pre-miRNA hairpin to produce a mature miRNA duplex. The duplex contains the mature miRNA, to be loaded into the RISC complex and the passenger strand miRNA. The passenger strand miRNA (sometimes referred to as the miRNA*) was originally thought to be degraded at this point. Although in most circumstances this is indeed the case, experimental evidence now suggests that some miRNA* species are loaded into the RISC complex an act as functional miRNAs (Okamura et al., 2009, 2008). Interestingly, numerous studies show that the regulation of each processing step during miRNA biogenesis can be regulated by non-processing factors (reviewed Krol et al., 2010; Siomi and Siomi, 2010; Winter et al., 2009).

Regulation of miRNA biogenesis can have important effects on controlling the abundance and availability of these small RNAs and consequently their biological function. This regulation is seen both at the transcriptional (Biemar et al., 2005; Chang et al., 2011; Chawla and Sokol, 2012; Ozsolak et al., 2008) and post-transcriptional

(Huang et al., 2012; Kim et al., 2009a; Suzuki et al., 2011; Trabucchi et al., 2009) stages of miRNA biogenesis.

Chang and colleagues demonstrated that the transcription activation of *miR-200c* by the tumour suppressor *p53* was an important component in the functional properties of *p53*. The expression of *miR-200c* was required to suppress two target genes - *BMI1* and *KLF4*. Both have functional roles in the regulation of the epithelial-mesenchymal transition (EMT), a cellular transition that when mis-regulated can enhance cancer metastasis. Thus, *p53* regulates EMT properties by ensuring the expression of *miR-200c* and therefore the repression of two important EMT related target genes (Chang et al., 2011).

The post-transcriptional regulation of miRNA biogenesis is emerging as an important factor in determining the functional capabilities of miRNAs within cellular and developmental biology. An interesting example highlighting the complexity of this mode of regulation was discovered in a study by Huang et al. The authors showed that the regulation of protein synthesis within neuronal synapses by *BDNF* was in part regulated through changes in miRNA biogenesis. The presence of *BDNF* in neurons led to the transcription-independent increase in *Dicer* protein levels, resulting in a general enhancement of mature miRNA levels within these neurons. Additionally, *BDNF* increased levels of *Lin-28*, a RBP known to down-regulate mature miRNA levels (Hagan et al., 2009; Heo et al., 2009). Thus *BDNF* activity both increases overall mature miRNA levels through enhanced *Dicer* function and selectively down-regulates a number of miRNAs targeted by *Lin-28* (Huang et al., 2012).

1.18 Characteristics of miRNA function during development

One of the most fascinating discoveries in the miRNA field was how deeply conserved some miRNAs are across long evolutionary distances. A small group of miRNAs, sometimes termed ‘ancient miRNAs’ have been discovered in both proteostome and deuterostome genomes indicating they may have been present in the last common bilaterian ancestor. This highly conserved nature of these miRNAs suggests that these genes have fundamental roles in animal biology. Yet, when individual miRNAs are removed from an animal, there are often very little phenotypic consequences. How to explain this disconnect?

The answer may lie in the manner in which miRNAs function. miRNAs are commonly seen performing two main regulatory functions. The first is ‘expression tuning’, where

miRNAs are actively down-regulating target transcripts, helping maintain the required level of target gene expression or by creating a stable 'miRNA switch' where only strong expression of a gene will lead to its correct function.

An excellent example of a miRNA tuning function was elucidated by Li et al, examining the role of *miR-9a* in the specification of external sensory cells in *Drosophila*. Peripheral sensory cells within *Drosophila* require the presence of the transcription factor *Senseless* (*Sens*) for their correct development. In non-sensory precursor cells, *Sens* is repressed by activated *Notch* signalling. It was seen that *miR-9a* was required in non-sensory precursor cells to also repress the expression of *Sens* through the inhibition of translation. Thus presence of *miR-9a* ensures that the expression of *Sens* is repressed within non-sensory precursor cells (Li et al., 2006).

Another study examining *miR-9* function in vertebrates highlighted an interesting example of a miRNA behaving in a 'switch-like' function. The *Notch* signalling effector protein *Hes1* is required for the continued proliferation of neural progenitors during development. For *Hes1* to function, its expression must be cyclical. Bonev and colleagues observed that *miR-9* was able to target *Hes1* transcripts within these neural progenitors and that *miR-9* transcription was also cyclical, however mature *miR-9* levels were very stable. Therefore mature *miR-9* expression levels constantly increase and concomitantly, their repression of *Hes1* transcripts also increase. Eventually the repressive effect of *miR-9* leads to limited *Hes1* expression levels and the disruption of *Hes1* function. This causes the neural progenitors to abandon their proliferative state. Here *miR-9* expression acts as a switch, eventually reaching certain level of expression that is able to fully terminate *Hes1* function (Bonev et al., 2012).

The second function is often termed 'expression buffering', where the miRNA acts to reduce any variation in target gene expression (Bartel and Chen, 2004; Herranz and Cohen, 2010; Hornstein and Shomron, 2006; Wu et al., 2009). An example of this miRNA function was uncovered by Li et al, in their analysis of *miR-7* function during sensory cell development in *Drosophila*. The authors found that *miR-7* was involved in the development of multiple types of sensory cells within the animal. However, expression of *miR-7* target genes changed little when the miRNA was removed. This was until these animals were placed in fluctuating temperature conditions during their development cycle. This environmental perturbation led to irregular expression of *miR-7* targets indicating this miRNA functions by acting as a genetic buffer, stabilising gene expression during development (Li et al., 2009).

In both these functional roles, the effect on gene expression by miRNAs is relatively weak, therefore, when most miRNAs are removed from an animal, the resulting phenotype maybe subtle and difficult to detect. This would explain why very few miRNA mutants have easily observable phenotypes.

The relationship between the level of target gene expression and the level of mature miRNA expression can have important implications for target-miRNA interactions. Using a cell based reporter testing system, Mukherji et al., explored the dynamics of target-miRNA concentrations and the effect on target gene repression. A key finding was that the level of translational inhibition by miRNAs was related to the abundance of the target transcripts compared with miRNA abundance. Lowly expressed mRNAs were greatly repressed by large amounts of miRNA. Increased target expression led to a reduction in target gene repression – something comparable to a 'fine-tuning' role by the miRNA (Mukherji et al., 2011).

An important characteristic when considering miRNA function is the high degree of pleiotropic targeting by an individual miRNA. The miRNA targeting mechanism is a 6-8nt 'seed' sequence. It is no surprise that many potential target genes will have a miRNA 'seed' site. Most estimates suggest each miRNA may have upwards of 100 targets within a cell at any given time.

Overall miRNAs provide subtle but very important regulatory behaviour within the cellular environment. Their ability to effect gene expression within the cytoplasm directly, gives them a fast acting regulatory activity that is perhaps not achievable through transcriptional control mechanisms alone. This allows miRNAs to act as intrinsic regulators of cell fate by maintaining the 'status quo' of gene expression within a cell, stabilising a particular cell phenotypic state. In some cases the miRNA profile within a cell can be used as a molecular marker for changing cell states. For example Neveu et al showed that similarities in miRNA profiles could be used to categorise pluripotent cell lines independent of their origin and that these profiles were indicative of *p53* function within these cell lines (Neveu et al., 2010).

1.19 Integration of miRNAs into complex gene regulatory networks

miRNAs are intrinsically embedded into the complex gene regulatory networks (GRNs) that govern animal development and are mis-regulated in disease (Cui et al., 2006; Mendell and Olson, 2012; Ooi et al., 2011; Pencheva and Tavazoie, 2013). Analysis of large scale GRNs that include miRNAs reveals a number of common and recurring

network motifs that can be related to different miRNA functions. For instance the 'expression tuning' function of a miRNA can be viewed as a coherent feed-forward loop motif, a transcription factor may repress a specific gene and activate a miRNA which also targets that gene. In this way, the transcription factor is re-enforcing the transcriptional decision to reduce gene expression by activating an additional negative repressor. The 'expression buffering' function of a given miRNA can be seen as an incoherent feed-forward motif, where a transcription factor can activate both its target gene and a miRNA to repress that target gene. The induced expression of the target gene is then buffered by the presence of the activated miRNA (Tsang et al., 2007).

An interesting biological example where miRNAs are embedded into a prominent gene regulatory network to control an essential cellular process is the maintenance of stem cell pluripotency. In this example, the main pluripotency factors *Oct4*, *Sox2, Nanog* and *Tcf3* transcriptionally induce a number of miRNAs which help fine-tune the expression of other pluripotency factor transcriptional targets. Equally a number of miRNAs known to contribute to cell fate decisions during mammalian development are transcriptionally silenced. This incorporation of miRNAs into the pluripotency gene network allows for network stabilisation, helping to maintain this particular cell phenotype (Marson et al., 2008).

1.20 Questions addressed in this study

As we have seen, the regulation of the *Ubx* expression through development is complex and multi-layered. Focusing on the regulation of transcription, there are many genetic interactions required at successive stages of development to produce a complex pattern of gene expression that varies depending on tissue type and developmental stage. But how variable is this expression at the cellular level? Are these transcriptional mechanisms accurate and reliable enough to ensure the correct levels of *Ubx* protein are achieved and maintained in individual cells? Studies highlighting the significance of post-transcriptional mechanisms, specifically the regulation of gene expression through the 3'UTR suggest that these mechanisms may have an equally important task in regulating the expression of potent genes like *Ubx* at the cellular scale.

How important are the correct levels of gene expression for Hox gene function? The complexities in regulating *Ubx* expression suggest that having the correct spatial and temporal abundance of this transcription factor is important for its function. Analysis of

a number of *Ubx* mutant alleles shows that cells can be sensitive to varying levels of *Ubx* expression and this can affect functional capabilities of this Hox gene.

Hox genes are fundamental regulators of appendage development in both vertebrates and invertebrates. Studying Hox gene function within appendage development allows us not only to address fundamental questions regarding how Hox gene expression and function is regulated but also to understand better, the role Hox genes have in helping build the diverse appendage morphologies seen within the animal kingdom.

In the first part of this thesis, using *Ubx* regulation of haltere development as a paradigm for Hox function, we look to further our understanding of *Ubx* regulation, specifically the role miRNAs may have in the fine-tuning of *Ubx* gene expression. Furthermore, we are interested in learning how this regulation relates to *Ubx* function. What can we learn about the role *Ubx* has in controlling and shaping the development of the haltere appendage?

Hox genes specify particular cellular fates during development. Yet, we know little regarding how Hox genes co-ordinate specific genetic programs in multiple cell and tissue types during developmental processes, like the formation of appendages. What other genetic factors are incorporated into the control and regulation of divergent gene regulatory programs instigated by the same gene?

In the second part of this thesis, we explore this question by asking to what extent potent gene regulators like miRNAs are recruited into the gene regulatory networks controlled by *Ubx* during haltere development. Which miRNAs are present during haltere development and how does this differ from other *Drosophila* appendages? What is the functional significance of these haltere miRNAs? How are these miRNAs incorporated into the *Ubx* gene regulatory programs guiding the development of the haltere appendage? In this study, we hope to address some of these questions.

CHAPTER 2

2. Materials & Methods

Total RNA Extraction and cDNA synthesis

Total RNA was extracted from all samples using TRI Reagent (Ambion) following manufacturers standard protocol. RNA quantity and quality was analysed using a NanoDrop spectrophotometer (Thermo Scientifc). cDNA synthesis from Total RNA was carried out using the RETROscript Kit (Ambion) using standard manufacturers protocol. For each individual synthesis reaction 1µg RNA was DNAseI treated (NEB) first, before cDNA Synthesis was carried out.

Ubx and miR-310C expression analysis (RT-PCR)

To detect differential *Ubx* 3'UTR isoform, primers were designed to detect either All Ubx isoforms (Ubx-universal) or extended 3'UTR isoforms (Ubx-distal). Ubx Universal Forward 5'-AGTGGAAGGAGCGCAGATTA-3' and Reverse 5'-CAGAATTTTGCTCGCATTCA-3', Ubx Distal Forward 5'-GAACGAAGGCAGATGCAAAT-3' and Reverse 5'-GGTAAGTGGTCGGATGCAGT-3'. Rp49 was used as control reaction across all samples. Rp49 Forward 5'-CCAGTCGGATCGATATGCTAA-3' and Reverse 5'–TCTGCATGAGCAGGACCTC– 3'. To detect *pri-miR-310C* transcripts, oligos were designed around the miR-313 gene, miR-313 Forward 5'-TACCCGACATCGTCTAGCC -3' and Reverse 5' AAAATGCAGAATTGCCCTTG-3'.

To determine range of the Δ310 deletion in the genome, oligos were designed to detect genes surrounding the *miR-310C* – *Quasimodo, Black, Nnf1a* - as well as primers within the *miR-310C* miRNA cluster. *Quasimodo* Forward 5'-TTCGGTGTGGTTTCGAGTCT-3' and Reverse 5'-GCAAACACACACAGCGAGTT-3', *Nnf1a* Forward 5'-TGCTATGGCCAAGAGCAAT-3' and Reverse 5'-TTGTCAGAAGTCGTTCAATGC-3', *Black* Forward 5'-GACAGGGTGATACGCCATTT-3' and Reverse 5'-AGACTTTGATGCCACCGAAC-3', and *miR-310* Forward 5'-CCGGCCTGAAAATATCAAGA-3' and Reverse 5'-GAGAAAAGCGAACTGGATT-3'.

PCR protocol was as standard for all reactions except for Ubx-universal and Ubx-distal. The cycle number for each pair of primers, required to produce an equivalent level of expression using a standard genomic template was determined first, to normalise reaction conditions before experimental testing of cDNA samples.

Table 2.1 Primers used for gene expression analysis

Gene	Forward Primer		Reverse Primer	
Ubx Universal	**UbxF1**	5'-AGTGGAAGGAGCGCAGATTA-3'	**UbxR1**	5'-CAGAATTTTGCTCGCATTCA-3'
Ubx Distal	**UbxF2**	5'-GAACGAAGGCAGATGCAAAT-3'	**UbxR2**	5'-GGTAAGTGGTCGGATGCAGT-3'.
rp49	**rp49F1**	5'-CCAGTCGGATCGATATGCTAA-3'	**rp49R1**	5'–TCTGCATGAGCAGGACCTC– 3'
pri-miR-310C	**313F1**	5'-TACCCGACATCGTCTAGCC -3'	**313R1**	5' AAAATGCAGAATTGCCCTTG-3'.
Quasimodo	**QuasF1**	5'-TTCGGTGTGGTTTCGAGTCT-3'	**QuasR1**	5'-GCAAACACACACAGCGAGTT-3'
Nnf1a	**NnfF1**	5'-TGCTATGGCCAAGAGCAAT-3'	**NnfR1**	5'-TTGTCAGAAGTCGTTCAATGC-3'
Black	**BlF1**	5'-GACAGGGTGATACGCCATTT-3'	**BlR1**	5'-AGACTTTGATGCCACCGAAC-3'
miR-310	**310F1**	5'-CCGGCCTGAAAATATCAAGA-3'	**310R1**	5'-GAGAAAAGCGAACTGGATT-3'
pri-miR-9b	**9bF1**	5'-CTGCAGGTCAATCGTCAGAA-3'	**9bR1**	5'-CGCGAGAAAAGTAAAGAATACCA-3'
pri-miR-986	**986F1**	5'- ATAGGAGCCGGAAAAGTCGT-3'	**986R1**	5'-AAGTGCCAGTAGCCCCATTA-3'
pri-miR-996	**996F1**	5'-GTGCAGGGGCAATAATCATC-3'	**996R1**	5'-CGTTGTGCTGACCCAACTTA-3'
pri-miR-999	**999F1**	5'-ACCCCGACATAGTCATACGG-3'	**999R1**	5'-CACCTGGCCGAACTTATTGT-3'
pri-miR-13a	**13aF1**	5'-AATTGGGCATAACGATTGGA-3'	**13aR1**	5'-AAGACGTGGTTCAGTCAGTCG-3'
pri-miR-137	**137F1**	5'-ATTACGGCCAGTGAAAGTGG-3'	**137R1**	5'-GCTCATTTAAACGGGTTTCG-3'
pri-miR-281-1	**281-1F1**	5'-GTCCTGTCCGTTGAGGTGTT-3'	**281-1R1**	5'-CTGAAAGGTGGGAAGGGATT-3',
pri-miR-283	**283F1**	5'-TGGGAGCGAGAGAGAGAGAG-3'	**283R1**	5'-TTCGTTTTGTTGCGCTTATG-3'
pri-miR-1013	**1013F1**	5'-CGTGCTGGAGAGGTGAGTTT-3'	**1013R1**	5'-TGACCCACCAGCATCTCATA-3'

SQ-RT-PCR analysis to determine Ubx expression levels

To assay the relative expression levels of Ubx long 3'UTR isoforms within the haltere, SQ-RT-PCR was performed using Ubx Universal and Ubx Distal primers. Reactions were run for each primer pair for successive cycle lengths (23, 26, 29, 32, 35) using genomic DNA as a template. At the same instance control reactions were run using Rp49 F1 and R1 primers. PCR products were run on 2% agarose electrophoresis gel and resulting bands were analysed using ImageJ software. The intensity of each Ubx Universal and Distal band was normalised to the intensity of the accompanying rp49 band at each successive cycle length. The resulting intensities can then plotted on a graph. For each primer pair, we looked to determine when the PCR reaction reached an exponential intensity. For SQ-RT-PCR it is desirable to run reactions at a cycle number preceding this exponential phase. Following this analysis it was determined that both Ubx Universal and Ubx Distal reactions could be run for 26 cycles before reaching this exponential phase.

miRNA Target Predictions

miRNA target predictions were carried out using the PITA algorithm (Kertesz et al., 2007) (http://genie.weizmann.ac.il/pubs/mir07/mir07_prediction.html). The *Ubx* extended 3'UTR sequence used for the target predictions was extracted from FlyBase (http://flybase.org/). Screening of results using published RNA Seq data (Ruby et al., 2007b) was done using *Microsoft Excel*.

Genetics

All stocks were raised at 25^{o}C on standard molasses medium. The *Oregon R* strain was used as the wild-type genotype.

To compare the extent of reduced Ubx expression within the haltere disc and the corresponding changes in haltere phenotype we used a series of genetic disruptions, which have varying effect on *Ubx* expression. The following Ubx alleles were used bx^{34e}, Ubx^{1} and Ubx^{61d} pbx^{1} composite chromosome.

Fig.2.1 Crossing scheme to generate *Ubx* allelic series

To generate the Ubx allelic series, each mutant alleles was crossed into the same genetic background using the *w ; MKRS / TM6b* stock (A-C). To generate severe homeotic haltere transformations, two mutant allele stocks were crossed together (D).

Fig.2.1 Crossing scheme for generating *Ubx* allelic series

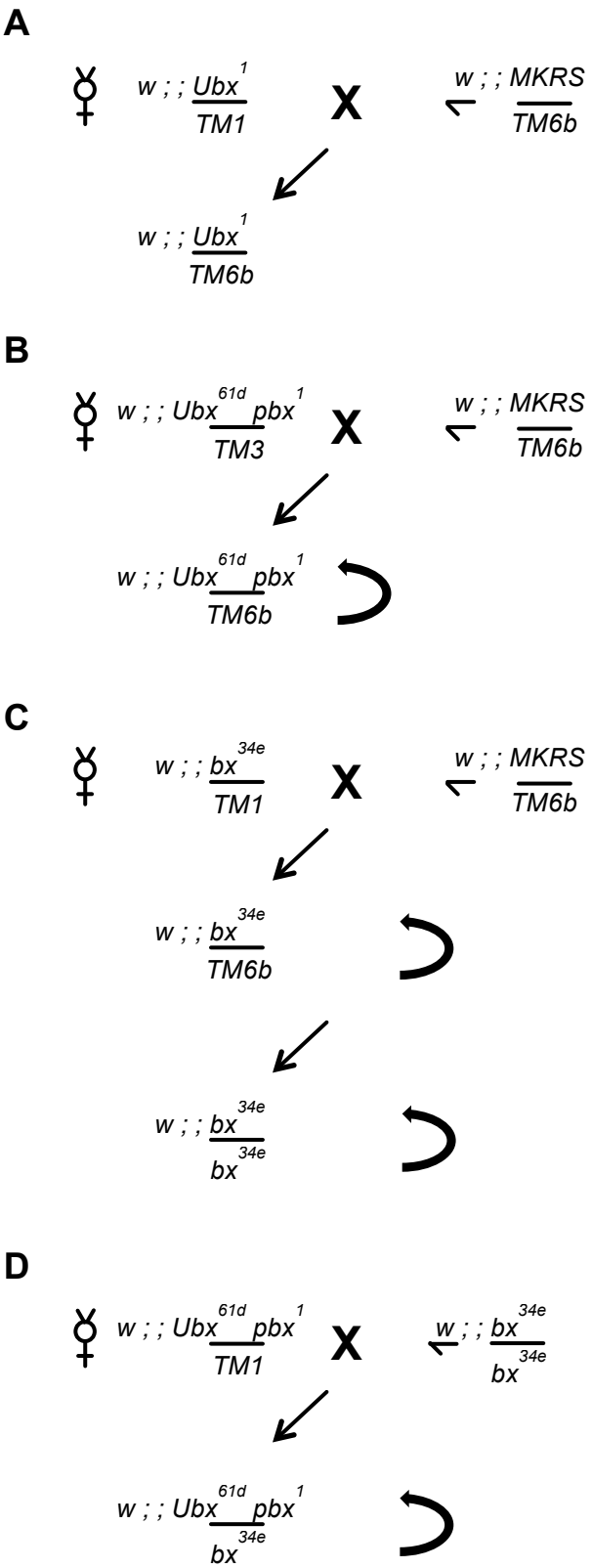

Fig.2.2 Crossing scheme to express mCherry constructs within the haltere

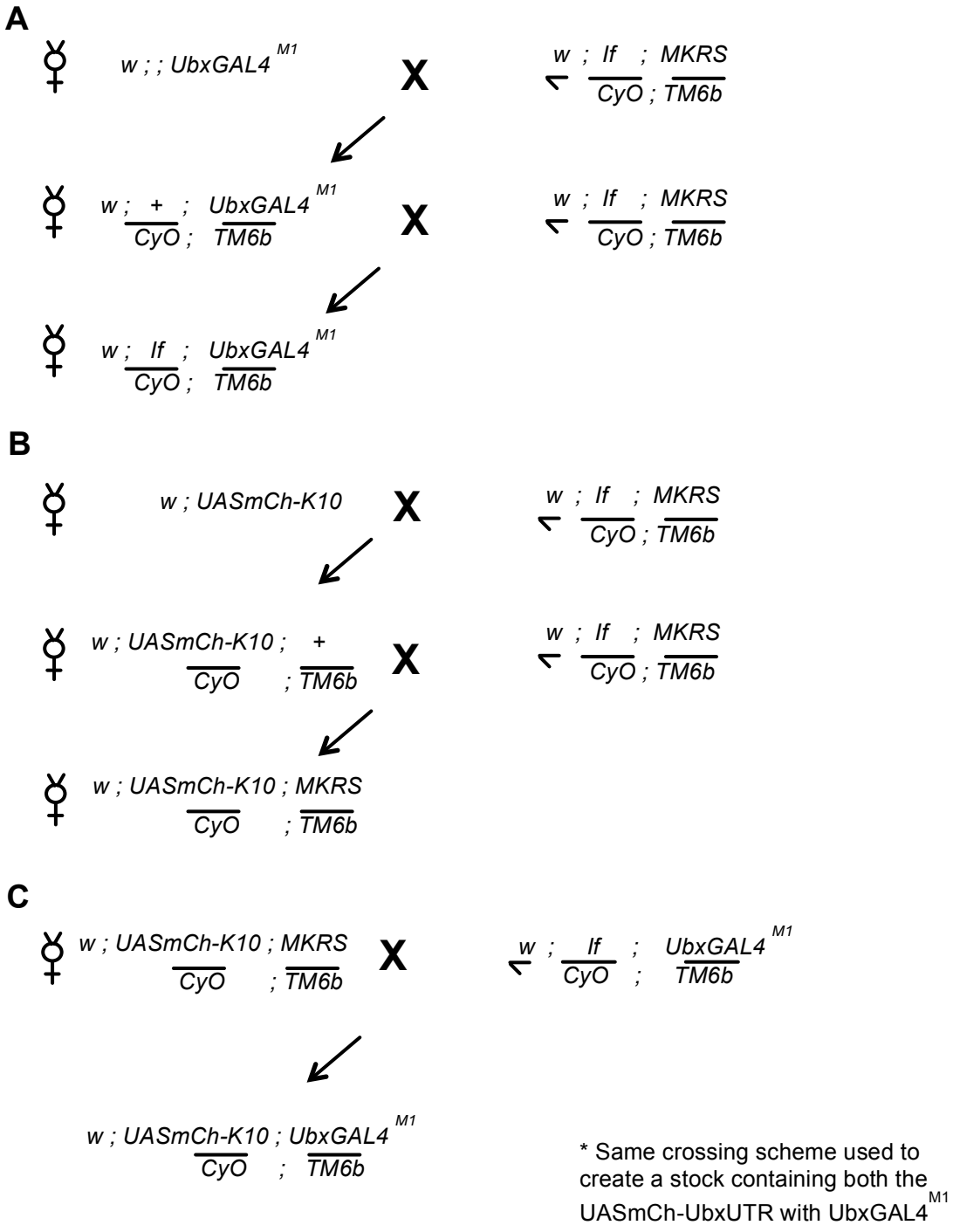

Fig.2.2 Crossing scheme to express mCherry constructs within the haltere

Each mCherry-UTR transgene and the Ubx-GAL4 driver were first all crossed into the same genetic background using the *w ; If/Cyo ; MKRS/TM6b* balancer stock (A-C). Each transgene was then crossed to the Ubx-GAL4 driver line to generate stable stocks which express the mCherry transgenes within the haltere (D).

Each of these alleles was crossed into the same generic background using the *w ; ; MKRS/TM6b* balancer stock (Fig.2.1). The *w ; ; Ubx ^{61d} pbx^{1}* chromosome was further crossed to *w ; ; bx^{34e}* to produce a more severe haltere transformation. The *bx^{34e}* allele is caused by the insertion of a Gypsy transposable element within an enhancer region of the *Ubx*. The *Ubx^{1}* allele is caused by the random insertion of the Doc transposable element downstream of the *Ubx* 5' exon disrupting all possible transcripts from this locus. The *pbx^{1}* allele is caused by a X-ray induced deletion of a upstream enhancer region of *Ubx.* The origin and nature of the *Ubx^{61}* mutations is unknown, however it is listed as a viable dominant allele on the Flybase repository (www.flybase.org)

The creation of the mCherry constructs has been previously described (Thomsen et al., 2010). Both constructs were inserted on 2nd chromosome in a *yellow white* background. These original lines were crossed with a UbxGAL4^{M1} line (De Navas et al., 2006a) (a gift from E. Sanchez-Herrero) previously balanced using a *w ; If/CyO ; MKRS/TM6b* (gift from Rob Ray) to create two mCherry expression stocks *w ; UASmCh-K10/CyO* ; *UbxGAL4^{M1}/TM6b* and *w ; UASmCh-UbxUTR/CyO ; UbxGAL4^{M1}/TM6b* (Fig 2.2).

The *miR-310C^{NP5941}* insertion (Bloomington Stock Centre; no:113798) containing a GAL4 transcriptional activator was used to drive expression of a *UAS::mCherryNLS* transgene *w ; UAS::mCherryNLS/CyO* and used as a reporter for *miR-310C* expression by recombining the insertion with the fluorescent reporter (Fig.2.3).

To overexpress the miR-310C miRNAs during imaginal disc development, the *miR-310C^{EP2587}* (Szeged Stock Centre) containing UAS promoter sequences upstream of the miR-310C miRNAs was crossed to a *NubbinGAL4* driver (Bloomington Stock Center; no: 38418) balanced over CyO generating *w ; Nub::GAL4/CyO* (Fig.2.4)

Fig.2.3 Crossing scheme to generate miR-310C-GAL stocks

The *miR-310C^{NP5941}* insertion was first crossed into the same *white* genetic background as the UAS-mCherryNLS reporter transgene (A). The insertion was then crossed to the reporter to monitor expression in the haltere (B). To create a stable reporter line (C), females containing both transgenes were crossed to a balancer stock, progeny of this cross were observed for possible recombination events within the female (see lightning bolt). Both transgenes contain mini-w+ marker leading to orange eye colours. Potential recombinant males were judged by looking for the appearance of dark orange - red eye colour.

Fig.2.3 Crossing scheme to generate *miR-310C*-GAL4 stocks

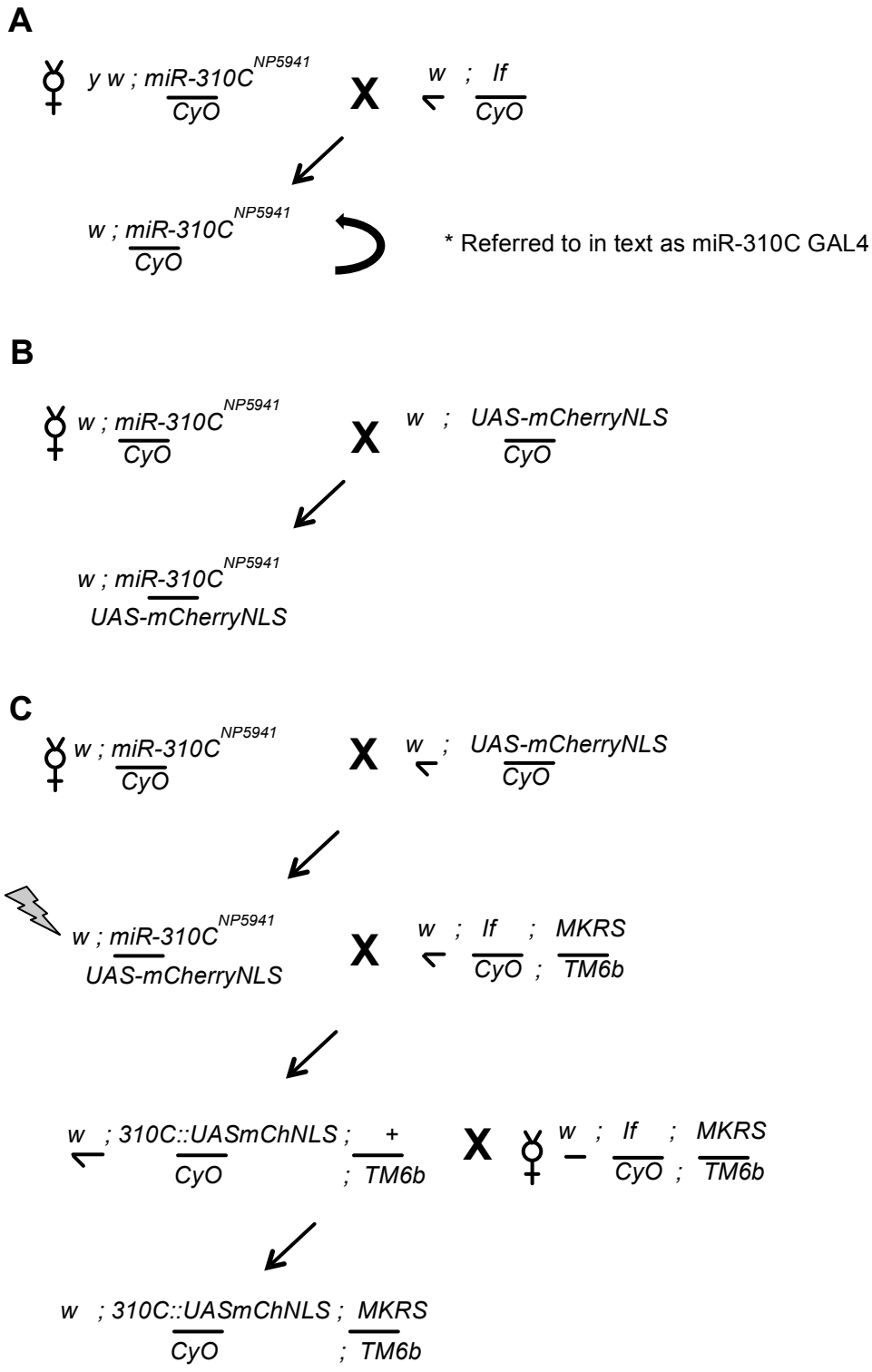

Ectopic expression of *EP2587* in Ubx null background was done by first balancing both *EP2587* and *NubbinGAL4* stocks with *w : If/Cyo ; MKRS/TM6* to create *w ; EP2587/CyO ; MKRS/TM6b* and *w ; NubbinGAL4/CyO ; MKRS/TM6b*. These two lines were then crossed to *Ubx* null chromosome, abx^1 bx^3 pbx^1 that had previously been balanced using the *w ; If/CyO ; MKRS/TM6b stock to produce w ; If/Cyo ;* abx^1 bx^3 pbx^1*/TM6b* This *Ubx* null chromosome is a composite of three separate alleles that each disrupt particular enhancer elements of *Ubx*. Together these three alleles severely limit post embryonic expression of this gene.. The final stocks produced *w ; EP2587/CyO ;* abx^1 bx^3 pbx^1*/TM6b* and *w ; NubbinGAL4/CyO ;* abx^1 bx^3 pbx^1*/TM6b* were crossed together to give *w ; EP2587/NubbinGAL4 ;* abx^1 bx^3 pbx^1*/TM6b* progeny, these were scored and analysed for haltere phenotypes (Fig.2.5).

To ectopically express the miR-310C miRNAs in clonal cells, the *EP2587* line was crossed to a *w hsFLP ; UAS::myrRFP/Cyo ; Act.FRT.STOP.GAL4/TM6b*. Resulting L3 larvae were heat shocked for 60 minutes at 37^{o}C to induce clone formation (Fig.2.6). Heat shock activated Flp recombinase is activated when larvae are exposed to ~37^{o}C. The Flp recombinase mediates the excision of a FRT flanked STOP cassette that separates the *Actin5c* promoter from the GAL4 cds. This excision of the stop cassette leads to clonal populations of cells that express GAL4 and lead to the induced expression of any UAS containing transgenes within the animal e.g. $miR\text{-}310C^{EP2587}$ and *UAS-myrRFP* as a reporter of activity.

The Δ310 deletion was created via P-element excision of the *EP2587* insertion (Tang et al., 2010). This line was put into a *white* background for phenotypic analysis. For genetic interaction analysis, the Δ310 deletion was combined with Ubx abx^1 bx^3 pbx^1 chromosome, used as a Ubx null allele. The Δ310 deletion was first balanced with *w ; If/Cyo ; MKRS/TM6b* creating *w ; Δ310/Δ310 ; MKRS/TM6b,* which was then crossed with *w ; If/Cyo ;* abx^1 bx^3 pbx^1*/TM6b* to produce *w ; Δ310/Δ310 ;* abx^1 bx^3 pbx^1*/TM6b* referred to as Δ310 $Ubx^{-/+}$ (Fig.2.7)

Ubx ectopic expression was achieved with the GAL4 GAL80 targeted mis-expression system by over expressing a $UAS::Ubx1a,\ tub.GAL80^{ts}$ stock (Pavlopoulos and Akam, 2011) (gift from Michael Akam, University of Cambridge) using the *NP5941* insertion (Fig.2.8). The presence of GAL80 prohibits activation of any UAS promoter sites by repressing GAL4 function. At desired developmental stages, this repression can be reversed by placing the animals at 29^{o}C which disrupts GAL80 function.

Fig.2.4 Crossing scheme to express UAS-*miR-310C* within the haltere

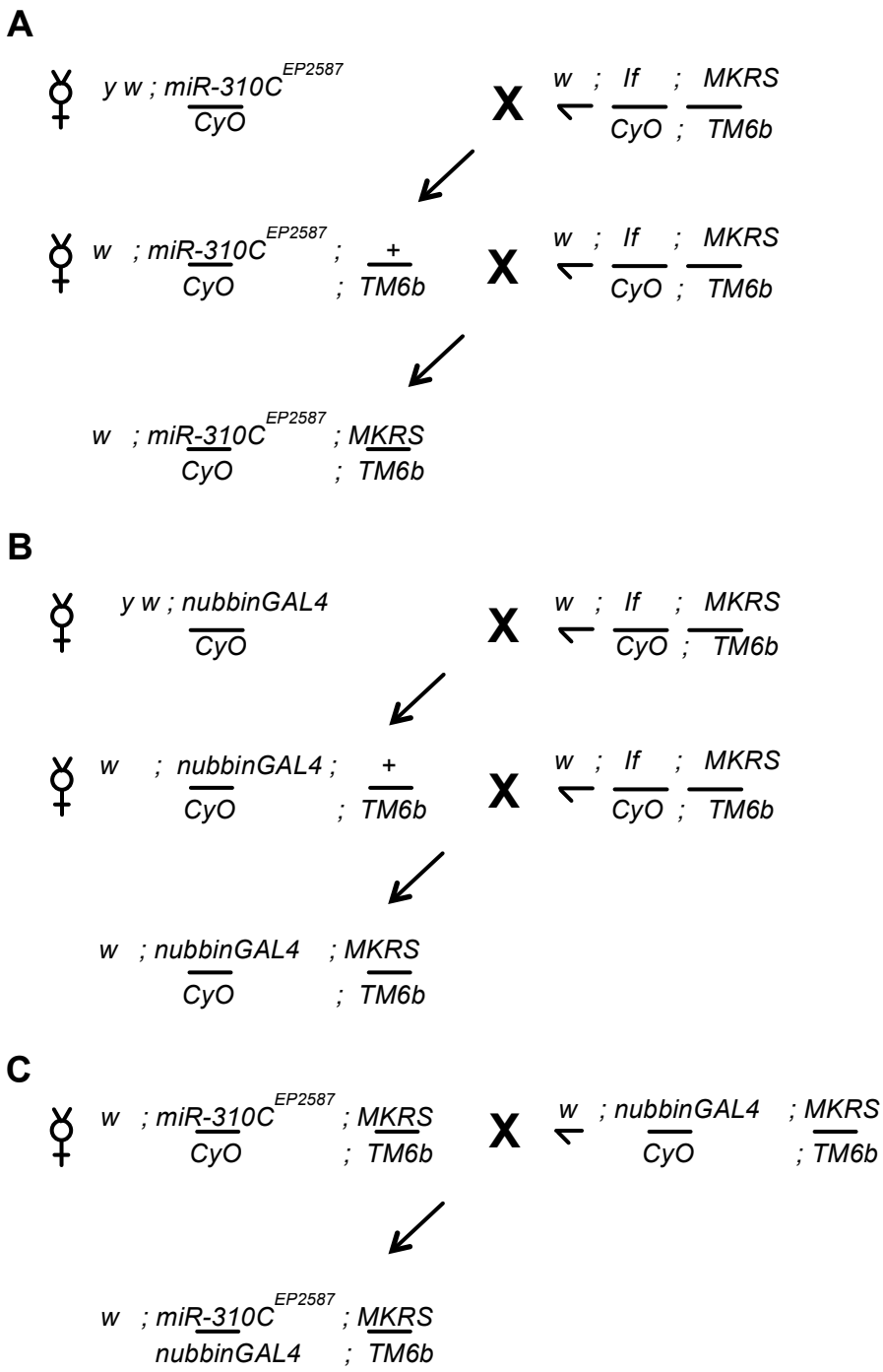

Fig.2.4 Crossing scheme to express UAS-miR-310C within the haltere.

The *miR-310C*^{EP2587} insertion was first placed into a *white* genetic background by crossing to a *w ; If/CyO ; MKRS/TM6b* balancer line (A). Additionally, the nubbinGAL4 driver was crossed into the same genetic background (B). To ectopically express the miR-310C miRNAs within the wing, these two new lines were crossed together (C).

Fig.2.5 Crossing scheme to express UAS-*miR-310C* in a *Ubx* deficient background

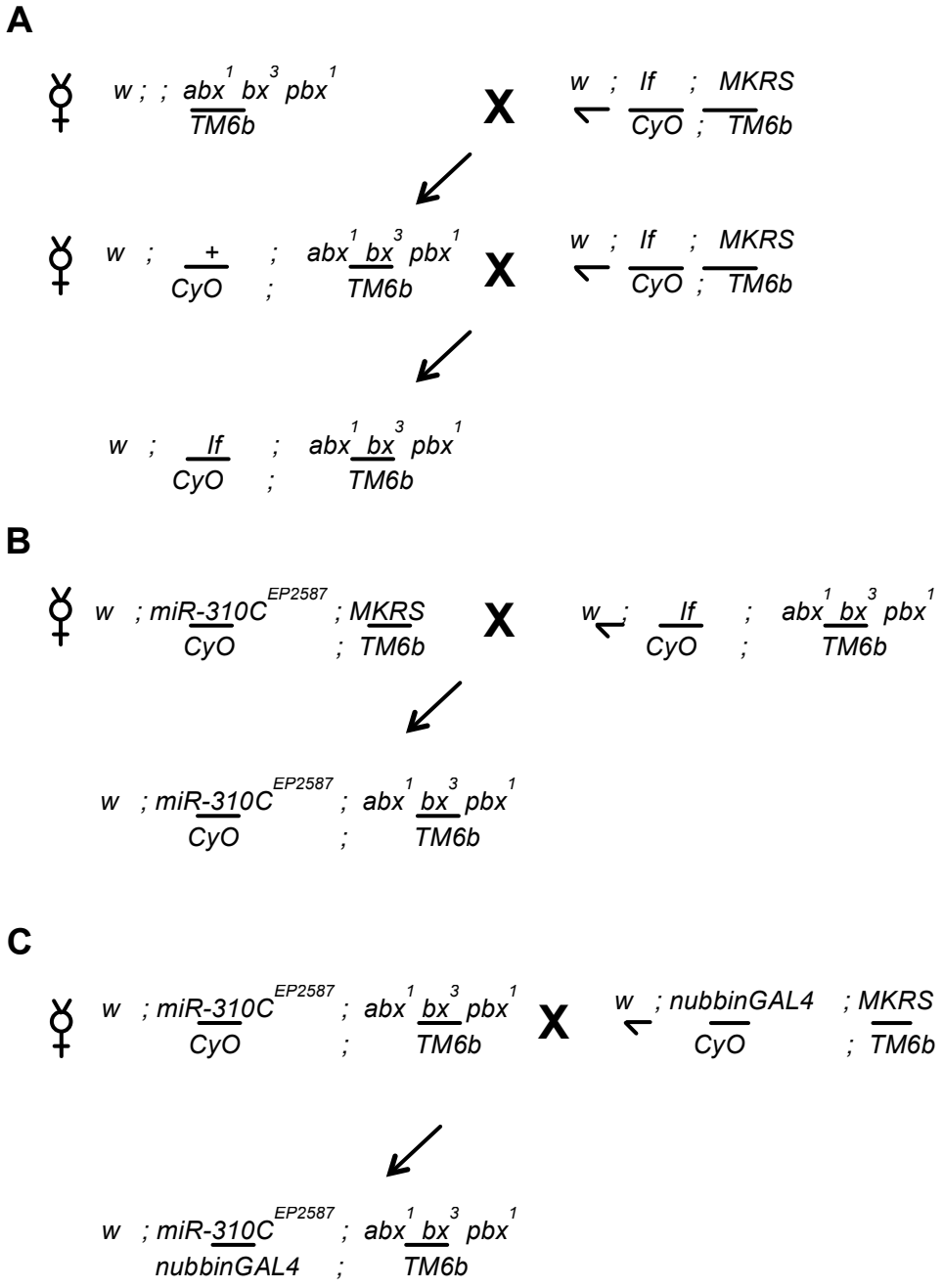

Fig.2.5 Crossing scheme to express UAS-*miR-310C* in a *Ubx* deficient background

First a *Ubx* null recombinant chromosome containing the abx^1 bx^3 pbx^1 mutant alleles was crossed into a *white* genetic background using the *w ; lf/Cyo ; MKRS/TM6b* stock (A). Using this line we crossed this *Ubx* deficient chromosome to line carrying the $miR\text{-}310C^{EP2587}$ insertion (B). This combined stock was then crossed to the balanced *nubbinGAL4* driver line to over-express the *miR-310C* miRNAs in a *Ubx* deficient background (C).

Fig.2.6 Crossing scheme to generate clones over-expressing *miR-310C* miRNAs

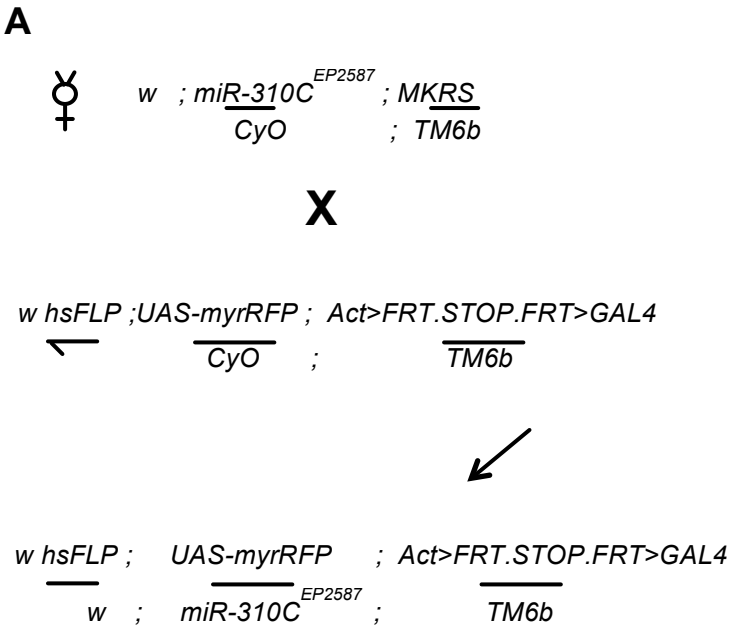

Fig.2.6 Crossing scheme to generate clones over-expressing UAS-*miR-310C*

To generate UAS-miR-310C expressing clones, the *miR-310C*^{EP2587} balanced stock was crossed to heat shock activated Actin-GAL4 FLP-OUT cassette containing stock

The co-expression analysis of *miR-310C* and *Neuralized* was achieved by crossing a *NP5941,UAS::mCherryNLS* recombinant chromosome (Fig.2.3C) balanced with *w ; If/CyO ; MKRS/TM6b* to give *w ; NP5941, UAS::mChNLS/CyO ; MKRS/TM6b* to a *NeuralizedLacZ* transgene (Bloomington Stock Centre 4369) balanced with *w ; If/CyO ; MKRS/TM6b* to give *w ; NP5941, UAS::mChNLS : NeurLacZ/TM6b* (Fig.2.9).

Analysis of the *H99* deletion (Bloomington Stock Centre; no:1576) was performed after first placing this deficiency in comparable genetic background to that found with our Δ310 and *Ubx* null stocks by first crossing to the *w ;; MKRS/TM6b* stock to give *w ; ; H99/TM6b*. This line was then combined with the Δ310 deletion, by first crossing to a *w ; If/CyO ; MKRS/TM6b* line and then crossed to *w ; Δ310/Δ310 ; MKRS/TM6b* to generate *w ; Δ310/ Δ310 ; H99/TM6b* (Fig.2.10).

Fig.2.7 Crossing scheme to place Δ310 mutation in *Ubx* deficient background

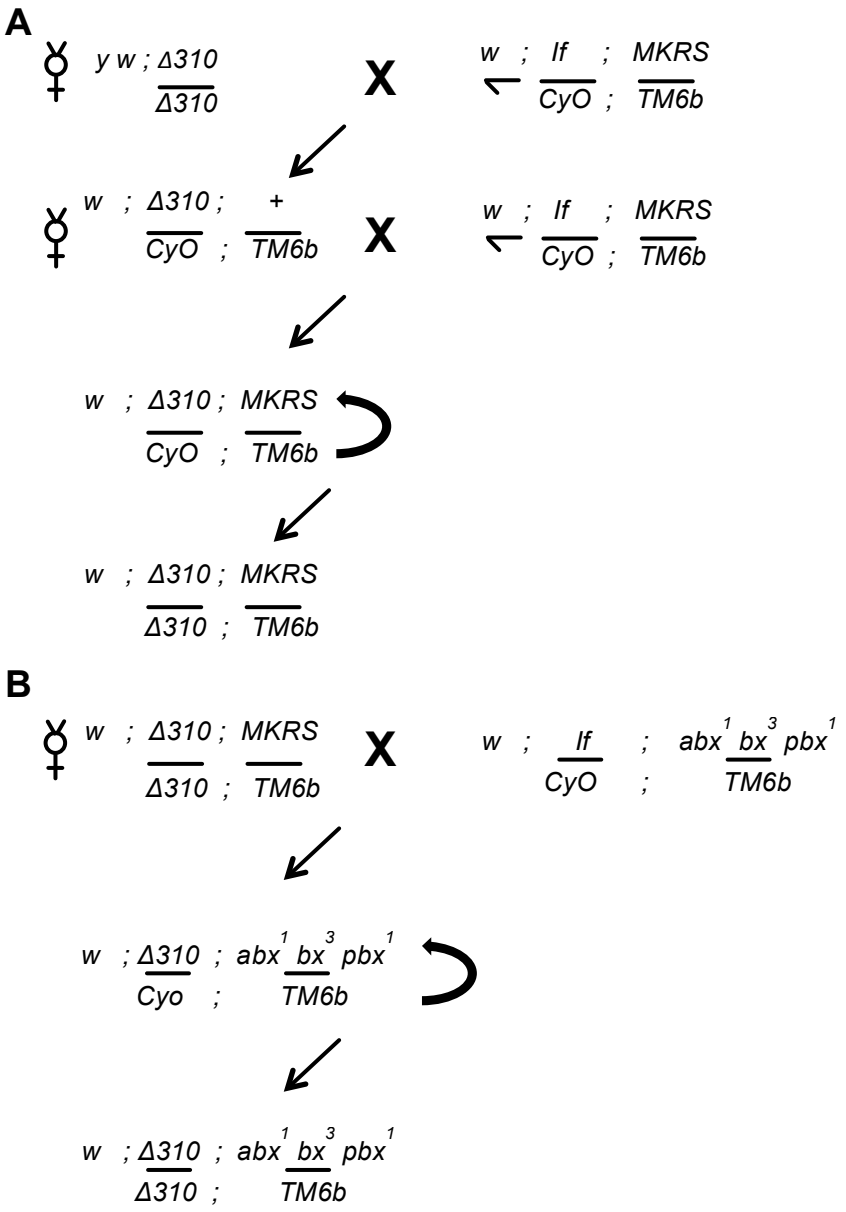

Fig.2.7 Crossing scheme to place Δ310 mutation in *Ubx* deficient background.

The Δ310 mutation was first placed into a *white* genetic background using *w ; If/Cyo ; MKRS/TM6b* line (A). This line was then crossed to the balanced *Ubx* null abx^1 bx^3 pbx^1 chromosome previously balanced (see Fig.2.5A) to place the Δ310 deletion in a *Ubx* deficient background (B).

For *Ubx – Dicer1* genetic interaction analyses, both the Ubx^{1} allele and the $dcr1^{Q1147X}$ (gift from Arno Muller, University of Dundee) were first crossed into a similar genetic background using *w; MKRS/TM6b.* These two alleles were then combined by crossing $w;Ubx^{1}/TM6b$ to $dcr1^{Q1147X}/TM6b$ to give $w;Ubx^{1}/dcr1^{Q1147X}$ (Fig.2.11).

Fig.2.8 Crossing scheme to ectopically express *Ubx* in *miR-310C* expression domains during development.

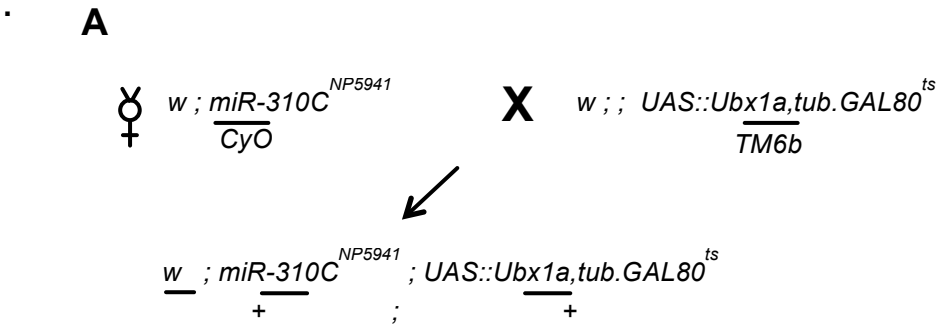

Fig.2.8 Crossing scheme to ectopically express Ubx in miR-310C expression domains during development.

To control the time and spatial domain of ectopic Ubx activity in the miR-310C expression domains, a *UAS-UbxIa* transgene recombined with a $tub\text{-}GAL80^{ts}$ repressor was crossed to the $miR\text{-}310C^{NP5941}$ GAL4 insertion. The resulting progeny could be placed at 29^{o}C during development when desired to inactivate the GAL80 protein and begin ectopic expression of the *UAS-UbxIa* transgene,

Fig.2.9 Crossing scheme to combine a 310C-mCherry reporter with SOP cell marker

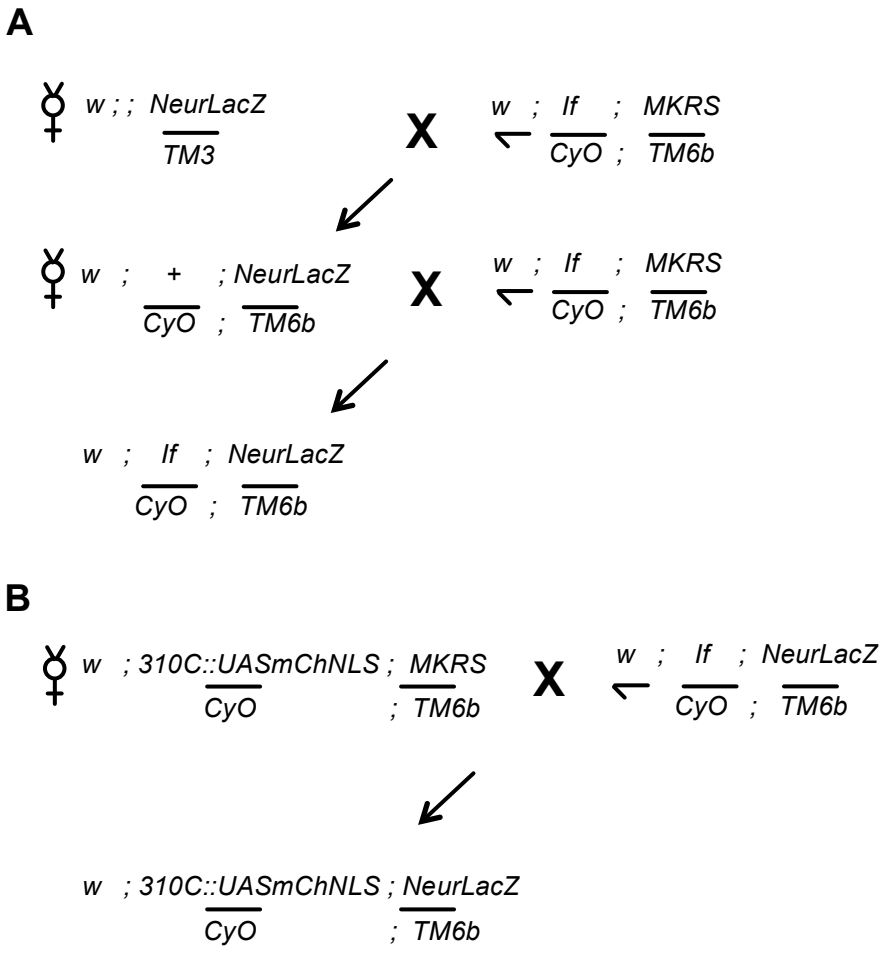

Fig.2.9 Crossing scheme to combine the a 310C-mCherry reporter with SOP cell marker

NeuralizedLacZ is LacZ enhancer trap known to mark sensory organ precursor (SOP) cells during development. This insertion was first crossed into a *white* genetic background using the *w ; If/CyO ; MKRS/TM6b* balancer line. This stock was then crossed to the miR-310C reporter line created earlier (see Fig.2.3C) to create a line that marked both the SOP cells and cells which transcribe the miR-310C miRNAs.

Fig.2.10 Crossing scheme to place H99 deletion into a Δ310 genetic background

The H99 deletion was first crossed into a *white* genetic background comparable to other genotypes (Δ310 and abx^1 *bx3* pbx^1) used in this study (A). This line was then crossed to the *w ; If/CyO ; MKRS/TM6b* stock (B) the generate a line that could easily be crossed the Δ310 genetic background generated earlier (see Fig.2.7A) to place the H99 deletion into Δ310 genetic background (C).

Fig.2.10 Crossing scheme to place H99 deletion in a Δ310 genetic background

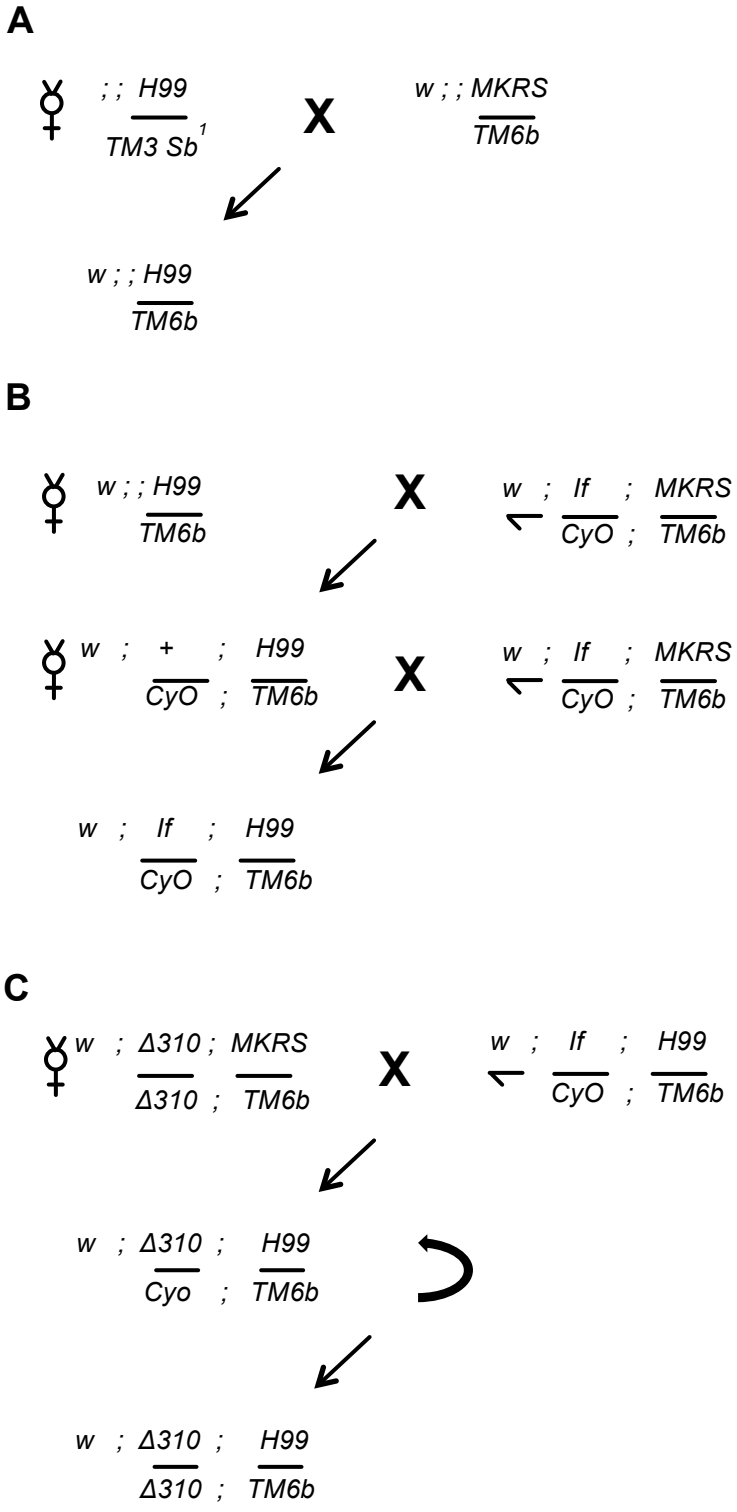

Fig.2.11 Crossing scheme to combine *Ubx*^{1} and *Dcr1*^{Q1147X} alleles

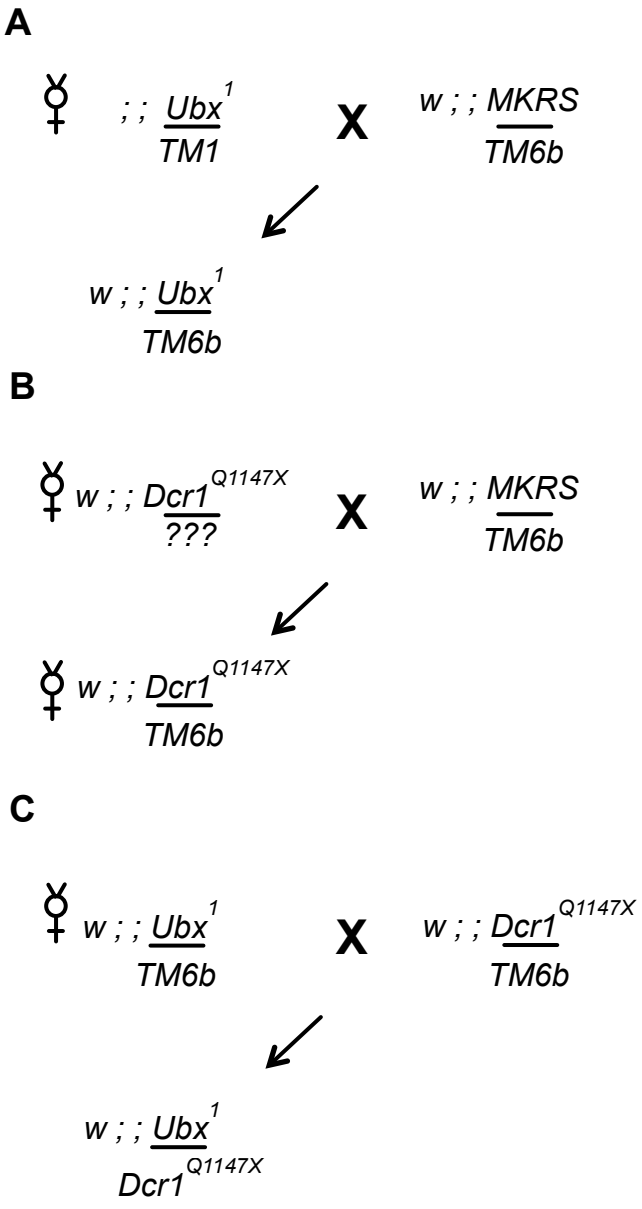

Fig.2.11 Crossing scheme to combine *Ubx*^{1} and *Dcr1*^{Q1147X} alleles

Both the *Ubx*^{1} and *Dcr*^{Q1147X} alleles were first crossed into the same white genetic background using the *w ; MKRS/TM6b* stock(A-B). These two lines were then crossed together combine both alleles in one line (C).

Table 2.2 Fly Stocks used or generated in this thesis

ABBREVIATED NAME	GENOTYPE	ORIGIN
-	*w ; UASmCh-K10/CyO*	Alonso Lab, Uni of Sussex
-	*w ; UASmCh-UbxUTR/CyO*	Alonso Lab, Uni of Sussex
-	*w ; UbxGAL4^{M1}/TM6b*	Gift from Sanchez- Herrero
-	*w ; UASmCh-K10/CyO ; UbxGAL4^{M1}/TM6b*	This study
-	*w ; UASmCh-UbxUTR/CyO ; UbxGAL4^{M1}/TM6b.*	This study
miR-310C Gal4	*w ; NP5491/Cyo*	Bloomington # 113798
UAS-miR-310C	*w ; EP2587/Cyo*	Szeged Stock Centre
Nubbin Gal4	*w ; Nub::GAL4/CyO*	Bloomington # 38418
-	*w ; EP2587/CyO ; MKRS/TM6b and*	This study
-	*w ; NubbinGAL4/CyO ; MKRS/TM6b*	This study
-	*w ; ; abx^{1} bx^{3} pbx^{1}/TM6b*	Alonso Lab, Uni. of Sussex
-	*w ; UAS::mCherryNLS/CyO*	Gift from Markus Affolter, Uni. Of Basel
-	*w ; lf/Cyo ; abx^{1} bx^{3} pbx^{1}/TM6b*	This study
-	*w ; EP2587/CyO ; abx^{1} bx^{3} pbx^{1}/TM6b*	This study
-	*w ; NubbinGAL4/CyO ; abx^{1} bx^{3} pbx^{1}/TM6b*	This study
-	*w ; EP2587/NubbinGAL4 ; abx^{1} bx^{3} pbx^{1}/TM6b*	This study
-	*w hsFLP ; UAS::myrRFP/Cyo ; Act.FRT.STOP.GAL4/TM6b*	Gift from Rob Ray
-	*yw ; 2b/2b*	Gift from Chung-I Wu, Uni. Of Chicago
Δ310	*w ; Δ310/Δ310*	This study
-	*w ; Δ310/Δ310 ; MKRS/TM6b*	This study
Δ310 Ubx$^{-/+}$	*w ; Δ310/Δ310 ; abx^{1} bx^{3} pbx^{1}/TM6b*	This study
-	*; ; UAS::Ubx1a, tub.GAL80^{ts}*	Gift from Michael Akam, Uni. Of Cambridge
-	*w ; NP5941.UAS::mChNLS/CyO ; MKRS/TM6b*	This study
-	*w ; ; NeurLacZ/TM6b.*	Bloomington #4369
-	*w ; NP5941, UAS::mChNLS : NeurLacZ/TM6b.*	This study
-	*; Df(3L)H99, kni^{ri-1} p^{p}/TM3, Sb^{1}*	Bloomington # 1576
H99	*w ; ; H99/TM6b*	This study
-	*w ; lf/CyO ; H99/TM6b*	This study
Δ310 H99	*w ; Δ310/ Δ310 ; H99/TM6b.*	This study
-	*; ; Ubx^{1} / TM1*	Bloomington #529
-	*; ; dcr1^{Q1147X} / TM3*	Gift from Arno Muller, Uni. Of Dundee
Ubx^{1}	*w ; Ubx^{1}/TM6b*	This study
-	*; ; dcr1^{Q1147X}/TM6b*	This study
-	*w ; ; Ubx^{1}/dcr1^{Q1147X}*	This study
bx^{34e}	*; ; bx^{34e}/TM1*	Bloomington #3437
Ubx^{61d} pbx^{1}	*; ; Ubx^{61d} pbx^{1}/TM3*	Bloomington #3435
-	*w ; ; MKRS/TM6b*	Gift from Rob Ray
-	*w ; lf/CyO ; MKRS/TM6b*	Gift from Rob Ray

Immunohistochemistry

Imaginal discs were fixed following dissection in 4% para-formaldehyde and stored at -20°C in 100% Methanol. Immuno-staining followed standard protocols based on (Nagaso et al., 2001). Briefly, samples were rehydrated from 100% Methanol to 1xPBS solution. Samples were pre-treated with 80% Acetone at -20°C for 20minutes, washed, then re-fixed with 4% para-formaldehyde and finally washed in 1xPBTwx (1xPBS, 0.1%Tween20, 0.1%TritonX). Samples were then blocked with 1% Milk Solution (Milkpowder, PBT) for 30 minutes. Primary antibodies were incubated overnight at 4°C. Primary antibodies then washed out in PBTwx and secondary antibodies incubated for 2 hours at room temperature. Samples were then washed in PBTwx and stored in 70% Glycerol/PBTwx at 4°C to await analysis. For microscopy, samples were mounted in Vectashield (Vector Laboratories) and imaged using a Leica DFC6000 with DFC340X digital camera. Antibodies used were α-*Ubx* FP3.38 (Mouse) 1:20 (Gift from Rob White, University of Cambridge) α-*RFP* (Rabbit) 1:1000 (Invitrogen) α-*Bgal* (Rabbit) 1:300 (Promega) α-Mouse Alexa A488 1:300 (Invitrogen) α -Rabbit Rhodamine 1:300 (Sigma-Aldrich).

Expression Analysis

Analysis of mCherry construct and Ubx expression patterns within the haltere pouch following immuno-staining was accomplished using the Plot Profile tool of ImageJ (http://rsbweb.nih.gov/ij/). Results were extracted to Microsoft Excel for further analysis.

Scanning Electron Microscopy

Adult flies were dehydrated in 25%, 50%, 100% EtOH solution. Instead of critical point drying, samples were washed three times with Hexamethyldisilazane (Sigma Aldrich). The solvent was left to evaporate by air drying samples for 24 hours. The adult thorax with the haltere appendages attached was isolated from the rest of the animal to allow for better manipulation when mounting samples.

Cuticle Preparation

Haltere appendages were analysed in detail following cuticle dissection and preparation as described by De Navas et al., 2006b. Flies were stored in Ethanol/Glycerol (3:1) Mixture. Flies were macerated in 10% KOH at 60oC for 60 minutes. Samples were washed and stored in Ethanol/Glycerol (3:1). Haltere appendages were dissected and mounted in 70% Glycerol/PBT solution.

Standard & UV Microscopy

For detailed analysis of morphological changes, appendages were imaged in both Brightfield and under UV light using a Leica DFC6000 with DFC340X digital camera. We found that the sensory structures of the pedicel and scabellum had a significant degree of auto-fluorescence when exposed to UV allowing for detailed analysis of morphological structure.

Wing and haltere RNA isolation and next-generation sequencing

To procure enough starting material for RNA sequencing, large numbers of wing and haltere imaginal discs were extracted over a period of three weeks. To ensure that the tissue populations were as homogenous as possible, only white-pre-pupae were chosen for dissection. This short life stage lasts approximately 60 minutes and has a number of easily distinguishable features – larvae cease moving and evert their anterior spiracles in anticipation of pupae formation. In total approximately 600 wing discs and 800 haltere discs were collected from *Oregon R* strain wild-type stocks. Dissections were carried out in collaboration with Ana Bomtorin (Visiting Student, Universidade de São Paulo, Ribeirão Preto, Brazil).

Wing and haltere tissues were pooled into two respective master collections. These total samples were then used to extract total RNA. Total RNA was extracted using Tri-Reagent (Ambion) following the manufacturer's protocol plus the following additional steps. For the precipitation of the final RNA pellet, 2µl of Glycogen (Ambion) was added to each extraction to aid in the precipitation of RNA. For the final precipitation step both samples were kept in a -80^{o}C freezer overnight before being spun down to generate the total RNA pellet.

For small RNA sequencing to be effective, the small RNA content of each total RNA sample had to be extracted. This is achieved usually by running all RNA content though a polyacrylamide gel which fractionates RNA content by size. The small RNA content can then be cut out from the gel and extracted. The following small RNA extractions can then be used to build a RNA-Seq cDNA library using Illlumina TruSeq Small RNA sample preparation kits (Illumina) before being run sequenced on an Illumina Genome Analyzer II platform (Illumina). The extraction of small RNA content, library preparation and sequencing was performed in-house by the High-Throughput Sequencing Facility at the University of North Carolina – Chapel Hill North Carolina.

Quality control of sequenced RNA libraries

Following sequencing of the wing and haltere samples, we performed two quality control steps on sequenced data. Using the Filter function of the *FASTX-Toolkit* (http://hannonlab.cshl.edu/fastx_toolkit/) from the public access *GALAXY* platform (https://main.g2.bx.psu.edu/) we filtered all reads from both samples for sequencing quality. We used a minimum quality score of 20 and a percentage level of 90. Therefore for a read to pass these parameters, 90% of its sequence must have a quality score greater than 20 (quality scale is 40 to -15). The next quality control measure was to trim reads that contain adapter sequences used during the Illumina sequencing process. Using the *Clip* function of the *FASTX-Toolkit* all reads were processed and adapter nucleotides were removed.

Alignment and quantification of small RNA libraries

Alignment of sequenced library was performed using the *BOWTIE* tool (Langmead et al., 2009) accessed from the *GALAXY* platform. Alignment was performed against the UCSC dm3 (BDGP5.6) *D.melanogaster* genome release. Alignments were made with one mismatch sequence allowed. Quantification of following alignments were performed using *CUFFLINKS* (Trapnell et al., 2010) accessed from the *GALAXY* platform. When running the small RNA libraries through *Cufflinks*, we used the Quartile Normalization function which improves the accuracy of low abundance estimations and the Bias Correction function which improves accuracy of transcript abundance estimates.

Analysis of mapped and quantified small RNA libraries

Analysis and manual annotation of the mapped sequenced libraries was performed using *Microsoft EXCEL*

Visualisation and Analysis

Visualisation and analysis of data was performed using *R Statistical Computing* (http://www.r-project.org/) using the following packages *Gplots*, *ggplot2* (http://ggplot2.org/) and *VennDiagram.*

Expression analysis of pri-miRNA transcription

For the analysis of primary-miRNA expression we extracted wing and haltere discs from white-pre-pupae stages larvae. Total RNA was extracted from disc samples using *Tri-Reagent* (Ambion) following standard manufacturers protocol. cDNA synthesis was performed using *RETROscript* (Ambion) following standard manufacturers protocol. PCR was performed using standard protocols. The following primers were used:- *pri-miR-9b* Forward 5'-CTGCAGGTCAATCGTCAGAA-3' Reverse 5'-CGCGAGAAAAGTAAAGAATACCA-3', *pri-miR-986* Forward 5'-ATAGGAGCCGGAAAAGTCGT-3' Reverse 5'-AAGTGCCAGTAGCCCCATTA-3', *pri-miR-996* Forward 5'-GTGCAGGGGCAATAATCATC-3' Reverse 5'-CGTTGTGCTGACCCAACTTA-3', *pri-miR-999* Forward 5'-ACCCCGACATAGTCATACGG-3' Reverse 5'-CACCTGGCCGAACTTATTGT-3', *pri-miR-13a* Forward 5'-AATTGGGCATAACGATTGGA-3' Reverse 5'-AAGACGTGGTTCAGTCAGTCG-3', *pri-miR-137* Forward 5'-ATTACGGCCAGTGAAAGTGG-3' Reverse 5'-GCTCATTTAAACGGGTTTCG-3', *pri-miR-281-1* Forward 5'-GTCCTGTCCGTTGAGGTGTT-3' Reverse 5'-CTGAAAGGTGGGAAGGGATT-3', *pri-miR-283* Forward 5'-TGGGAGCGAGAGAGAGAGAG-3' Reverse 5'-TTCGTTTTGTTGCGCTTATG-3', *pri-miR-1013* Forward 5'-CGTGCTGGAGAGGTGAGTTT-3' Reverse 5'-TGACCCACCAGCATCTCATA-3'

miRNA gene target predictions

Target gene predictions of selected microRNAs were downloaded from *TargetScanFly* (http://www.targetscan.org/fly_12/) and were curated manually using *Microsoft EXCEL*

Gene Ontology profiling analysis

Gene ontology profiling analysis was performed in *R* using the *GOprofiles* package (url http://estbioinfo.stat.ub.es/pubs). Results were visualised using the *ggplot2* package

Analysis of published microarray data and miRNA target predictions

The top 10% Ubx down-regulated and up-regulated transcripts were obtained from analysing available transcriptomic data from (Pavlopoulos and Akam, 2011). Data was analysed using the *GEO2R* tool available at the NCBI (http://www.ncbi.nlm.nih.gov/geo/geo2r/). Once the regulated transcripts were identified, their corresponding 3'UTR sequences were obtained using the *GenomicFeatures* package in *R*. Each 3'UTR sequence was run through the *PITA*

target prediction software (Kertesz et al., 2007) against the haltere miRNA profile defined in our study. All *PITA* results were manually grouped into the three experimental cohorts - Down-regulated and Up-regulated and Neutral *Ubx* targets for further analysis.

Analysis of RBPs expression patterns was achieved using the data output of the *GEO2R* tool, manual annotation of RBPs was done through *Microsoft EXCEL* and all data was visualised using the *ggplots2* package in *R*.

CHAPTER 3

3. Post-transcriptional regulation of the *Drosophila* hox gene *Ultrabithorax* by miRNAs during appendage formation

3.1 Chapter Overview

Hox genes are evolutionarily conserved transcription factors and fundamental regulators of cellular and developmental biology. They function to initiate distinct genetic programmes within cells along the head-to-tail axis of animals. Additionally, they are required for the correct growth and differentiation of animal appendages in both vertebrates and invertebrates.

Cells and tissues are very sensitive to different levels of Hox gene expression and can alter their developmental fates accordingly. For this reason, Hox gene expression is precisely controlled throughout development, both spatially and temporally. Disruption to this regulation can lead to dramatic changes in body morphology.

miRNAs are small non-coding RNAs that have emerged as potent regulators of gene expression in cell and developmental biology and have been shown to regulate Hox gene expression in both vertebrates and invertebrates. However up to now, the biological consequences and importance of this regulation is not fully understood.

In Drosophila, the haltere flight appendage is under strict developmental regulation by the Hox gene *Ultrabithorax (Ubx)*. The cells that build the haltere are known to be sensitive to varying levels of *Ubx* expression. Thus, this tissue provides a suitable developmental context in which to study to what extent miRNA regulation is required to accurately define *Ubx* expression and function within the developing haltere.

In this chapter we identify a family of miRNAs - the *miR-310C*, that regulate *Ubx* expression during the post-embryonic development of the haltere. Detailed analysis of animals lacking these miRNAs reveals subtle altered morphologies within the haltere appendage, specifically in the correct formation of the haltere sensory cells. Through genetic interaction experiments, we show that this phenotype is due to altered *Ubx* expression which affects the sensory tissue architecture of the haltere. This study reveals a novel miRNA-Hox interaction during appendage development and offers insight into how *Ubx* directs the correct development of haltere morphology.

3.2 *Ubx* isoform distribution during post-embryonic development

To be able to understand the regulation of *Ubx* by miRNAs through targeting of the 3'UTR during haltere development, we first needed to determine which *Ubx* 3'UTR isoforms were present during the post-embryonic development of *Drosophila* and specifically, the haltere imaginal discs.

After embryogenesis, *Drosophila* development continues through three larval developmental stages (L1-L3), a short pre-pupal stage (WPP) and pupal development (P) in which the metamorphosis of the adult occurs (A). Early studies in *Ubx* transcript processing and expression suggested that APA of the *Ubx* 3'UTR is actively regulated during embryonic development (Kornfeld et al., 1989; O'Connor et al., 1988). These studies suggested that through the use of a proximal (PAS1) and distal (PAS2) poly-adenylation site, both a short and long 3'UTR isoform was present during larval and pupal development (Fig.3.1A).

We first confirmed these results by determining the relative transcript levels of *Ubx*-short and *Ubx*-long 3'UTR isoforms during post-embryonic development.

Fig.3.1 *Ubx* 3'UTR isoform distribution and functionality during post-embryonic development

(A) Genomic map of *Ultrabithorax*, the gene spans approximately 75kbs. Exon sequences are identified in grey boxes. The 3' exon and UTR are shown in expanded sequence. The two active poly-adenylation sites are shown. The extended 3'UTR sequence is approximately 2kb in length. (B) Analysis of *Ubx* 3'UTR isoforms during post-embryonic development. Amplicons representing all *Ubx* transcripts are shown in blue, amplicons representing *Ubx* transcripts containing extended 3'UTR are shown in red. Respective relative expression levels are plotted in blue and red. Error bars represent standard deviation (variation) between biological replicates. Values are calculate by averaging three technical replicates for each biological sample (C) mCherry constructs used in 3'UTR expression analysis, the control mCh-K10 construct carries a viral *K10* 3'UTR sequence, the experimental mCh-Ubx construct carries an extended *Ubx* 3'UTR lacking PAS1.(D - E) Sample images of mCh-K10 and mCh-Ubx expression in haltere imaginal disc. Yellow boxes highlight regions measured for expression analysis. (F) Plot profile showing expression analysis of mCh-K10 and mCh-Ubx constructs. (G) Magnification of areas measured for expression intensity of mCh-K10 and mCh-Ubx constructs. Scale bar represents 25μm.

Fig.3.1 *Ubx* 3' UTR isoform distribution and functionality during post-embryonic development

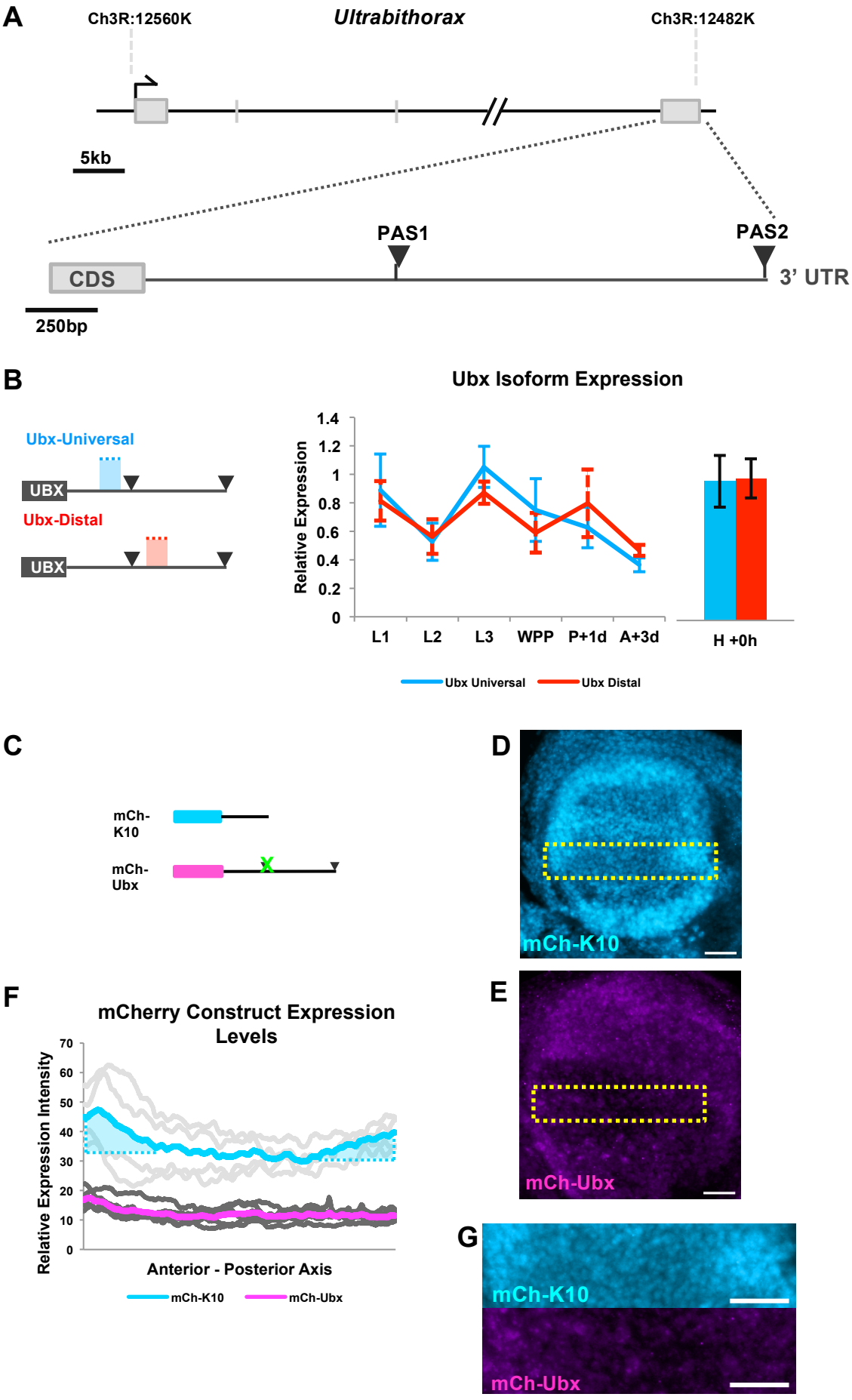

Using a semi-quantitative RT-PCR approach (SQ-RTPCR), we determined the total *Ubx* mRNA levels using oligonucleotides that amplify a ~200bp amplicon of the 3'UTR proximal to the first poly-adenylation site. This was termed the *Ubx*-universal amplicon. The relative expression levels of *Ubx*-long isoforms were detected by oligonucleotides that amplified a ~200bp region distal to the first poly-adenylation site and termed the *Ubx*-distal amplicon (Fig.3.1B). As a control reaction across all samples and technical replicates, we designed oligonucleotides to detect the ribosomal protein *rp49*. Using this experimental strategy we could determine the total levels of *Ubx* transcript expression and the abundance of *Ubx*-long isoform specific transcripts across multiple post-embryonic stages and within the haltere imaginal discs.

Our results show that total levels of *Ubx* vary greatly during post-embryonic development (Fig.3.1B). *Ubx* expression initially decreases from L1 to L2 stages; a point in which the larvae are growing rapidly, expression of *Ubx* then increases to its highest level at L3 stage, a time when the imaginal discs are undergoing extensive pre-patterning. From this developmental time point, expression gradually decreases through the WPP stage (where the larvae begins to form the pupae) and pupal stage (where the larvae begins its transformation into the adult form). When the adult emerges, levels of *Ubx* expression reach their lowest point, likely reflecting the diminished number of cells and tissues still expressing *Ubx*. Over these developmental stages, the expression levels of *Ubx*-long isoforms matched total *Ubx* transcript expression. From this data we can infer that during post-embryonic development the majority of *Ubx* transcripts carry the *Ubx*-long 3'UTR. To determine if this distribution is seen in the haltere imaginal discs specifically, we assayed expression of *Ubx* in haltere discs dissected from WPP stages larvae. Our data indicates that the dominant isoform among all *Ubx* transcripts during post-embryonic development carry the extended long 3'UTR.

Having determined the dominant *Ubx* 3'UTR isoforms present within the developing haltere imaginal disc, we next looked for evidence that this 3'UTR was regulated in a manner that could affect expression patterns in the haltere. To achieve this we monitored the expression of a transgenic *UAS::mCherry* fluorescent reporter protein coupled to either a control viral *K10* 3'UTR or *Ubx*-long 3'UTR (Thomsen et al., 2010) (Fig.3.1C). Expression of these transgenic insertions was driven by the *UbxGAL4*^{M1} (De Navas et al., 2006a) which expresses throughout the haltere imaginal disc.

We determined the relative signal intensity of *mCherry* expression across the dorsal pouch region of the haltere in both control and experimental UTRs (Fig.3.1D-E). The

average signal intensities of each construct from left to right of the anterior-posterior axis in the disc were plotted (Fig.3.1F). It is clear that overall *mCherry* expression is greatly reduced by the presence of the *Ubx* 3'UTR. The relative intensity of mCherry-K10 expression is on average between 35 and 45 units whereas mCherry-Ubx expression is between 10 and 20 units. There are also distinct peaks of intensity at the far left and far right of the mCherry-K10 plot (see blue shaded areas), these are noticeably absent in the mCherry-Ubx plots. This may indicate the corresponding regions within the imaginal disc are under a high degree of negative regulation. Interestingly, we note that individual measurements of the mCh-K10 expression patterns (light grey lines) are far more varied than the individual measurements seen with the mCh-Ubx samples. This suggests that there is a great deal of transcriptional variation at the *Ubx* locus, picked up by the *UbxGAL4*^{M1} insertion, but perhaps masked by the presence of regulatory elements present within the *Ubx* 3'UTR.

Through semi-quantitative RT-PCR analysis, we have seen that *Ubx* mRNA levels vary during the post-embryonic life cycle of *Drosophila*, peaking at late larval and pre-pupae stages. This peak of expression correlates with the latter stages of a prolonged phase of growth and differentiation. We show that the dominant 3'UTR isoform among the total *Ubx* mRNAs is that of the extended long 3'UTR. Specific analysis of the haltere imaginal disc also shows this isoform distribution. The complex transition of different 3'UTR isoforms caused by APA during embryogenesis is not seen post-embryonically.

3.3 Identification of miRNA target sites within the *Ultrabithorax* 3'UTR.

Having determined the *Ubx* 3'UTR isoform distribution during post-embryonic development and specifically within haltere imaginal disc, we next looked to identify the possible miRNA regulators of *Ubx*. To begin, we used bio-informatic analysis to predict possible miRNA "seed" sites within the *Ubx* 3' UTR.

Fig.3.2 *Ubx* 3'UTR miRNA target predictions

(A) Venn diagram illustrating proportion of all *Drosophila* miRNAs that are predicted to have 'seed' sites within the Ubx 3'UTR. (B) Proportion of miRNAs that potentially target *Ubx* that have experimentally validated expression profiles in imaginal discs. (C) Top 20 candidate miRNAs that potentially target *Ubx* and are present in imaginal discs. (D) Diagram showing possible seed sites of *miR-313*, a top candidate to target the *Ubx* 3'UTR.

Fig. 3.2 The *Ubx* 3'UTR miRNA target predictions

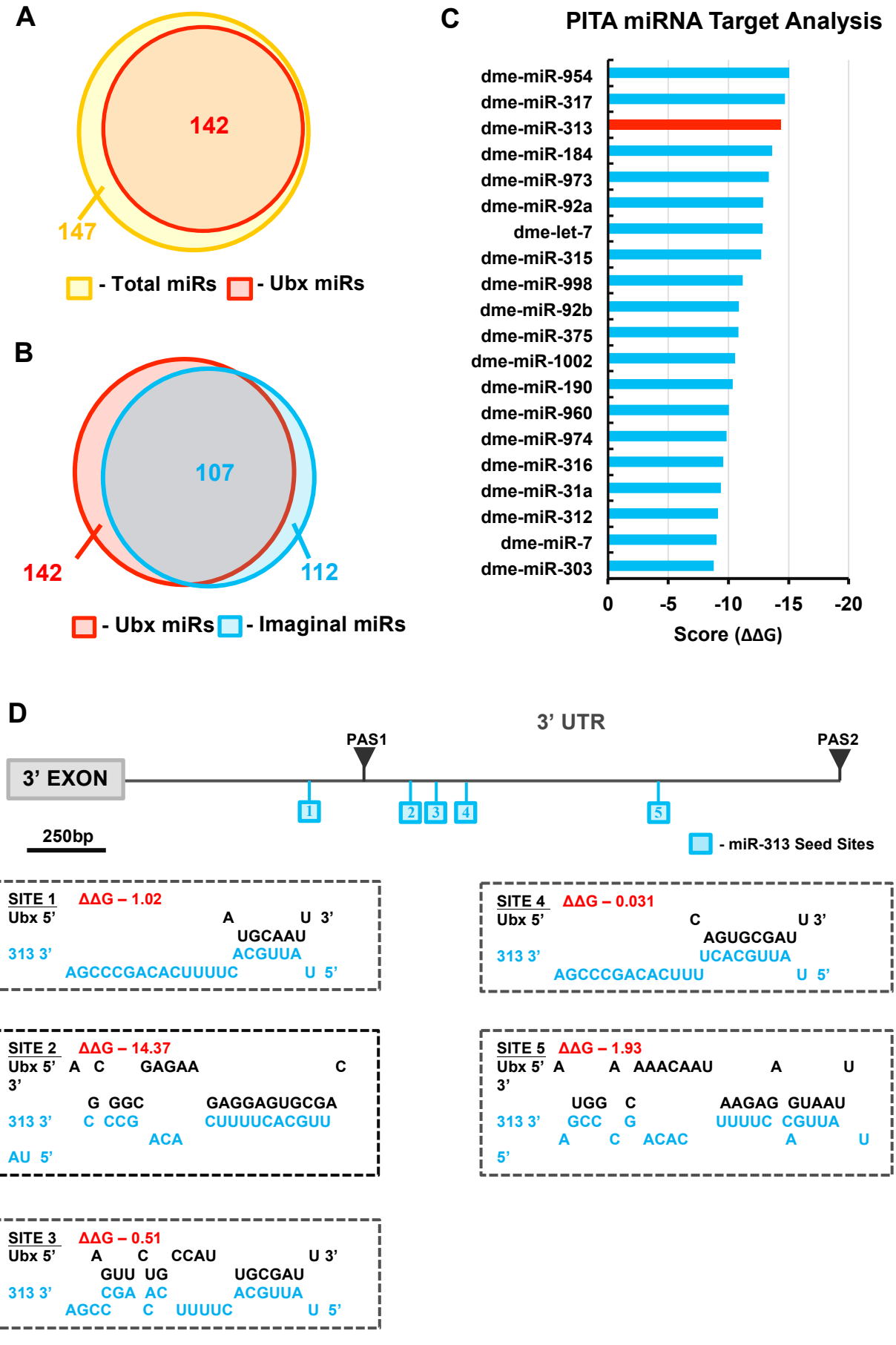

Target site prediction was performed by applying the PITA target site prediction algorithm to the extended 3'UTR isoform (Kertesz et al., 2007). This prediction tool differs from other commonly used methods in that its prediction scores are based on changes in RNA structure and stability that will occur if a given miRNA binds to the 3'UTR of a target gene. It does not take in to account the evolutionary conservation of the miRNA or the potential miRNA seed sites in related species.

The results of this prediction tool revealed potential seed sites for 142 out of the 147 miRNAs (Fig.3.2A) that had been identified within the *Drosophila* genome at the time of analysis. To further reduce the number of potential miRNA regulators of *Ubx*, we screened out all potential miRNAs that did not have experimentally determined expression in imaginal discs, using miRNA profiling data generated through small RNA

next-generation-sequencing (Ruby et al., 2007b). Out of the 112 mature miRNAs detected in imaginal disc tissue samples, 107 have predicted seed sites within the 3' UTR (Fig.3.2B). Unfortunately, at the time of this analysis, there was no haltere specific miRNA profile data to utilise.

Overall this analysis allowed us to produce a candidate list of miRNAs that have high value target prediction scores and are also potentially expressed in the haltere imaginal disc (Fig.3.2C), therefore being in the correct cellular environment for possible *Ubx*-miRNA interactions to occur. The next step was to experimentally validate these miRNA predictions. A top candidate to start this analysis was *miR-313*. This miRNA has 5 potential seed sites situated within the *Ubx* 3'UTR, one site in particular (SITE 2) showed a very high sequence match and potential binding score (Fig.3.2D).

3.4 The *miR-310C* - sequence and expression analysis

The *miR-313* miRNA is positioned within an intergenic region of the *Drosophila* genome flanked by 7 other miRNAs all within 100-200 nucleotides distance of each other (Fig.3.3A). These miRNAs are likely transcribed together as a single poly-cistronic transcript that subsequently undergoes further processing via the miRNA biogenesis pathway. Sequence conservation analysis comparing *miR-310*, *miR-311, miR-312* and *miR-313* pre-microRNA sequences show that they share high sequence identity with each other (Fig.3.3B). Specifically, the seed sequence (labelled red Fig.3.3B) is identical in all four miRNAs. These miRNAs are likely genomic duplications that consequently diverged in overall sequence structure, whilst maintaining the seed sequence. Since all four miRNAs share the same seed sequence, they are all

predicted to target the *Ubx* 3'UTR. However their individual targeting strengths, as predicted by the PITA algorithm, vary due to differences in the remaining mature miRNA sequence (labelled pink Fig.3.3B).

To be viable regulators of *Ubx*, we verified that these miRNAs were transcribed and expressed in the haltere imaginal discs. We tested for expression of the primary *miR-310-313 (miR-310C)* transcript using RT-PCR with oligonucleotides flanking the *miR-313* gene. We detected expression of this transcript in both the wing and haltere imaginal disc tissue (Fig.3.3C). Having shown that the *miR-313* miRNA was expressed at the transcript level, we determined any specificity in the spatial expression patterns within the developing haltere tissue.

To examine the spatial pattern of miR-310C expression within the developing haltere disc, we made use of a *miR-310C*^{NP5941} P-element insertion upstream of the miR-310C miRNAs (see blue triangle, Fig.3A). This P-element contains the GAL4 transcriptional activator CDS and was designed to function as an enhancer trap. These insertions can be used to drive the expression of a suitable UAS-reporter constructs revealing the spatial and temporal transcriptional activity at the site of insertion. Using this *miR-310C*^{NP5941} insertion crossed to lines containing a *UAS-mCherryNLS* fluorescent reporter transgene (Fig.2.3), we documented the spatial patterns of miR-310C expression within the haltere.

Fig.3.3 The *miR-310C* sequence conservation and expression analysis

(A) Genomic map of miR-310-313 cluster. Two P-element insertions are shown – *miR-310C*^{EP2587} carrying multiple UAS sequences and *miR-310C*^{NP5941} containing a GAL4 coding sequence (B). Alignment of the *miR-310C* pre-microRNA sequences showing evolutionary conservation. Mature miRNA sequences are shaded blue, seed sequences are shaded light blue (C). RT-PCR expression analysis of the *pri-miR-310C* transcripts in wing and haltere imaginal discs, third lane shows a No RT control reaction (D) *miR-310C*^{NP5941} (*miR310C::GAL4*) was used to drive mCherry (*UAS-mCherryNLS*) expression in the haltere imaginal disc. (D') Enhanced view of haltere pouch region, areas of high *miR-310C* expression are denoted by *. (E) Schematic of haltere imaginal disc showing regions of high and intermediate levels of *miR-310C* expression. (F) Expression of *miR-310C* co-stained for *Ubx* expression. (F') Enhanced view of haltere pouch showing variable *Ubx* expression and *miR-310C* expression. (F'') An enhanced view of the haltere pouch showing only Ubx expression. Areas showing high *miR-310C* expression and low *Ubx* expression are denoted by *. Scale bar for panels D-F & D'-F'' is 30μm.

Fig.3.3 The *miR-310C* sequence conservation and expression analysis

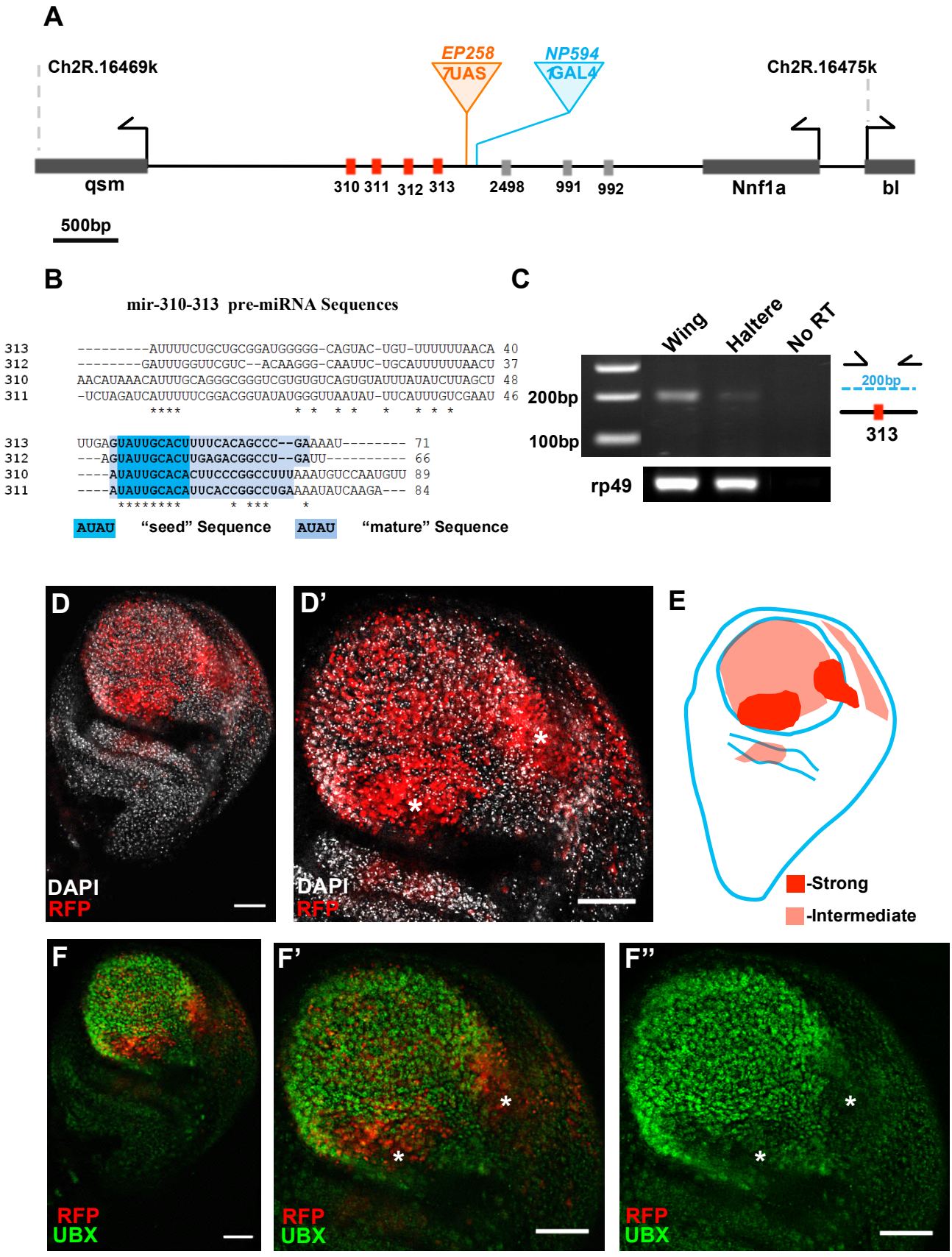

mCherry expression was detected using an α-RFP antibody. We see that the expression pattern is largely contained within the pouch region of the imaginal disc. This section of the haltere corresponds to presumptive haltere appendage as opposed to the thoracic body. The transgene is active throughout the pouch region (Fig.3.3D') but is specifically strong in two areas (denoted with * Fig.3.3D'). A schematic of the *miR-310C* haltere expression pattern is shown (Fig.3.3E). To understand how the expression of the *miR-310C* related to *Ubx*, we co-stained samples for UBX protein expression (Fig.3.3F-F''). We see that the regions with strong *miR-310C* signal (* in Fig.3.3F'-F'') correspond to regions with low levels of *Ubx* expression.

Overall our data shows that *miR-313* is situated within a miRNA cluster, containing three other miRNAs which share an identical seed sequence. Using RT-PCR, we see that all four of these miRNAs are transcribed together as a poly-cistronic transcript within the haltere imaginal disc. Through the use of GAL4 promoter trap insertion upstream of *miR-313*, we analysed the spatial expression of the *miR-310C* miRNAs. The *miR-310C* exhibits a defined spatial pattern of transcriptional expression centred within the pouch region of the haltere disc. There are two specific areas of strong expression, each area correlates with reduced levels of *Ubx* expression. This data suggests that a possible function of the *miR-310C* may be to reduce *Ubx* function within this region.

3.5 *miR-310C* gain-of-function results in phenotypic changes linked to *Ultrabithorax* loss-of-function.

The *miR-310C* miRNAs seemed excellent candidates to test for possible regulatory interactions with *Ubx* due to their high scores through bio-informatic analysis as well as their apparent active expression within the developing haltere. To test if the *miR-310C* could regulate *Ubx* expression we used the GAL-UAS expression system to over-express the *miR-310C* within the developing haltere and look for changes in phenotype and *Ubx* expression.

To assess the gain-of-function effects of the miR-310C miRNAs, we made use of the *miR-310C*^{EP2587} insertion upstream of *miR-313*. This P-element based insertion contains UAS sites that be used to ectopically express downstream transcripts (in this instance, the miR-310C). Animals carrying this insertion were crossed to a NubbinGAL4 containing stock (*Nubbin::GAL4)*, a driver which expresses specifically in the "pouch" region of both the wing and haltere imaginal discs. (Fig.2.4).

To assess if there is any effect on *Ubx* expression following ectopic induction the *miR-310C*, we first looked for phenotypic changes appearing in the adult haltere appendage.

miR-310C gain-of-function (GOF) led to noticeable phenotypic changes within the haltere appendage. Specifically, the appearance of ectopic sensory bristles within the haltere structure (arrowheads Fig.3.4B & Fig.3.4B'). The wild type haltere appendage clearly lacks these large sensory cells (Fig.3.2A & Fig.3.2A'). The ectopic sensory cells seen in the *miR-310C* GOF animals would normally be found along the margin of the wing appendage and may be considered a "homeotic transformation". Indeed when analysing halteres from animals that are heterozygous for a *Ubx* null allele, these ectopic sensory cells can be clearly seen (Fig.3.4C-C'). This similarity of phenotype resulting from a *Ubx* loss-of-function (LOF) allele and *miR-310C* GOF expression suggests that the *miR-310C* phenotype could be due to reductions in *Ubx* expression levels.

To test this further, we over-expressed the *miR-310C* in a genetic background that was heterozygous for a *Ubx* null allele. Any increase in phenotypic severity in these animals would suggest that the *miR-310C* was negatively regulating *Ubx* expression. We saw that this was indeed the case (Fig.3.4D-D'), there is a clear increase in phenotypic severity of this genotype. These data suggests that *miR-310C* GOF negatively regulates *Ubx* expression, resulting in marked phenotypic changes within the haltere appendage.

Fig.3.4 *miR-310C* gain-of-function leads to homeotic transformations.

(A-D) The ectopic expression of *miR-310C* miRNAs using the *miR-310C*^{EP2587} insertion leads to homeotic transformations. (A-A') A WT haltere shows no large sensory bristles. (B-B') miRNA overexpression using *Nub::GAL4* leads to the appearance of large ectopic sensory bristles denoted by arrowhead. (C-C') A haltere taken from a *Ubx* null heterozygote (*w ;; abx*^{1} *bx*^{3} *pbx*^{1}/+) showing the appearance of ectopic bristles. (D-D') *miR-310C* GOF in a *Ubx* null genetic background leads to a severe haltere transformation. (E) Induction of clonal cells in haltere imaginal disc over-expressing *miR-310C*, marked by *RFP*. (F) The same clonal cells co-stained for *Ubx* protein expression. (H-J) Images show magnified area of the haltere imaginal disc. (H) Clonal cells marked by *RFP*. (I) Haltere disc showing *Ubx* expression. Decreased expression of *Ubx* is seen in clonal cells marked with white dashed circles. (J) DAPI staining of haltere imaginal disc, nuclei are still visible in clonal cells. Scale bars for panels A-D are 40μm, panels A'-D' are 25μm. The scale bars for E-F represent 20μm and for panels H-J 10μm.

Fig.3.4 *miR-310C* gain-of-function leads to homeotic transformations

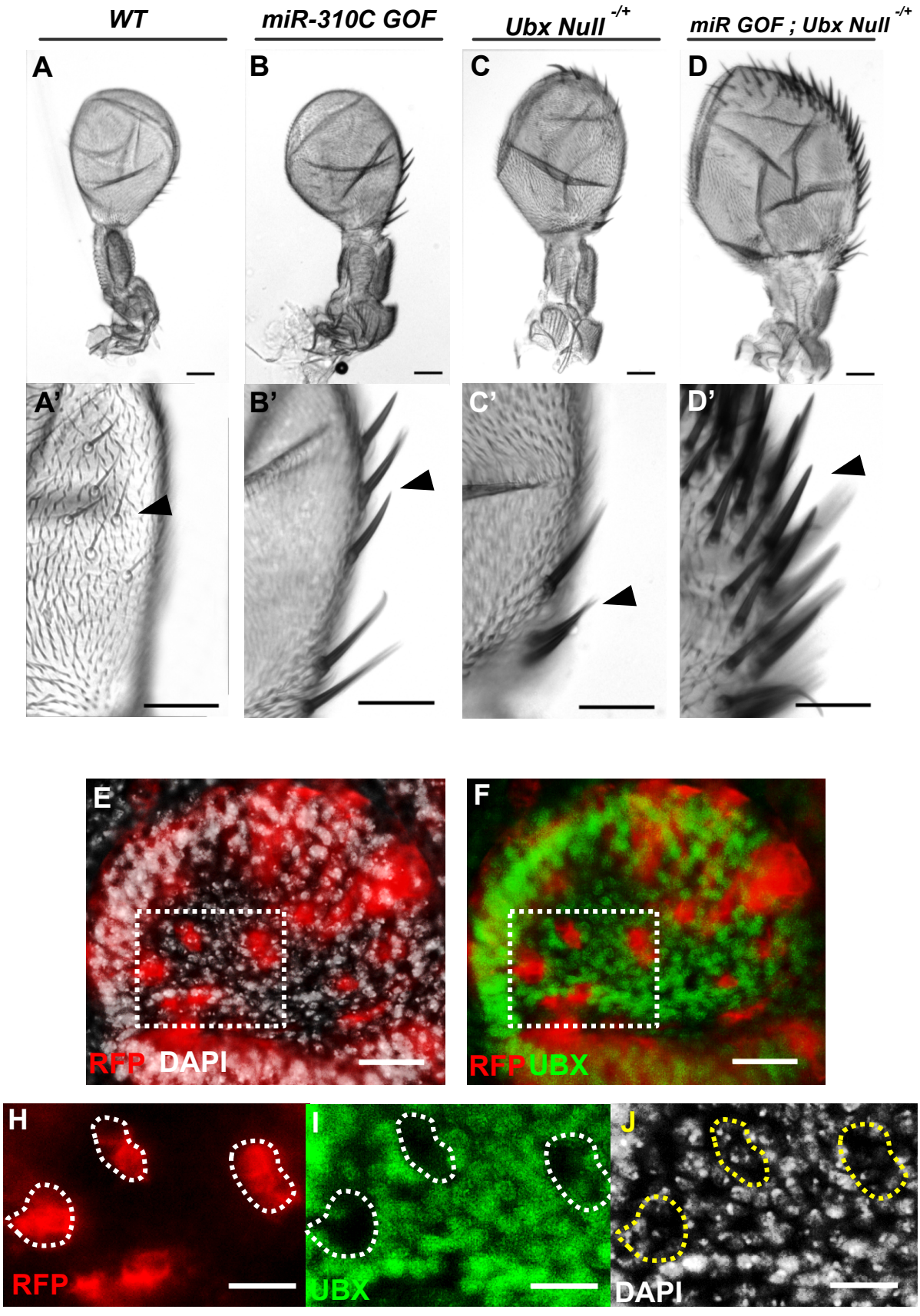

Following on from these initial results, we considered to what extent *miR-310C* GOF affected *Ubx* protein levels within the haltere. Using clonal analysis, we induced ectopic *miR-310C* expression in clonal cell populations by crossing the *miR-310C*^{EP2587} (UAS-miR310C) insertion to Actin-GAL4 'FLP-OUT' stock which also carried a *hs-FLP* recombinase and a *UAS::myrRFP* reporter construct (Fig.2.6). Progeny of this cross were exposed to 37^{o}C heat shock treatment during first larval instar growth phases. This heat shock treatment induced the expression of the FLP recombinase which excises the FRT-Stop cassette which separates the Actin promoter sequence from the GAL4 driver. FRT excision can only occur when cells are dividing therefore the result of the heat shock treatment is a stochastic activation of the Actin GAL4 driver, which induces the expression of the target UAS-miR310C insertion and the *UAS::myrRFP* reporter. Haltere discs were dissected from white-pre pupae animals and stained for Ubx expression. This technique has the advantage of inducing ectopic miRNA expression in small subsets of cells marked with an independent RFP reporter which can then be compared with the remaining haltere tissue.

We used immuno-histochemistry to monitor changes in *Ubx* protein expression in *miR-310C* over-expressing cells. Small groups of clonal cells, marked by *myrRFP* (see dashed box Fig.3.4E) were co-stained with the nuclear stain DAPI and *Ubx* antibody (Fig.3.4F). Close inspection of these cells (Fig.3.4H) shows that they appear to have little detectable levels of *Ubx* protein (Fig.3.4I). This loss in *Ubx* expression is not attributable to the cell death within the clonal cell populations as there is clear staining of DNA within nuclei still present in these cells (Fig.3.4J).

Overall, through genetic analysis we see that *miR-310C* GOF leads to phenotypic changes during the development of the haltere appendage. Furthermore, we also see that this phenotype can be affected by changes in endogenous *Ubx* levels. Through clonal analysis in the developing haltere imaginal disc, we see that *miR-310C* GOF leads to a visible reduction in *Ubx* protein expression. Together these results show that *miR-310C* is physiologically capable of negatively regulating *Ubx* expression levels.

3.6 A *miR-310C* deletion leads to increased *Ubx* expression

Our results showing the effects of *miR-310C* ectopic expression on both haltere phenotype and *Ubx* protein levels suggest that these miRNAs are capable of regulating *Ubx* expression during haltere development. However, these GOF experiments increase miRNA levels above the normal physiological levels. To determine if there is

any interaction between the *miR-310C* and *Ubx in vivo*, during normal haltere development, we must look for changes in *Ubx* expression following the removal of *miR-310C* expression. If the *miR-310C* miRNAs do indeed negatively regulate *Ubx*, then we would expect to see increases in *Ubx* expression within the haltere imaginal discs following the removal of the miRNAs.

To examine changes in *Ubx* expression following removal of the *miR-310C*, we used a previously established deletion of the *miR-310C* miRNAs, which we will denote as Δ310 (Tang et al., 2010). The Δ310 deletion was created by P-element excision of the *EP2487* insertion line. Only the *miR-310C* miRNAs are removed, the surrounding genes remain intact (Fig.3.5A).

To analyse changes in *Ubx* expression, wild-type (WT) and Δ310 larvae were identically staged and the haltere imaginal discs dissected and fixed. Following immuno-staining for *Ubx*, the resulting *Ubx* expression patterns from both genotypes were analysed. The intensity of expression signal was determined using the *Plot Profile* tool in *Image J* (Fig.3.5B). A discrete section of the imaginal disc was selected to determine signal intensity in both WT and Δ310 discs. This section can be determined by studying the morphology of the imaginal discs (see white box, Fig.3.5B). All samples from both genotypes were compared and profiled for signal intensity. Importantly, only samples which were immuno-stained at the same instance were compared together to control for variation between experiments. An example comparison between WT and Δ310 can be seen in the Fig.3.5B. The signal intensity of *Ubx* expression from left to right of the imaginal disc is plotted. The light grey lines represent intensity profiles for individual WT discs, the dark grey lines represent individual Δ310 discs.

Fig.3.5 *miR-310C* removal results in increased *Ubx* expression levels.

(A) Genomic map of *miR-310C* cluster of miRNAs in WT and Δ310 genotypes. Genomic PCR highlights the extent of the Δ310 deletion and shows that neighbouring genes remain intact. Primer positions for each gene are marked by arrows. (B) Profile of *Ubx* expression intensities within the haltere imaginal discs in WT and Δ310 (*w ; Δ310/Δ310*) genotypes. (C) Average differences in signal intensity between WT and Δ310 genotypes in both a Control (Orange Box) and Experimental (Pink Box) test regions. The average differences in three independent experiments are shown. Each experiment analysed a minimum of 5 halteres of each genotype. Students T-test was used to determine statistical significance *** - $p<0.001$.

Fig.3.5 *miR-310C* removal results in increased *Ubx* expression levels

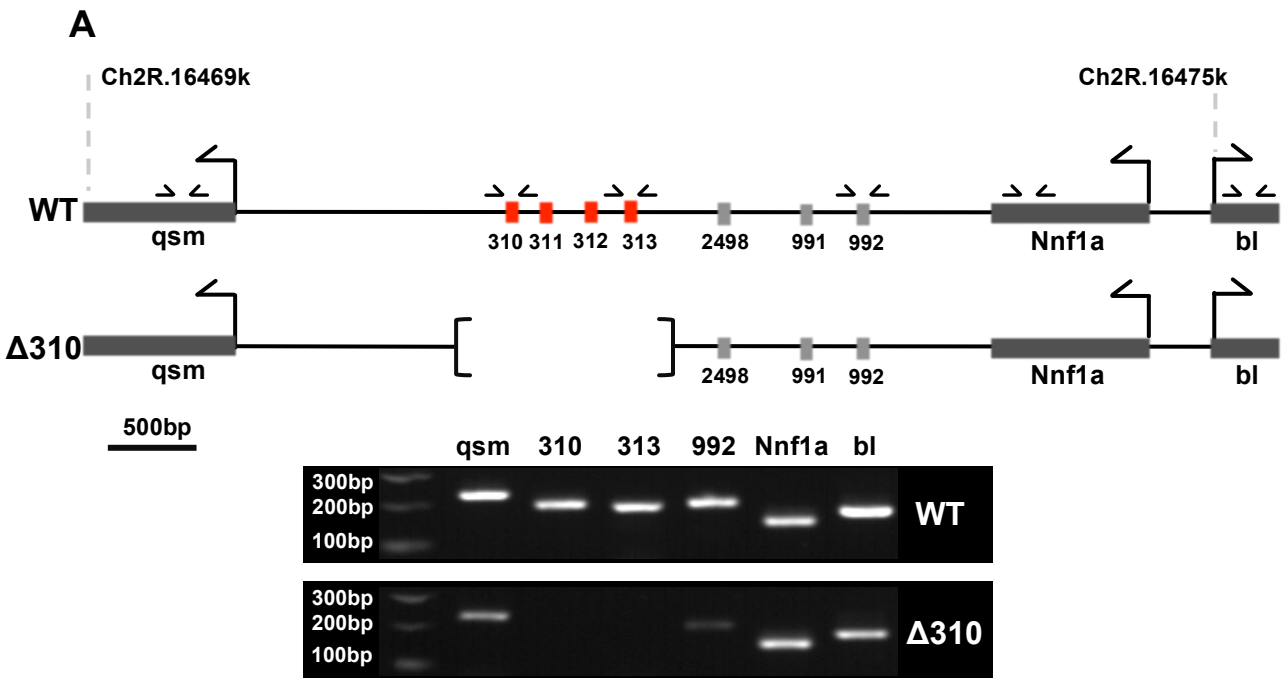

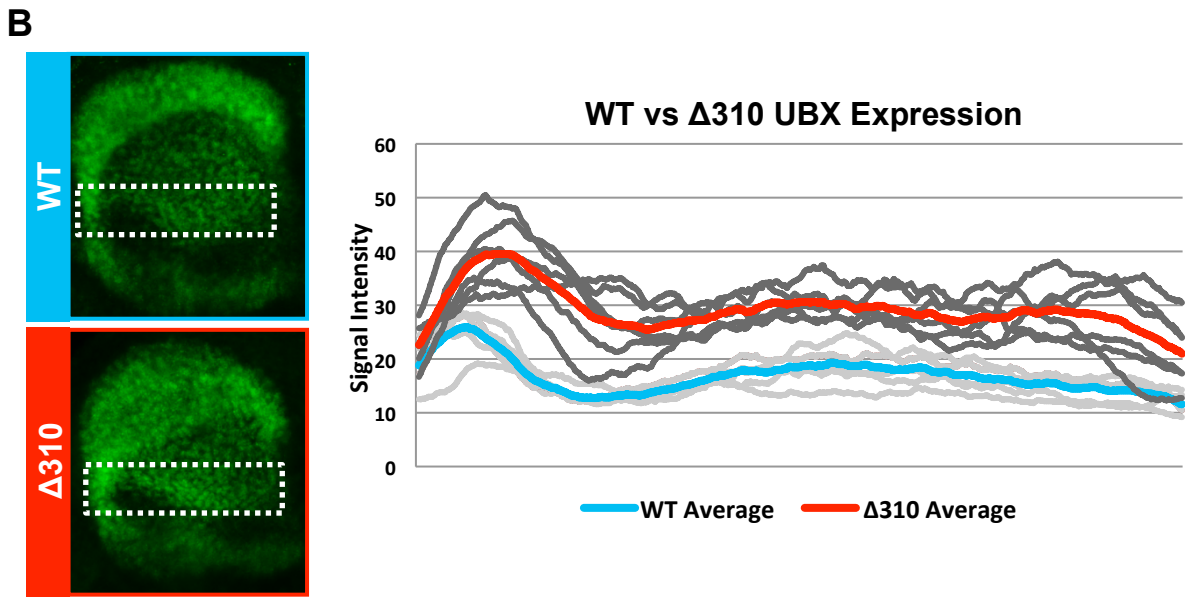

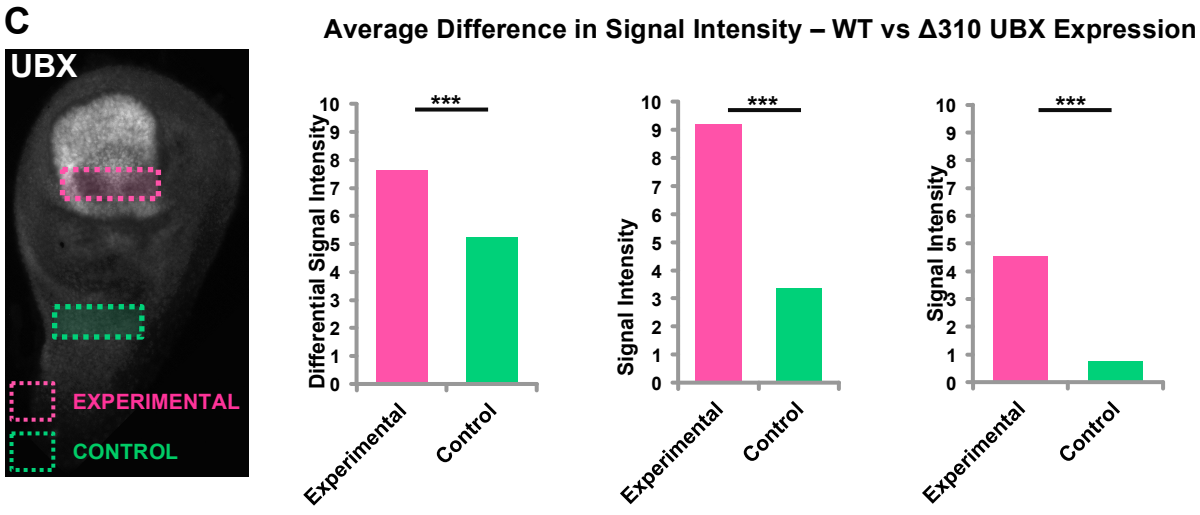

The light blue line represents the average WT expression intensity, the red line representing the average Δ310 expression intensity. A clear difference in signal intensity can be seen when comparing both genotypes, the Δ310 samples showing increased levels of *Ubx* expression.

Despite our experimental precautions, there is a possibility that these detectable differences in signal intensity are due to variation in the experimental protocol. To demonstrate that this was not the case, we looked for possible changes in signal intensity between genotypes in a region of the imaginal disc where we do not expect to find miRNA activity. In Fig.3.5C the previously defined experimental testing region is highlight by the pink box, the chosen control region is shown in an orange box. This region was not seen to have *miR-310C* transcriptional activity as detected by the *miR-310C::GAL4* transgenic line (Fig.3.3D). Signal intensity levels were determined for each genotype in both selected regions following three independent experimental repeats. For both regions, the differences in average signal intensity was calculated by subtracting the signal intensity levels of the WT sample from that of the Δ310 sample. The average difference in signal intensity when comparing both the experimental and control regions of three independent experiments are shown (Fig.3.5C). In each independent experiment there were detectable differences in signal when comparing the control region within the imaginal discs. However, differences within the experimental region, comparing both genotypes was always significantly greater than that of the control region ($p < 0.001$ comparing Experimental with Control).

Overall, the analysis of *Ubx* expression in the Δ310 genotype suggests that when the *miR-310C* is absent, there are significant increases in *Ubx* protein expression. This strongly suggests that these miRNAs are capable of targeting *Ubx* transcripts *in vivo* during the development of the haltere imaginal disc. When examining the miR-310C expression pattern, we noted that there appeared to be a correlation between the spatial pattern of miR-310C expression and apparent decreases in Ubx signal intensity suggesting that perhaps the presence of the miR-310C had an effect in reducing Ubx expression in these regions (Fig.3.3F-F''). However, our analysis of Ubx expression patterns within the Δ310 mutant discs shows that in most samples assayed, we detected a general increase in Ubx expression across the disc with a dip in Ubx expression was still visible albeit at a higher level of intensity. This data suggests that the decreases in Ubx expression observed before are not entirely due to the presence of miR-310C miRNAs. An interpretation of these results is that the 'dip' in expression is predominantly the result of transcriptional regulation at the Ubx locus. Therefore removing miR-310 activity would not lead to changes in these levels of transcription.

However, the fact that removing the miR-310C does lead to clear increases in Ubx protein expression suggests that the role for these miRNAs is to fine-tune the expression of Ubx across the haltere disc, not a more active role in shaping the Ubx expression pattern. In this manner these miRNAs may be supplying a robustness mechanism in the regulation of Ubx expression during haltere development.

3.7 Loss of the *miR-310C* leads to phenotypic changes in haltere morphology.

Having shown that there were significant differences in *Ubx* expression levels within the haltere imaginal discs when comparing WT and Δ310 genotypes, we next considered to what extent the loss of these miRNAs would affect the morphology of the haltere appendage.

Previous studies involving *miR-310C* miRNAs noted there were no obvious phenotypic changes in morphology resulting from miRNA deletion (Pancratov et al., 2013; Tang et al., 2010; Tsurudome et al., 2010). We reasoned that the effects of the miRNA removal may be very subtle. To fully assess if any morphological changes occurred following miRNA removal, we used Scanning Electron Microscopy (SEM) and Light Microscopy to examine the haltere structure in detail.

Fig.3.6 Loss of the *miR-310C* miRNAs leads to changes in haltere morphology

(A) The haltere appendage can be divided into three main compartments – *scabellum*, *pedicel*, and *capitellum*. (B) Each compartment had its own unique array of sensory cells. (C-E) The Δ310 deletion (*w ; Δ310/Δ310*) leads to diverse array of phenotypic changes in the arrangement of sensory cells of the pedicel. (C) The normal sensory field arrangement from a WT haltere. (D-E) Δ310 halteres show different phenotypic changes within the sensory fields. (F) Quantification of the phenotypic penetrance comparing WT and Δ310 genotypes. (G) Halteres from Δ310 animals have visibly large Capitellum. (H) Quantification of the Capitellum

size increase. (I) Box plot comparing the distributions of total capitellum sensilla in WT and Δ310 genotypes. (J) The capitella sensilla are found within the capitellum, see arrowhead. For analysis of phenotype penetrance and capitella sensilla cell number the following *n* numbers were used. *WT* – 46, *Δ310* – 42. For the analysis of haltere capitellum size the following *n* numbers were used. *WT* – 20, *Δ310* – 20. Scale bar for panel A is 25μm, panel B-E is 10μm, panel G is 10μm. Statistical analyses was performed using Students t-test, *** - $p<0.001$.

Fig.3.6 Loss of the *miR-310C* leads to altered haltere morphology

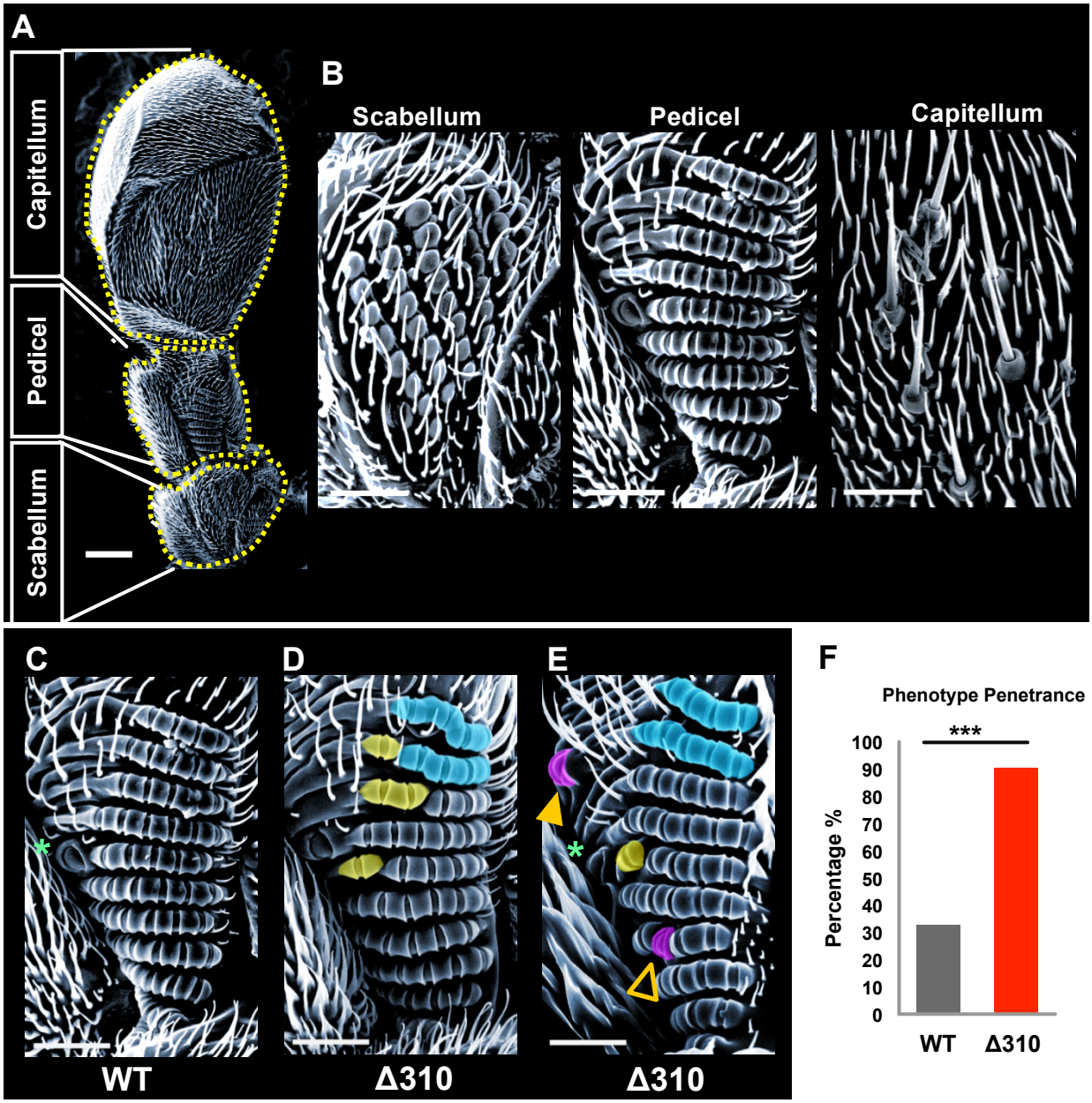

Much like the *Drosophila* wing, which can be separated into the wing blade and wing hinge regions, the haltere can be broken down into multiple compartments. The haltere is formed of the capitellum – a rounded balloon like compartment, the scabellum – the base of the appendage and the functional attachment to the body wall, and the pedicel – interconnecting tissue that links the capitellum to the scabellum (Fig.3.6A).

Each compartment is filled with a number of mechano-sensory cells that are arranged in various sensory fields throughout the appendage – the *campaniform sensilla* (Cole and Palka, 1982). Within each compartment of the haltere, each sensory field is composed of sensory cells with particular morphologies and spatial arrangements (Fig.3.6B).

The pedicel compartment contains a unique sensory field comprised of multiple rows of campaniform sensilla arranged along the anterior posterior axis (Fig.3.6C). These particular sensory cells have a very distinct morphology. They are stacked next to each other and are linked together by a shared cuticle that covers the majority of the sensory cell surface. The other campaniform sensilla cell type found within the pedicel is not connected to the sensory rows, is larger and covered less by overlying cuticle (see * Fig.3.6C). Altogether these sensory fields have a very stereotyped architecture.

Following our close inspection of WT and Δ310 haltere appendages, we noticed a number of morphological abnormalities occurring in the formation of the sensory fields within the pedicel and scabellum compartments. Two example sensory fields taken from Δ310 halteres can be seen in the Fig.3.6D & Fig.3.6E. In these samples, we see three distinct changes in morphology within the haltere pedicel. Cells false coloured yellow are sensory cells that have disconnected from the main sensory rows which form the sensory fields. The disconnected cells, share the same morphology as those cells still present in the rows, but have now lost their attachment to the main grouping of cells. Cells false coloured blue have still formed into their composite rows, however these rows are now orientated incorrectly. Instead of forming straight along the antero-posterior axis, they are now mis-directed, moving away from the main body of campaniform sensilla. Cells which are false coloured purple appear to be cell-types that do not belong in the area they have appeared, the normal cell that should occupy that space has been transformed into an alternative form. The purple cell (see arrowhead Fig.3.6E) has the same morphology as the large sensory cell adjacent to the sensory rows (* in Fig.3.6E). However, this new cell is separated from the rest of the sensory rows, positioned amongst normal cuticle tissue. The second purple cell (empty arrowhead Fig.3.6E) also appears to be a transformed cell-type. Here a large sensory

cell has appeared, replacing one of the smaller campaniform sensilla found within the sensory rows. These phenotypes are also easily seen and distinguished using standard light microscopy.

To determine how often these changes in morphology occur in Δ310 animals, we analysed a large cohort of haltere appendages and quantified the phenotypic penetrance in both WT and Δ310 genotypes (Fig.3.6F). Our analysis shows that there is a ninety per cent penetrance effect seen in the Δ310 genotype. Although we also found morphological abnormalities in the halteres of the WT population, the penetrance of these defects were significantly lower than that seen in the Δ310 halteres.

Having ascertained that there were clear morphological defects in the pedicel and scabellum of the Δ310 halteres. We next ascertained if there were any changes in the morphology of the haltere capitellum. Firstly, we investigated if capitella size was altered in the Δ310 genotype by measuring the area of the haltere capitella. We see an increase in average capitella size when comparing Δ310 to WT halteres (Fig.3.6H). We next looked for alterations to the sensory cells found within the capitellum – the *capitella sensilla*. These cells have a different morphology to those seen within the pedicel and scabellum (Fig.3.6B). The capitella sensilla most resemble the large sensory bristles found along the margin of the wing. Our analysis revealed that there were no changes in sensory cell specification of the sensilla. Analysis of total sensilla cell numbers within the capitellum tissue showed there are no significant differences between WT and Δ310 genotypes (Fig.3.6I). Interestingly, we do see that the variation in sensilla number appears to be reduced in the Δ310 halteres.

In summary, this data shows that the Δ310 genotype not only leads to detectable increases in *Ubx* protein levels, but also results in many morphological abnormalities within the haltere appendage. We uncovered both sensory cell patterning defects in the pedicel and scabellum compartments as well as a significant increase in capitellum size of the appendage.

3.8 The Δ310 phenotype is sensitive to *Ubx* dosage.

Having confirmed that removal of the *miR-310C* leads to morphological abnormalities within the haltere appendage as well as a significant increase *Ubx* protein expression levels, we next looked to determine the relationship between the Δ310 phenotype and abnormal *Ubx* levels.

We hypothesised that the morphological changes detected in the genotype were due to increased levels of *Ubx* within the developing haltere imaginal disc, caused by the loss of the *miR-310C*. We therefore tried to "rescue" these changes by genetically reducing the levels of *Ubx* expression. We combined the Δ310 genotype with a *Ubx* heterozygote null strain, generating animals that were homozygous for the Δ310 deletion and heterozygous for the Ubx null allele – $\Delta 310^{-/-}$ $Ubx^{-/+}$ (Δ310 Ubx). Like the Δ310 genotype, these animals are viable and appear to have no obvious defects in fitness occurring from the combination of these two alleles.

To fully understand if the Δ310 phenotype could be altered by reducing levels of *Ubx,* we performed a more extensive documentation of the morphological changes seen in the WT, Δ310 and Δ310 Ubx genotypes. We first subdivided the morphological changes we had previously detected into eight categories – *Wild-Type*, *Wobble*, *Disconnect, Transformation*, *Join*, *Gain*, *Loss* and *Disruption*.

The '*Wobble*' phenotype class is defined by the appearance of sensory cell rows within the pedicel that have changed orientation away from the main body of cells. Fig.3.7C shows two rows of cells (highlighted red) orientate away from the main sensory field. The final cell within the row (looking from left to right) is not positioned adjacent to the cell below it (marked with *) causing a wobble in the row formation.

The '*Disconnect*' phenotype class contains halteres which show individual sensory cells that are of the same cell-type found within the sensory rows but are now located apart from the organized sensory field. For example Fig.3.7B shows three disconnected cells that are set apart from the main sensory rows.

Fig.3.7 Genetic interactions between *miR-310C* and *Ubx*

(A-I) The different phenotypic classes found in Δ310 halteres documenting the array of morphological abnormalities. For full details of phenotypic changes, see main text. (J) Quantification of phenotypic penetrance comparing WT, Δ310 (*w ; Δ310/Δ310*) and Δ310 Ubx (*w ; Δ310/Δ310 ; abx^1 bx^3 $pbx^{\prime}$/+*) genotypes. (K) Quantification of phenotype expressivity using a measure of multiple phenotypic class occurrences comparing WT, Δ310 and Δ310 Ubx genotypes. (L) Quantification of phenotype severity using a measure of total number of phenotypic changes comparing WT, Δ310 and Δ310 $Ubx^{-/+}$ genotypes. Statistical test used was the Students t-test. For analysis of phenotype penetrance and severity, the following *n* numbers were used. *WT* – 46, *Δ310* – 42, *Δ310 Ubx* – 54. Scale bar is 10μm for all images.

Fig.3.7 Genetic interactions between the *miR-310C* and *Ubx*

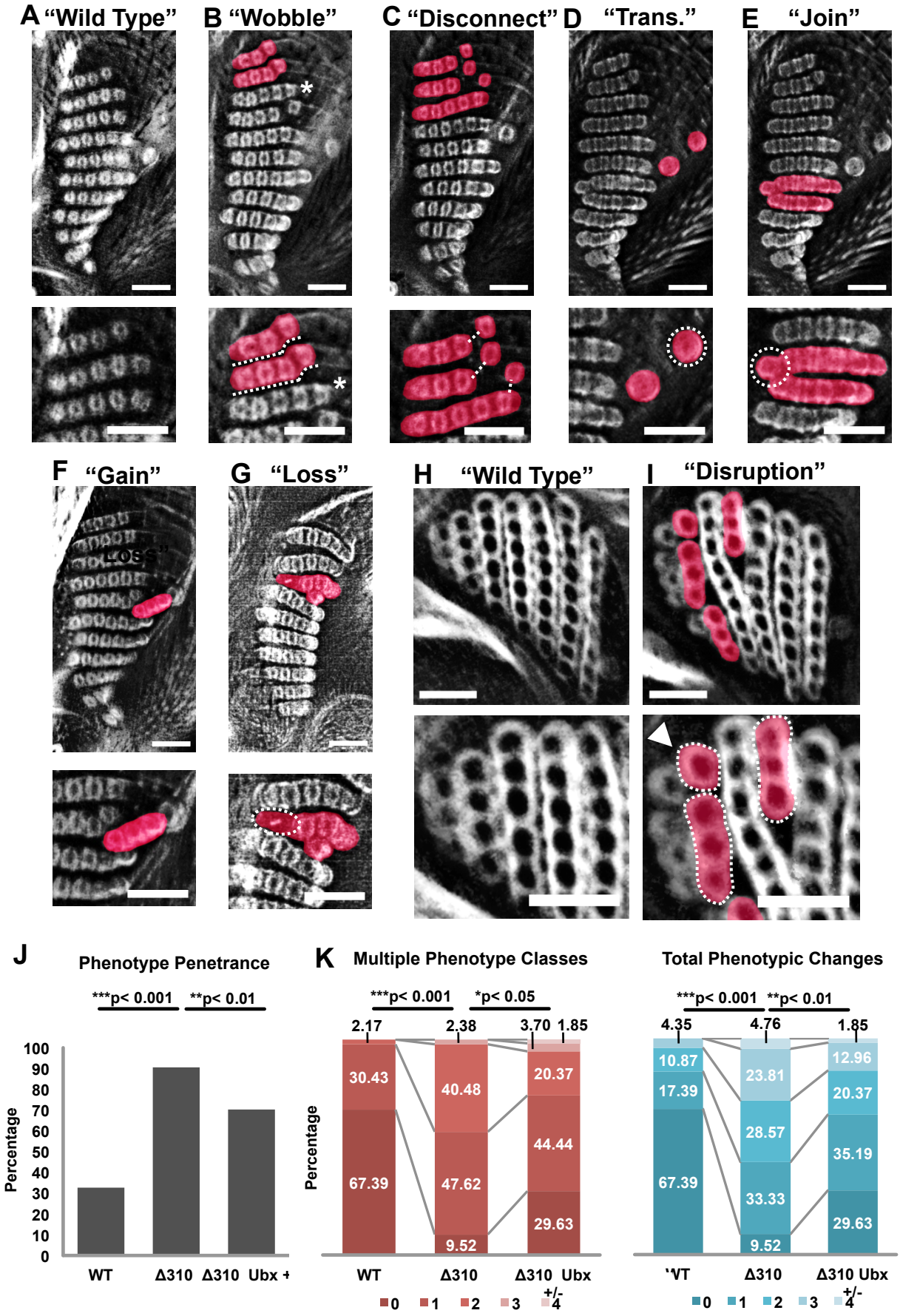

The majority of the cases we encountered were single cells that had become disconnected, however there were a small number of samples that showed two or three cells joined together, but together had separated from the main body of sensory rows.

The '*Transformation*' phenotype class contains halteres that have ectopic sensory cells that are not of the same type seen within the sensory rows and appear within the vicinity of the pedicel sensory fields. An example of the most common occurrence can be seen in Fig.3.7D, here we see an ectopic large sensory cell (dashed white circle) of the type normally found sitting adjacent to the sensory field.

The '*Join*' phenotype occurs when two rows of the sensory field share one or more cells, thus joining the rows. In wild-type halteres, the rows of cells sit very close together with a minimal gap between them but are still clearly distinct structures. In this phenotypic class, this arrangement is disrupted by the cells from adjacent rows joined together. In Fig.3.7E, the cell to the far left (dashed circle) forms part of both rows of cells (highlighted red) therefore joining both rows.

The '*Gain*' phenotype class contains halteres which show a clear gain in the number of campaniform sensilla within sensory rows. Fig. 7F shows an example where three ectopic sensory cells have formed an extra row of cells situated between two normal sensory rows. These cells break the organized formation normally seen within this sensory field.

The '*Loss*' phenotype class contains halteres that show an obvious gap in the cell arrangement, an example is seen Fig.3.7G. Here, a sensory row can be identified (highlighted in red) which contains only three sensory cells, as opposed to the normal 4-5 cells. In place of the missing cell (see white dashed oval) a small white trichome appears indicating the appearance normal haltere cuticle. In this case, the sensory cell that should be positioned in this gap is missing from the structure and a normal cuticle cell has filled the void.

The above morphological changes all occur within the pedicel compartment of the haltere. The final phenotypic class occurs within the dorsal sensory field of the scabellum (Fig.3.7H). The '*Disruption*' phenotype class includes any changes in morphology of scabellum sensory rows. Two examples of the '*Disruption*' class are shown in Fig.3.7I. On the left (marked with arrowhead) we see that the long row of cells normally spaced next to each other have become disjointed into three groups of cells. In the middle of the sensory field we also see that an ectopic grouping of cells is

positioned between two normal rows. This ectopic grouping is splitting the two main rows of cells from each other.

After establishing our main phenotypic classes, we first analysed the phenotype penetrance in the three experimental genotypes – WT, Δ310 and Δ310 Ubx. In particular, was there a change in penetrance between the Δ310 and Δ310 Ubx genotypes? We had previously seen that the penetrance of morphological traits in the Δ310 animals was significantly greater than WT halteres. Following our analysis of the Δ310 Ubx halteres, we saw that the phenotype penetrance in this genotype was significantly reduced ($p<0.01$) when compared to the Δ310 animals (Fig.3.7J). To investigate further, we analysed the morphological changes in terms of phenotypic severity – first, the percentage of haltere samples that had multiple phenotypic classes present and secondly, the total number of phenotypic changes occurring within the haltere samples.

We initially grouped our samples dependant on how many different phenotypic classes were visible within the halteres. We identified that there was a range of zero (no phenotypic alterations) to four (different classes of phenotype) multiple phenotype occurrences (Fig.3.7K). The data is displayed as a stacked bar chart representing the relative contributions of each grouping as a percentage of all halteres analysed. There was a highly significant increase in multiple phenotypic classes occurring when comparing the Δ310 and WT genotypes ($p<0.001$). Comparing the Δ310 and Δ310 Ubx, we see a small but statistically significant decrease in the occurrence of multiple phenotypic classes ($p<0.05$) in the Δ310 Ubx genotype. Our second approach was to study the total number of phenotypic changes within the haltere, irrespective of particular phenotypic classes. This analysis showed that the most severely altered halteres could have up to four visible changes in morphology (Fig.3.7L). There was a highly significant increase in the total morphological alterations appearing in the Δ310 halteres when compared to WT ($p <0.001$). We observed a significant decrease in the total number of morphological changes when comparing the Δ310 to Δ310 Ubx genotypes ($p<0.005$).

Both of these approaches demonstrate that removal of the *miR-310C* not only increases the likelihood of morphological defects to develop within the halteres but also the severity of phenotypic change when compared to the WT genotype. Our data also shows that this affect was lessened when levels of *Ubx* were reduced.

In summary, we wanted to determine to what extent the morphological changes observed in the Δ310 mutant halteres were caused by increased levels of *Ubx*

expression within the developing haltere imaginal disc. We examined in detail the haltere morphology of animals lacking the *miR-310C* and determined there were 7 visibly distinct classes of phenotypic change occurring in these halteres. Using a genetics methodology, we reduced *Ubx* availability in animals also lacking the *miR-310C*. Assaying for phenotypic penetrance and severity we see significant decreases when comparing the Δ310 and Ubx Δ310 genotypes. Overall this data suggests that the Δ310 phenotype we have documented is dependent on increased levels of *Ubx* within the developing haltere, indicating a relationship exists between the Δ310 phenotype and altered *Ubx* levels. We hypothesise that the loss of the *miR-310C* disrupts the regulation of *Ubx* expression leading to increased levels of *Ubx* protein. This disrupts *Ubx* functionality in specifying the correct patterning or specification of the sensory field architecture within the haltere.

3.9 *Ubx* ectopic expression phenocopies the Δ310 phenotype.

Having shown that the phenotypic changes seen in Δ310 halteres are likely due to the increased levels of *Ubx* expression, we next undertook to substantiate this finding by attempting to experimentally reproduce the Δ310 phenotype by ectopically inducing *Ubx* within the developing haltere.

Using the binary GAL4-UAS expression system, coupled to a GAL80 temperature sensitive GAL4 repressor (McGuire et al., 2003), we induced expression of a *UAS::Ubx1a, tub::GAL80^{ts}* transgene (Pavlopoulos and Akam, 2011) with the *miR310C::GAL4* driver. To determine the effect different doses of ectopic *Ubx* protein would have on the development of the haltere sensory fields, we used the temperature sensitive GAL80 transgene to control when the *UAS::Ubx1a* construct was activated. At different larval and pupal developmental time points - the L1, L2, L3 larval phases and during Pupae formation (P0), we initiated Ubx1a transgene expression by placing the animals at 29^{o}C (Fig.3.8A). This temperature disables the GAL80 protein which is a repressor of GAL4, thus leading to the activation of the UAS promoter. Using this experimental design we generated four data sets plus a control in which the experimental genotype but was kept at 25^{o}C throughout development, thus never initialising *mir310C::GAL4-UAS::Ubx1a* expression.

These experimental data sets were analysed using the phenotypic classes established in our previous documentation of the Δ310 phenotype. Example halteres from each experimental time-point are shown (Fig.3.8B). Altered morphologies are false-coloured

blue, highlighting abnormalities within the haltere structures. It is apparent that many of the phenotypes seen in the Δ310 halteres were recapitulated after expressing the *UAS::Ubx1a* transgene. For example we saw evidence of both the '*Wobble*' (see *) and '*Join*' phenotypes (see arrowhead) in the same haltere (Fig.3.8B L3). Analyses of all halteres show a definite increase in morphological changes as the time of *UAS::Ubx1a* activation was increased. As an example, the sensory field shown in the Fig.3.8B L1

in sensory cell number has a very severe disruption to the normal morphology. This is presumably a result of the prolonged exposure to increased levels of *Ubx* protein.

We quantified the changes in phenotype observed amongst our data sets as previously done when examining the Δ310 phenotype. We observed that as time of *Ubx* exposure increased, there were no significant changes in phenotype penetrance between the P0/L3 samples and the control. However, a clear increase in phenotype penetrance was seen in the L2 and L1 data sets when compared to their preceding time-points ($p<0.05$ and $p<0.005$ respectively).

We next assessed to what extent increasing levels of *Ubx* affected the phenotype expressivity of our datasets. The experimental cohorts were grouped dependant on how many different classes of morphological alterations were observed (Fig.3.8D). There were no statistically significant increases in multiple phenotype classes between the P0/L3 datasets when compared to the control group. The L2 and L1 data sets again showed significant changes ($p<0.05$ and $p<0.001$ respectively) when compared to the preceding experimental groups. In particular, the transition between the L2 and L1 dataset was much more severe than the transition between the L3 and L2 groups.

Fig.3.8 *Ubx* gain-of-function phenocopies the Δ310 phenotype

(A) Experimental scheme to ectopically express *Ubx* during different post-embryonic developmental stages. *miR310C::GAL4* induction of *UAS::Ubx1a* transgene occurs by shifting incubation temperature from 25^{o}C to 29^{o}C in-activating the temperature sensitive GAL80 repressor. (B) Examples of haltere phenotypes occurring following induction of *Ubx* expression comparing all experimental groups. (C) Quantification of phenotypic penetrance at all experimental stages. (D) Quantification of phenotype severity using a measure of multiple phenotype occurrences comparing all experimental groups. (E) Box plots showing the distribution of total sensilla number in the capitellum sensilla comparing all experimental groups. Statistical test used was the Students t-test, p-values are shown in the figure. The following *n* numbers were used for analysis. *Control* - 18 , *P0* - 10 , *L3* - 15 , *L2* - 18 , *L1* – 19. Scale bar for all images is μm. Statistical significance was determined using Student's t-test.

Fig.3.8 *Ubx* gain-of-function phenocopies the Δ310 phenotype

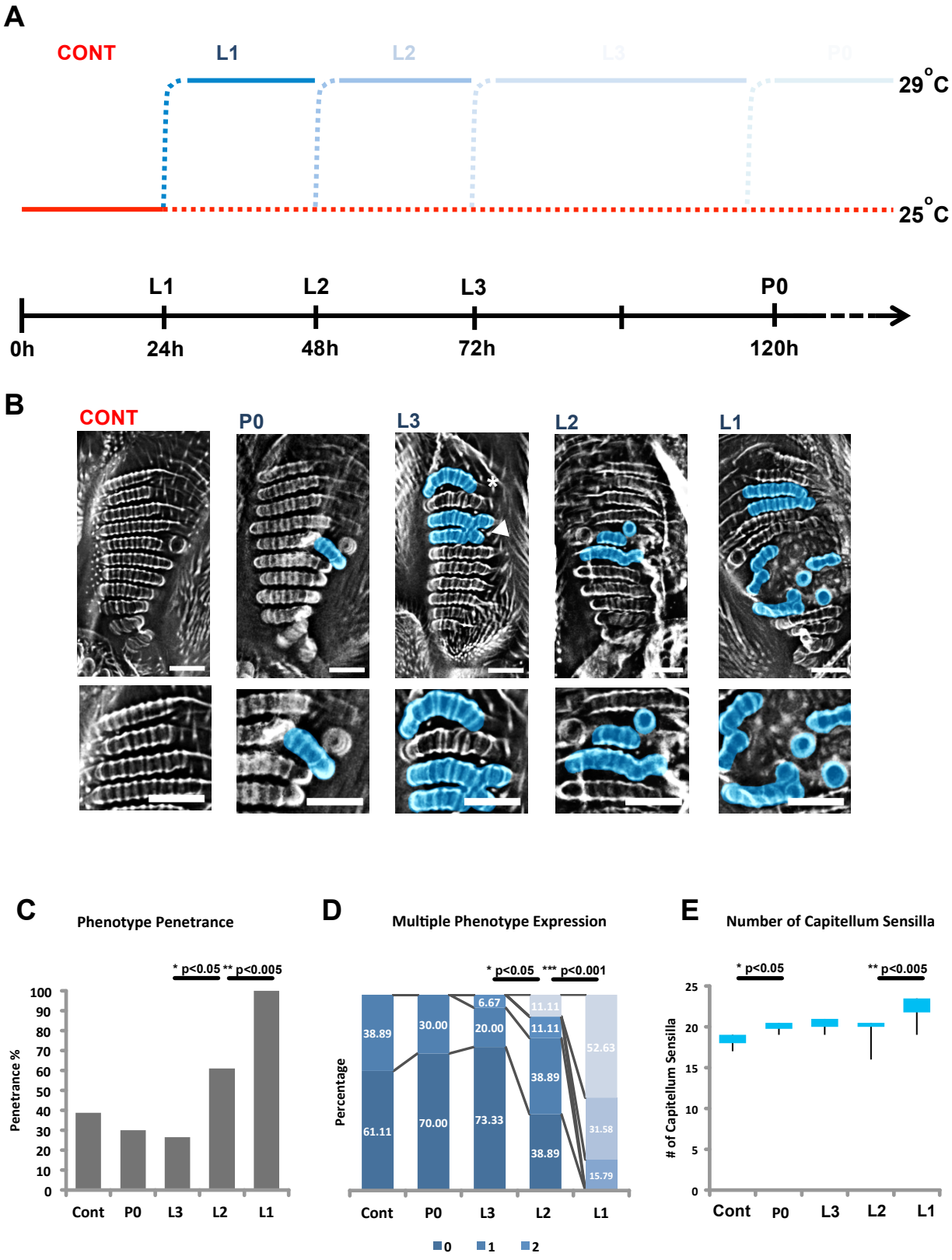

Up to this point our analysis had been restricted to phenotypic changes within the pedicel/scabellum compartments of the haltere. We next looked for changes in sensory cell specification within the haltere capitellum. We did not observe any alterations to sensory cell morphology within the capitellum. However, our analysis of capitella sensilla cell number shows that there was a small but significant increase ($p<0.05$) in the number of sensilla when comparing P0-L2 stages with control (Fig.3.8E). A much more significant increase in sensilla cell number was seen when comparing the L1 to L2 datasets ($p<0.005$).

In summary, we had wanted to verify if the observed Δ310 phenotypes were due to increased levels of *Ubx* expression within the developing haltere. By experimentally inducing ectopic *Ubx* in a controlled manner, we looked for Δ310-like phenotypic changes in the resulting haltere phenotypes. We see that ectopic *Ubx* expression induced using a *Ubx* transgene coupled to a *miR310C::GAL4* driver was able to phenocopy a number of the morphological alterations seen in the Δ310 halteres. This experiment also highlights that the *miR-310C* is transcribed in the presumptive pedicel and scabellum compartments of the haltere imaginal disc. We identified a graded response to increasing levels of *Ubx* in the pedicel/scabellum compartments. The longer the *UAS::Ubx1a* transgene was activated, the more drastic the morphological changes within the haltere. Interestingly we did not see the same graded response when examining the number of sensilla cells present in the capitellum. The most significant changes in capitella sensilla number occurred between the L2 to L1 experimental groups. This suggests that different regions and/or cell types within the haltere have different sensitivities to increasing *Ubx* levels and are able to avoid alterations to their developmental programs that may lead to changes in haltere morphology.

3.10 *miR-310C* regulation of *Ubx* leads to changes in sensory field architecture but not through direct specification of sensory cells

Our results indicate that *Ubx* has an important role in the correct development of the haltere sensory fields and that this function is disrupted when the *miR-310C* is absent. We next wanted to define what role *Ubx* performs during development of the haltere sensory fields. Is *Ubx* function required during the initial specification of the sensory precursor cells? Or rather, is *Ubx* function indirect, controlling general sensory tissue formation and organisation?

There are many classes of external sensory cells found within *Drosophila*, all have a shared mechanism of initial specification. Every external sensory cell differentiates from a common pre-cursor, termed the Sensory Organ Precursor (SOP) cell. The specification of an SOP cell occurs through a process termed lateral inhibition (Heitzler and Simpson, 1991). Lateral inhibition involves the specification of a single cell from among a number of competent cells within the presumptive sensory tissue. The process of lateral inhibition is achieved through the *Notch/Delta* cell signalling system. Once the SOP cell has been selected, it undergoes a series of asymmetric divisions that result in a collection of daughter cells which coalesce to form the functioning sensory apparatus (Gho et al., 1999). It is during these asymmetric divisions that the particular class of sensory cell is specified, for example – the decision between mechano-sensory or chemo-sensory cell types (Blochlinger et al., 1991; Jan and Jan, 1994; Nottebohm et al., 1994).

We wanted to determine to what extent the expression pattern of the *miR-310C* overlapped with SOP cells specified during haltere imaginal disc development. To visualise SOP cells we monitored the expression of *Neuralized* – a transcription factor expressed following SOP specification – using a *Neuralized-LacZ* transgenic line. This transgene was crossed into animals containing a *miR-310C::GAL4-UAS::mChNLS* recombinant chromosome. Monitoring expression of both *Neuralized-LacZ* and *miR-310C::mChNLS* at three developmental time points – larvae, pre-pupae and pupae (Fig.3.9A-C), no significant changes in *miR-310C* expression patterns were observed through these developmental phases. The majority of *miR-310C* expression is still located within the pouch region of the haltere disc. Co-staining for *Neuralized-LacZ* with *miR-310C* expression showed that the SOP cells are specified in regions of tissue that were also surrounded by *miR-310C* expression (white dashed boxes Fig.3.9A'-C')). Although *miR-310C* expression intensity does vary within these regions (see inset panel Fig. 9A'), there seems to be no correlation between which cells express either high or low levels of *miR-310C* and their proximity to a SOP cell. There is little evidence of co-expression between *miR-310C* and *Neuralized-LacZ* in single SOP cells. This data suggests that once specified, it is unlikely that *miR-310C-Ubx* regulatory interactions affect the differentiation and development of the SOP cells.

However, the close spatial relationship between *miR-310C* positive and *Neuralized-LacZ* positive cells warranted further investigation. Could *miR-310C* regulation of *Ubx* affect the initial specification process of SOP cells? A role for *Ubx* has been identified in SOP specification within leg imaginal discs (Rozowski and Akam, 2002). We compared SOP cell numbers between WT and Δ310 haltere imaginal discs within the

presumptive pedicel tissue (white boxes Fig.3.9A'-C', dashed region Fig.3.9D) – a region of the haltere with a prominent sensory field in the adult appendage. Our analysis showed a small but statistically significant increase in the distribution of total SOP cells in the Δ310 imaginal discs. Ectopic sensory cells could be a viable explanation for many of the phenotypes we documented in the Δ310 haltere appendages. Thus we wanted to confirm that an increase in sensory cell number was still apparent in the mutant haltere appendages. We re-analysed the haltere appendages from the WT, Δ310 and Δ310 Ubx genotypes and determined the total number of sensory cells present within the dorsal pedicel sensory fields. Although there was variation in the total number of sensory cells of all genotypes, there were no significant changes in total cell number within the dorsal pedicel when comparing these genotypes (Fig.3.9E). We further looked for differences in the organisation of the haltere sensory fields by documenting the number of rows (green bracket Fig.3.9F) and calculating average number of cells per row (yellow bracket Fig.3.9F) within each haltere sensory field.

Fig.3.9 Effects of Δ310 allele on sensory cell formation during haltere development.

(A-C) Expression patterns of *miR-310C* shown alongside *Neuralized* expression marking SOP cells during three stages of imaginal disc development. *miR310C::GAL4* was used to monitor *miR-310C* expression. A *Neuralized-LacZ* transgene was used to monitor SOP cell formation. (A-A') Example late larval stage haltere imaginal disc showing the expression of *miR-310C* and *Neuralized* (B-B') Example pre-pupal haltere imaginal disc showing the expression of *miR-310C* and *Neuralized*. (C-C'). Example pupal imaginal disc showing expression of *miR-310C* and *Neuralized* (D). Quantification of the distribution of SOP cell populations in WT and Δ310 (*w ; Δ310/Δ310*) genotypes at the pre-pupal stage of development. (E) Quantification of the distribution of total sensory cell numbers in haltere appendages comparing WT, Δ310 (*w ; Δ310/Δ310*) and Δ310 Ubx (*w ; Δ310/Δ310 ; abx^{1} bx^{3} pbx^{1}*/+) genotypes. (F) Image of the dorsal Pedicel sensory field. This field of cells was analysed in terms of number of rows within sensory field (green bracket) and number of cells per row (blue bracket). (G) Quantification of the distribution of the number of rows found within the sensory field comparing WT, Δ310 and Δ310 Ubx genotypes. (H) Quantification of the distribution of the average number of cells per row within the sensory field comparing WT, Δ310 and Δ310 Ubx genotypes. Statistical test used was the Students t-test, p values are given in figures. For analysis of SOP cell number in imaginal discs, the following n numbers were used. *WT* – 16, *Δ310* – 20. For analysis of sensory field cell number and organisation, the following *n* numbers were used. *WT* – 42, *Δ310* – 37, *Δ310 Ubx* – 42.Scale bar for images is 25μm.

Fig. 3.9 Effects of Δ310 allele on sensory cell formation during haltere development

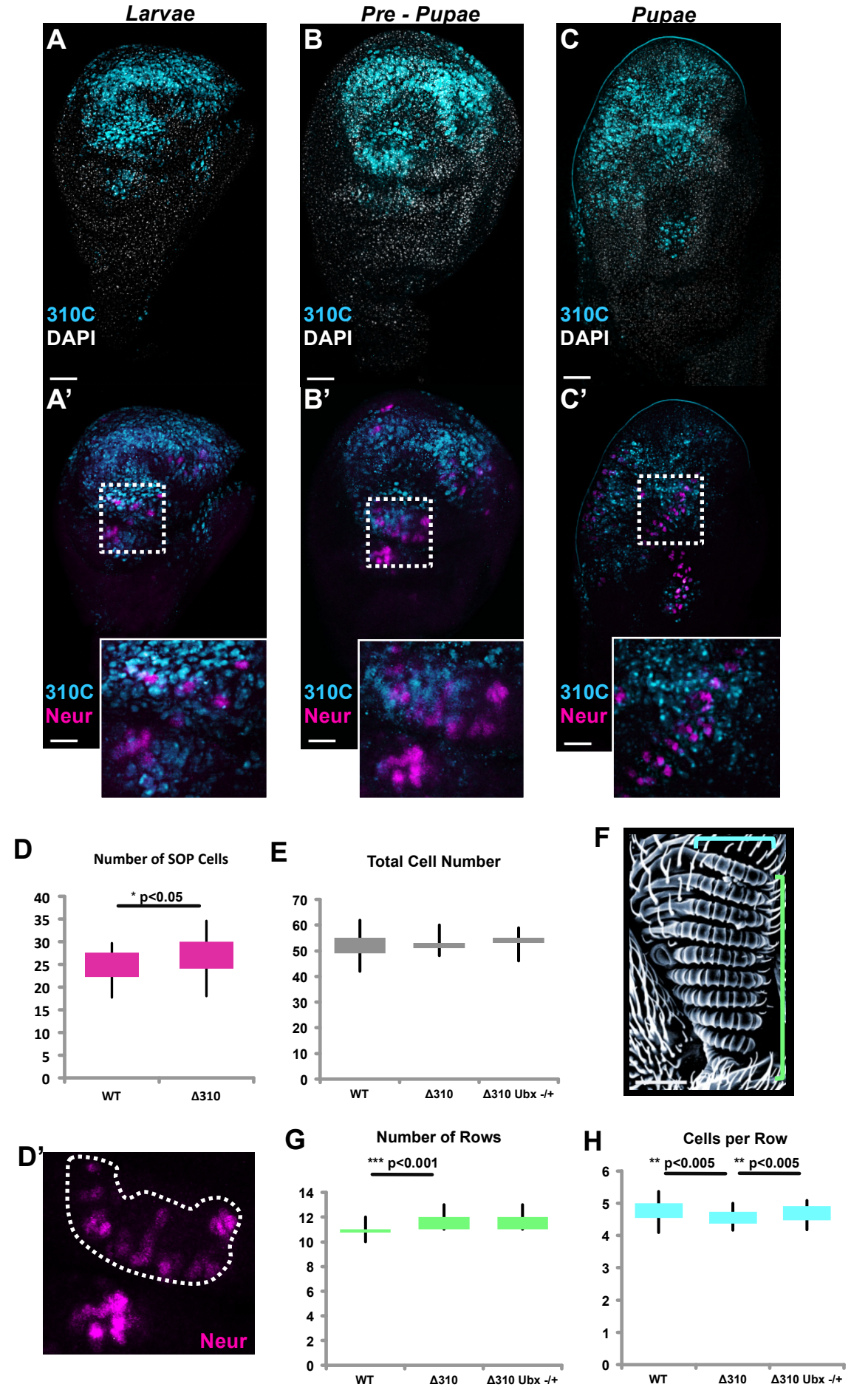

Analysis of row number within the sensory field showed that there was a significant tendency for an increased number of rows in the Δ310 genotype compared to WT (Fig.3.9G). Furthermore, there was also a significant decrease in the distribution of the number of cells per sensory row in the Δ310 genotype (Fig.3.9H). To understand if these changes in tissue architecture were due to increased *Ubx* levels resulting from lack of *miR-310C* regulation, we compared the dorsal pedicel sensory fields of the Δ310 and Δ310 Ubx genotypes. We found no significant changes in total row number (Fig.3.9E & 9G), however we did see a significant increase in distribution of cells per row when comparing the Δ310 Ubx halteres to those of the Δ310 genotype (Fig.3.9H).

This data thus suggests that the loss of the *miR-310C* does not alter the total number of sensory cells seen within the dorsal pedicel, but does affect the manner in which the sensory field is organised. Specifically we see alterations to the number of rows and number of cells per row within the sensory field. Additionally, we show that these alterations in sensory field architecture are in part rescued in the Δ310 Ubx genotype.

Our previous analysis of the phenotypic changes resulting from loss of the *miR-310C* showed that the majority of the documented morphological alterations were related to changes in sensory cell patterning and formation. We investigated the relationship between *miR-310C* expression and the specification of SOP cells during three stages of haltere disc development. Our analysis showed that there is a close spatial relationship between *miR-310C* positive tissue and SOP cells. We hypothesized the role of the *miR-310C* regulation of *Ubx* would directly or indirectly control the number of sensory cells specified within the developing tissue. Analysis of SOP cell populations at a specific developmental stage within the presumptive dorsal pedicel region of the haltere imaginal disc showed a small but significant increase in SOP cell number when comparing WT to Δ310 discs. This result suggested that the role of *Ubx* maybe to limit the number of sensory cells produced within the presumptive sensory field. Our analysis of total sensory cell numbers in the adult haltere appendages showed that there are no significant differences between WT and Δ310 genotypes. However, examination of the sensory field organisation did reveal statistically significant increases in the number of sensory cell rows and a decrease in the number of cells per row. Performing the same analysis in the Δ310 Ubx genotype we documented an increase in the number of cells per row when compared to the Δ310 genotype. This suggests that the changes in tissue architecture present in the Δ310 genotype are linked to increases in *Ubx* expression levels.

In summary, we find no evidence that *Ubx* regulation by the *miR-310C* defines any developmental or differentiation processes of SOP cells once they are specified within the haltere disc. Our analysis of SOP cell populations during haltere development and the sensory cells within the adult appendage, suggest that the *miR-310C-Ubx* regulation may play a role in the overall organisation of sensory field tissue architecture within the haltere. Analysis of SOP cell populations within Δ310 haltere discs suggest that disrupting *miR-310C-Ubx* regulation would result in increased sensory cell numbers, however this is not observed in the adult appendages. An explanation for this could be that the loss of the *miR-310C* leads to early specification of SOP cells during haltere development but not the total number of cells specified. Alternatively, there may be a surveillance mechanism that detects and corrects errors in SOP specification during early imaginal disc development, therefore maintaining the correct cell number in the adult appendage.

3.11 A role for apoptosis during haltere sensory field formation

We hypothesised that a possible mechanism in which *Ubx* could directly affect the formation of haltere sensory fields was via the induction of programmed cell death in the presumptive sensory tissue. It has been documented that Hox genes can induce apoptosis to sculpt tissue morphology during embryogenesis (Lohmann et al., 2002). Disruption to this function by increasing levels of *Ubx* could explain some of the phenotypic changes seen in the haltere sensory field. The induction of SOP cells occurs through the process of lateral inhibition, because of this, it is unlikely that the sensory cells form in pre-determined rows. Therefore a mechanism must exist that can lead to the cell re-arrangement required to create each row of sensory cells. It is possible that to aid this process, excess cells – both sensory and epithelial, maybe removed from the presumptive sensory field. This cell pruning effect via the apoptotic pathway would lead to correct formation of the sensory fields (Fig.3.10A).

This hypothesis has two testable predictions. Firstly, any disruption to the apoptotic pathway would lead to similar phenotypic changes to those seen in the Δ310 genotype. Second, reducing apoptotic function in Δ310 background would lead to increased phenotype penetrance and severity. To test these predictions we analysed the haltere appendages of animals heterozygous for the H99 deletion (White et al., 1994) which removes the three main pro-apoptotic genes – *head involution defective (hid)*, *grim* and *reaper* (*rpr*) (Fig.3.10B) in both WT and Δ310 genetic backgrounds.

Analysis of the H99 haltere appendages revealed similar morphological alterations to those seen in the Δ310 genotype. There are clear examples showing the '*Wobble*' and '*Disruption*' phenotypes previously observed in Δ310 halteres (Fig.10D & Fig.10D''). We determined the phenotypic penetrance of the H99 deletion in both a WT and Δ310 genetic backgrounds and compared this with our previous WT and Δ310 data (Fig.3.10E). There was a significant increase in phenotype penetrance (78%) when comparing WT and H99 genotypes, however no significant changes between the H99 and Δ310 genotypes. Comparisons between the Δ310 and Δ310 H99 $^{-/+}$ (Δ310 H99) genotypes showed a nominally significant decrease in penetrance.

We documented phenotypic severity of the H99 deletion in both WT and Δ310 backgrounds as before, by monitoring increases in the number of multiple phenotypic classes and the total phenotypic changes present within the haltere.

Fig. 3.10 A role for apoptosis during haltere appendage formation.

(A) Schematic showing hypothetical role for programmed cell death during the formation of sensory fields within the haltere. (B) Genomic map showing the extent of the H99 deletion. Pro-apoptotic genes *hid, grim* and *rpr* are removed. (C-D) Comparison of haltere phenotypes seen in WT and H99 genotypes. (C-C'') Formation of dorsal pedicel and scabellum in WT genotype. (D-D'') Formation of dorsal pedicel and scabellum in H99 genotype. (E) Quantification of phenotype penetrance comparing WT, H99 (*w ;; H99/TM6b*), Δ310 (*w ; Δ310/Δ310*) and Δ310 H99 $^{-/+}$ (*w ; Δ310/ Δ310 ; H99/TM6b*) genotypes. (F) Quantification of phenotype severity using a measure of multiple phenotypic class occurrences comparing WT, H99, Δ310 and Δ310 H99 genotypes. (G) Quantification of phenotype severity using a measure of total number of phenotypic changes comparing WT, H99, Δ310 and Δ310 H99 genotypes. (H) Image of the dorsal Pedicel sensory field. This field of cells can be analysed in terms number of rows within sensory field (green bracket) and number of cells per row (blue bracket). (I) Quantification of the distribution of total sensory cell numbers in haltere appendages comparing WT, H99, Δ310 and Δ310 H99 genotypes. (J) Quantification of the distribution of the number of rows found within the sensory field comparing WT, H99, Δ310 and Δ310 H99 $^{-/+}$ genotypes. (K) Quantification of the distribution of the average number of cells per row within the sensory field comparing WT, H99, Δ310 and Δ310 H99 $^{-/+}$ genotypes. Statistical test used was the Students t-test, p-values are shown within the figure. For analysis of phenotype penetrance and severity, the following *n* numbers were used. *WT* – 46, *H99 - 15 , Δ310* – 42, *Δ310 H99* – 16. For analysis of sensory field cell number and organisation, the following *n* numbers were used. *WT* – 44, *H99 - 18 , Δ310* – 39, *Δ310 H99* – 19. Scale bar for all images is 10μm.

Fig.3.10 A role for apoptosis during haltere appendage formation

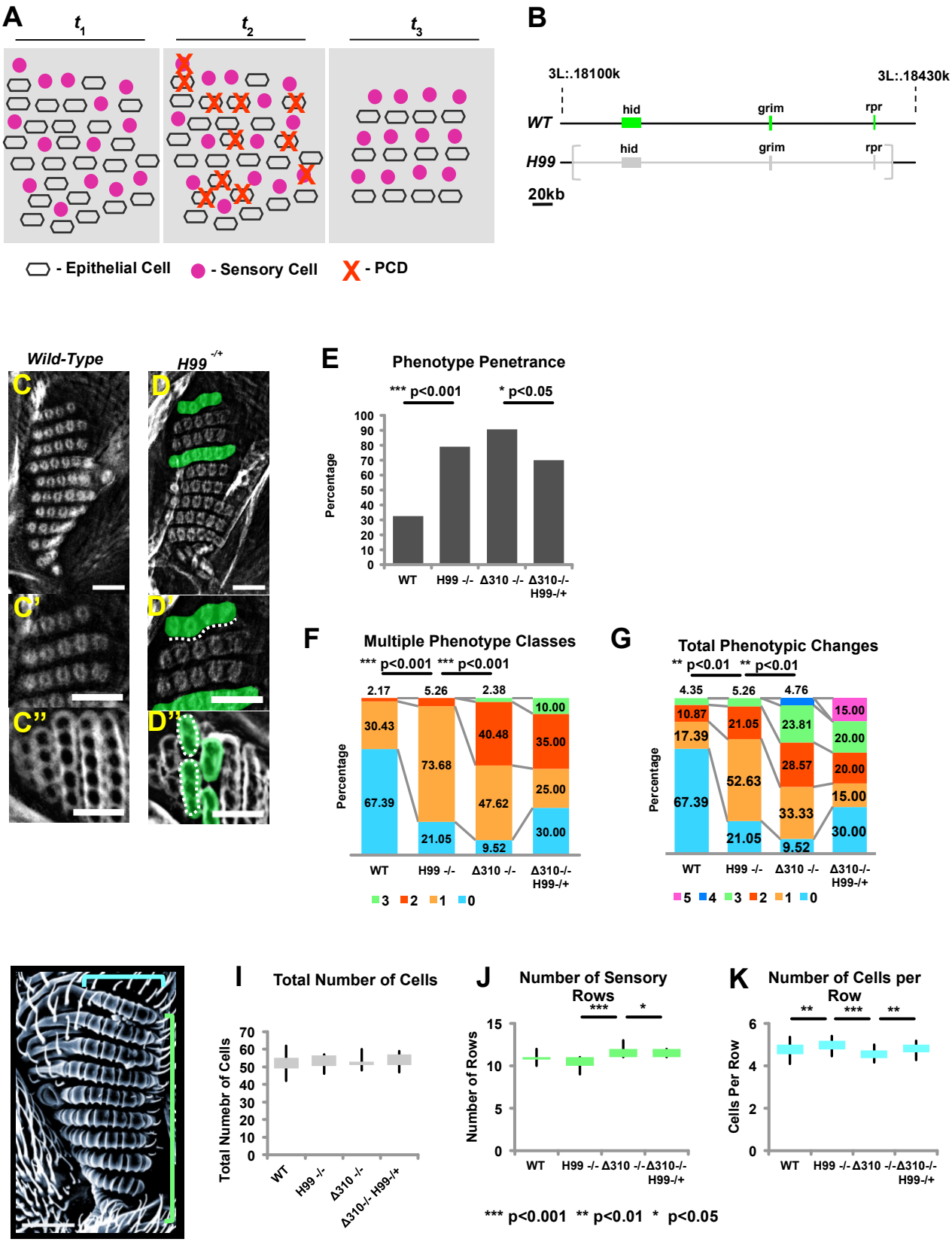

Analysing the number of multiple phenotypic changes showed there were significant differences in phenotypic severity between the WT and H99 genotypes, mirroring the increase in phenotype penetrance (Fig.3.10F). This data indicates that the majority of H99 halteres show only a single morphological alteration. This contrasts with the data of the Δ310 genotype where a large proportion of halteres have at least two types of phenotypic class present. There was in fact a significant increase in multiple phenotypic changes when comparing H99 and Δ310 genotypes; however we did not see any significant difference comparing the Δ310 and Δ310 H99 genotypes.

The analysis of the total phenotype occurrences in the four experimental genotypes showed similar results (Fig.3.10G). Once again there was a significant increase in total phenotype occurrences between WT and H99 genotypes and a significant increase when comparing the H99 and Δ310 genotypes. However, there were no significant changes when comparing the Δ310 and Δ310 H99 genotypes.

Taken together, we show that the H99 deletion leads to the same phenotypic changes seen in Δ310 animals. However, although both mutants show a similar degree of phenotypic penetrance, there are significant differences in phenotype severity. The loss of the *miR-310C* leads to more severe morphological alterations. In addition, we show that combining both the H99 and Δ310 deletions does not lead to increased phenotype penetrance or severity.

Having previously shown that the Δ310 deletion resulted in alterations to the overall architecture of the dorsal pedicel sensory tissue, we set out to determine if the H99 deletion also replicated this phenotype. We again analysed total sensory cell numbers, total row number and the average number of cells per row in the dorsal pedicel sensory field (Fig.3.10H), looking at the H99 deletion in both WT and Δ310 genetic backgrounds. Our analysis showed there were no significant changes in total cell number between the genotypes assayed (Fig.3.10I). Comparisons of the total sensory row numbers (Fig.3.10J) revealed no significant differences between WT and H99 deletions. However, we observed a significant difference between H99 and Δ310 genotypes, a clear tendency towards more sensory rows in the Δ310 genotype. When comparing the Δ310 and Δ310 H99 genotypes, a nominally significant decrease in the number of sensory rows of the Δ310 H99 genotype was determined.

Finally, we examined the number of cells present in each row (Fig.3.10K) and saw an increase when comparing the H99 and WT genotypes, which was also significantly different to that observed in the Δ310 genotype. When both the H99 and Δ310 deletions were combined, there was an increase in the number of cells per row when

compared to the Δ310 genotype, the distribution sitting in between that seen in the H99 and Δ310 genotypes.

To summarise, we hypothesised that phenotypic changes seen in the Δ310 halteres could be caused by the mis-regulation of the apoptotic pathway due to increased *Ubx* expression levels. We documented the haltere sensory fields of animals with H99 deletion in both WT and Δ310 genetic backgrounds, looking for any morphological changes. We see that disruption to the apoptotic pathway leads to similar phenotypic changes observed in the Δ310 animals. These phenotypic changes are at an equivalent penetrance in both the H99 and Δ310 populations. However, analysis of phenotype severity showed significant differences between the H99 and Δ310 genotypes. Halteres from Δ310 animals are more likely to show an increased number of phenotypic classes and total phenotypic changes. Although both H99 and Δ310 deletions exhibit the same phenotypic changes, when combined, there are no significant increases in phenotype penetrance or severity.

Examination of the sensory field architecture in halteres from the H99 genotype shows that disruption to the apoptotic pathway has an opposing effect to that seen in the Δ310 genotype. Whereas the latter deletion caused an increased number of sensory rows and a decreased number of cells per row, the H99 deletion had no significant effect on row number but a significant increase in the number of cells per row.

These results suggest that apoptosis does have a role in helping shape and define the correct architecture of the haltere sensory fields. However, this process is not linked to *Ubx* regulation through *miR-310C* activity.

3.12 DISCUSSION

The regulation and expression of the Hox transcription factor *Ubx* during *Drosophila* development is dynamic and complex, encompassing epigenetic, transcriptional and post-transcriptional mechanisms. In this study, we looked to expand our knowledge of the post-transcriptional regulation of *Ubx* expression and its consequences for *Ubx* function during the development of the haltere imaginal disc. *Ubx* is expressed throughout the haltere imaginal disc and is vital for the appropriate development and patterning of the haltere appendage. Although present in all haltere cells, *Ubx* expression is heterogeneous amongst different cell populations. Furthermore, these cells are sensitive to *Ubx* expression levels and will alter their developmental fates accordingly.

We hypothesised that post-transcriptional regulators, specifically miRNAs, could have an important role in the dynamic regulation of *Ubx* levels within the haltere imaginal disc, helping maintain the heterogeneity of *Ubx* expression within the haltere and consequently an important role in instructing the appropriate development of this appendage.

Identifying candidate miRNA regulators of *Ubx* during haltere development

The most common mechanism of miRNA regulation occurs through the targeting of 6-8 nucleotide sequences within the 3'UTR. *Ubx* is known to undergo developmentally regulated APA during development. Using SQ-RTPCR we confirmed that the most common *Ubx* 3'UTR isoform expressed during *Drosophila* post-embryonic development contains the extended long 3'UTR.

Bioinformatic analysis predicted a large number of possible miRNA seed sites within this *Ubx* 3'UTR. Screening these candidates for miRNAs whose expression had previously been detected in imaginal disc tissue (Ruby et al., 2007b), we generated a list of ~100 miRNAs which could potentially target the *Ubx* 3'UTR during post-embryonic development.

One of the top candidates was *miR-313*. Inspection of *miR-313* within the genome showed that this miRNA was present alongside three closely related miRNAs - *miR-310*, *miR-311* and *miR-312* (*miR-310C*). All four miRNAs are related to the ancient *miR-92* family. Analysis of the *miR-310C* expression patterns within the haltere showed

that these miRNAs were transcribed within the haltere imaginal disc with a specific spatial expression focused on the pouch region of the disc.

To know if the *miR-310C* was capable of repressing *Ubx* expression, we ectopically expressed these miRNAs in the developing haltere imaginal disc. This miRNA GOF causes drastic changes in haltere morphology that resemble classic *Ubx* LOF phenotypes. Furthermore, ectopic expression of this miRNA cluster in a *Ubx* deficient genetic background leads to increased phenotypic severity of the haltere. This strongly suggests that the *miR-310C* GOF phenotype is due to decreased *Ubx* expression levels. Clonal over-expression of the *miR-310C* within the haltere imaginal disc confirmed that these miRNAs can repress *Ubx* protein expression.

To determine if the *miR-310C* miRNAs were true regulators of *Ubx*, we monitored *Ubx* expression patterns in animals lacking the *miR-310C* (Δ310 genotype). This analysis revealed *Ubx* levels increased significantly within the haltere imaginal disc. Previous studies had concluded that there were no morphological alterations to animals lacking the *miR-310C* (Pancratov et al., 2013; Tang et al., 2010; Tsurudome et al., 2010). Our detailed analysis of Δ310 haltere appendages revealed significant alterations to haltere morphology. These included multiple aberrations in the formation of the many sensory cell-types within the haltere. To our knowledge, this is the first description of morphological phenotypes associated with this miRNA cluster and adds to the study by Arif et al., demonstrating the capacity for miRNA regulation to affect body morphology (Arif et al., 2013). Taken together, through bioinformatic and genetic analysis, we have identified a true miRNA regulator of *Ubx* expression during post-embryonic development.

The *miR-310C* – *Ubx* regulatory axis affects sensory tissue formation and patterning within the developing haltere

Using a genetic interaction assay, we set out to prove that the Δ310 phenotype was due to altered levels *Ubx* expression. We combined the Δ310 allele with a *Ubx* LOF mutation and documented in detail the resulting changes in phenotype penetrance and severity. This analysis shows that reducing *Ubx* expression in a Δ310 genetic background led to decreases in both phenotypic penetrance and severity, thus 'rescuing' the Δ310 phenotype. We were also able to show that controlled ectopic expression of a *Ubx* transgene was able to reproduce aspects of the Δ310 phenotype. Taken together our data strongly points to a direct genetic interaction between the *miR-*

310C and *Ubx* and that these miRNAs are genuine regulators of *Ubx* expression. To our knowledge, these miRNAs are the first identified to regulate *Ubx* during post-embryonic development.

The morphological aberrations following *miR-310C* removal involve the disruption to the correct patterning of the many sensory cells found within the haltere. Analysis of SOP formation in haltere imaginal discs showed a small increase in SOP cell number within Δ310 haltere discs compared to WT. However analysis of sensory cell numbers in the adult appendages showed no significant differences when comparing these two genotypes. Detailed observations of the dorsal pedicel sensory field in the haltere appendage showed significant differences in the overall organisation of the sensory rows as well as the specific morphological defects seen in Δ310 halteres. It is also interesting to note that we detected a large degree of variation in the number of sensory cells found within the WT sensory field, which was reduced in the Δ310 halteres.

What cellular processes are required to produce these complex tissue arrangements? How does the regulation of *Ubx* levels relate to proper specification of this tissue architecture?

We hypothesised that programmed cell death may be an important cellular process involved in shaping the developing sensory fields of the haltere. This pathway has been previously associated with Hox gene regulation of tissue development (Lohmann et al., 2002). Animals heterozygous for the H99 deletion showed that disruption of the apoptotic pathway leads to morphological changes similar to those seen in the Δ310 genotype. However combining both H99 and Δ310 deletions did not increase either phenotype penetrance or severity.

Why do we not see a Δ310-H99 interaction, yet both genotypes lead to similar morphological defects in the haltere? A possible explanation for this could be that the Δ310 allele already causes a saturating effect on the extent to which morphological changes can occur in the haltere without leading to animal lethality. Trying to increase the phenotype severity by adding further disruptions via the H99 allele is therefore ineffective.

Examining the effect of the H99 allele on sensory tissue organisation within the dorsal pedicel, we again detected no significant changes in total cell number or any differences in the number of sensory rows; however we did detect an increase in the number of sensory cells per row. These results indicate that the H99 deletion leads to a

different effect on the sensory tissue formation compared to the Δ310 allele. Overall, we were unable to show any direct link between the changes observed in the Δ310 allele and defects in the apoptotic pathway. However, our evidence suggests that programmed cell death does play a role in the determination of the final tissue architecture of the haltere sensory fields.

A role for *Ubx* in defining the haltere sensory field size and organisation

We have shown that *Ubx* expression levels are regulated by *miR-310C* and that this regulation is required for correct sensory tissue formation. Absence of this fine-tuning regulatory level leads to specific cellular phenotypes as well as a general lengthening of the sensory field along the proximo-distal axis of the haltere appendage. In addition, we also show that the apoptotic pathway contributes to formation of the sensory field architecture independently of the *miR-310C-Ubx* regulatory axis. It is unclear if *Ubx* may still regulate the apoptotic pathway in this context. However, we find no evidence linking the Δ310 phenotype to mis-regulation of apoptosis during haltere development.

Our data indicates that in Δ310 animals, elevated *Ubx* expression levels lead to an increased length of sensory field without affecting total cell numbers within the sensory field. One explanation to this phenomenon is that incorrect *Ubx* activity allows for SOP cells to be specified within a wider area of presumptive sensory tissue. Consequently when the sensory rows form together, the overall sensory field is extended (Fig.3.11A-B). The ineffectual forming of sensory rows would also explain many of the other morphological defects seen in Δ310 animals e.g. the '*Disconnect*' phenotype. It is important to note that this analysis highlights one aspect of *Ubx* function in the development of the haltere but does not include all aspects of *Ubx* activity, which may not be regulated by the *miR-310C*. For instance, what role does *Ubx* have in determining the specific sensory cell-types seen within the haltere, which are morphologically dissimilar to their counterparts seen within the wing? Many studies have shown evidence linking the Hox gene activity to the specification of specific sensory cell types. Unfortunately there seems to be no unifying point of Hox regulatory input between these different biological examples (Gutzwiller et al., 2010; Li-Kroeger et al., 2012; Rozowski and Akam, 2002).

How does *Ubx* shape the developing sensory fields within the haltere? One possibility would be that *Ubx* provides a regulatory input into the process of lateral inhibition involving the *Notch*/*Delta* pathway, perhaps limiting the area of presumptive sensory

Fig.3.11 Model of *miR-310C-Ubx* interactions during haltere development

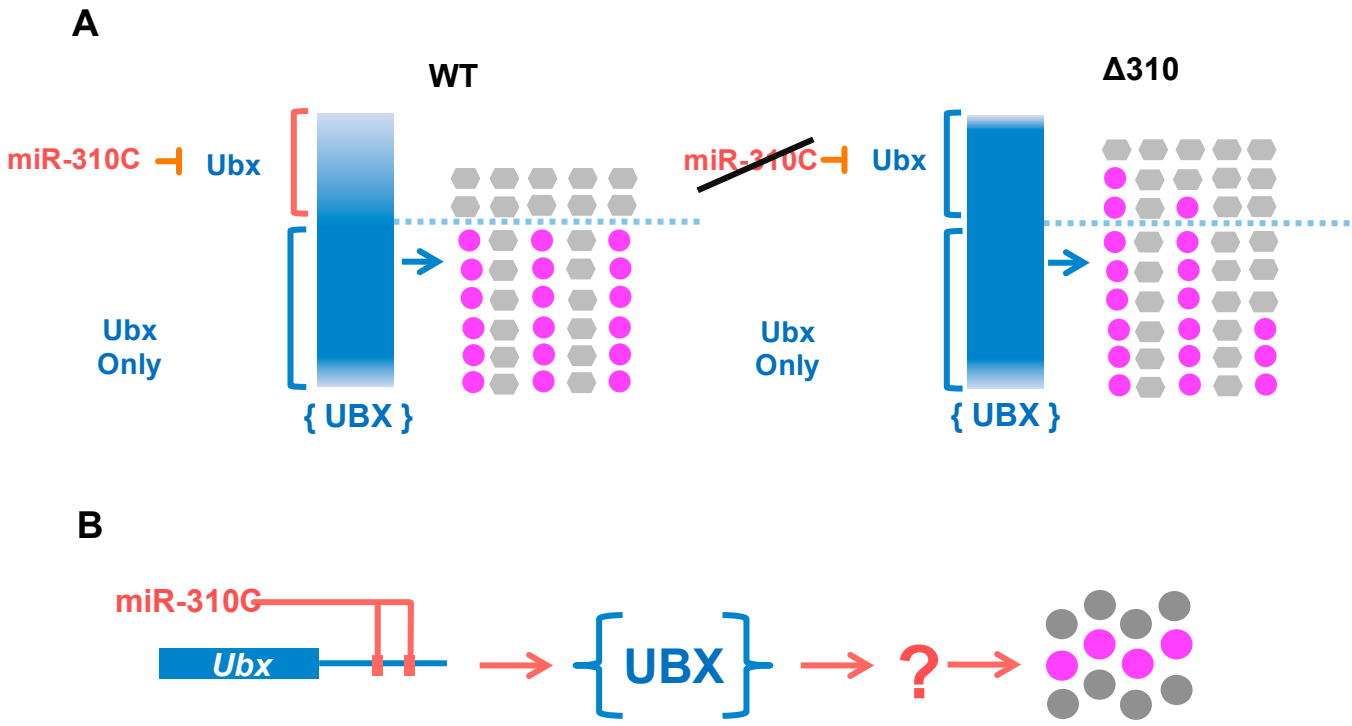

Fig.3.11 Model of *miR-310C-Ubx* interactions during haltere development

(A) Schematic illustrating the effect on Ubx expression and consequently sensory field architecture when the *miR-310C* is removed from haltere. Loss of miRNA activity leads to an increased area of high *Ubx* expression. This results in changing the sensory field organisation within the haltere. (B) Schematic illustrating the regulatory axis of *miR-310C* regulation of *Ubx* leading to correct sensory field patterning. Question mark highlights the missing link that connects *Ubx* expression to directing sensory field organisation.

tissue in which this process takes place. Elevated levels of *Ubx* caused by lack of *miR-310C* regulation, outside of the normal presumptive sensory field could lead to an increased area of competent tissue containing cells capable of undergoing lateral inhibition. In this example, the increasing *Ubx* levels may lead to an ectopic *Ubx* inductive function – usually only occurring within the normal sensory field, there by instigating an increased sensory field capable of forming SOP cells. Alternatively, the role of *Ubx* may be to suppress sensory tissue competency outside of the normal tissue area. Increased *Ubx* levels disrupt this function leading to a greater presumptive tissue for sensory cell formation. Considering these possibilities, the disrupted

regulation caused by the Δ310 deletion may be creating a GOF or LOF effect on *Ubx* activity.

Interestingly, a study by Takács-Vellai et al., 2007, showed that the correct specification of vulvar cells in *C.elegans* required Hox transcriptional input into the *Notch/Delta* pathway and Shroff et al., 2007, showed that different patterns of microchaetae sensory cells in *Drosophila* T1 and T3 legs were due to Hox regulation of *Delta* expression. Furthermore, a number of *Ubx* genomics studies identified members of this signalling pathway as being bound by *Ubx* within the nucleus (Choo et al., 2011; Slattery et al., 2011) and being receptive to *Ubx* transcriptional inputs (Pavlopoulos and Akam, 2011). Future studies could explore the relationship between *Ubx* activity and *Notch*/*Delta* function in specifying the correct sensory field architecture during haltere development.

The complexities in regulating *Ultrabithorax* expression

It is interesting to note that the *miR-310C* miRNAs are a relatively new addition to the *Drosophila melanogaster* genome. This group of miRNAs varies greatly between the other sequenced Drosopholids, with changes in the number miRNA present in the cluster or in some species, being completely absent. Additionally, these miRNAs are not found in any species outside of the Drosophilids but do have orthologues in other species – *miR-92a/b*, *miR-25*. We provide evidence that the loss of the *miR-310C* in *Drosophila melanogaster* has definitive consequences on the development and morphology of the haltere appendage. When considering Drosopholids that lack these miRNAs, we speculate as to what takes their regulatory place? Have alternative miRNAs taken up this regulatory role? Has the regulation of *Ubx* expression in this developmental context been alternatively wired in these species? Perhaps, more interesting is how novel regulators like new miRNAs become integrated into the gene-regulatory networks vital for the correct development of an organism? These questions are of interest in trying to understand the complex genetic relationships which emerge to control development through evolution.

The control of *Ubx* expression is complex and multi-faceted. The transcriptional regulation of *Ubx* has been thoroughly documented. These analyses revealed an array of cis-regulatory regions at the *Ubx* locus which regulate the transcriptional and epigenetic mechanisms that lead to the appropriate expression patterns of this gene. It becomes apparent that a further cis-regulatory code exists post-transcriptionally, with

regulators like miRNAs being vital for the correct functioning of the *Ubx* gene. There are doubtless many other miRNA capable of regulating *Ubx* expression. The haltere imaginal disc would provide a useful testing ground to first identify these regulators of *Ubx*, and second, to define how their regulation leads to the correct *Ubx* function and the appropriate development of the haltere. This system would also allow one to study the extent to which the possible co-ordination of multiple miRNA regulators is required for correct *Ubx* expression and how these regulatory inputs are integrated with the transcriptional regulation of *Ubx*. Elucidating these miRNA-*Ubx* regulatory interactions could serve as a paradigm for understanding miRNA-transcription factor interactions and their consequences for development.

The regulation of transcription factor activity not only depends on when and where it appears within a developing organism or the DNA sequences that it may bind to. It is increasingly apparent that subtle changes in expression levels can have direct consequences on the transcription factors functional capabilities (Zhang et al., 2012). It is in this context that important gene regulators like miRNAs must be viewed - the ability to fine-tune expression levels above or below the required limits of transcription factor activity.

Why is the *Ubx* gene under such regulatory control – both at the transcriptional and post-transcriptional level? The answer is surely due to the class of gene it belongs, the Hox genes. As transcription factors this gene family have a fundamental ability to influence countless other genes within the genome and thus must be carefully controlled. What is particularly important is the powerful ability of Hox genes to direct cell and tissue identity and function. Disruption to this function can lead to many developmental defects and disease states. As a consequence, complex regulatory mechanisms have evolved to ensure the correct functioning capabilities of these genes are maintained.

CHAPTER 4

4. miRNA expression profiling of *Drosophila* wing and haltere imaginal discs using next-generation RNA sequencing technology

4.1 Chapter Overview

Hox genes encode transcription factors which are able to direct and influence a diverse range of cell developmental programmes, dependant on spatial position and temporal window during development. How can one Hox gene define the many diverse cell fates required during animal development? Misregulation of Hox function can lead to abnormal developmental and disease phenotypes. How is the accuracy of Hox function ensured through development? What other factors within the genome, help to install and regulate the Hox genetic programmes that govern development. miRNAs are pleiotropic regulators that can act quickly to alter gene expression within any given cell. We considered to what extent, these small non-coding RNAs are utilised by powerful gene regulators, such as Hox transcription factors to implement and maintain the required gene expression changes need during development.

Ubx regulation of haltere development provides a suitable developmental context in which to assess these possible interactions. All the developmental changes which occur during haltere development are ultimately direct or indirectly regulated by *Ubx*. Thus it becomes easier to understand how miRNAs within this tissue, function alongside *Ubx* in the generation of the haltere.

To elucidate the potential roles miRNAs may have in haltere developmental programmes, we must first know which miRNAs are present within the haltere imaginal disc, and secondly, how specific or general this miRNA expression is, by first identifying the miRNAs present within a similar tissue – the wing imaginal disc.

In this chapter we describe the miRNA profiling during the development of two serially homologous appendages – the wing and haltere, using next generation sequencing technology. Comparing these miRNA profiles reveal that the repertoire of miRNAs within the haltere is more diverse, with many miRNAs only detectable within this tissue when compared to the wing. We also reveal that the expression of a small group of miRNAs represent the majority of total miRNA expression in both tissues. Through analysis of miRNA expression levels within each tissue we hypothesise that the differential miRNA expression seen between these tissues is generated at a post-transcriptional stage of miRNA biogenesis.

4.2 Small RNA profiling of *Drosophila* imaginal discs

To understand the relationship between miRNA activity and *Ubx* regulation of haltere development, we set out to document the full mature miRNA content of the wing and haltere imaginal discs using next-generation RNA sequencing.

The pipeline used to generate the wing and haltere small RNA libraries is summarised in Fig.4.1A. Wing and haltere imaginal discs were collected from the white pre-pupal developmental stage (Fig.4.1B). At this point in development, the larvae are preparing for the process of metamorphosis where they will subsequently undergo their transformation into the adult form. This developmental stage was chosen because it is representative of an interesting developmental transition, a point in which the imaginal discs of the larvae are at the end of a long period of growth, cell proliferation and extensive pre-patterning. During pupal development, the simple epithelial tissue of the imaginal disc will differentiate into the complex structures of the adult appendages. Experimentally, this time-point was also useful in that the morphological markers of white pre-pupae larvae are easy to identify and allow for the collection of multiple samples of developmentally homogenous wing and haltere tissue. In order to produce enough RNA for sequencing, wing and haltere imaginal discs were collected in separate rounds of dissection to minimise the chances of cross-contamination. Total RNA was isolated and sent to the University of North Carolina Sequencing Facility. Here, the small RNA content of each sample was isolated, processed and submitted for Illumina sequencing.

Having received the raw sequencing data, we next had to perform the necessary quality control steps before in depth analysis of the small RNA profiles could begin. All sequencing data processing was performed using the public access GALAXY platform. The quality filter and trimming results are summarised in Fig.4.1C.

Fig.4.1 Small RNA profiling of *Drosophila* imaginal discs

(A) Schematic of experimental pipeline to obtain sequenced small RNA libraries of wing and haltere imaginal discs. (B) Developmental timeline of post-embryonic *Drosophila* development. Samples for sequencing were taken from the pre-pupal developmental stage (blue-shadow). (C) Summary of quality control filters used on the sequenced libraries. (D) Summary of genomic alignments performed with sequenced libraries. (E-F) Summary of aligned RNA content present in wing and haltere small RNA libraries, the majority of sequenced reads align to miRNA genes.

Fig.4.1 Small RNA profiling of Drosophila imaginal discs

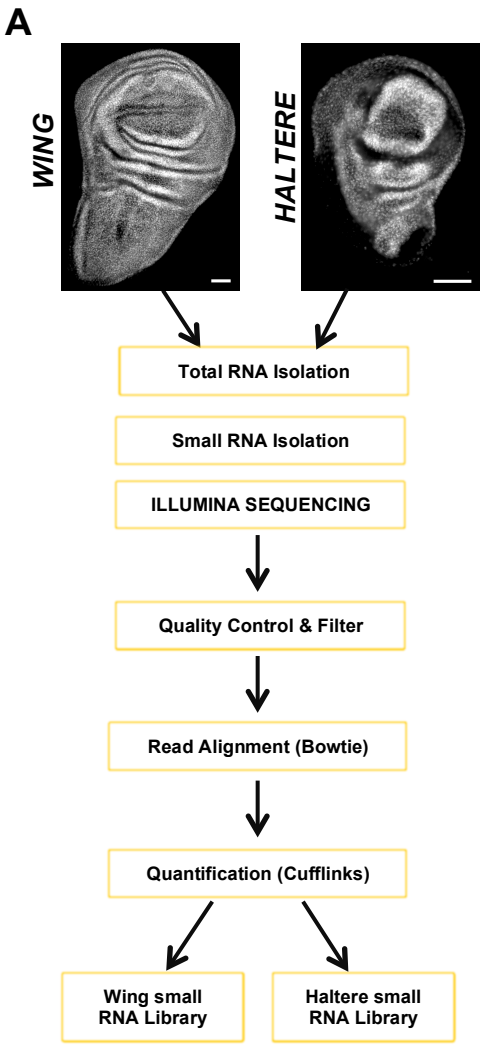

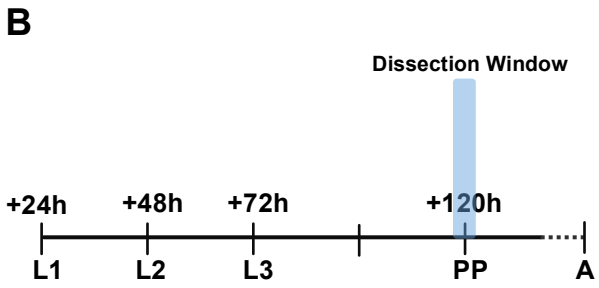

C

	Wing (Reads)	Haltere (Reads)
Illumina Library	19,439,402	124,112,017
Quality Filter	-1,534,527	-7,232,308
Trim Filter	-15,705,428	-105,883,019
Final Count	2,054,481	10,996,690

D

	Wing	Haltere
All Reads	2,054,481	10,996,690
Aligned Reads	~2,000,000	~10,000,000

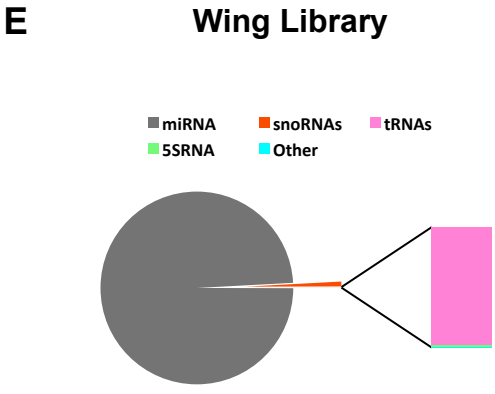

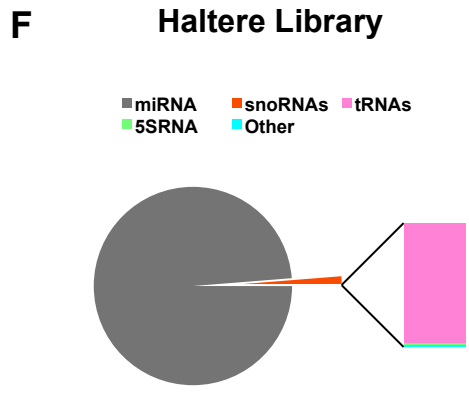

We began by performing a read quality filter on all reads from both libraries. Following sequencing, the Illumina methodology results in every nucleotide of each read given a quality score. In applying a read quality filter, we remove reads that don't meet certain criteria dependant on these quality score. To filter our reads, we used a minimum score cut-off of 20 and minimum percentage of 90. Essentially, these two criteria mean that only reads that have a minimum score of 20 or above across 90 percent of the nucleotides within each read will pass this filter.

During the Illumina protocol, our cDNA libraries are ligated to specific adaptor sequences, which are required for the Illumina methodology to work. If the ligated small RNA is smaller than the total sequencing length of the Illumina run, sections of the ligated adapter will also be sequenced (for example, a 20 nucleotide microRNA ligated to an adapter that undergoes 35bp Illumina sequencing would result in 15 nucleotides of the read output belonging to the ligated adapter). Because of this phenomenon, our second quality control and filter step involved trimming unwanted adaptor sequences and then filtering the remaining reads by size, only allowing reads with a minimum of 18 nucleotides to pass. The resulting RNA read libraries could then be used to map and quantify the small RNA profiles of each tissue. When comparing both our samples, it was seen that the trim filter removed a greater number of reads from the haltere sample compared to wing.

Close analysis of some of the reads being removed showed that a large proportion of the raw haltere read library contained reads that were the result of sequencing the ligated adaptors. One explanation for this would be that in preparing the libraries for sequencing, an error occurred which resulted in a large proportion of un-ligated adaptor sequences which would subsequently be removed using the trimming filter. This could possibly be due to lack of abundant small RNAs within the haltere sample and therefore an abundance of un-ligated adaptors. Alternatively, a problem could have occurred in the ligation step leading to a large number of free adaptor sequences that were consequently sequenced. Due to the fact that a third party (North Carolina High-Throughput Sequencing Facility) facility performed library preparation and sequencing we are unable to resolve this issue or determine the extent to which this may affect our results.

The resulting libraries of small RNA reads were aligned to the most current published *Drosophila melanogaster* (BDGP5.6) genome annotation using *Bowtie* (Langmead et al., 2009) within the *GALAXY* platform. The library alignments are summarized in

Fig.4.1.D. Quantification of read alignments was achieved using the *Cufflinks* (Trapnell et al., 2010) program available through *GALAXY*.

Using this pipeline, we generated small RNA libraries from wing and haltere imaginal discs aligned to the *Drosophila* genome. To assess the quality of our libraries, we quantified the percentage of reads mapped to miRNA genes within the *Drosophila* genome compared to other RNA elements detected within our small RNA libraries. The small RNA isolation step performed at the beginning of the pipeline should ensure that the majority of the libraries will be constituted by miRNA reads. We see that this is indeed the case, both wing and haltere samples contain over 99% reads mapped to miRNAs. The remaining reads were aligned to tRNAs, snoRNAs and 5S ribosomal RNAs. A very small percentage aligned to other mRNAs within the genome, likely resulting from the sequencing of degraded mRNA products present within our total RNA samples.

4.3 The miRNA profiles of *Drosophila* wing and haltere imaginal discs.

The initial aim of this study was to document the miRNA content present within two similar tissues at a specific developmental transition. Having initially shown that our small RNA libraries primarily contained miRNAs, we next documented in detail which miRNAs were present within the wing and haltere and to what extent miRNAs were differentially expressed between these two tissues.

Fig.4.2 miRNA profiles of *Drosophila* wing and haltere imaginal discs

(A) Summary analysis of miRNAs present in either wing or haltere tissue, present in both tissues or present in neither tissue. (B) Summary analysis demonstrating the number of common and distinct miRNAs found in wing and haltere tissue. (C) Scatterplot showing the expression levels (FPKM) of wing and haltere miRNAs. Arrowheads indicate highly expressed miRNAs (D) Scatterplot focusing on miRNAs highlighted in pink box of panel C. Arrowheads highlight a number of miRNAs preferentially expressed in the haltere. (E) Scatterplot summarising miRNA expression in wing and haltere tissue along a transformed LOG scale. Arrowheads highlight tissue specific miRNA expression in the wing and haltere respectively (F). Same LOG transformed scatterplot. Highlighted are miRNAs from the *miR-310C*. In the previous chapter we show that these miRNAs are functionally active in the haltere.

Fig.4.2 miRNA profiles of Drosophila wing and haltere imaginal discs

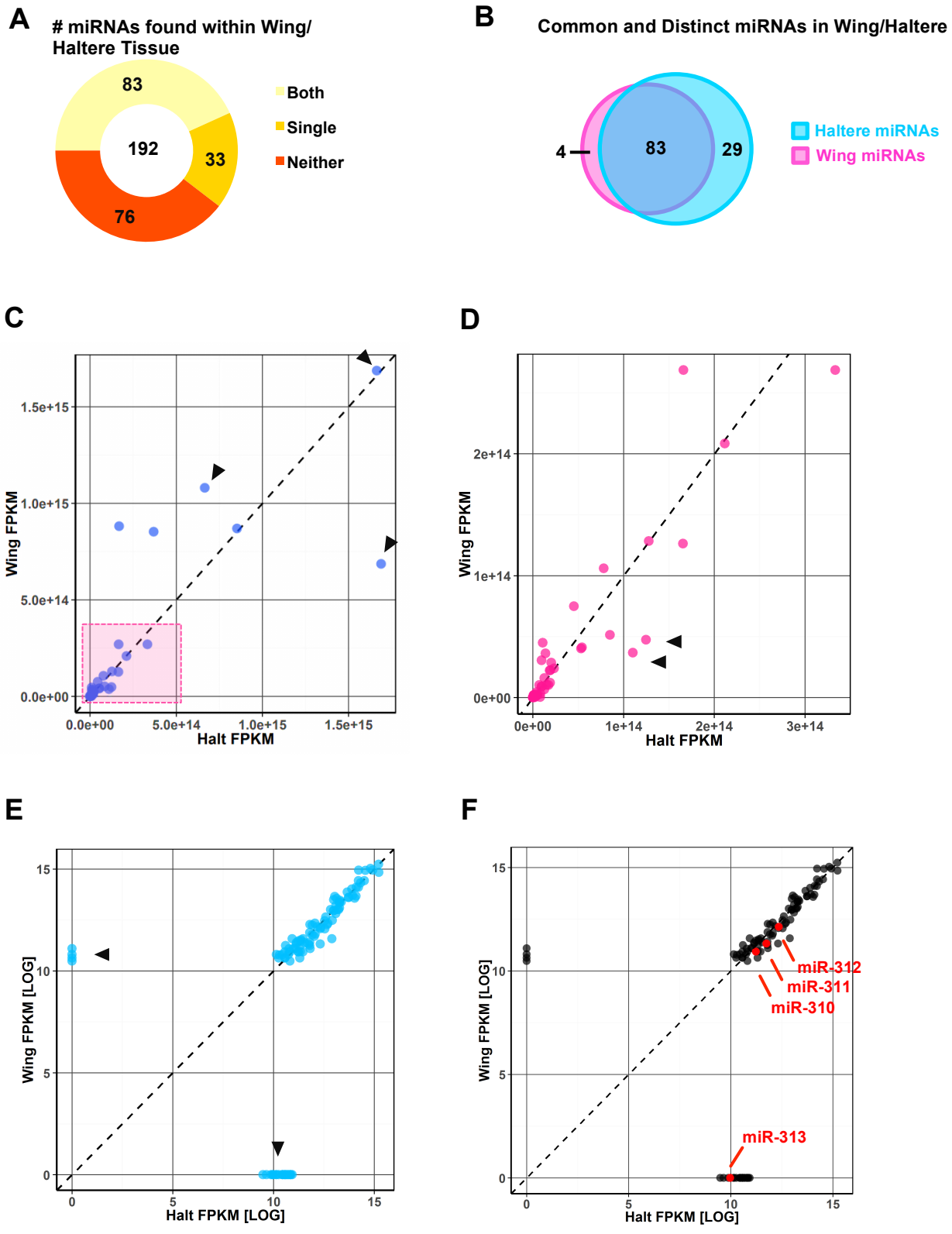

The analysis of our aligned small RNA libraries showed that out of the 192 mature miRNAs annotated within the *Drosophila* genome, 116 were expressed in either wing or haltere tissue. Of these 116 miRNAs, 83 were detectable in both tissues, whereas 33 miRNAs had expression in only one of either wing or haltere (Fig.4.2A). Of the 33 miRNAs found in only one tissue, 29 were present in the haltere tissue specifically (Fig.4.2B). Overall we see a total of 87 and 112 miRNAs present within wing and haltere tissue respectively.

We next examined the differences in miRNA expression levels between the two tissues. Relative levels of miRNA expression were calculated as FPKM abundance (Fragments Per Kilobase of exon per Million fragments mapped) which allows us to compare samples with varying numbers of sequenced reads mapped to the genome.

The relative expression levels of all miRNAs found within wing and haltere tissue were plotted together (Fig.4.2C). We see that the majority of miRNAs have relatively low levels of expression (pink box Fig.4.2C), although a number of miRNAs have much higher levels of expression in both wing and haltere tissue (arrowheads Fig.4.2C). Examining in detail the miRNAs which exhibit lower levels of the expression, (pink box Fig.4.2C), we see that the majority of miRNA expression varies little between wing and haltere tissue (Fig.4.2D). However, examples can be seen where one tissue exhibits preferential expression of individual miRNAs (arrowheads Fig.4.2D). Viewing miRNA expression along LOG transformed FPKM scales (Fig.4.2E) highlights the similarities in overall expression of miRNAs expressed in both tissues. Also easily seen are the tissue specific miRNAs, which have lower levels of overall expression when compared to the remaining cohort of miRNAs (arrowheads Fig.4.2E).

Fig.4.3 Differential expression of miRNAs in wing and haltere tissue

(A) Scatterplot showing relative log fold changes in miRNA expression when comparing haltere to wing tissue. A manual threshold of 2-fold increase or decrease in expression was used to differentiate between haltere enriched miRNAs (blue points) compared to wing enriched miRNAs (pink points). (B) Scatterplot showing miRNAs expressed in wing and haltere tissue colour coded by their differential expression class. (C) All miRNAs were sorted into 5 miRNA expression group's dependant on their differential expression levels in wing and haltere tissue. (D) Graph highlighting the top differentially expressed miRNAs when comparing wing and haltere tissue.

Fig.4.3 Differential expression of miRNAs in wing and haltere tissue

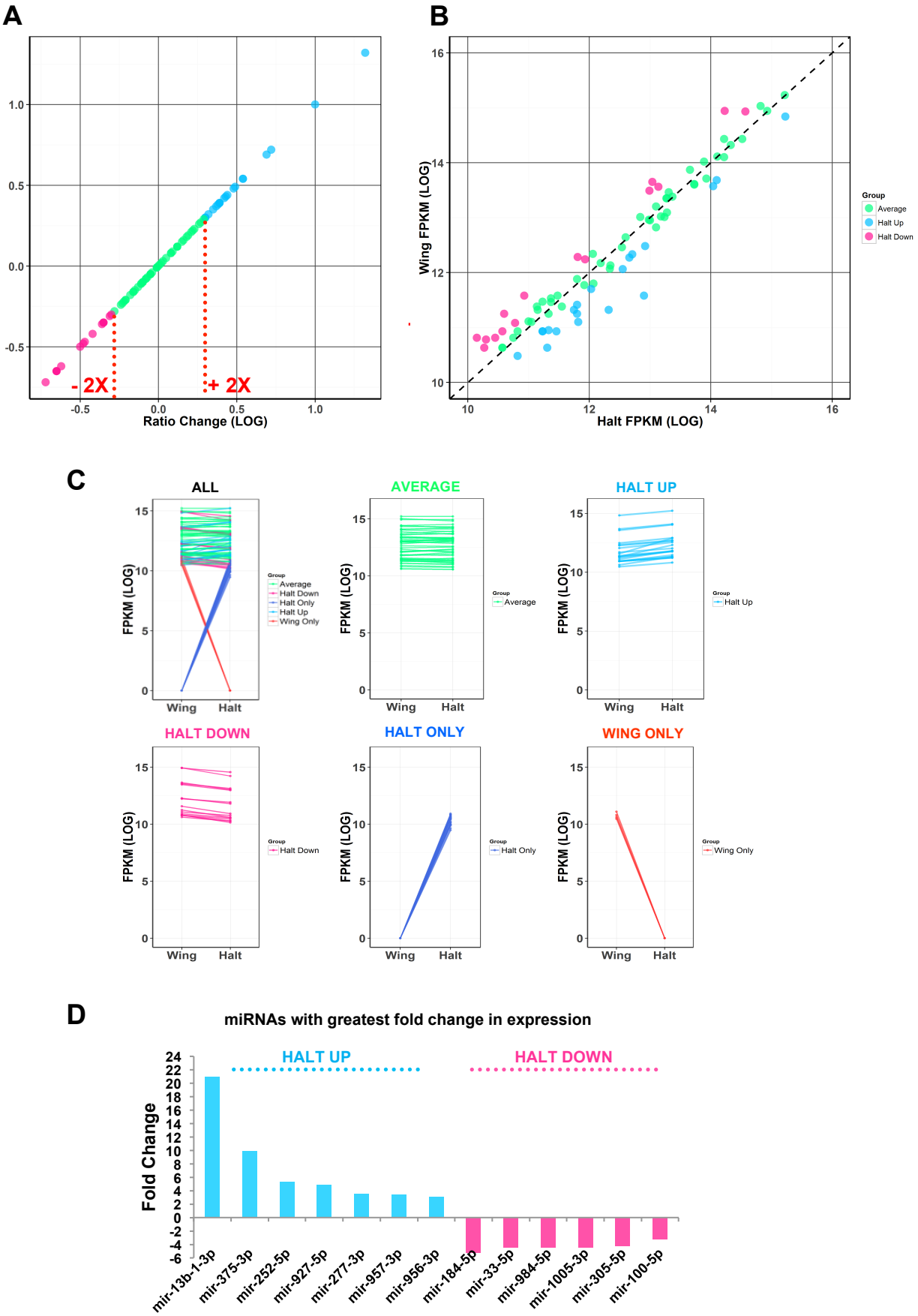

As a proof of principle to show that our datasets had picked up miRNAs that were functionally active within the haltere, we looked whether the *miR-310C* miRNAs were expressed. In the previous chapter we gathered genetic evidence indicating that these miRNAs regulated *Ubx* expression during haltere development. We observe that all four *miR-310C* miRNAs were present within haltere tissue (Fig.4.2F), including *miR-313* which was solely detected within the haltere.

Having analysed the general patterns of miRNA expression levels, we next analysed in detail at which miRNAs were expressed in both tissues, particularly to what extent their expression levels varied. We grouped individual miRNAs together dependant on their differences in expression when comparing wing and haltere samples. For this analysis

we used a two-fold increase or decrease in expression as a cut-off point to mark a preferential changesin expression patterns (Fig.4.3A). miRNAs preferentially expressed within the haltere are marked by light blue data points, those preferentially found within the wing are coloured magenta, miRNAs which exhibit less than two-fold expression changes are coloured green (Fig.4.3B).

To summarise this differential expression analysis, all miRNAs, including those detected in only one tissue were sorted into five 'miRNA Expression Groups' – Average, where miRNA expression neither increased or decreased past the two-fold limit between each tissue, the Halt Up group containing miRNAs with haltere enriched expression, the Halt Down group with miRNAs displaying wing enriched expression and finally the Halt Only and Wing Only groups where miRNAs are only detected in one tissue respectively (Fig.4.3C). Generally we see that the miRNA expression changes are not greater than a two to three fold between the two tissues, however there are notable exceptions. For example, *miR-13b-1* shows an approximate 20-fold increase in expression within the haltere compared to the wing. Overall, only a small group miRNAs exhibit a three-fold or greater change in expression (Fig.4.3D).

4.4 Analysis of miRNA content from wing and haltere imaginal discs

Having sorted miRNAs from both wing and haltere imaginal discs into five groups based on their expression profiles, we next examined in detail the characteristics of these groups.

We began by analysing the number of miRNAs within each expression group (Fig.4.4A). In both tissues, the biggest complement of miRNAs belongs to the Average

expression group, followed by the Halt Up and Halt Down expression groups respectively. The Wing Only expression group contains the fewest number of miRNAs out of all the expression groups, a stark contrast to the Halt Only group which contains an abundance of miRNAs, the second largest contingent within the haltere. Overall, we see that the haltere tissue contains an expanded complement of miRNAs compared to the wing, in particular, expressing a large number of tissue specific miRNAs.

We analysed the distribution of miRNA expression profiles per group in each tissue (Fig.4.4A-B). In general, we see that the three expression groups, representative of miRNAs present in both tissues (Halt Up, Halt Down, Average) display a wide distribution of expression levels. The tissue specific miRNAs are expressed at the lower end of the scale compared with the shared miRNA expression groups. This could be a concern in evaluating whether these tissue specific, but lowly expressed miRNAs, could be artefacts in the miRNA profiling protocol and therefore biologically meaningless. However, miRNAs from the three main expression groups (Average, Halt Up & Halt Down) are also represented at these lower expression levels suggesting that this is not the case (see bars to the left of the dotted lines Fig.4.4A-B).

We assessed the contribution that each miRNA group makes to the total miRNA content of each tissue (Fig.4.3D-E). The largest contribution to total miRNA levels is the Average expression group, containing 66% and 64% of total wing and haltere miRNA reads respectively. As was maybe expected, the Halt Up expression group is the next highest contributor to total haltere miRNA expression, conversely the Halt Down miRNAs are the second highest contributor to the wing miRNA content.

Interestingly, in both tissues, the complements of tissue specific miRNAs contribute a very small percentage of total expression (Fig.4.3D-E). This could indicate that the expression of these miRNAs is discrete within the imaginal discs but that they may provide a very specific regulatory function.

Fig.4.4 Analysis of miRNA content from wing and haltere imaginal discs

A) Comparison of miRNA content in wing and haltere tissue. miRNA contributions colour coded by their miRNA expression group association. miRNAs which are appendage specific are delineated from miRNAs present in both tissues. (B-C) Histograms showing the distribution of miRNA expression values in wing (B) and haltere (C) tissue. Distributions are separated and colour coded by miRNA group association. (D-E) Contributions of each miRNA expression group to the total miRNA content present in the wing (D) and haltere (E).

Fig.4.4 Analysis of miRNA content in wing and haltere imaginal discs

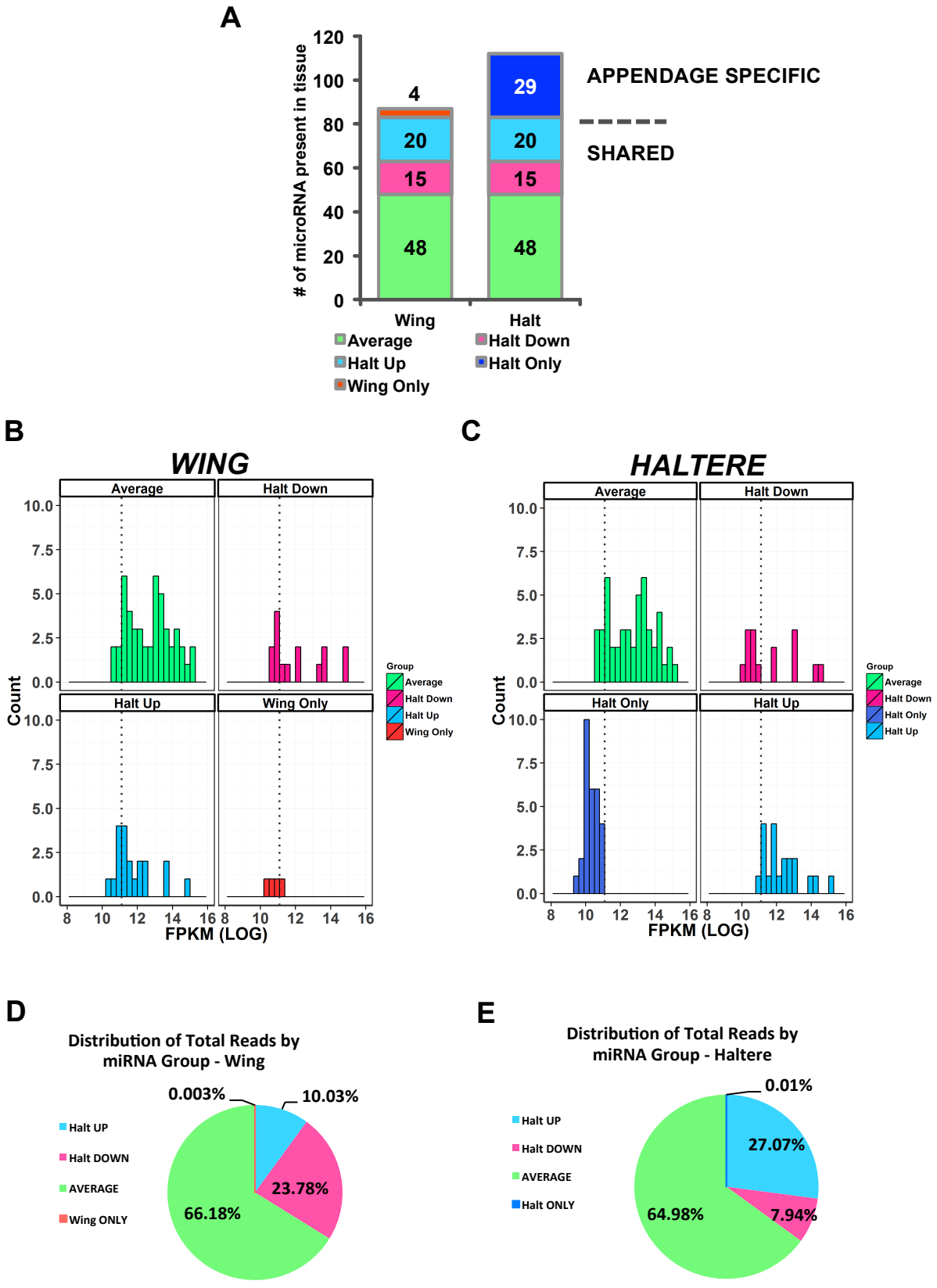

Another possibility is that these miRNAs have particular spatially restricted expression patterns which generate a small expression profile.

Having quantified the contribution of each miRNA expression group to the total miRNA content within each tissue, we next examined the contribution of individual miRNAs to each miRNA expression group (Fig.4.5A). For miRNAs present in both tissues, we used the haltere expression data for this analysis. For the Wing Only and Halt Only expression groups we used their tissue specific expression data respectively. In these stacked bar charts, each rectangle represents the relative contribution of an individual miRNA to each respective expression group. In the three main groups, representing the most significant contributions to total miRNA content – the Average, Halt Up and Halt Down groups - only a small number of individual miRNAs contribute a large proportion of the total reads attributed to each expression group. Alternatively, in the Halt Only and Wing Only tissue specific groups, which contribute least to total miRNA levels, the proportion of reads attributed to each individual miRNA is smaller and consequently the distribution of total reads is spread amongst many.

Finally, we examined the miRNAs which contribute most to the total miRNA levels in wing and haltere tissue (Fig.4.5B-C). Both tissues exhibit a similar set of miRNAs in the top echelons of expression, albeit with varying contributions. The main difference between the two tissues is the presence of *miR-9b-5p* within the wing and *miR-275-3p* within the haltere. In both tissues, the top fifteen miRNAs make up approximately 94% of total miRNA expression in each tissue.

Overall, this analysis shows that the total miRNA content of both wing and haltere tissue is dominated by a small group of miRNAs, each exhibit a large level of expression in both tissues. The majority of miRNAs within each tissue contribute little to total expression levels. Future studies may be able to address the functional significance of this heavily weighted distribution in total miRNA expression for wing and haltere development. Do highly expressed miRNAs regulate basic cellular and developmental processes? Do lowly expressed miRNAs have specific functions related to appendage development and morphological diversity?

Fig.4.5 Individual miRNA contributions to total miRNA content in wing and haltere imaginal discs

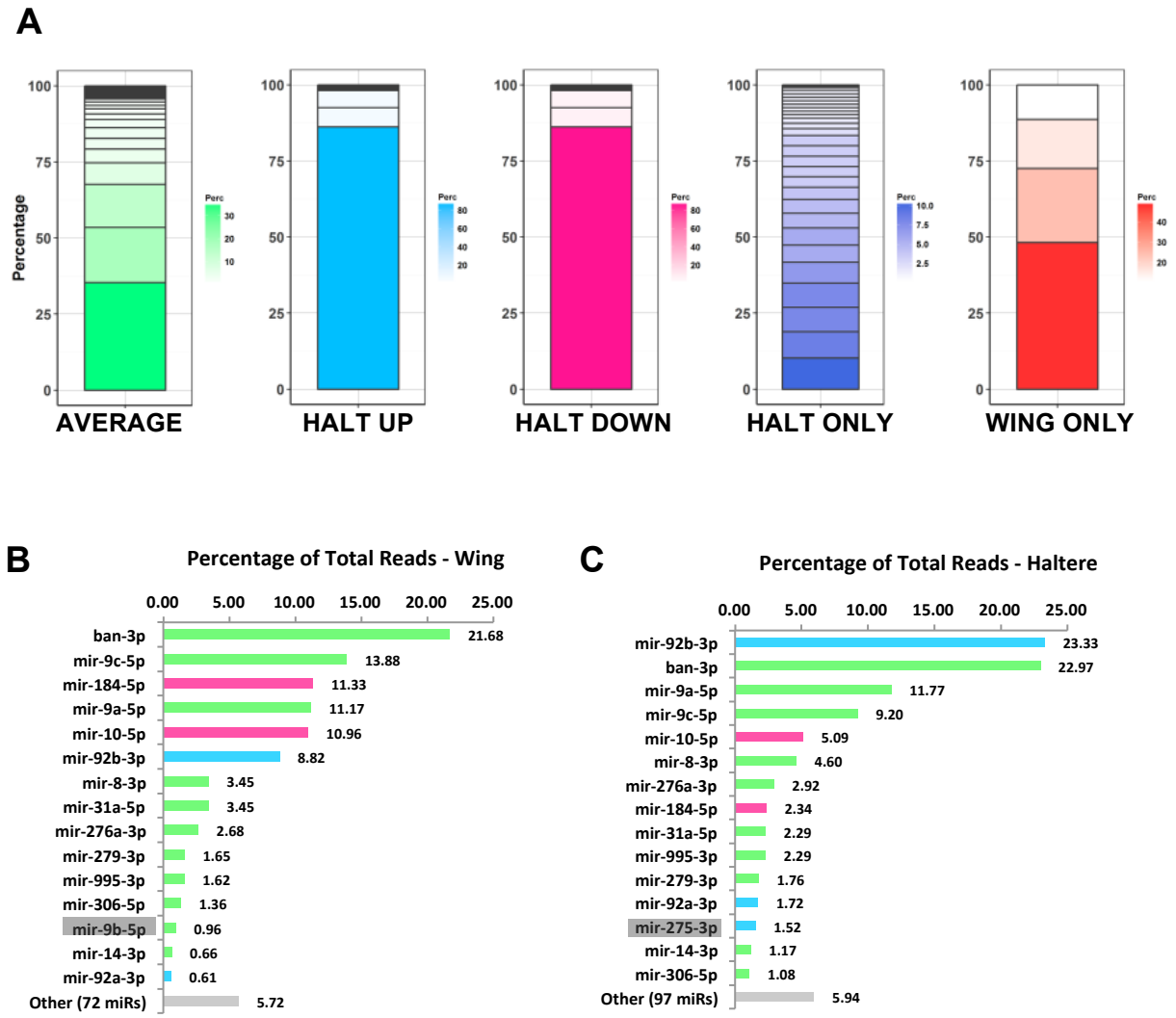

Fig.4.5 Individual miRNA contributions to total miRNA content in wing and haltere imaginal discs

(A) Analysis of individual miRNA contributions to total expression levels in each miRNA expression group. Each coloured rectangle represents an individual miRNA expression contribution as a percentage of the total. (B-C) Analysis of the most highly expressed miRNAs in wing and haltere samples.

4.5 Differential miRNA expression through the regulation of miRNA transcription

The analysis of our RNA sequencing data revealed a high level of differential expression amongst miRNAs within the wing and haltere imaginal discs. We were intrigued as to how this differential expression was achieved. Was it possible that regulation of primary miRNA transcription could lead to the establishment of different levels of mature miRNAs in the wing and haltere tissue? Could *Ubx* be the controlling factor in regulating this differential transcriptional activity?

To address this question we quantified the expression levels of a number of pri-miRNA transcripts in wing and haltere tissue to understand if pri-miRNA levels were indicative of the mature miRNA expression detected in our sequencing libraries.

There are currently 192 annotated miRNAs within the *Drosophila* genome. Due to the phenomena of miRNA clustering and miRNA/miRNA* processing, these annotated miRNA are situated at 120 transcriptional loci within the genome. The analysis of our sequencing data shows that 69% of these loci (83 transcriptional sites) are active in either the wing, haltere or both tissues (Fig.4.6A). When we look closely at these active loci, we see that only half of these sites are situated in intergenic regions of the genome (Fig.4.6B). The remaining active miRNAs are positioned within the introns of protein coding genes. This could be of potential importance when considering how these miRNA transcriptional loci are regulated.

To examine the relationship between pri-miRNA transcript levels and mature miRNA expression, we collected total RNA from developmentally staged white pre-pupae to match the staged collections used for small RNA sequencing.

Fig.4.6 Differential miRNA expression through the regulation of miRNA transcription

(A) Summary of active/inactive miRNA transcriptional loci in the wing and haltere imaginal discs. (B) Summary of intergenic/intronic nature of active miRNA transcriptional loci. (C) Summary bar charts of primary-miRNA expression levels for four miRNAs belonging to the Average miRNA expression group. (D) Summary bar charts of primary-miRNA expression levels for five miRNAs belonging to the Halt Only expression group. Expression levels were determined by averaging 3 technical repeats for biological samples of wing and haltere imaginal discs. Error bars indicate standard deviation of each biological sample average. Statistical significance was determined using Student's t-test, p-values given in figure.

Fig.4.6 Differential miRNA expression through the regulation of miRNA transcription

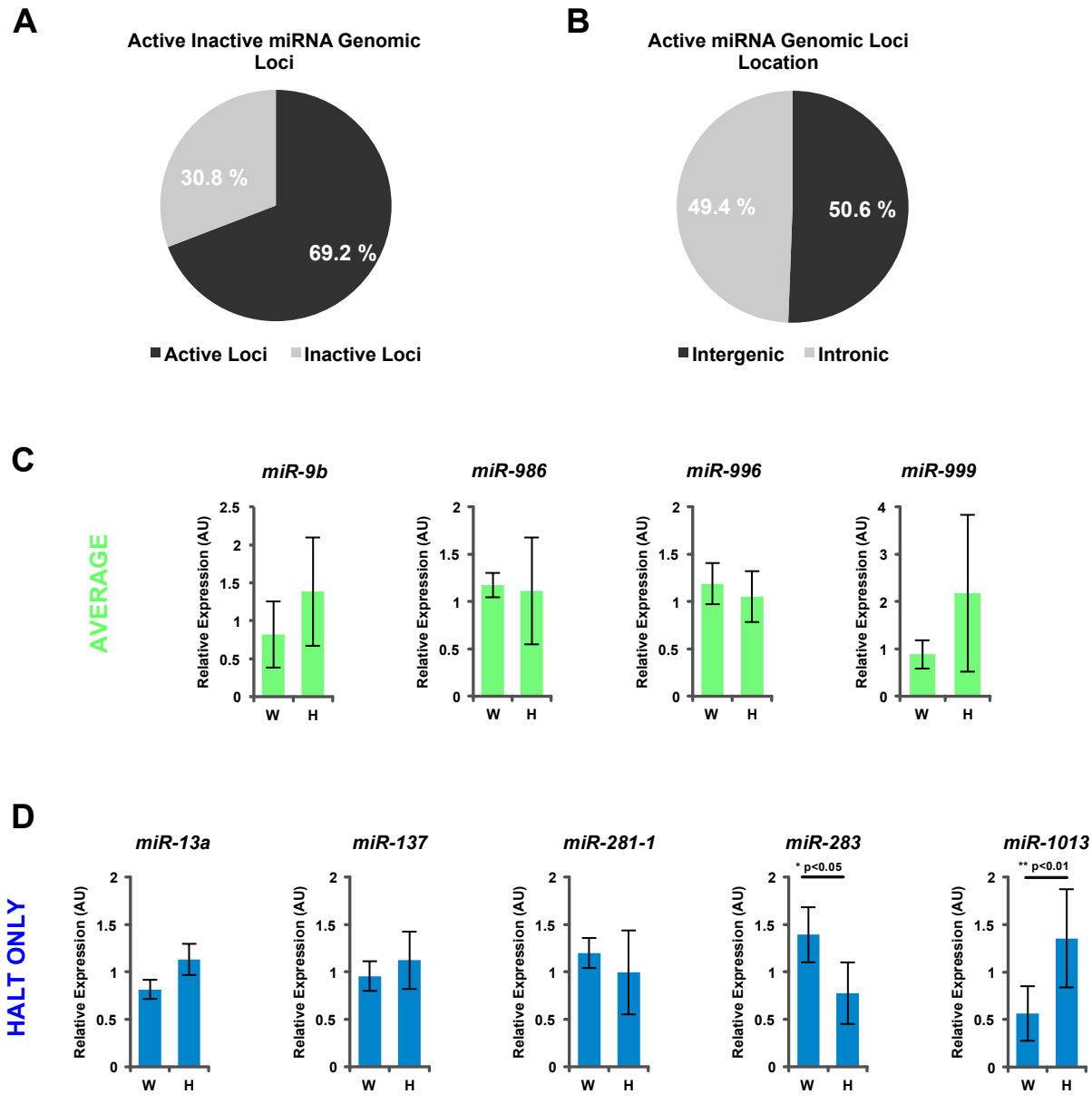

A selection of candidate miRNAs from the Average and Halt Only expression groups were tested for pri-miRNA expression levels using SQ-RTPCR. If pri-miRNA transcriptional regulation was a leading factor in generating differential miRNA expression, we would expect to see differential pri-miRNA expression that would match mature miRNA levels.

We first analysed the expression levels of four pri-miRNAs – *miR-9b-306-79-9b*, *miR-986*, *miR-279-996*, *miR-999* containing miRNAs from the Average expression group (Fig.4.4C) in wing and haltere tissue. Our results show that none of these pri-miRNAs showed any significant changes in expression level between the two tissues. This matches with our mature miRNA sequencing data for these miRNAs. We next analysed the expression levels of five pri-miRNA transcripts – *miR-13a-13b-2c*, *miR-137*, *miR-281-1/2*, *miR-283-304-12*, *miR-1013*, each containing miRNAs from the Halt Only expression group. Interestingly, each pri-miRNA tested had detectable expression in the wing and haltere tissue, including *pri-miR-283-304-12* and *pri-miR-1013,* the two pri-miRNAs which did display significant differential expression between wing and haltere tissue. This data does not match that seen at the mature miRNA level where expression is only detected in the haltere.

The fact that all five pri-miRNAs containing haltere specific mature miRNAs are also transcribed in the wing suggests that it is unlikely that the regulation of miRNA transcription is a driving force in generating differential mature miRNA expression in the wing and haltere. The caveat to this observation is that our sequencing data and these experiments examine one developmental time point. Since the biogenesis of mature miRNAs relies on a number of biochemical processing steps, it is conceivable that changes in mature levels lag behind the regulation of pri-miRNA expression. Detailed analysis of miRNA content at both the pri-miRNA and mature miRNA level during a progression of developmental time points can resolve this issue.

4.6 Analysis of miRNA cluster expression

Our analysis of pri-miRNA levels in wing and haltere tissue suggest that the transcriptional regulation of miRNA expression is unlikely to be the mechanism in which differential miRNA expression patterns are generated in the wing and haltere. This leaves the post-transcriptional regulation of miRNA biogenesis as the most viable path in which diverse miRNA expression levels are created in these two tissues.

To assess to what extent the post-transcriptional regulation of miRNA biogenesis maybe responsible for generating differential miRNA expression, we looked in detail at the miRNAs situated in 'miRNA clusters' within the *Drosophila* genome. These clusters contain several pre-miRNA sequences that are transcribed as a long polycistronic pri-miRNA transcript which is then processed into a multiple pre-miRNAs and subsequently, multiple mature miRNAs. These clusters are under the same transcriptional regulation, therefore any differences in mature expression levels must result from regulation of miRNA biogenesis. If post-transcriptional regulation of miRNA biogenesis does take place within the wing and haltere imaginal tissues, we would expect to see evidence of this within the expression levels of clustered miRNAs.

There are 192 miRNAs annotated within the *Drosophila* genome, 75 of these are positioned within a "miRNA cluster" (Fig.4.7A). Analysis of our miRNA expression data revealed that out of the 75 clustered miRNAs, 48 (64%) had detectable expression in either the wing, haltere or both imaginal tissues (Fig.4.7B). The 75 clustered miRNAs are situated within 20 genomic loci. The size of each miRNA cluster varies from two to eight miRNAs, the majority of miRNA clusters containing two to three miRNAs (Fig.4.7C). A miRNA cluster can be situated in either intergenic or intronic regions of the genome (12 intergenic loci, 8 intronic loci). Analysis of clustered miRNA expression patterns shows that 87% of the miRNA clusters exhibit differential expression within a cluster. (Fig.4.7D).

We examined the distribution of clustered miRNA expression patterns to assess if there is a preferential association for a particular miRNA expression group to miRNA clusters. The largest contributing miRNA expression groups were the Average, Halt Only and None expression groups (Fig.5E).

Fig.4.7 Expression analysis of miRNA clusters in wing and haltere tissue

(A) Summary of the number of clustered and non-clustered miRNA out of the 192 miRNAs annotated in *Drosophila*. (B) Division of the 75 clustered miRNAs expressed or not-expressed in wing and haltere tissue. (C) Distribution of miRNA cluster sizes found in *Drosophila*. (D) Summary analysis of heterogeneous or homogenous expression patterns of miRNA clusters in wing and haltere tissue. (E) Analysis of expression group associations of example miRNA clusters. (F) Diagram of *miR-13b-13a-2c* miRNA cluster and accompanying expression levels in wing and haltere tissue. Bracketed values represent log fold changes between wing and haltere tissue. (G) Diagram of *miR-310-313* cluster and accompanying expression levels in wing and haltere tissue.

Fig.4.7 Expression analysis of miRNA clusters in wing and haltere tissue

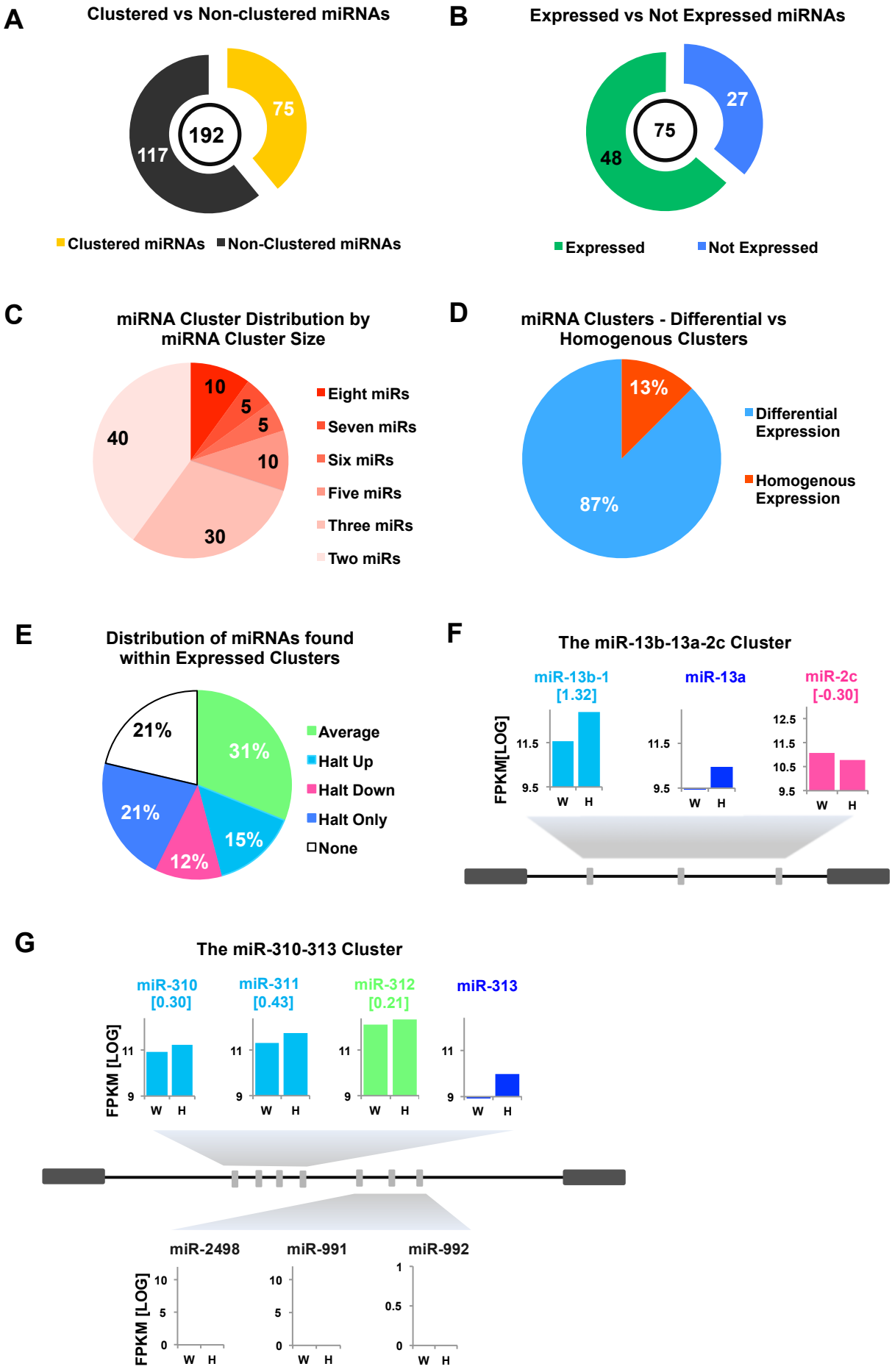

These ratios reflect that these groups contain the most miRNAs, therefore would be more likely to be represented within miRNA clusters. There is likely no overt preference for clustered miRNAs to belong to a particular expression profile.

The miRNA expression patterns within a cluster can vary, both in terms of differential expression between wing and haltere as well as the general level of expression within one tissue. For example, the *miR-13b-13a-2c* cluster contains three miRNAs (Fig.4.5F), each display differential expression patterns between wing and haltere. The three miRNAs belong to the Halt Up, Halt Only and Halt Down expression groups respectively. There are also significant differences in total levels of expression. The expression of *miR-13b-1* in both the wing and haltere is much higher than *miR-2c* and *miR-13a* expression. The *miR-310-313* cluster contains eight miRNAs (Fig.4.5G) which exhibit both differential expression and differences in total expression (*miR-310*, *miR-311*, *miR-312* and *miR-313*). Additionally, three miRNAs within the cluster are not detected in either the wing or haltere tissue (*miR-2498*, *miR-991*, *miR-992*).

Overall, our analysis reveals that a large degree of differential expression exists within miRNA clusters. We find that the majority of miRNAs found within clustered loci display differential expression patterns when compared to other miRNAs within the cluster. In some cases a cluster may have miRNAs expressed with high abundance as well as being completely absent. If all miRNAs from each cluster are under the same transcriptional regulation (the production of a long poly-cistronic primary transcript) then we must reason that the underlying cause of this differential expression is regulation at post-transcriptional stages of miRNA biogenesis. Alternatively, differential degradation and stability of mature miRNAs within each tissue could possibly lead to different expression patterns.

4.7 Analysis of dual strand selection from miRNA hairpins

During miRNA biogenesis, a key processing step is the excision of the mature miRNA duplex from the pre-miRNA hairpin. Following cleavage, the mature miRNA strand is loaded into the *Argonaute1* (*Ago1*) protein of the RISC complex and the passenger strand or miRNA* sequence is degraded. It is becoming evident that in some cases, the miRNA* species is not degraded but instead loaded into a RISC complex. This dual processing of the miRNA hairpin is significant in that in can produce two mature miRNA species (from the 5’ and 3’ arm of the pre-miRNA sequence) with differing ‘seed’ targeting sequences from one genomic location.

Our analysis of miRNA cluster expression suggests differential miRNA expression can be generated by post-transcriptional regulation of miRNA biogenesis. To look further into this aspect of miRNA regulation we examined instances where both the mature miRNA and miRNA* species are generated from the pre-miRNA hairpin and questioned if dual arm processing could represent a regulated post-transcriptional event during appendage development.

There are currently 21 genomic loci within *Drosophila* which have been shown to generate stable miRNAs from both arms of the pre-miRNA hairpin. Analysis of our sequencing data showed that just under half (47%) of these loci show expression of at least one mature miRNA from either the wing, haltere or both tissues (Fig.4.8A).

We compared the expression levels of both mature miRNA species (5p Arm/3p Arm) produced from the mature miRNA duplex in both wing and haltere tissue (Fig.4.8B). Six of the ten dual arm miRNA loci have detectable expression levels of both miRNA species from the mature miRNA duplex. Our analysis shows that in both wing and haltere tissues, similar levels of expression are not seen when comparing mature miRNAs originating from the same hairpin. This indicates that for a number of miRNA loci, both mature arms of the miRNA duplex are processed but this does not result in equivalent levels of mature miRNA. Whether these differences in expression are a result of active regulation of miRNA maturation is not known.

We assessed which miRNA expression groups were associated with miRNA loci that exhibit differential arm expression in wing and haltere tissue. We find that all expression groups were represented by these dual arm miRNAs (Fig.4.6C). Specifically, the Average, Halt Down and Halt Only expression groups accounted for the majority of miRNA group associations. Interestingly, only 35% of the miRNAs belonged to the Average expression group.

Fig.4.8 Analysis of dual strand processing from pre-miRNA hairpins

(A) Summary of expressed vs non-expressed annotated dual arm miRNA loci wing and haltere tissue. (B) Expression analysis of dual arm loci in wing and haltere tissue, shades of colour are representative of FPKM values, black boxes represent no detectable expression in either tissues. (C) Summary of overall group associations for dual arm miRNAs. (D) Comparison of group association from miRNAs originating from the same pre-miRNA hairpin. (E) Analysis of 3p/5p ratio of dual arm processing comparing wing and haltere tissue.

Fig.4.8 Analysis of dual strand processing from pre-miRNA hairpins

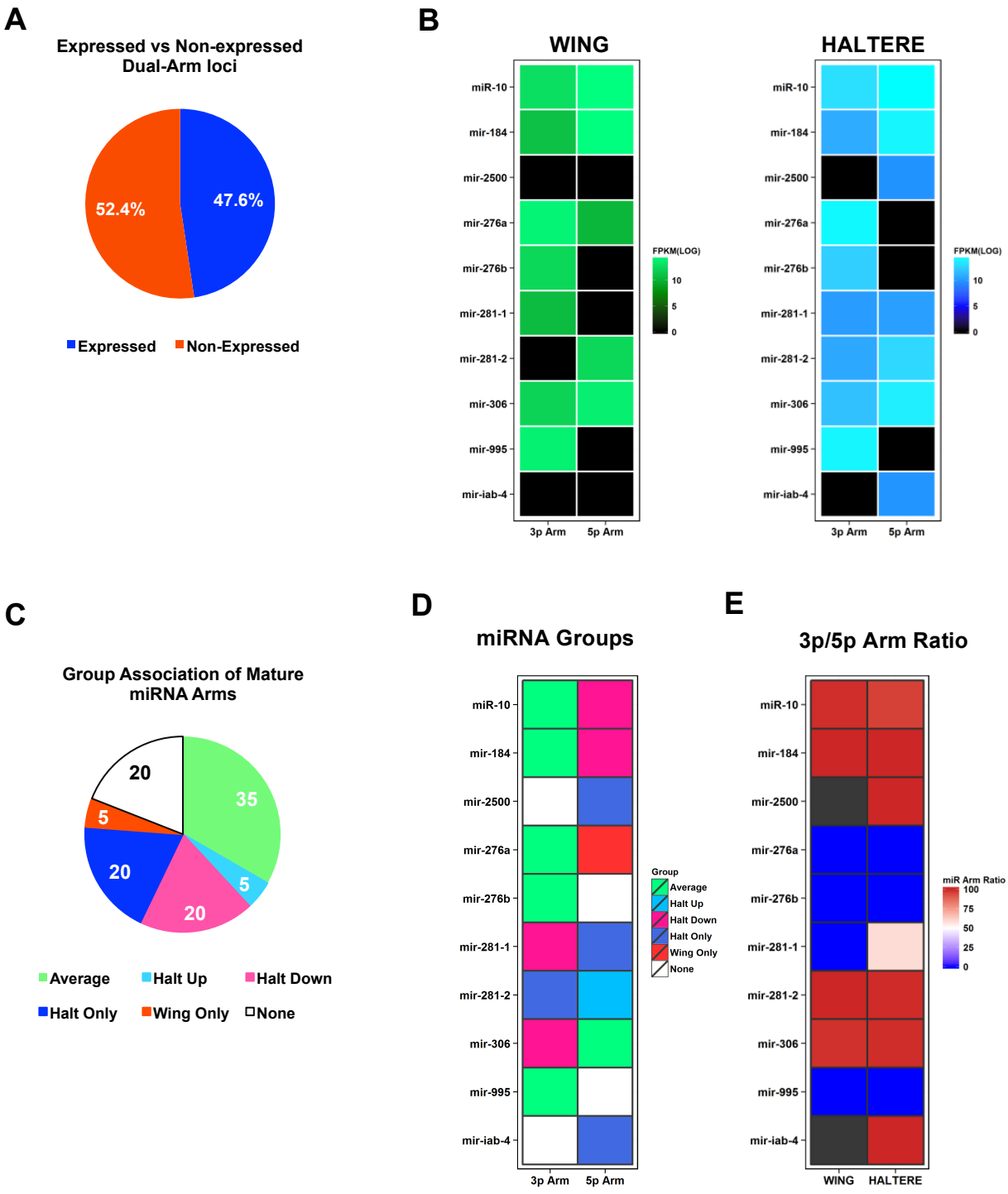

The indication is that that the majority of dual arm miRNAs exhibit differential expression between wing and haltere tissue as well as the differential expression between mature miRNA and miRNA* species.

Comparing the specific group associations of both the 5p and 3p mature miRNAs from each miRNA loci (Fig.4.8D) we see that no dual arm loci contained miRNAs belonging to the same expression group. This would be expected since we observed little similarity in mature miRNA levels coming from the same loci (Fig.4.8B). Interestingly, there appears to be a particular bias for 3p Arm miRNA species to belong to the Average expression group. This could suggest that the 5p arm of the pre-miRNA hairpin is under greater regulatory pressure within wing and haltere tissue.

Our analysis of miRNA expression levels and expression group association indicate a tendency towards one mature miRNA of the duplex being dominantly expressed. To look at this phenomenon more closely, we used our sequencing data to generate a ratio of 5p to 3p processing from each miRNA hairpin in both wing and haltere tissues (Fig.4.8E). In general, we confirm that the majority of miRNA dual arm loci predominately express one miRNA species from each duplex. We do not see a preference to which arm of the miRNA duplex is the dominant strand. Counting both tissues, there are ten instances that show strong bias towards the 5p arm compared with seven instances where the bias is towards 3p arm processing.

Our analysis also shows that for most loci there are no significant changes in arm choice between wing and haltere tissue. The exception to this observation is *miR-281-1* which changes in arm bias when comparing wing and haltere tissue. In wing tissue, only expression from the 3p arm is detected. However, expression from both 5p and 3p arms is observed within the haltere. Furthermore, the arm bias ratio is just over 50% towards the 5p arm indicating both miRNA species from this duplex are processed in approximately equal measure. Further investigation can determine how this change in bias is generated and the functional implications that this may have.

Overall our assessment of differential processing from dual arm miRNA duplexes shows that there is a high degree of differential expression between the miRNA and miRNA* species as well as differential expression between wing and haltere tissues. We also document notable bias in which strand is expressed more highly. These observations reinforce the notion that differential miRNA expression between wing and haltere two tissues is generated at post-transcriptional stages of miRNA biogenesis. However, apart from the change in arm bias exhibited by *miR-281-1*, it is not clear if

differential expression of dual strand miRNAs is actively regulated or perhaps a by-product of varying stabilities found within different mature miRNA sequences.

4.8 DISCUSSION

In the previous chapter, we uncovered a miRNA-*Ubx* regulatory interaction that affected *Ubx* function during haltere development. In this and the following chapter we explored the notion that miRNAs are recruited into the *Ubx* regulated genetic networks that govern haltere development.

Since there are no current published studies comparing wing/haltere miRNA content, we first set out to describe the miRNA profiles of these two serially homologous tissues. Using next-generation RNA sequencing technology, we document the total miRNA content of wing and haltere imaginal discs at a specific developmental transition, the white pre-pupae.

Although we were able to successfully profile the small RNA content of both wing and haltere tissue, at present our data comes with two prominent caveats. First, we generated two libraries with a substantial difference in numbers of read, our haltere library containing five times greater number of quality reads than the wing library. What is the cause of this difference and how could this fact impact our results? Theoretically, this difference in read numbers could reflect that the haltere tissue is generally enriched in small RNAs. An alternative explanation could be that differences in sample preparation by the sequencing facility, perhaps in the small RNA size fractionation step, led to a greater number of small RNAs being prepared from total RNA we extracted from the haltere tissue.

These issues highlight one of the problems which can occur when a significant degree of sample processing and preparation is performed by a third party, if problems or anomalies do occur, it is then hard to troubleshoot these issues.

The comparative differences in total read numbers could affect to what extent we are accurately detecting miRNA abundance in both tissues and the conclusions we draw from these observations. Essentially, if our coverage of wing tissue small RNAs is reduced because of technical reasons, we may be missing a number of microRNAs that are lowly expressed but present within this tissue. In particular, this may affect the status of miRNAs we group as ‘Halt Only’ miRNAs – that we detect them only in the haltere tissue. Potentially, these miRNAs are present within the wing but are lowly abundant, thus we may not detect these miRNAs in our Wing library due to insufficient read coverage. Additionally, miRNAs that we detect with low abundance FPKM values in the wing may in fact be present at a higher level, which we are not detecting.

Secondly, our results are based on the analysis of two read libraries generated for wing and haltere tissue respectively, essentially a single biological replicate for each tissue. Thus for further in depth analysis and follow up experimentation, validation of our results would be required. Ideally a second round of sequencing would take place on a second set of tissue preparations, failing that, quantitative-PCR detecting a number of mature miRNAs in both samples would be able to confirm the presence of particular miRNAs within each tissue and provide a relative estimation of abundance which could be compared with our sequencing data.

Encouragingly, when comparing our data sets to a similar study (Jones et al., 2013), which analysed mature miRNA content within wing imaginal discs at an earlier developmental stage, we see that many of the abundant miRNAs we detect within our wing samples, are also present within their data sets, for example *bantam* and *miR-9a*.

Our analysis shows that each tissue has significant miRNA content; more than half of the annotated miRNAs within the *Drosophila* genome were expressed in at least one, if not both of these appendages. Furthermore, there is a considerable degree of differential expression amongst miRNAs when comparing these tissues. A large number of miRNAs are expressed in both tissues, 50% of these display differential expression at two-fold or higher magnitudes when comparing wing and haltere samples. We grouped miRNAs dependant on their expression profiles in both tissues. We find that a large cohort of miRNAs are preferentially enriched within the haltere or were specifically expressed in the haltere when compared to the wing.

The diversity in miRNA expression observed when comparing these two closely related but morphologically distinct appendages is indicative of the important role miRNAs perform in the regulation of the divergent developmental programmes. In particular, it is interesting to highlight that the repertoire of miRNAs within the haltere is greater than that of the wing. The haltere appendage is a derived form of the ‘ground state’ wing appendage. It is intriguing to speculate that the haltere specific developmental programmes instigated by *Ubx* require an increased level of miRNA regulation to ensure the correct development of this tissue.

Our miRNA profiling shows that the majority of total miRNA expression (~95% of total miRNA content) found within both wing and haltere tissue is due to the expression of a small collection of miRNAs. The extreme abundance of these miRNAs indicates that they may have fundamental roles in the biology of these tissues. Future studies will be needed to identify the function these miRNAs perform during the development of these tissues. Additionally to determine to what extent miRNA expression is spatially

restricted within these appendages. Could miRNAs with lower overall expression levels, as detected in our profiling experiments, have specific expression domains?

Since the haltere is a derived form of the more ancestral wing appendage, we assume that the wing miRNA content is the fundamental profile found within these tissues. Our next aim was to understand the possible mechanisms that could generate divergent miRNA expression patterns in the haltere.

The starting point of all miRNA expression begins with the initial transcription of the pri-miRNA, either as an intergenic sequence or that of a transcribed mirtron. We hypothesised that pri-miRNA sequences may form part of the *Ubx* controlled transcriptome within the haltere, and that *Ubx* function in the haltere could regulate alternative miRNA profiles. Using SQ-RTPCR analysis we looked for evidence of differential pri-miRNA expression between wing and haltere tissues. We were unable to identify expression patterns that match that which we detected at the mature miRNA level. This data suggests that *Ubx* transcriptional control does not directly affect miRNA expression levels. Since transcriptional regulation seemed an unlikely cause for differential miRNA expression we re-examined our sequencing data looking for evidence that post-transcriptional regulation of miRNA biogenesis may cause differential expression. Our analysis of clustered miRNA expression and miRNA/miRNA* dual arm processing suggests that mechanisms influencing the biogenesis of mature miRNAs and/or their stability thereafter, may play an important role in generating diverse expression patterns between wing and haltere tissue. Specifically, our analysis showed a tendency for heterogeneous expression amongst miRNAs present in genomic clusters (and transcribed as a long poly-cistronic transcript).

Although these results indicate *Ubx* may not be directly involved in generating differential miRNA expression within the haltere, it remains to be seen if *Ubx* may function indirectly to generate these diverse miRNA profiles. For example, the transcriptional up-regulation of RBPs by *Ubx* may favour the biogenesis of certain miRNAs within the haltere.

In summary, we describe the miRNA expression patterns of the wing and haltere imaginal discs at a specific developmental transition. Our results show that the haltere imaginal disc contains an expanded repertoire of miRNAs compared to the more ancestral wing appendage. The generation of these divergent expression profiles likely occurs at the post-transcriptional level of miRNA biogenesis. In the following chapter we explore the functional significance of these alternative miRNA expression profiles

and investigate the potential for haltere miRNAs to be integrated into the *Ubx* GRNs that govern haltere development.

CHAPTER 5

5. The functional analysis of miRNAs present within the haltere imaginal disc and their relationship to *Ubx* regulation and function

5.1 Chapter Overview

In the previous chapter we profiled the miRNA content present in wing and haltere imaginal discs at a transitional phase in development. Analysis of these profiles showed that the haltere contained a more diverse and expanded set of miRNAs, including 29 miRNAs only found within the haltere and not present in the wing. Why would this particular tissue require more miRNAs during its developmental cycle? The miRNAs present within the haltere tissue can also be grouped into multiple miRNA expression groups, dependant on their expression levels relative to that seen in the wing tissue. Do these grouped miRNAs share similar functionality within the haltere?

We know that the Hox gene *Ubx* is the fundamental regulator of haltere development. How are these miRNAs, present within the haltere, integrated into the *Ubx* controlled developmental programs?

In this chapter, we explore these questions. Utilising miRNA-target prediction profiles we show that miRNAs which share similar expression patterns between wing and haltere tissue are predicted to target similar groups of genes. Furthermore, miRNAs that have predominately haltere enriched expression are more likely to share similar gene targets than miRNAs not enriched or present in the haltere. Integrating our haltere miRNA expression profiles with available *Ubx* transcriptomic data reveals that haltere miRNAs are more likely to target transcripts up-regulated by *Ubx*. Using genetic analysis we show that general miRNA function is required for the correct development of the haltere appendage instigated by *Ubx*. Synthesising this data, we propose a hypothesis in which the main requirement of miRNA function in the haltere is to buffer and maintain the changing transcriptome within this tissue, directed by *Ubx*. In this manner miRNAs function as a robustness mechanism ensuring the correct Hox genetic programs proceed within the developing haltere.

5.2 Functional similarities amongst similarly expressed miRNAs

Through our analysis of miRNA expression patterns in wing and haltere tissue, we were able to group these miRNAs into a number of different miRNA expression groups. The question remains if there is functional purpose for this differential miRNA expression. Is it possible that regulatory mechanisms exist to manipulate miRNAs into particular expression patterns dependant on tissue type? If so, are there functional similarities between the miRNAs found within the same expression groups? Using target gene predictions of each miRNA as a measure of miRNA functionality, we looked at the potential for co-ordinated gene targeting by miRNAs with similar expression. We used this analysis as evidence to assess if miRNA expression may have functional implications to the development of the wing and haltere appendages.

We collated the predicted gene targets of each miRNA within the five main expression groups - Average, Halt Up, Halt Down, Halt Only and None. We also included a randomised control group which featured miRNAs from each of the main expression groups. For the Average and None expression groups, a set of 20 miRNAs was chosen to keep numbers similar to those found in the Halt Up, Halt Down and Halt Only miRNA groups. Predicted gene targets for each miRNA tested were obtained from TargetscanFly. The overall patterns of gene targeting by different miRNA expression groups are shown as heat maps (Fig.5.1A-F). Overlap of similarly targeted genes was ascertained by hierarchically clustering all gene targets per miRNA (left-side dendrogram Fig.5.1A-F). miRNAs with similar sets of gene targets were also hierarchically clustered (top dendrogram Fig.5.1A-F).

Fig.5.1 Gene target similarities amongst expression group miRNAs

(A-F) Gene target analysis of miRNAs from each miRNA expression group. Left dendrogram of each heatmap represents genes targeted by similar sets of miRNAs from within the miRNA expression group. The top dendrogram represents the clustering of miRNAs which are predicted to target similar sets of genes. For each heatmap, a section (white dashed box) has been scaled up to show the detail within each map. Each coloured line represents a predicted miRNA-target gene interaction (see magnified regions of each heatmap). Black lines represent no predicted interactions between a miRNA and a target gene. miRNA-gene target interactions cluster together when similar cohort of miRNAs targets a particular gene. This is seen in the heat map as a large coloured area (a collection of individual coloured lines representing each individual miRNA-gene target interaction).

Fig.5.1 Gene target similarities amongst expression group miRNAs – Part 1

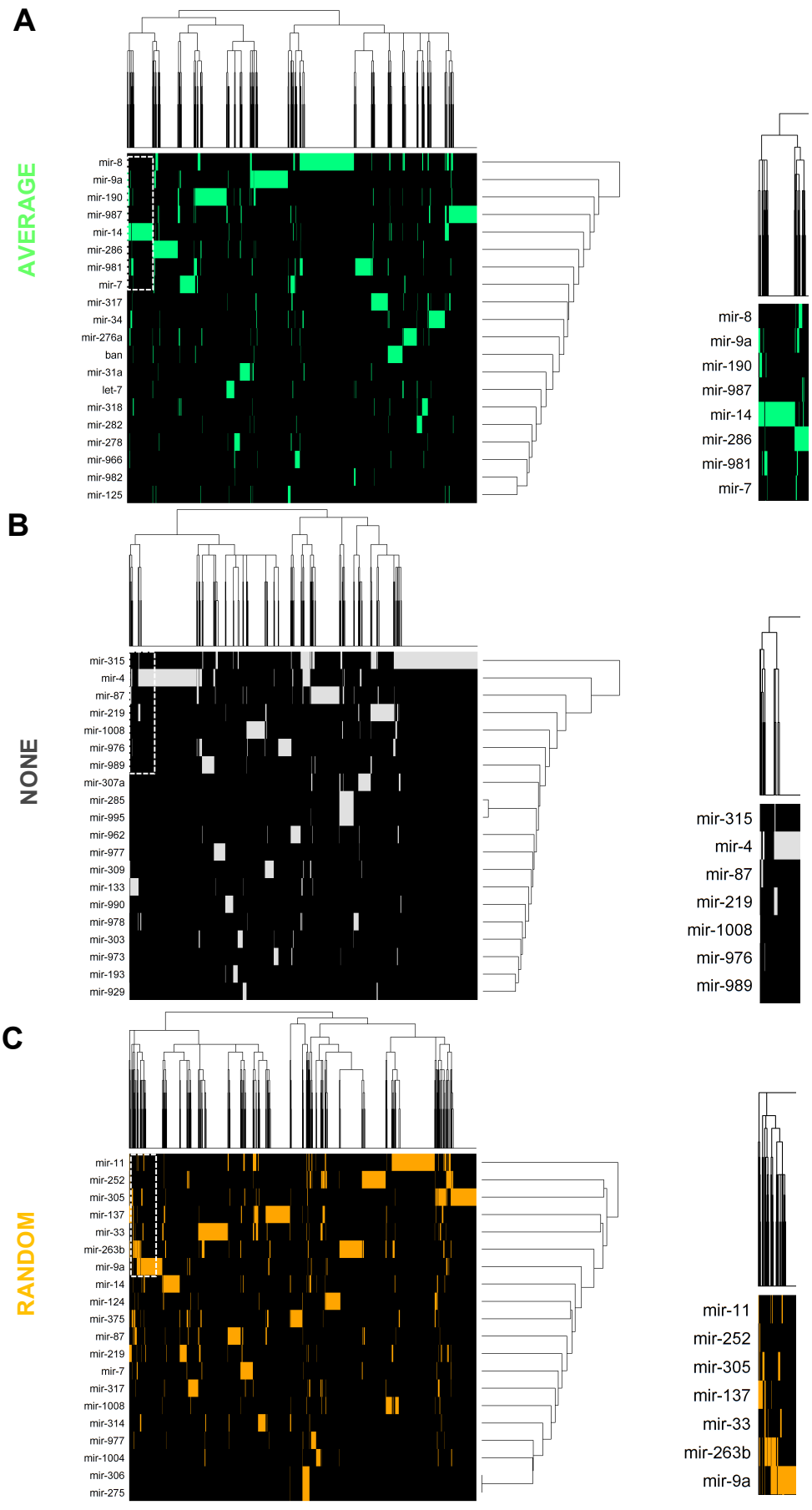

Fig.5.1 Gene target similarities amongst expression group miRNAs – Part 2

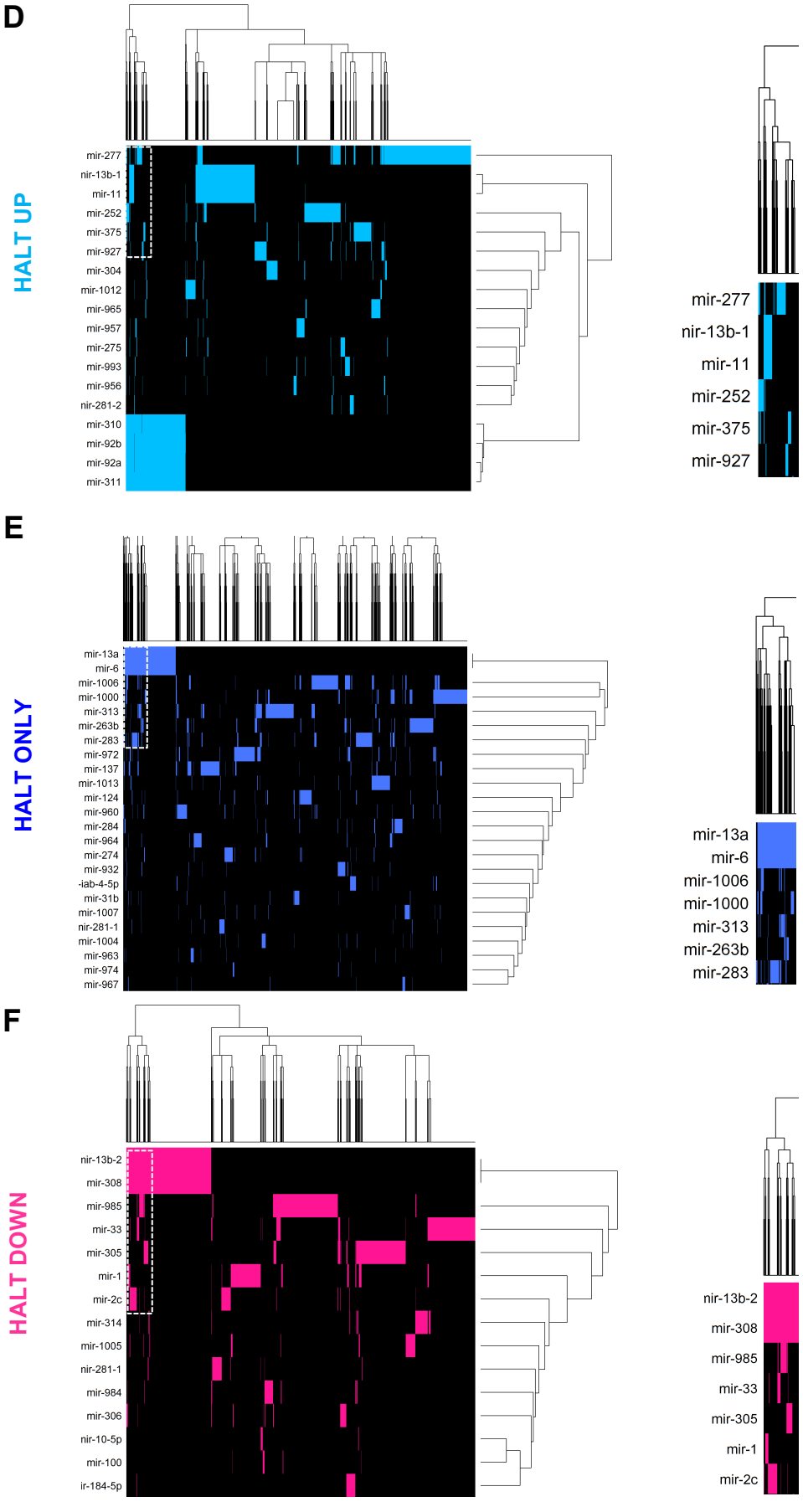

Analysis of the gene target clustering shows that each expression group contains a number of genes which are similarly targeted by multiple miRNAs.

For the majority of expression groups, there is no clear evidence for miRNAs to cluster together based on their gene targets. This suggests that within the miRNA expression groups, there are no prominent sub-groups of miRNAs with specific sets of gene targets. However, there are exceptions which can be explained by the fact that these miRNAs share similar seed sequences and thus are predicted to target the same gene transcripts. These include *miR-310*, *miR-311*, *miR-92a*, *miR-92b* and *miR-13b-1*, *miR-11* belonging to the Halt Up group and *miR-13a*, *miR-6* which form part of the Halt Only expression group.

A numerical analysis of the degree of miRNA co-targeting within each miRNA expression group was performed (Fig.5.2). We calculated the percentage of miRNAs within each expression group that are predicted to target each gene within that group. We then collated target genes together dependant on the percentage of miRNAs they

would be predicted to be targeted by – 0-10%, 11-30%, 21-30%, 31-40%, 41% and higher respectively. Analysis of these percentages shows little evidence for large scale co-targeting of genes. The majority of genes within this survey are targeted by 10% or less of miRNAs within each expression group. The exceptions to this are the Halt Up, Halt Down and Halt Only groups, which have significant increases in the number of genes targeting by between 11 and 40% of miRNAs within each group. Interestingly, these three groups all show differential expression between wing and haltere imaginal tissue. Analysis of these target gene distributions showed there were significant differences when comparing the Average expression group to Halt Up, Halt Down and Halt Only expression groups. There were also significant differences in distribution when comparing the Halt Up, Halt Down and Halt Only groups themselves ($p<0.001$ for all combinations, Mann-Whitney u-test). We further detected significant differences when comparing the Random to the Average and None expression groups. This likely reflects that the Random expression group is made up of miRNAs from each group that displays significant co-targeting.

Fig.5.2 Analysis of shared targeting amongst miRNA expression groups

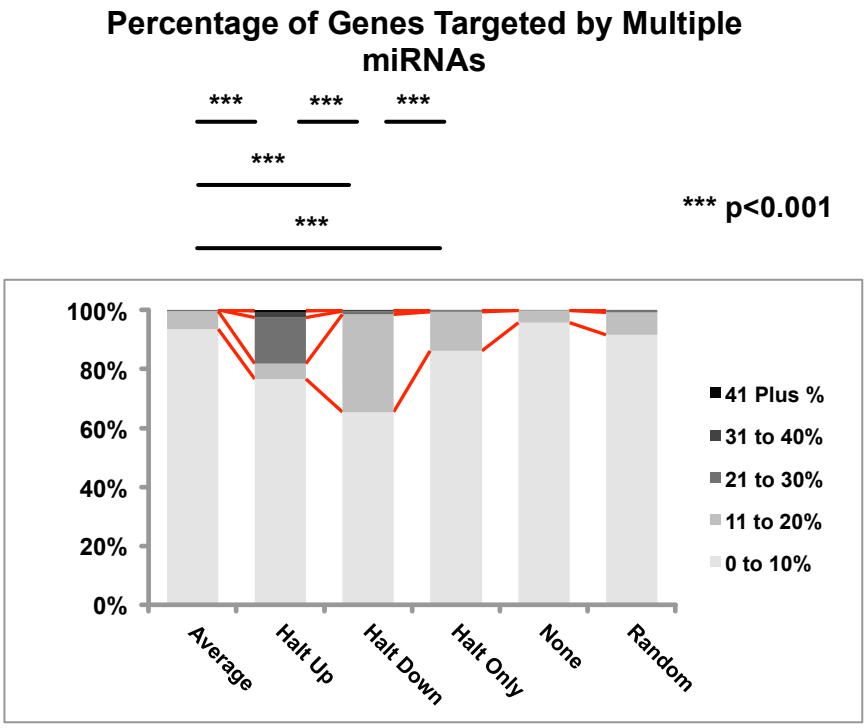

Fig.5.2 Analysis of shared targeting amongst miRNA expression groups Numerical analysis of co-ordinated gene targeting amongst miRNA expression groups. Stacked bar plots signify percentage of total gene targets per group that are targeted by increasing numbers of microRNAs within each expression group. Statistical analysis performed using Mann-Whitney u-test, p-values shown in figure.

Overall, this data suggests that within each miRNA expression group, there is a large degree of target gene overlap. Importantly, when we quantify the percentage of genes targeted by increasing levels of miRNAs within each expression group, three display an increased tendency to co-target genes with multiple miRNAs – Halt Up, Halt Only and Halt Down. It is tempting to speculate that this tendency towards targeting of similar gene sets may have important implications to miRNA function during the development of these tissues and could possibly be the cause or consequence of similar expression patterns across wing and haltere tissue.

5.3 Targeting overlap and specificity amongst miRNA expression groups

Having previously analysed the targeting overlap amongst miRNAs found within defined miRNA expression groups, we next assessed to what extent genes were specifically targeted by particular miRNA expression groups and how much targeting overlap existed between miRNA expression groups.

We first condensed our previous data of genes targeted by miRNAs within each miRNA expression group into a collective data set containing all genes targeted by each miRNA expression group (combining individual miRNA target lists into one target list per group). We performed hierarchical clustering on both the genes targeted by each miRNA expression group (left-side dendrogram Fig.5.3A) and which miRNA expression groups have similar sets of gene targets (top dendrogram Fig.5.3A). This analysis shows that there is a large degree of target overlap amongst all five expression groups. Possibly of most interest is the observation that the Halt Up and Halt Only groups cluster together, indicating in particular, that they share high proportion of target genes.

We repeated this analysis, now considering the extent of co-targeting of each gene by miRNAs within the same expression group. Once again, individual miRNA target lists for each expression group were collated, however each gene target is now given a score dependant on how many miRNAs within the expression group were predicted to target that particular gene. Again hierarchical clustering was performed for both genes similarly targeted by miRNA expression groups and for the expression groups which share similar groups of target genes (Fig.5.3B). As before we see a large degree of clustering amongst target genes (left-sided dendrogram) indicating multiple sets of genes are targeted by the same miRNA groups. Significantly, the Halt Up and Halt Only expression groups once again cluster together (top dendrogram) indicating that that groups of targets genes are targeted by multiple miRNAs from both expression groups. We also observed that the Halt Down group now clusters independently from the Average and None expression groups, likely reflecting the fact that this expression group was observed to have a higher degree of multiply targeted genes than the Average and None expression groups (Fig.5.2).

To look more closely at the number of genes co-targeted by the various miRNA expression groups and the number of specific gene targets for each expression group, we performed a Venn analysis of all genes targeted by the main miRNA expression groups (Fig.5.3C). We observed a large degree of target overlap between the various miRNA expression groups. For example there are 142 genes predicted to be targeted by miRNAs contained within all five expression groups. This analysis revealed that

there are large sets of genes predicted to be specifically targeted by individual miRNA expression groups. The exception is the Average expression group which has relatively few specific target genes.

To understand to what extent the degree of targeting overlap or target specificity amongst expression groups was a consequence of the large number of genes being assessed in this analysis, we analysed the number of overlapping targets, looking at genes targeted by a minimum ten percent of miRNAs found within each individual miRNA expression group – the 'Ten Percent' cohort of genes (Fig.5.8D). This approach reduced the number of genes shared amongst multiple expression groups. However, large numbers of group-specific genes still remained. These group specific genes, co-targeted by multiple miRNAs may have some functional significance for the correct development of the haltere.

Our data so far indicates that miRNA expression groups are likely to co-target a number of genes. To consolidate this data, we performed pair-wise comparisons of each miRNA expression group to determine the number of shared targets between each group. The average number of genes shared between expression groups was 690. There were four pairwise group comparisons that shared genes above this number.

Fig.5.3 Target overlap and specificity amongst miRNA expression groups

(A) Analysis of the degree of shared targeting amongst miRNA expression groups. Left dendrogram represents clustering of genes targeted by similar miRNA expression groups. Top dendrogram represents clustering of miRNA expression groups with similar sets of gene targets. (B) Analysis of shared targeting amongst miRNA expression groups. Each gene target is now given a score dependant on the number of miRNAs targeting the gene from within the expression group. Left dendrogram represents clustering of genes targeted by similar miRNAs. Top dendrogram represents genes clustering of miRNA expression groups with similar sets of target genes. (C) Venn diagram depicting the shared and specific target genes of each miRNA expression group. (D) Venn diagram depicting the shared and specific target genes of each miRNA expression group. Analysis is limited to only genes targeted by a minimum of ten percent of microRNAs within each cohort. (E) Pairwise comparisons of shared gene targets between miRNA expression groups. (F) Pairwise comparisons of shared gene targets between miRNA expression groups. Analysis is limited to only genes targeted by a minimum of ten percent of microRNAs within each cohort.

Fig.5.3 Target overlap and specificity amongst miRNA expression groups

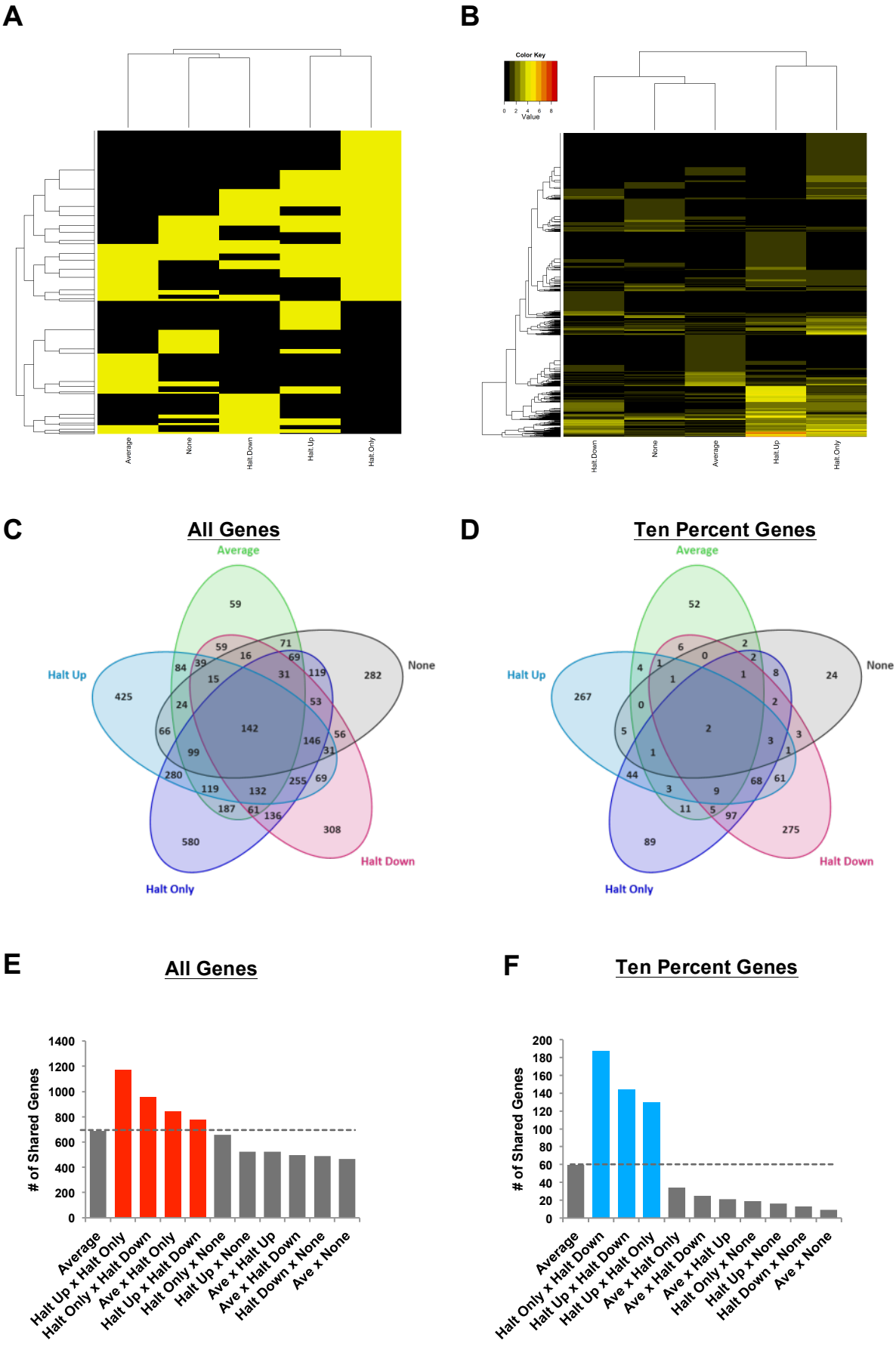

The Halt Up and Halt Only expression groups sharing the most target genes. We also observe a large degree of shared targeting between the Halt Only x Halt Down, Average x Halt Only and Halt Up x Halt Down groups (Fig.5.3E). To further this analysis, we determined the shared targeting amongst groups using the 'Ten Percent' gene list generated earlier (Fig.5.3F). With this refined data set, the average number of shared genes falls to 59. There are three pairwise comparisons that exceeded this number - the Halt Up x Halt Only, Halt Up x Halt Down, Halt Only x Halt Down. This analysis suggests that these three groups co-target a specific set of genes through their constituent miRNAs. This may have implications for the functional capabilities of these miRNA expression groups during development. For example, do genes targeted by haltere enriched miRNAs (Halt Up and Halt Only) have specific roles that must be regulated by miRNA activity during haltere development.

In summary we attempted to deduce to what extent genes were co-targeted by multiple groups of miRNAs and how many targets were specific to each expression groups. Our analysis shows there is a large degree of gene target overlap amongst multiple miRNA expression groups. In particular there seems to be an association between the Halt Up and Halt Only expression groups. This could indicate a functional significance, since these miRNAs have enriched haltere expression. We also observe significant groups of genes specifically targeted by each miRNA expression group. Additionally, there was still an enrichment of these group specific targets when analysing only genes targeted by a minimum ten percent of the miRNAs from each expression group. This suggests that a number of possible gene targets are co-ordinately regulated during haltere development and morphogenesis. One caveat is that the predicted target data sets used for this analysis do not take into account when and where these genes are expressed during *Drosophila* development. However, these findings still hold merit in indicating that certain miRNA expression groups may have similar functionality during development, particularly within the haltere imaginal disc.

5.4 miRNA groups associate with specific biological processes

Our analysis of potential co-targeting by miRNAs within the same expression groups revealed significant numbers of genes could be targeted by specific miRNA expression groups. Additionally, we observe increased levels of co-targeting between similar expression groups e.g. Halt Up and Halt Only suggesting that each miRNA expression group may exhibit specific functionality. To follow on from these observations we used

Gene Ontology analysis to look for evidence that miRNA expression group target genes share a molecular or biological specificity.

We first performed pair-wise comparisons of gene ontology terms of the five miRNA expression groups using the 'All', 'Ten Percent' gene sets previously identified and a 'Specific' gene set containing only genes targeted specifically by each individual miRNA expression cohort. As a control group we used the Random miRNA expression group used previously for the 'All' and 'Ten Percent' genes, and a 'Common' gene set (containing gene targets shared by all expression groups) as a control for the Specific genes. For these comparisons we interrogated the Molecular Function and Biological Process gene ontologies of each target gene set.

Analysis of Molecular Function gene ontologies for the 'All' and 'Ten Percent' gene sets (Fig.5.4A-B) showed negligible differences between the five main expression groups. The most significant differences in gene ontology were observed when comparing each main expression group to the Random control group (bright magenta symbolising a significant p-value). However, analysis of the 'Specific' gene set revealed a different picture (Fig.5.4C). Here, most pairwise comparisons showed statistically significant differences in gene ontology. Perhaps more telling are the two comparisons that were not statistically significant, the Halt Up x Halt Only and Average x None groups.

We assessed the same data sets looking for significant differences in Biological Process gene ontologies. Analysis of the 'All' genes data (Fig.5.4D) showed significant differences when comparing a number of miRNA expression groups to the Random control group (bright green indicating significant p-values). Unlike the analysis of Molecular Function, other pairwise comparisons did approach statistical significance – Halt Down x Average, Halt Only x Average, Halt Only x Halt Down.

Fig.5.4 miRNA groups associate with specific molecular and biological processes

(A-C) The pairwise analysis of the significant differences between miRNA expression groups in molecular function gene ontologies. Analysis performed on (A) 'All' (B) 'Ten Percent' (C) 'Specific' gene sets. Colour of tile represents significance p-value, bright magenta represents $p<0.05$ or lower. (D-F) The pairwise analysis of the significant differences between miRNA expression groups in biological process gene ontologies. Analysis was performed on (D) 'All' (E) 'Ten Percent' (F) 'Specific' gene sets. Colour of tile represents significance p-value, bright green represents $p<0.05$.

Fig.5.4 miRNA groups associate with specific molecular and biological processes

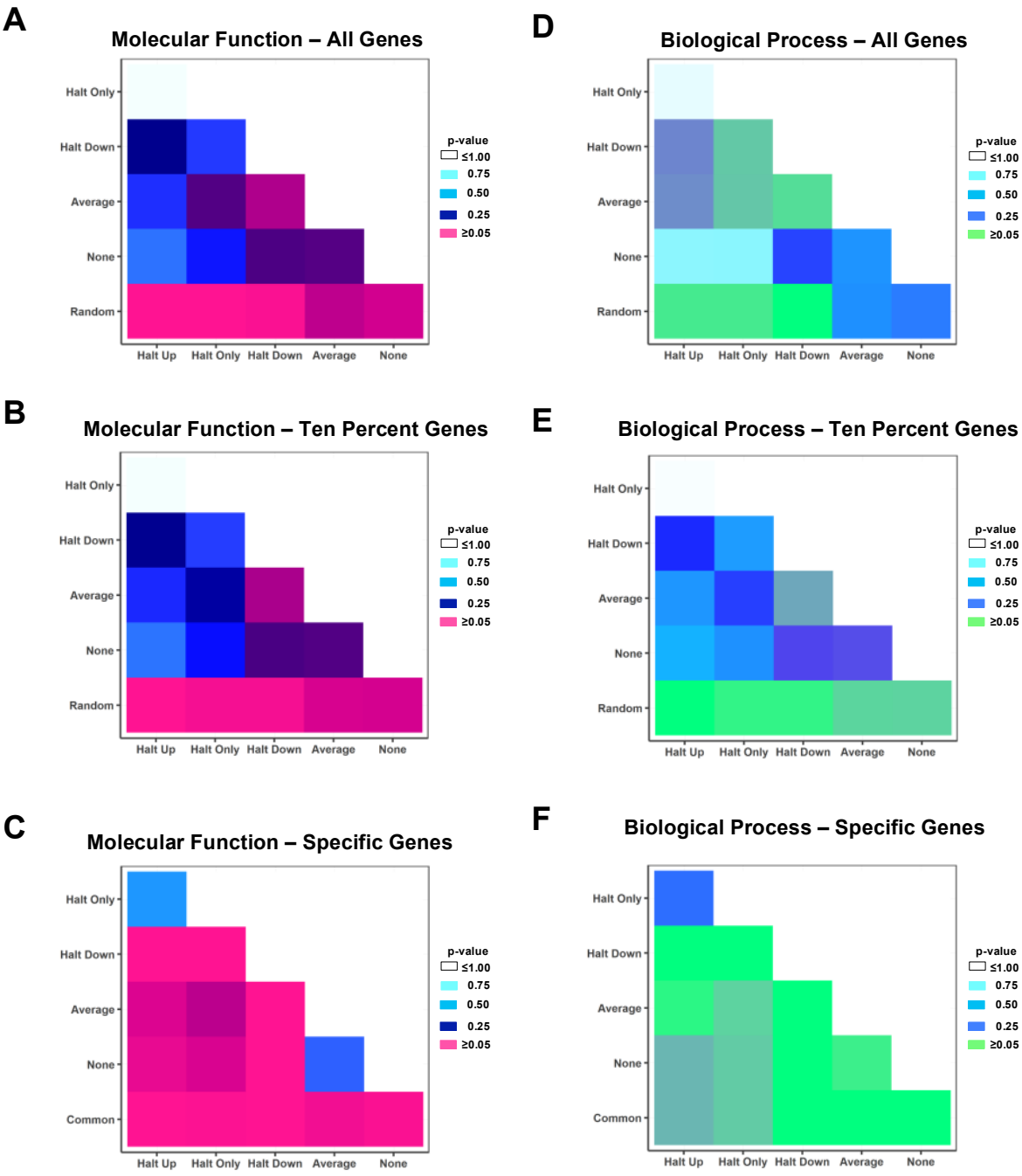

Analysis of the ‘Ten Percent’ gene set (Fig.5.4E) showed only significant differences between the main expression groups and the Random control group. Assessing the significance of the ‘Specific’ gene set (Fig.5.4F) showed that most pairwise comparisons differed significantly in Biological Process. These results match with what we see in the analysis of the Molecular Function ontologies. Again the Halt Up x Halt Only comparison shows that these gene sets are not significantly different in biological process.

Overall, this analysis indicates that the ‘Specific’ genes of each miRNA expression group have particular molecular or biological functions when compared to the other expression groups. This specific functionality amongst groups could be the reason for maintaining differential miRNA expression within the developing haltere tissue. We highlight that the Halt Up and Halt Only group appear to share the same functionality, both molecularly and biologically. This may be of importance when trying to decipher why these particular miRNAs are enriched within the developing haltere tissue. We do not observe the same degree of functional differences between groups when assessing the ‘All’ and ‘Ten Percent’ gene sets. This is likely due to the large overlap in gene targets observed amongst miRNA expression groups.

The reason for such an overlap amongst miRNAs which display differential miRNA expression patterns is an open question. One intriguing possibility is that these overlapping target genes may have fundamental roles in general appendage development and therefore have evolved multiple miRNA-target interactions.

To further these results, we documented which gene ontology categories were most represented amongst the miRNA expression groups and how these associations change as the specificity of each gene set increases. We assessed the percentage of genes contributing to the top ten Molecular Function and Biological Process gene ontologies present within the ‘All’, ‘Ten Percent’ and ‘Specific’ gene sets. The percentage contribution of each ontology is displayed as a ‘dotplot’, the size of each dot indicates the relative percentage contribution to all ontologies. Analysis of the molecular function ontologies (Fig.5.5A-C) showed that in each grouping of genes, the same top categories appear, including the ‘nucleic acid binding’ and ‘sequence specific DNA binding transcription factor activity’. The enrichment of these ontologies may be representative of the fact that miRNAs are often seen to be prominent regulators of transcription factors in cellular and developmental biology.

In general, there is little change in gene contribution amongst the miRNA expression groups across each ontology category within the ‘All’ and ‘Ten Percent’ gene sets. The

one exception is within the ‘nucleic acid binding’ category of the ‘All’ dataset. Here the Halt Down group is notably enriched for genes contributing to this category (Fig.5.5A). Analysis of the ‘Specific’ gene set (Fig.5.5C) shows that the relative contribution to each ontology category was reduced amongst the miRNA expression groups when compared to the ‘All’ and ‘Ten Percent’ datasets. This indicates that these smaller sets of genes are not enriched for any particular molecular function ontologies. The exception to this observation is the Halt Down group where again a significant contribution is made from genes related to ‘nucleic acid binding’. These results indicate that there could be a requirement for the highly regulated expression of a number of nucleic acid binding genes (transcription factors/co-factors) required within the developing haltere. Therefore, expression of miRNAs which may negatively regulate these factors is reduced within the haltere.

Analysis of biological process ontologies for each miRNA expression group reveals slight changes in the top ontology categories of these gene sets (Fig.5.5D-F). Common to all datasets were general categories such as ‘regulation of cellular process’ and ‘regulation of biological process’ but also included developmentally specific ‘multicellular organismal development’ and ‘anatomical structure development’ ontologies. The ‘All’ and ‘Ten Percent’ genes both contained ‘cellular developmental process’ as a top category (Fig.5.5D-E). Interestingly, we observe large asymmetrical contributions of genes to different categories within each miRNA expression group. For example ‘regulation of cellular process’, ‘regulation of biological process’ and ‘anatomical structure development’ within the ‘All’ and ‘Ten Percent’ gene sets have a far greater contribution of genes than the remaining categories. This asymmetrical distribution of genes is not seen in the majority of miRNA expression groups from the ‘Specific’ genes data set (Fig.5.5F). Here, contributions are spread evenly across the top ontology categories. The exception to this observation is again the Halt Down expression group where particular ontology categories have large contributions in each set of genes.

Fig.5.5 Top gene ontology categories associated with specific miRNA groups

(A-C) Dot plots displaying the percentage of genes each expression group makes to the top ontology categories for molecular function. Results shown from the (A) ‘All’ (B) ‘Ten Percent’ (C) ‘Specific’ gene sets. (D-F) Dot plots displaying the percentage of genes each expression group makes to the top ontology categories for biological processes. Results shown are from (A) ‘All’ (B) ‘Ten Percent’ (C) ‘Specific’ gene sets. Each dot is representative of the percentage contribution of genes to a category from each miRNA expression group.

Fig.5.5 Top gene ontology categories associated with specific miRNA groups

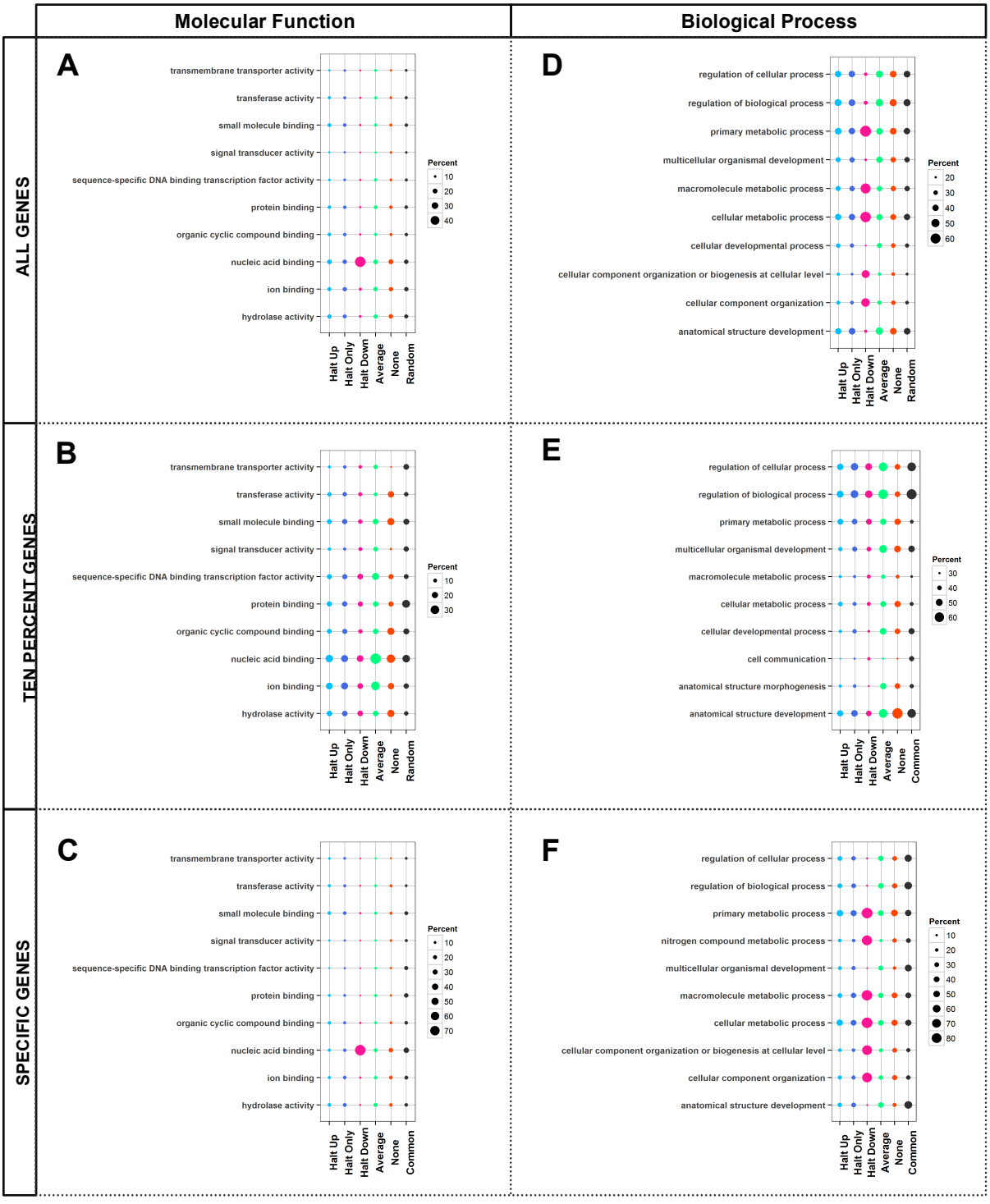

In summary, we attempted to assign a level of molecular and biological functionality to genes regulated by different miRNA expression groups. We observed that the larger 'All' and 'Ten Percent' datasets show no significant differences in gene ontology associations amongst the main miRNA expression groups. However, analysis of the 'Specific' gene sets revealed that all the miRNA expression groups showed significant differences in gene ontology at both the molecular function and biological process level. The exception to this is the Halt Only and Halt Up groups which suggests genes targeted by these miRNA expression groups share particular functionalities.

Close inspection of the top molecular function ontology categories showed no differences between the main miRNA expression groups and gene data sets. However, differences in the top biological process categories were seen when comparing each gene data set. We observed that particular categories are enriched for genes within each miRNA expression group. Overall, this data suggests that the genes predicted to be targeted by each miRNA expression group have similar molecular functions. In general, these genes also contribute to similar biological functions. An exception to this conclusion, are the target genes of the Halt Down expression group. Although these genes have similar molecular and biological functions to other expression group targets, their relative contribution to each category is very distinct from the other miRNA groups. We have not analysed in detail categories with smaller contributions of genes and how these may be similar or dissimilar amongst miRNA expression groups.

5.5 Functional consequences of haltere miRNA expression – The Regulation of *Ultrabithorax*

In the Chapter 3, we showed that the fine-tuning of *Ubx* expression by miRNAs can be an important regulatory step in controlling *Ubx* functionality. Now, with a better understanding of the miRNA content within the haltere, we re-assessed likely *Ubx*-miRNA interactions during the development of this appendage. We were interested in first examining the relationship between predicted miRNA targeting strength and miRNA expression group association, and secondly, miRNA targeting strength and overall miRNA expression level within the haltere. Were miRNAs that are preferentially or highly expressed in the haltere, more or less likely to target *Ubx* transcripts?

We submitted the long isoform of the *Ubx* 3'UTR to the PITA target prediction algorithm using the most current miRNA annotations within the *Drosophila* genome (BDGP5.6). We analysed the PITA results, cross-referencing with our documented haltere miRNA

expression profile data. At the time of analysis there were 192 mature miRNAs annotated within the *Drosophila* genome. Following PITA target prediction, we see that 154 (78%) miRNAs have one or more target sites within the *Ubx* 3'UTR (Fig.5.6A). How do these 154 *Ubx* targeting miRNAs distribute amongst the miRNA expression groups defined in our profiling experiments? We observe that just over 70% of all *Ubx* targeting miRNAs had detectable expression within the haltere, the largest contingent of miRNAs belonging to the Average expression group. This would be expected since the Average expression group contained the most miRNAs and therefore would by chance have more miRNAs capable of targeting *Ubx*. Interestingly, the Halt Only expression group had the second highest contribution of miRNAs targeting *Ubx* (Fig.5.6B). We next analysed the relationship between individual miRNA target sites of the *Ubx* 3'UTR and their associated PITA prediction scores by plotting these two factors against each other (Fig.5.6C). In this scatter plot, each data point represents a specific region of the *Ubx* 3'UTR along the x-axis and the PITA ΔΔG score associated with each target site along the y-axis. There are 503 predicted target sites within the *Ubx* 3'UTR with a negative ΔΔG. Overall, we observe an increased density of target sites with a ΔΔG score between 0 to -8 (represented by white dashed line). There are noticeably fewer miRNA sites with scores lower than this. This may be of significance when considering which miRNAs could be potent regulators of *Ubx* (the more negative the ΔΔG score, the more likely a miRNA-target interaction will occur). Using this analysis we do not see obvious differences in the distribution of target sites along the length of the *Ubx* 3'UTR, suggesting there are no specific regions within the 3'UTR where miRNA targeting elements are enriched.

Fig.5.6 miRNA group associations and potential for *Ubx*-miRNA regulatory interactions

(A) Summary of the number of miRNAs predicted to target the extended *Ubx* 3'UTR. (B) Group associations for miRNAs predicted to target the extended *Ubx* 3'UTR. (C) Scatter plot displaying the relationship of Ubx targets sites along the *Ubx* 3'UTR and their predicted targeting strength. (D) Analysis of miRNA target score distributions broken down into the respective miRNA expression groups. (E) Scatter plot displaying the association between a miRNAs overall targeting strength against Ubx and the number of target sites predicted within the *Ubx* 3'UTR. (F) Distribution analysis of the number of target sites detected for each miRNA predicted to target Ubx, broken down into each miRNA group. In panels C & E, white vertical line represents approximate location of the first poly-adenylation site.

Fig.5.6 miRNA group associations and potential for *Ubx*-miRNA regulatory interactions

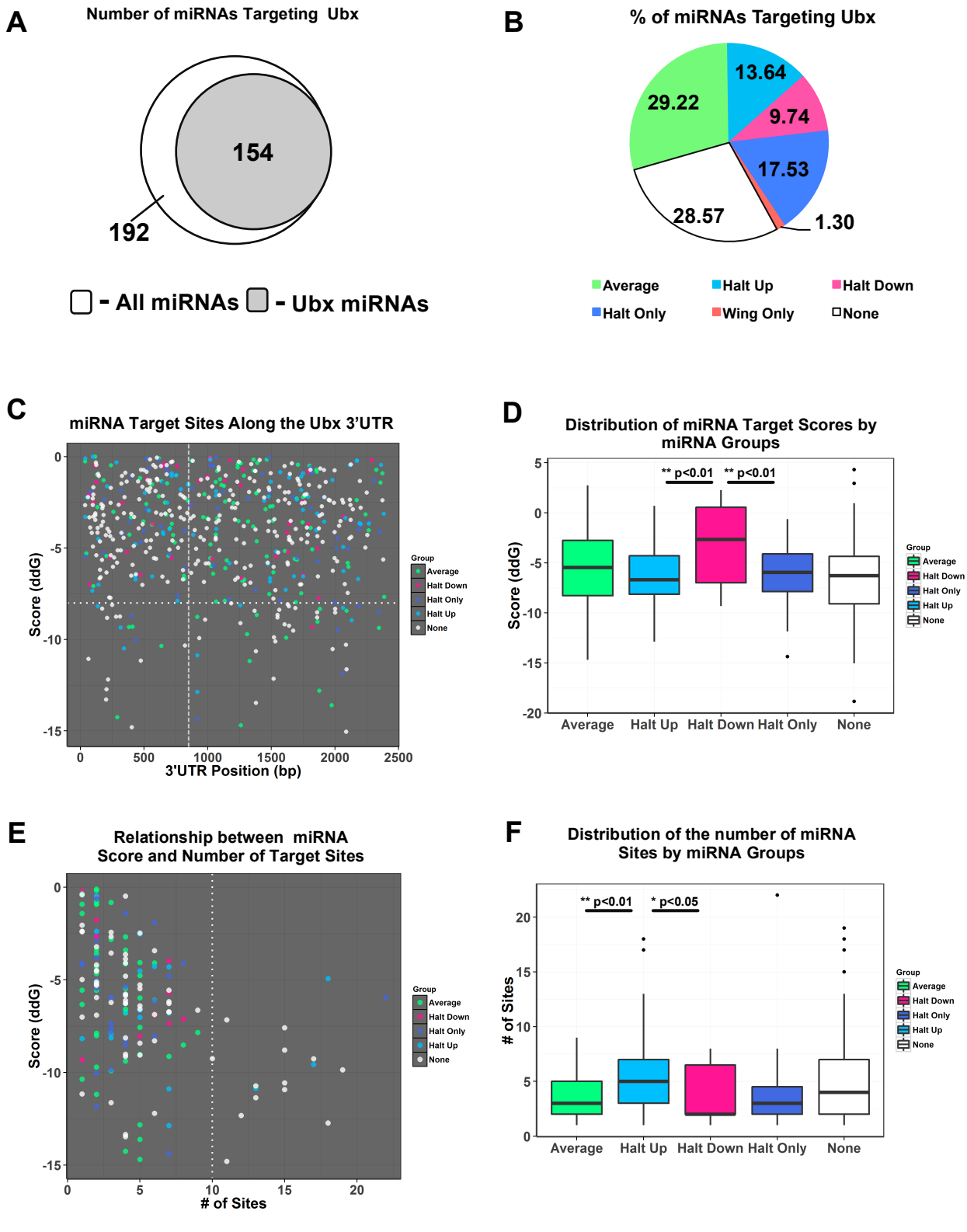

We analysed the distribution of overall miRNA targeting strength (the collective score of all individual target sites for each miRNA) for all miRNA expression groups (Fig.5.6D). We observe that each expression group except the Halt Down miRNAs have similar ΔΔG score distributions. The Halt Down expression group had a significant decrease in ΔΔG score distribution corresponding to their associated miRNA target sites ($p<0.002$ comparing Halt Up x Halt Down and Halt Down x Halt Only). These target scores (only one below -8) suggest that these miRNAs are less likely to target the *Ubx* 3'UTR within the developing haltere tissue.

We next assessed the association between the number of sites per miRNA and the overall score for each miRNA (Fig.5.6E). Again there is a notable threshold in miRNA density with relatively few miRNAs having more than 10 target sites within the 3'UTR. Of the 12 miRNAs to have more than 10 target sites, only four had detectable expression within the haltere. Analysis of miRNA distributions showed no obvious correlation between the number of target sites and the overall ΔΔG score. This suggests that in general, most miRNAs that potentially target *Ubx* have a small number of sites which could lead to miRNA-target interactions.

We analysed the distributions of target site number per miRNA within each miRNA expression group (Fig.5.6F). Here, the Halt Up group has a small but significant increase in the target site distribution ($p<0.01$ comparing Average x Halt Up, $p<0.05$ comparing Halt Up x Halt Down). Thus miRNAs within the Halt Up cohort tend to have an increased number of miRNA target sites within the *Ubx* 3'UTR.

Having seen that specific miRNA expression groups have certain associations with either target score distribution or the number of target sites, we next assessed to what extent the expression levels of each miRNA may correlate with the likelihood of targeting the *Ubx* 3'UTR.

We examined the association between each miRNA target site and its corresponding ΔΔG score. However, we now took into context the expression level of each miRNA within the haltere, defined by our sequencing data and shown by the changing colour of each target site data point (Fig.5.7A). Overall we see that the most highly expressed miRNAs have target sites associated with higher ΔΔG values. This suggests that these miRNAs would be less likely to target the *Ubx* 3'UTR. However this was not a definitive association, a number of miRNA target sites with very negative ΔΔG scores are associated with highly expressed miRNAs within the haltere (see arrowheads Fig.5.7A).

To analyse these associations in more detail, we grouped each miRNA into one of five Haltere Expression Groups – Very High, High, Medium, Low and None dependant on their expression value within the haltere. Each miRNA association with a particular expression group was determined by calculating the quartile ranges of all miRNA expression values within the haltere. miRNAs with no expression in the haltere were automatically grouped into the None expression group.

Having sorted each miRNA into their respective haltere expression groups, we examined the distribution of overall miRNA target scores (Fig.5.7B). Although the distributions of the Very High and High expression groups are greater than the Medium, Low and None, these differences are not statistically significant. This suggests there is no correlation between overall expression level within the haltere and the likelihood of a miRNA targeting *Ubx* transcripts.

We next investigated the associations between the number of target sites, the ΔΔG score of individual miRNAs and their respective expression values (Fig.5.7C). The most striking observation to be made when analysing this data is that none of the miRNAs with numerous target sites are highly expressed within the haltere tissue. To examine this further, we determined the distribution of target sites amongst the miRNA associated haltere expression groups (Fig.5.7D). Although there appears to be very little change in distribution between groups, there are statistically significant differences. miRNAs present within the Very High expression group tend to have fewer sites per miRNA than the Medium expression group ($p<0.05$). Additionally, we observe that miRNAs with no expression in the haltere tend to have more target sites per miRNA than the Low expression group ($p<0.01$).

To summarise, 70% of all potential miRNA regulators targeting *Ubx* are expressed within haltere tissue. The analysis of miRNA target score distributions shows that there is no particular miRNA expression group more likely to target *Ubx* than another. However, our data does indicate that miRNAs down-regulated in the haltere (Halt Down group) are less likely to target *Ubx* transcripts. Analysis of target site number for each miRNA group association shows that miRNAs enriched for haltere expression are more likely to have an increased number of target sites within the *Ubx* 3'UTR. This may be evidence of the evolution of target sites within the 3'UTR for miRNAs preferentially expressed within this tissue.

Fig.5.7 miRNA expression levels and the effect on potential Ubx-miRNA regulatory interactions

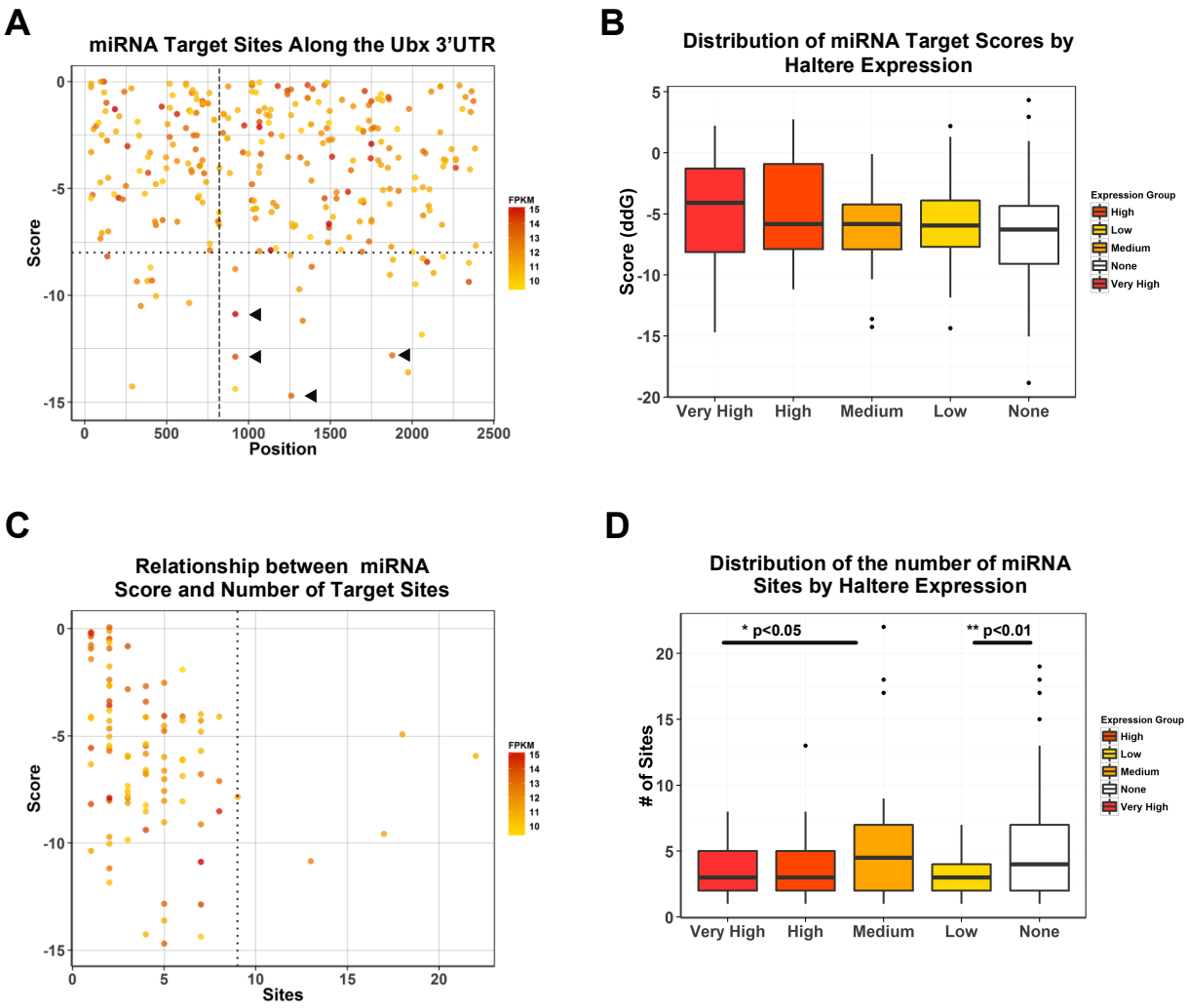

Fig.5.7 miRNA expression levels and the effect on potential *Ubx*-miRNA regulatory interactions

(A) Scatter plot displaying the relationship of *Ubx* targets sites along the *Ubx* 3'UTR and their predicted targeting strength. Each miRNA dot colour is representative of the miRNA expression level detected in the haltere. (B) Analysis of miRNA target score distributions broken down into five expression groups based on the miRNA expression level detected in the haltere. (C) Scatter plot displaying the association between a miRNAs overall targeting strength against *Ubx* and the number of target sites predicted within in the *Ubx* 3'UTR. Each miRNA dot colour is representative of the miRNA expression level detected in the haltere. (D) Distribution analysis of the number of target sites detected for each miRNA predicted to target Ubx, broken down into the five haltere expression groups. Statistical significance determined using Students' t-test, p-values given in figure. In panels A & C, white vertical line represents approximate location of the first poly-adenylation site.

Interestingly, we see no correlation between miRNA expression levels and the likelihood of targeting *Ubx*. This could be an indication that high expression levels are not required to evolve potential miRNA-target interactions. However, an intriguing observation is that highly expressed miRNAs show a small but significant tendency to have fewer target sites within the *Ubx* 3'UTR. An interpretation of these observations is that miRNAs with low expression levels are compensated by an increased number of target sites within a 3'UTR to compete with highly expressed miRNAs.

5.6 The integration of miRNA regulation into the *Ubx* regulated transcriptome of the haltere

We wanted to assess to what extent miRNA regulation may be integrated into the *Ubx* directed transcriptome during haltere development. Many published studies indicate that *Ubx* directly and indirectly regulates countless numbers of transcripts within the haltere imaginal disc (Hersh et al., 2007; Pavlopoulos and Akam, 2011). This regulation is negative and positive, many transcripts increasing or decreasing expression levels. We were interested in how the miRNA content of the haltere imaginal disc may be integrated into the global regulation of gene expression within the haltere. Do the miRNAs help reduce the expression levels of genes transcriptionally down-regulated by *Ubx* or alternatively help fine-tune and buffer the transcriptionally up-regulated genes within the haltere?

To try and answer these questions we integrated our haltere miRNA expression profiles with available microarray transcriptomic data published by Pavlopoulos and Akam, 2011, which experimentally uncovered transcriptional targets of *Ubx*. Using this data, we generated three cohorts of genes, containing the top 10% of transcripts significantly down-regulated or up-regulated by *Ubx*. These were termed '*Ubx Downregulated*' and '*Ubx Upregulated*' respectively. Additionally, we included a '*Ubx Neutral*' set of transcripts representing 100 genes that show no response to *Ubx* transcriptional activity to be used as a control group.

For all genes in each cohort, the 3'UTR sequence was obtained and submitted to the PITA Target Prediction software (Kertesz et al., 2007) along with our experimentally defined set of miRNAs present within the haltere. The resulting target scores for every gene within each cohort was collated. The resulting data was hierarchically clustered using similarities in miRNA targeting scores (Fig.5.8A-C). Comparison of these three target score maps shows that most genes within each cohort have a high potential for

targeting interactions with haltere miRNAs. What is noticeable when comparing the three gene cohorts is that the Ubx Upregulated cohort appears to contain a greater number of genes targeted by each individual miRNA. Additionally, genes within the Ubx Downregulated cohort appear to have a higher prediction score values for each miRNA interaction indicated by the darker orange hues presented within the heat map.

We examined these two points further. Since the number of genes within each *Ubx* regulated cohort differs, we first calculated the number of genes targeted by each miRNA as a percentage of the total number of genes found within each respective cohort. Analysing the distributions of these Gene Target percentages, comparing each cohort, we revealed a highly significant difference in target percentage when comparing the Ubx Upregulated cohort to both the Ubx Neutral and Ubx Downregulated cohorts respectively ($p<0.001$ Fig.5.8D). There was no significant difference in score distribution when comparing the Ubx Downregulated to Ubx Neutral cohorts. Together this data indicates that miRNAs found within the haltere are predicted to target a greater percentage of genes transcriptionally up-regulated by *Ubx*.

We furthered this analysis by examining the gene target percentages when each cohort distribution was segregated into the respective miRNA expression groups (Fig.5.8E). There is a general trend amongst expression groups where each tends to target a greater percentage of the Ubx Upregulated cohort. There are no significant changes in percentage score distributions comparing Ubx Upregulated and Ubx Downregulated genes within the Halt Down and Halt Up expression groups, indicating these miRNAs can efficiently target genes in both cohorts.

Fig.5.8 Integration of miRNA regulation into the *Ubx* directed haltere transcriptome

(A-C) Heatmaps displaying the potential regulatory interactions between transcripts from the Ubx Downregulated (A), Ubx Upregulated (B) and Ubx Neutral (C) gene cohorts miRNAs present in the haltere. (D) Box plots displaying the distributions of the percentage of Ubx regulated genes targeted by individual miRNA within the haltere comparing Ubx Downregulated, Ubx Upregulated and Ubx Neutral gene cohorts (*** $p<0.001$ Mann-Whitney U-test). (E) The same distribution analysis, now showing changes in target percentages between Ubx regulated cohorts in each miRNA expression group (*** $p<0.001$, ** $p<0.01$ Mann-Whitney U-test) (F) Box plots displaying the distributions of the average scores for each haltere miRNA in the Ubx regulated gene cohorts (* $p<0.05$). (G) The same analysis average score distributions in each miRNA expression group.

Fig.5.8 Integration of miRNA regulation into the *Ubx* directed haltere transcriptome

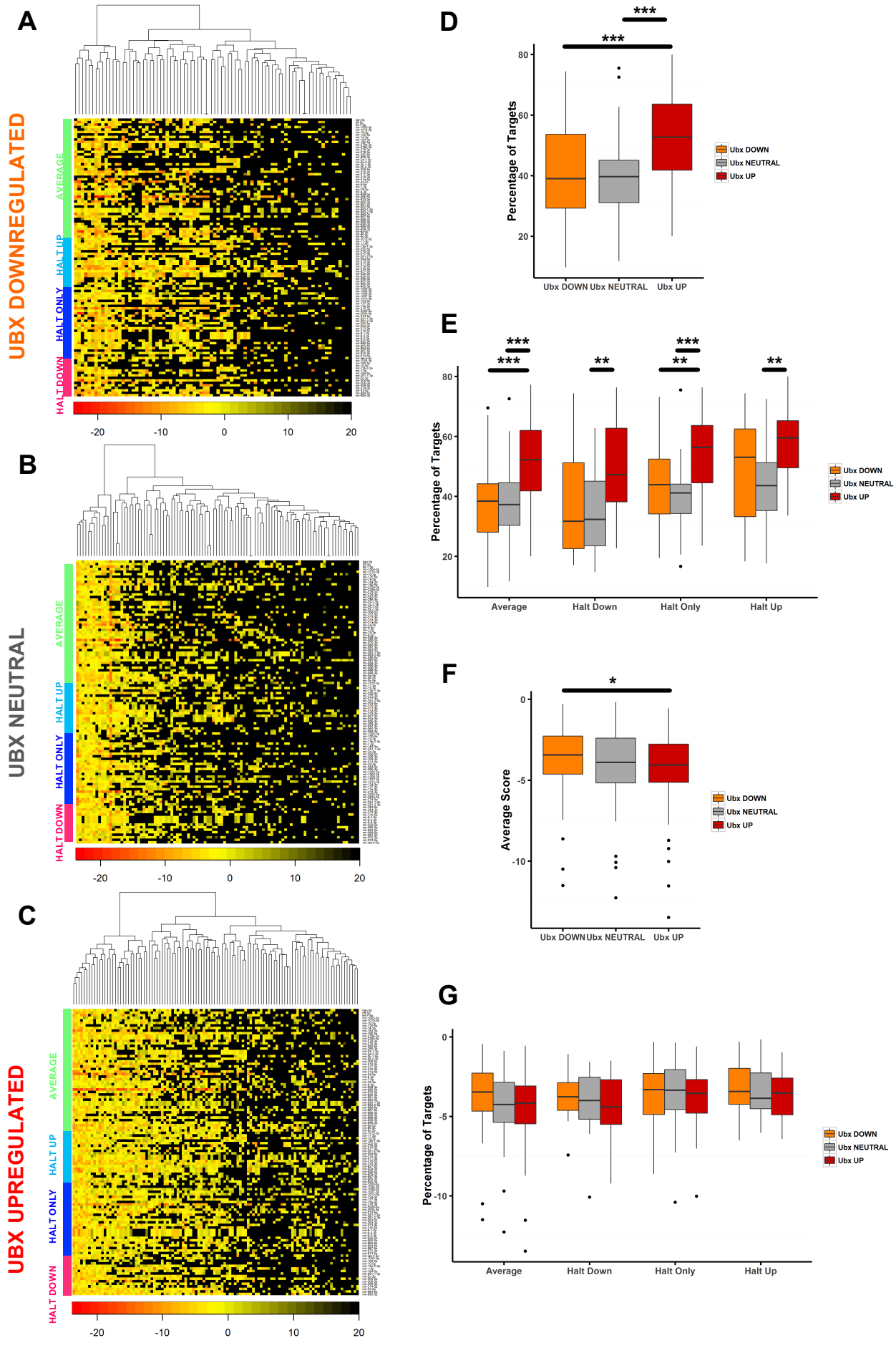

In summary, we see that all expression groups are more likely to target Ubx Upregulated transcripts, however the Halt Up and Halt Down groups are also still likely to have a strong regulatory influence on Ubx Downregulated transcripts. It is intriguing to speculate that perhaps the causative reason for differentially expressed miRNAs within the haltere, is their differing abilities to target *Ubx* regulated transcripts.

Previously we noted that genes from the Ubx Downregulated cohort appeared to have stronger target predictions when compared with the other cohorts. We explored this further by calculating the Average Score of targeting strength for each miRNA, looking for differences in Average Score distribution (Fig.5.8F). We observe a nominally significant ($p<0.05$) change when comparing the Ubx Upregulated and Ubx Downregulated cohorts. Transcripts up-regulated by *Ubx* tend to have more negative average scores implying these genes are under greater targeting pressure by haltere miRNAs. This analysis does not correspond to our initial observations of the data. We further analysed the Average Score distributions broken down by miRNA expression group (Fig.5.8G). Here we see a general trend where the average scores of the Ubx Upregulated genes tend to be more negative, however there are no significant disparities when comparing each miRNA expression group.

Finally, we documented the top predicted miRNA regulators in both *Ubx* regulated cohorts (Fig.5.9A-B). In each grouping of genes, the major miRNA expression group represented is that of the Average expression group (see pie-chart inserts). Interestingly, each gene cohort is targeted best by the same two miRNAs suggesting that these RNAs could be fundamental regulators required during haltere development. Comparing both lists, we see a 75% similarity in miRNAs within each list. This may indicate that these miRNAs have important roles in regulating the general haltere transcriptome. Interestingly, in both cases there are 5 miRNAs which are specific to each cohort. It is intriguing to think that these miRNAs may have particular roles in helping *Ubx* regulate haltere development.

In summary, we explored the possibility that the miRNAs were integrated into the *Ubx* regulated transcriptome of the developing haltere. Analyses of target prediction scores suggest that *Ubx* up-regulated transcripts are more likely to undergo miRNA targeting and subsequent regulation of gene expression. However, we still observe that transcripts undergoing negative transcriptional regulation by *Ubx* are also likely to be targeted.

Fig.5.9 Top predicted miRNA regulators of the *Ubx* instructed transcriptome

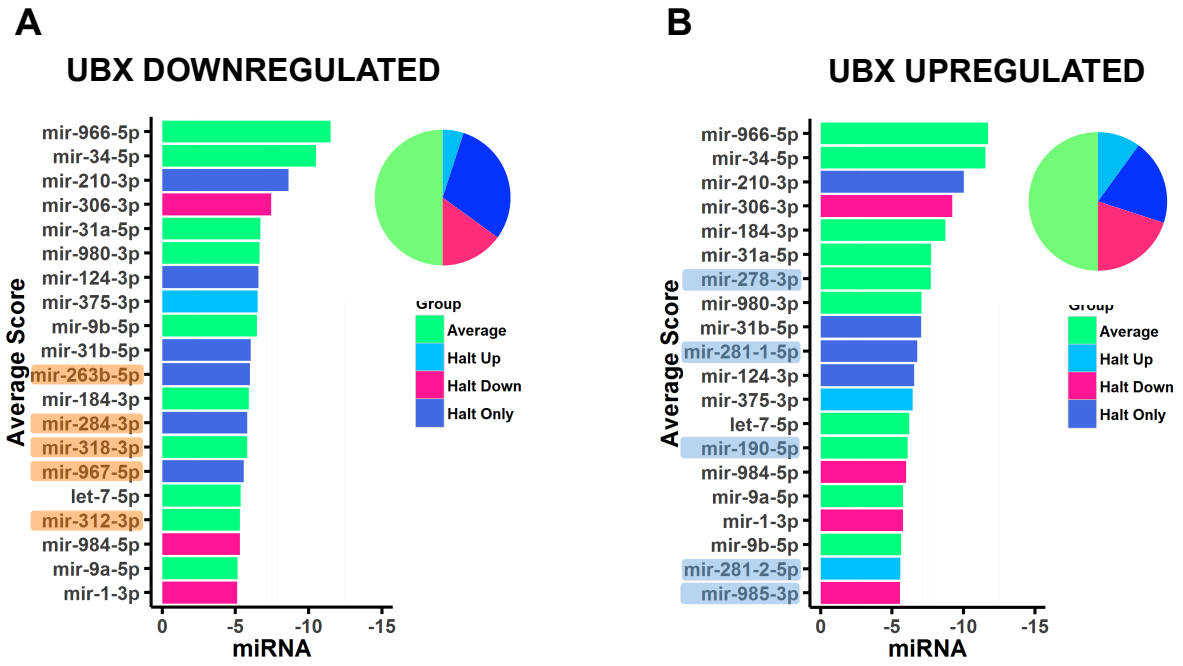

Fig.5.9 Top predicted miRNA regulators of the *Ubx* instructed transcriptome

Summary bar plots of the top targeting miRNAs detected for the Ubx Downregulated and Ubx Upregulated gene cohorts respectively. miRNAs which are specific to each top 20 list are shaded orange and blue respectively.

In general these results raise the intriguing possibility that a main requirement for miRNA activity within the developing haltere is to help buffer and fine-tune the positive transcriptional regulation induced by *Ubx* during haltere development. We also identify a number of miRNAs that are prominent in their targeting abilities of both down-regulated and up-regulated genes within the developing haltere. It will be of interest to look further at these miRNAs and their relationship to *Ubx* activity and function. This analysis may also serve as a starting point in the study of the potential combinatorial regulation of gene targets by multiple miRNAs. Many genes from both cohorts are predicted to be targeted by multiple miRNA. The analysis of these genes, the miRNAs that potentially target them and their role in the development of the haltere are exciting potential avenues of further research.

5.7 Differential miRNA expression through the regulation of RBPs

Our analysis of the potential integration of miRNAs into a *Ubx* regulated transcriptome suggests that the miRNAs found within the haltere may have an important role in the development of this appendage. We again returned to the question of how haltere enriched miRNA expression is generated. In particular, does *Ubx* recruit miRNAs into the gene regulatory networks that govern haltere development?

Earlier analysis of the haltere miRNA expression data suggested that the generation of divergent miRNA expression profiles was likely regulated at a post-transcriptional level of miRNA biogenesis. Possible candidates for this regulation would be RBPs, which have been shown to influence miRNA expression profiles. Again utilising available *Ubx* transcriptome data (Pavlopoulos and Akam, 2011), we searched for evidence that *Ubx* may regulate RBP expression patterns, and in this manner, could control the miRNA expression levels within the haltere (Fig.5.10A).

Comparing the genome wide expression data of tissue with and without *Ubx* present, we looked for RBPs that showed significant changes in expression. The log-fold change for all genes assayed in this experiment was plotted against the significance value of each fold change (Fig.5.10B). Genes which display significant differential expression are highlighted red. There are 155 RBPs present within the microarray platforms used for this experiment. Of these 155 RBPs, 19 had a significant change in expression between the experimental conditions (Fig.5.10C). Interestingly, included within these *Ubx* responsive RBPs, were three fundamental factors associated with canonical miRNA biogenesis – *Drosha*, *Dcr1* and *Loqs*, all showed increased expression in response to the presence of *Ubx*.

Fig.5.10 *Ubx* transcriptional regulation of RBP expression

(A) Schematic highlighting potential relationship between *Ubx* control of miRNA expression through the up-regulation of RBPs. (B) Volcano plot showing changes in gene expression when comparing *Ubx* positive and *Ubx* negative tissue, red data points highlight statistically significant changes in gene expression. Green data points show RBPs detected in this experiment. Data taken from (Pavlopoulos and Akam, 2011). (C) Volcano plot showing only RBP expression changes from the same data set. Red data points highlight statistically significant changes in gene expression. Four RBPs associated with miRNA biogenesis and expression control are highlighted red. (D) Summary of all RBPs with statistically significant changes in gene expression. Yellow bars represent genes associated with miRNA biogenesis and expression control.

Fig.5.10 *Ubx* transcriptional regulation of RBP expression

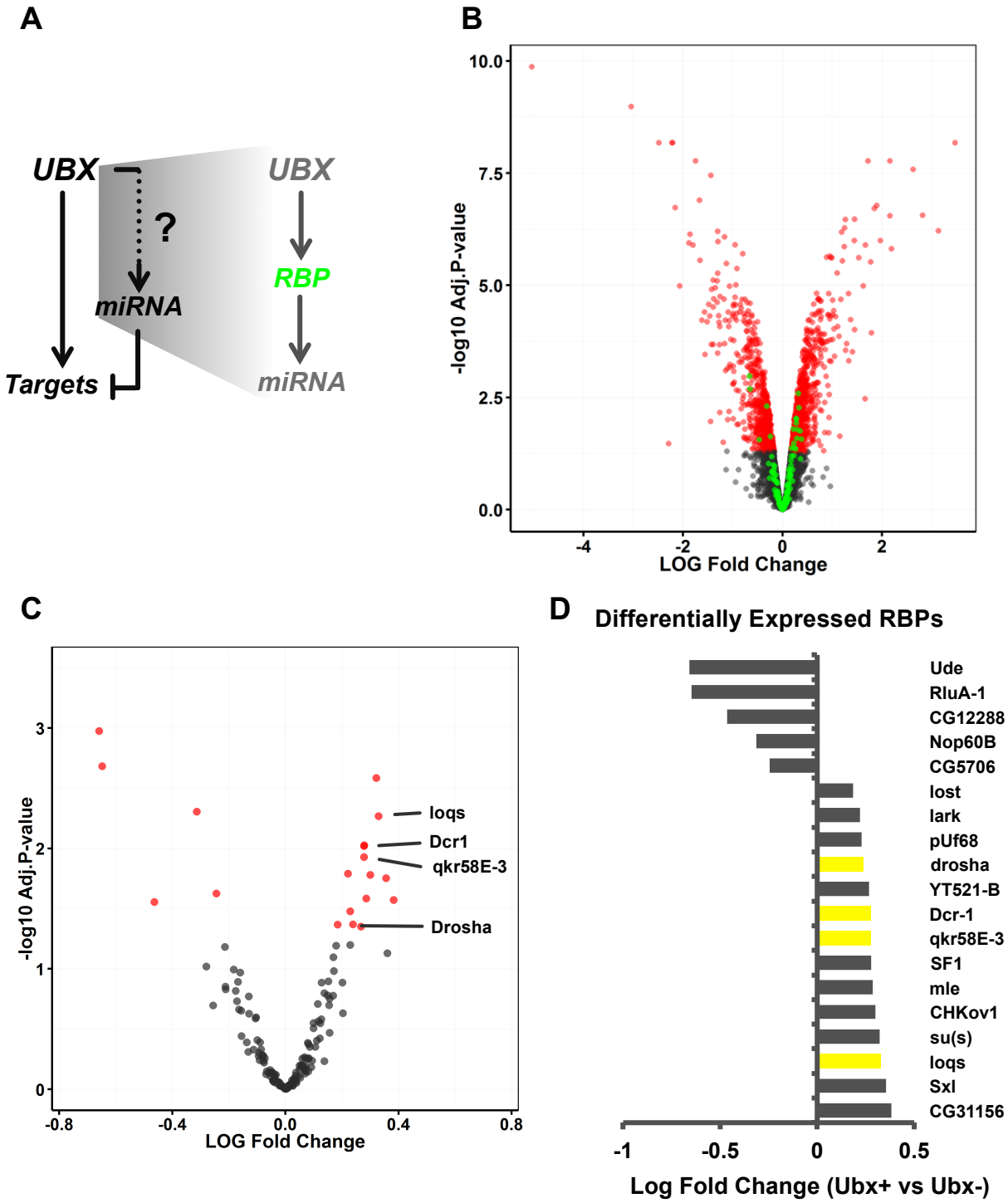

An additional RBP which displayed a significant response to *Ubx* expression was *quaking-related 58E-3 (qkr58E-3).* Intriguingly, vertebrate members of the *Quaking* family of RBPs have been shown to influence miRNA biogenesis (Chen et al., 2012a). Overall, the changes in expression influenced by *Ubx* activity are relatively small compared to many genes seen in this study (Fig.5.10D), however many of these RBPs including those highlighted above approach a 2-fold increase (0.3 log-scale) in expression when *Ubx* is present.

In summary, this analysis reveals that a number of RBPs associated with miRNA biogenesis are responsive to *Ubx* presence in a positive manner. This finding raises an intriguing hypothesis in the manner in which *Ubx* expression could lead to differential miRNA expression within the haltere. *Ubx* transcriptional activity could increase expression levels of core miRNA biogenesis factors like *Drosha*, *Dcr1* and *Loqs*, enhancing the capacity of mature miRNA processing from a pool of pri-miRNA transcripts present within the haltere cells. This elevated miRNA biogenesis and processing would then result in an enrichment of certain susceptible miRNAs within the haltere. This hypothesis of course does not explain the regulation of miRNAs which are down-regulated within the haltere tissue but does highlight the potential importance of RBP activity on miRNA biogenesis. Apart from a few notable examples (*Pum* and many splicing factors) we do not have a full understanding of RBP function during development. It is not impossible that a number of RBPs are capable of fine-tuning the miRNA content in both wing and haltere tissue. Future work could explore these interactions more closely, especially in the context of tissue development. Equally, consolidating the link between *Ubx* activity and RBP regulation of miRNA biogenesis could highlight novel mechanisms in which Hox genes control gene expression indirectly through miRNA activity.

Fig.5.11 Analysis of *Ubx-Dcr1* genetic interactions

(A-D) Sample haltere phenotypes from the four genotypes assayed – *WT*, *Dcr1*$^{-/+}$, *Ubx* $^{-/+}$, *Ubx*$^{-/+}$ *Dcr1*$^{-/+}$. (C'-D') Magnification of homeotic transformations found in *Ubx* $^{-/+}$, *Ubx*$^{-/+}$ *Dcr1*$^{-/+}$genotypes. Black arrowhead marks region were extra ectopic bristles appear in the *Ubx*$^{-/+}$ *Dcr1*$^{-/+}$ genotype compared to *Ubx*$^{-/+}$. (E) Analysis of ectopic bristle distributions seen in the *Ubx* $^{-/+}$, *Ubx*$^{-/+}$ *Dcr1*$^{-/+}$genotypes. Statistical significance determined using Student's t-test, *** represents $p<0.001$. (F) Summary of the relationships between Ubx and miRNA function during haltere development in – *WT*, *Ubx* $^{-/+}$, *Ubx*$^{-/+}$ *Dcr1*$^{-/+}$. For this analysis, the following *n* numbers were used. *WT* - 28, *Dcr1* - 20 , *Ubx* - 36 , *Ubx Dcr1* – 17.

Fig.5.11 Analysis of *Ubx-Dcr1* genetic interactions

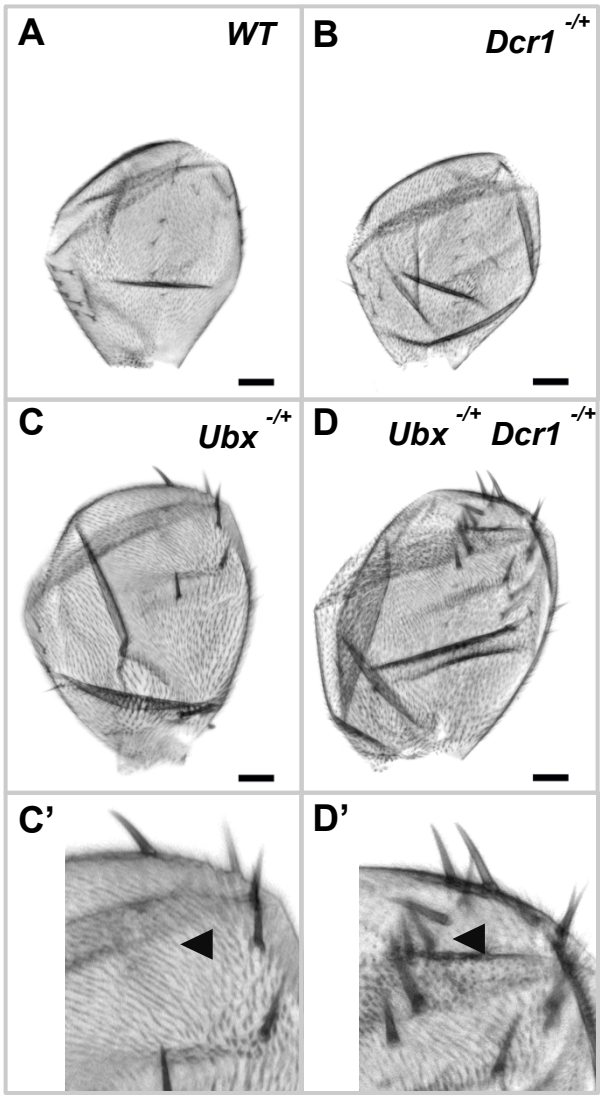

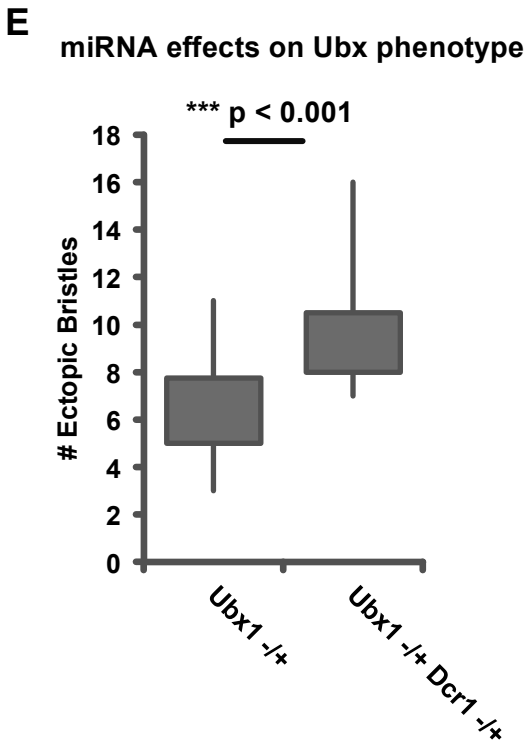

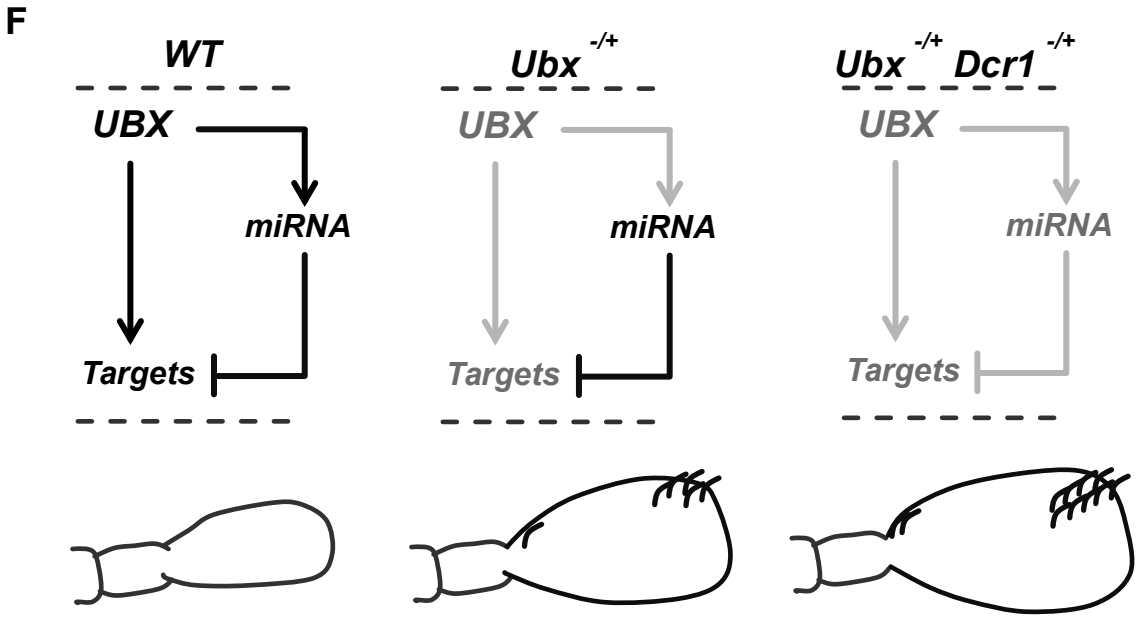

5.8 Genetic interactions between *Ubx* and *Dcr1* affect haltere development

Our analysis of *Ubx*-miRNA interactions suggest that the haltere expressed miRNAs are incorporated into the *Ubx* instructed transcriptome to help regulate these transcripts during development. If this was to be the case, we would expect that disruption to this miRNA activity would be detrimental to *Ubx* function and regulation during haltere development. To test this proposal, we used a genetic interaction assay during haltere development. Animals that are heterozygous for a *Ubx* null allele develop halteres with distinctive partial homeotic transformations – the appearance of large sensory bristles. By combining *Ubx* and *Dcr1* null alleles, we can use the appearance of these homeotic transformations as a read-out of *Ubx* activity. If miRNAs are required for *Ubx* directed haltere development, decreasing *Dcr1* function, and therefore miRNA biogenesis should enhance any *Ubx* homeotic transformations within the haltere. We monitored the appearance of ectopic bristles in four genotypes – *WT*, $Ubx^{-/+}$, $Dcr1^{-/+}$ and $Ubx^{-/+}$ $Dcr1^{-/+}$ (Fig.5.11A-D). Ectopic bristles were detected in only the $Ubx^{-/+}$ and $Ubx^{-/+}$ $Dcr1^{-/+}$ genotypes (Fig.5.11C'-D'). A numerical analysis of these ectopic bristles was performed (Fig.5.11E). We find that the number of ectopic bristles appearing within $Ubx^{-/+}$ $Dcr1^{-/+}$ halteres is significantly increased ($p<0.001$). This data suggests that there is a requirement for correct miRNA functionality within the developing haltere and that the primary role for this miRNA activity is in helping *Ubx* regulate the development of this appendage (Fig.5.11F).

5.9 DISCUSSION

In the previous chapter we described the miRNA profiles of wing and haltere imaginal discs at a specific developmental time point. Here we assessed the functionality of these alternative miRNA profiles and investigated to what extent, these haltere miRNAs are required for the correct development of the haltere appendage.

We were interested in understanding the potential significance of differential miRNA expression, in particular, was there a shared functionality between miRNAs which exhibit similar expression patterns when comparing wing and haltere tissue.

We had previously grouped miRNAs present in the wing and haltere dependant on their relative expression levels between the two tissues. Interestingly, we find that miRNAs which display similar, differential expression profiles tend to have similar sets of predicted target genes. We further show that miRNAs either enriched within the haltere or only expressed within the haltere (Halt Up & Halt Only expression groups) share many predicted target genes. This data suggests that the differential expression patterns of miRNAs may have functional consequences to the biology of the imaginal discs.

To explore this possibility further, we used gene ontology analysis to examine how similar or dissimilar each miRNA expression group is in terms of function. Through this analysis, we uncover significant differences when comparing gene ontologies of specific target genes from each miRNA expression group. These results lend weight to the notion that there may be a functional reason for the differential expression patterns seen between the wing and haltere.

We assessed to what extent *Ubx* regulation and function was integrated with the miRNA content found within the haltere. First, we re-analysed the potential for miRNA targeting of *Ubx* transcripts within the haltere using our understanding of the miRNA content within this tissue. Interestingly, we find no evidence that miRNAs enriched within the haltere, or miRNAs expressed at high levels within the haltere are less likely to target *Ubx*. In fact, the most statistically significant finding was that miRNAs down-regulated within the haltere (Halt Down expression group) are less likely to target *Ubx*. It is hard to discern if miRNAs not enriched within the haltere lack *Ubx* seed sites because they have decreased expression, or rather, because they do not target *Ubx*, there is reduced regulatory pressure to maintain their presence within the haltere. It is important to note that the miRNAs that are enriched in the wing do not necessarily have low levels of expression within the haltere. Overall, these results suggest that *Ubx*

is under a large degree of potential regulatory pressure by miRNAs within the haltere and that these regulatory interactions have evolved to maintain the strict regulation of *Ubx* expression within this tissue.

We next investigated the potential recruitment of the haltere miRNA content into the *Ubx* regulated transcriptome. Combining our sequencing data with available transcriptomic studies, we show that there is greater potential for haltere miRNAs to target genes directly up-regulated by *Ubx* transcriptional activity. This finding suggests that the regulatory input of miRNAs into the *Ubx* transcriptome is required to fine-tune and buffer active transcription within the haltere, not to behave as primary regulators of gene-expression assisting *Ubx* in turning over the haltere transcriptome during development. In this manner we believe a substantial proportion of miRNAs within the haltere are sub-ordinate to *Ubx*, recruited by this Hox factor to help regulate and maintain the developmental programmes of the appendage.

In the previous chapter we observed little evidence to indicate that transcriptional regulation accounts for differing miRNA expression profiles. If *Ubx* does incorporate miRNA activity into its genetic programmes during haltere development, how does it achieve this? To try answer this question, we analysed *Ubx* transcriptomic data as before, looking for evidence that RBPs – common regulators of miRNA biogenesis, are differentially expressed due to *Ubx* activity, potentially facilitating the generation of divergent miRNA profiles. Interestingly, we find that three core components of miRNA biogenesis were up-regulated within the haltere. Our hypothesis is that enhanced miRNA biogenesis leads to increased levels of miRNAs in the haltere. We know little regarding the exact dynamics of miRNA biogenesis and mature miRNA stability. It is possible that some miRNA species require a greater level of biogenesis factors for efficient processing from the pri-miRNA. Alternatively, some miRNAs require constant processing to maintain their required levels. The reason for increased levels of RBP expression induced by *Ubx* and their relationship to miRNA processing are areas for future research. In this context, the haltere provides an excellent developmental model tissue for this work.

To determine the regulatory impact of interactions between haltere miRNAs and *Ubx* function during haltere development, we used a genetic interaction assay to determine the effect reducing miRNA function had on haltere development. Genetically disrupting the expression of *Dcr1*, a miRNA biogenesis factor in a *Ubx* deficient genetic background led to significantly greater homeotic transformations in the haltere. This data suggests that the main requirement for miRNA function during haltere

development is to assist *Ubx* in regulating the haltere transcriptome, not in regulating *Ubx* expression itself.

Overall we believe our analysis will provide an important addition in the effort to understand how Hox genes regulate developmental programmes through co-ordinated global changes in the transcriptome, using *Ubx* regulation of haltere development as a paradigm for Hox. In particular, by integrating our miRNA expression profiles with available transcriptomic data, it will be possible to elucidate and test candidate gene regulatory network motifs formed within the developmental programmes which build the haltere (Fig.5.12A). Through this experimental approach, we may uncover the regulatory pathways used by *Ubx* in specifying particular tissue and cellular fates. This knowledge may provide insight into understanding the potential risks of disruptions to Hox regulatory networks and how they may lead to developmental abnormalities and disease.

What role may global miRNA activity have in the development of the haltere? The primary functions of miRNAs are often documented as either having an 'expression tuning' or 'expression buffering' functions. During the development of the haltere, both modes of action maybe relevant. The increased miRNA content of the haltere may have evolved to fine-tune and buffer the haltere transcriptome, re-enforcing the changing transcriptional programme installed by *Ubx* and ensuring the correct development of this appendage (Fig.5.12B-E). Additionally, the co-ordination and integration of miRNAs to fine-tune and buffer *Ubx* expression cannot be overlooked (Fig.5.12F-G). In this manner, we hypothesise that the main role for miRNAs within the haltere could be viewed as a robust regulatory force which helped the canalisation of the haltere developmental programme induced by *Ubx* during the evolution of haltere morphology.

Fig.5.12 *Ubx*-miRNA integrated gene regulatory networks

(A) Overview of how miRNAs are potentially integrated into the Ubx regulated haltere transcriptome. (B-C) Example coherent feed forward network motifs where a miRNA forms an 'Expression Tuning' role. (D-E) Example incoherent feed forward network motifs where a miRNA forms an 'Expression Buffering' role. (F-G) Example network motifs where miRNAs form 'Expression Tuning' (F) and 'Expression Buffering' (G) network motifs to regulate *Ubx* expression.

Fig.5.12 *Ubx*-miRNA integrated gene regulatory networks

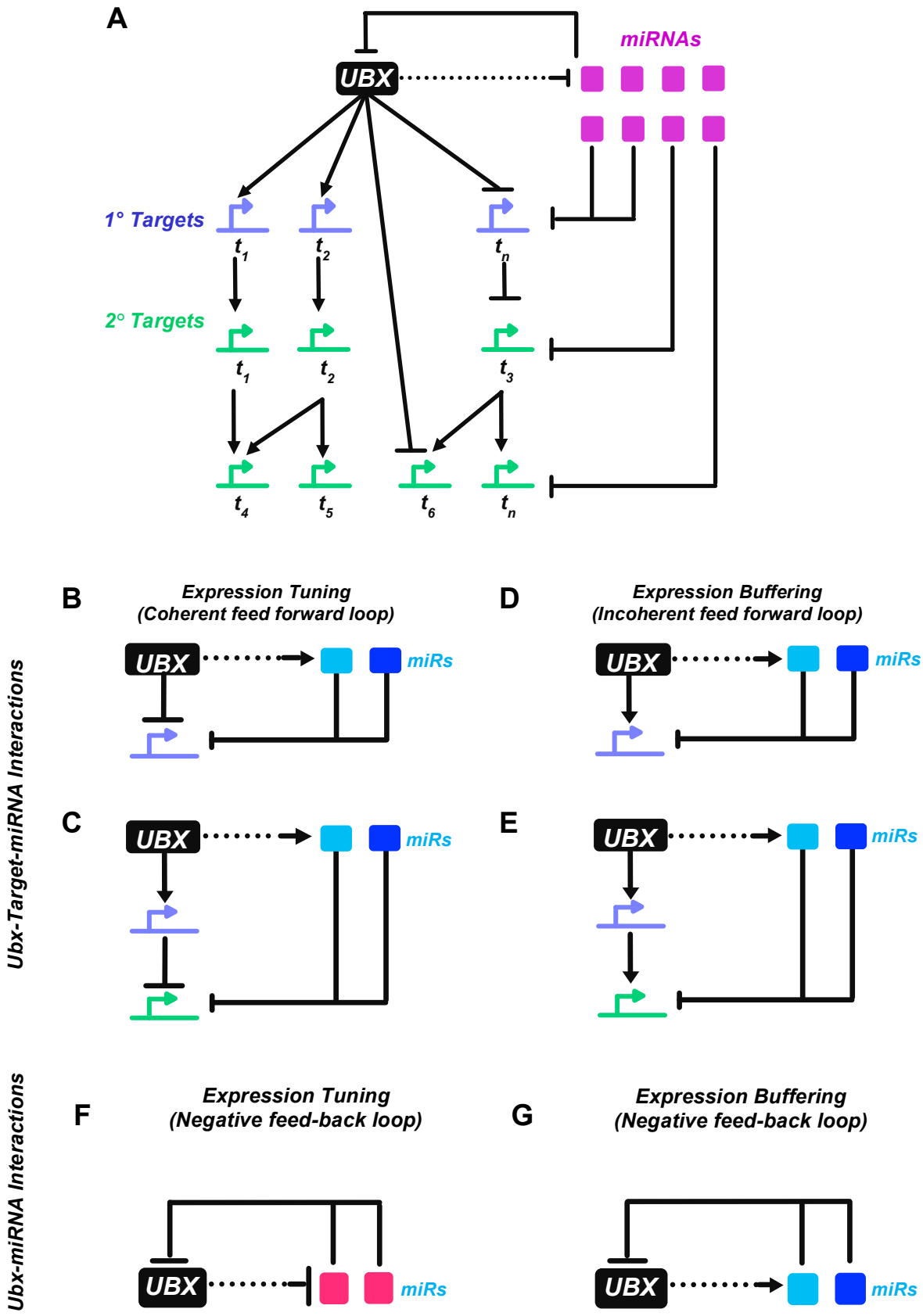

CHAPTER 6

6. Final Discussion

Hox genes encode transcription factors that are fundamental regulators of developmental biology in all animals. They function to regulate cell fate along the antero-posterior axis of all complex animals. Additionally they contribute to the co-ordination and development of animal appendages.

The regulation of Hox gene expression in both spatial and temporal dimensions involves a complex set of genetic interactions and instructions. Failures in these regulatory machinations can lead to severe developmental abnormalities and disease.

Over the last two decades, miRNAs have emerged as fundamental components in the regulation of cellular and developmental biology. So far, their role in helping regulate Hox gene expression and function is not fully understood.

In this thesis we set out to explore two aspects of miRNA-Hox regulatory interactions during development. To uncover to what extent miRNA regulation of *Ubx* expression occurs during development, and importantly, what is the biological significance of these regulatory interactions. Additionally, to understand the relationship between global miRNA activity and *Ubx* function. Specifically, are miRNAs integrated into *Ubx* instructed genetic programmes required for development?

To achieve our objectives we used the *Drosophila* Hox gene *Ubx* and its control of haltere appendage development as a paradigm for Hox function. We first show that the *miR-310C* is required to fine-tune *Ubx* expression in particular regions of the haltere and that this regulation is important for the correct patterning and organisation of the sensory apparatus present within this appendage.

What are the implications of these findings for general Hox function? Although transcriptional regulation of Hox gene expression will always be the fundamental process in which the patterns of Hox gene expression are generated, our results suggest that miRNAs function to fine-tune this expression in certain regions or cell-types during development. This data fits with that seen in vertebrate embryogenesis (Brend et al., 2003; Hornstein et al., 2005) and invertebrates (Bender, 2008; Thomsen et al., 2010) where post-transcriptional mechanisms of regulation are required to accurately define the boundaries of Hox expression. Importantly, we show that this regulation of Hox expression fine-tunes Hox function during development, with implications for the correct development of appendage morphology.

During vertebrate limb development, many Hox genes are expressed within varying regions of the developing limb bud, sometimes in overlapping domains. As the limb develops and extends away from the main body, these domains of expression change. It is intriguing to speculate to what extent miRNAs are involved to help regulate the spatial changes in expression exhibited by different Hox genes. Furthermore, because of their overlapping domains of expression, many cells within the limb bud express multiple Hox genes. We wonder to what extent multiple miRNAs within these cells could manipulate the expression of individual Hox genes and how this fine-tuning of expression could affect Hox function within these cells.

Although Hox genes have been well studied and characterised, we still understand relatively little regarding how Hox genes instruct particular genetic programs in cells and tissues during development. Each given Hox gene may be able to activate or silence hundreds of genes within the genome, but how much does this regulated transcriptome vary between different cell-types and at different developmental transitions? How do Hox genes ensure that the correct changes in gene expression required for development are instigated and maintained? We speculated that miRNAs may be recruited for this function by Hox genes during cell and tissue development. The potential for an individual miRNA to target many transcripts makes them highly pleiotropic regulators. Additionally, the relatively fast-acting nature of miRNA regulation means that these small RNAs are good candidates to function quickly, regulating the changing gene networks installed by Hox activity.

To explore this notion, we identified the full repertoire of miRNAs within the developing tissue of two serially homologous but morphologically distinct appendages – the wing and haltere. Our results show that these two tissues have divergent miRNA profiles which include a number of miRNAs with appendage specific expression patterns. Analysing the functional implications of this data, we suggest that the main role of miRNA activity within the haltere is to assist *Ubx* in regulating the genetic programs that govern the development of this appendage. In particular, we see that transcripts up-regulated by *Ubx* activity are more likely to be targeted by miRNAs within the haltere. The implication from this observation is that *Ubx* may recruit miRNAs to stabilise and maintain transcript expression levels, through the formation of incoherent feed-forward gene-network motifs within the haltere GRNs. Additionally, our study of the genetic interactions between *Ubx* and miRNA biogenesis factor *Dcr1* show that miRNA activity is required for the appropriate development of the haltere, either through the suppression of wing identity and/or the promotion of haltere fate.

Going forward, how may we further these findings into *Ubx*-miRNA interactions and provide insight into the functional requirement for possible *Ubx*-miRNA regulation during haltere appendage development.

A first step is to fully define the nature in which certain miRNA expression levels are controlled in one tissue compared to another. Specifically, are miRNA levels controlled at the transcriptional or post-transcriptional level within that Haltere, and what role does *Ubx* play in this. Our data indicates that this regulation occurs at the post-transcriptional level but how to proves this? A first step would be to repeat our analysis of primary miRNA transcript levels present in wing and haltere tissue using a more sensitive technique than SQ-PCR, for instance quantitative PCR. Do we see altered expression levels of pri-miRNAs that correspond to the detected changes in mature miRNA expression levels? Further to this analysis, a gain-of-function experimental approach could be used. If Ubx activity changes primary miRNA transcript levels, inducing *Ubx* expression within the wing with controlled bursts of Ubx transcriptional activity using the GAL4-GAL80^{ts} binary system (Pavlopoulos and Akam, 2011) should lead to changes to primary miRNA transcript levels.

If this refined analysis again indicates that altered mature miRNA levels are not due to transcriptional regulation of pri-miRNAs, analysing the potential role RBPs may play in this regulation could be further elucidated. Our analysis of previous Ubx transcriptomic studies suggests that *Ubx* has the ability to alter the expression levels of a number of RBP transcripts. A first step would be to define the endogenous levels of these RBPs in both the wing and haltere, minimally at the transcript level and ideally at the protein level. For suspected enriched RBPs within the haltere, a parallel genetic experimental approach could look to determine if disrupting the function of these RBPs could enhance or suppress a *Ubx* phenotype within the haltere, as done with our analysis of *Ubx-Dcr1* interactions within the haltere (Fig.5.11). This approach could indicate which RBPs may be required for the development of the haltere and their relationship to *Ubx* activity.

We hypothesise that *Ubx* recruits miRNAs to help in regulating the changing transcriptome of the haltere during development. A key test of this hypothesis is to determine the function of particular miRNAs within the haltere. To what extent are they required for haltere development and how does this requirement fit with the development of the haltere?

An efficient experimental approach for this would be to select a small cohort of miRNAs and test to what extent they are required for haltere development by removing these

miRNAs from the haltere. This would require the generation of a number of miRNA deletions, not a trivial task. A possible approach would be to use the cis-FRT deletion strategy (Thibault et al., 2004). The suitable candidate list of miRNAs to be investigated could be chosen by looking for those that are most enriched for targets which have also been defined as Ubx transcriptional targets through large-scale transcriptomic studies (Choo et al., 2011; Pavlopoulos and Akam, 2011; Slattery et al., 2011). Candidate miRNAs could be further divided dependant on whether they are predicted to preferentially target transcripts down-regulated or up-regulated or both by *Ubx* activity (Fig.5.8).

An additionally approach would be to look at the developmental role miRNAs that are expressed highly or specifically within the haltere (Halt Up and Halt Only expression groups) have during haltere development and determine to what extent these functions relate to Ubx activity during appendage development.

A long-standing problem within developmental biology has been to define how Hox genes influence cellular development. Carrying on from above analysis, an interesting experimental path into this problem is to first define a *Ubx*-miRNA interaction and then focus on which cellular components are regulated by that specific miRNA. It can then be determined to what extent these factors are also regulated by *Ubx*. The advantage of this approach is by focusing on a specific miRNA (factors implicated in cytoskeletal regulation), we potentially narrow down the possible genetic interactions of *Ubx*, miRNAs and shared target genes making experimental analysis far more approachable. In this manner, we may begin to decipher the small gene regulatory networks present within the haltere and also reveal how Hox genes (in this case *Ubx*) regulate cellular development and the generation of specific morphologies.

How extensive is the recruitment of miRNAs into Hox developmental regulation? In many developmental contexts, Hox genes are expressed within different tissues and cells. In each instance, the Hox gene must instigate a specific developmental programme. For example, during *Drosophila* post-embryonic development, *Ubx* is expressed within specific cells of the VNC (Marin et al., 2012). The function of *Ubx* in these cells differs, instructing both cell-death and cell-survival as well as specifying particular differentiation programs and axonal morphologies. To achieve these different developmental fates, each cell must use an alternative developmental program, in part through the activity of *Ubx*. It would be fascinating to investigate if alternative sets of miRNAs are recruited to help regulate and maintain these genetic programs. It remains

to be seen how specific Hox recruitment of miRNAs can be with regards to different cell and tissue types as well as alternative Hox inputs.

Overall, this work explores different aspects of Hox-miRNA regulatory interactions and their functional consequences during animal development. We believe that our findings offer insight into the important regulatory capacity of miRNAs and their ability to assist Hox function in shaping the development and morphology of complex appendages.

CHAPTER 7

7. Bibliography

Agrawal, P., Habib, F., Yelagandula, R., Shashidhara, L.S., 2011. Genome-level identification of targets of Hox protein Ultrabithorax in Drosophila: novel mechanisms for target selection. Sci Rep 1, 205.

Akam, M.E., Martinez-Arias, A., 1985. The distribution of Ultrabithorax transcripts in Drosophila embryos. EMBO J. 4, 1689–1700.

Alonso, C.R., 2012. A complex “mRNA degradation code” controls gene expression during animal development. Trends Genet. 28, 78–88.

Arif, S., Murat, S., Almudi, I., Nunes, M.D.S., Bortolamiol-Becet, D., McGregor, N.S., Currie, J.M.S., Hughes, H., Ronshaugen, M., Sucena, É., Lai, E.C., Schlötterer, C., McGregor, A.P., 2013. Evolution of mir-92a underlies natural morphological variation in Drosophila melanogaster. Curr. Biol. 23, 523–528.

Asli, N.S., Kessel, M., 2010. Spatiotemporally restricted regulation of generic motor neuron programs by miR-196-mediated repression of Hoxb8. Dev. Biol. 344, 857–868.

Baek, M., Enriquez, J., Mann, R.S., 2013. Dual role for Hox genes and Hox co-factors in conferring leg motoneuron survival and identity in Drosophila. Development 140, 2027–2038.

Bartel, D.P., 2009. MicroRNAs: target recognition and regulatory functions. Cell 136, 215–233.

Bartel, D.P., Chen, C.-Z., 2004. Micromanagers of gene expression: the potentially widespread influence of metazoan microRNAs. Nat. Rev. Genet. 5, 396–400.

Bello, B.C., Hirth, F., Gould, A.P., 2003. A pulse of the Drosophila Hox protein Abdominal-A schedules the end of neural proliferation via neuroblast apoptosis. Neuron 37, 209–219.

Bender, W., 2008. MicroRNAs in the Drosophila bithorax complex. Genes Dev. 22, 14–19.

Bender, W., Akam, M., Karch, F., Beachy, P.A., Peifer, M., Spierer, P., Lewis, E.B., Hogness, D.S., 1983. Molecular Genetics of the Bithorax Complex in Drosophila melanogaster. Science 221, 23–29.

Bentley, D.L., 2014. Coupling mRNA processing with transcription in time and space. Nat. Rev. Genet. 15, 163–175.

Béthune, J., Artus-Revel, C.G., Filipowicz, W., 2012. Kinetic analysis reveals successive steps leading to miRNA-mediated silencing in mammalian cells. EMBO Rep. 13, 716–723.

Biemar, F., Zinzen, R., Ronshaugen, M., Sementchenko, V., Manak, J.R., Levine, M.S., 2005. Spatial regulation of microRNA gene expression in the Drosophila embryo. Proc. Natl. Acad. Sci. U.S.A. 102, 15907–15911.

Blair, S.S., Brower, D.L., Thomas, J.B., Zavortink, M., 1994. The role of apterous in the control of dorsoventral compartmentalization and PS integrin gene expression in the developing wing of Drosophila. Development 120, 1805–1815.

Blochlinger, K., Jan, L.Y., Jan, Y.N., 1991. Transformation of sensory organ identity by ectopic expression of Cut in Drosophila. Genes Dev. 5, 1124–1135.

Bonev, B., Stanley, P., Papalopulu, N., 2012. MicroRNA-9 Modulates Hes1 ultradian oscillations by forming a double-negative feedback loop. Cell Rep 2, 10–18.

Brend, T., Gilthorpe, J., Summerbell, D., Rigby, P.W.J., 2003. Multiple levels of transcriptional and post-transcriptional regulation are required to define the domain of Hoxb4 expression. Development 130, 2717–2728.

Brennecke, J., Hipfner, D.R., Stark, A., Russell, R.B., Cohen, S.M., 2003. bantam encodes a developmentally regulated microRNA that controls cell proliferation and regulates the proapoptotic gene hid in Drosophila. Cell 113, 25–36.

Burt, R., Palka, J., 1982. The central projections of mesothoracic sensory neurons in wild-type Drosophila and bithorax mutants. Dev. Biol. 90, 99–109.

Bushati, N., Cohen, S.M., 2007. microRNA functions. Annu. Rev. Cell Dev. Biol. 23, 175–205.

Capdevila, J., Guerrero, I., 1994. Targeted expression of the signaling molecule decapentaplegic induces pattern duplications and growth alterations in Drosophila wings. EMBO J. 13, 4459–4468.

Chan, C.S., Rastelli, L., Pirrotta, V., 1994. A Polycomb response element in the Ubx gene that determines an epigenetically inherited state of repression. EMBO J. 13, 2553–2564.

Chang, C.-J., Chao, C.-H., Xia, W., Yang, J.-Y., Xiong, Y., Li, C.-W., Yu, W.-H., Rehman, S.K., Hsu, J.L., Lee, H.-H., Liu, M., Chen, C.-T., Yu, D., Hung, M.-C., 2011. p53 regulates epithelial-mesenchymal transition and stem cell properties through modulating miRNAs. Nat. Cell Biol. 13, 317–323.

Chawla, G., Sokol, N.S., 2012. Hormonal activation of let-7-C microRNAs via EcR is required for adult Drosophila melanogaster morphology and function. Development 139, 1788–1797.

Chen, A.-J., Paik, J.-H., Zhang, H., Shukla, S.A., Mortensen, R., Hu, J., Ying, H., Hu, B., Hurt, J., Farny, N., Dong, C., Xiao, Y., Wang, Y.A., Silver, P.A., Chin, L., Vasudevan, S., Depinho, R.A., 2012a. STAR RNA-binding protein Quaking suppresses cancer via stabilization of specific miRNA. Genes Dev. 26, 1459–1472.

Chen, Y., Takano-Maruyama, M., Fritzsch, B., Gaufo, G.O., 2012b. Hoxb1 controls anteroposterior identity of vestibular projection neurons. PLoS ONE 7, e34762.

Choo, S.W., White, R., Russell, S., 2011. Genome-wide analysis of the binding of the Hox protein Ultrabithorax and the Hox cofactor Homothorax in Drosophila. PLoS ONE 6, e14778.

Cohen, B., McGuffin, M.E., Pfeifle, C., Segal, D., Cohen, S.M., 1992. apterous, a gene required for imaginal disc development in Drosophila encodes a member of the LIM family of developmental regulatory proteins. Genes Dev. 6, 715–729.

Cole, E.S., Palka, J., 1982. The pattern of campaniform sensilla on the wing and haltere of Drosophila melanogaster and several of its homeotic mutants. J Embryol Exp Morphol 71, 41–61.

Crickmore, M.A., Mann, R.S., 2006. Hox control of organ size by regulation of morphogen production and mobility. Science 313, 63–68.

Cui, Q., Yu, Z., Purisima, E.O., Wang, E., 2006. Principles of microRNA regulation of a human cellular signaling network. Mol. Syst. Biol. 2, 46.

Dasen, J.S., Liu, J.-P., Jessell, T.M., 2003. Motor neuron columnar fate imposed by sequential phases of Hox-c activity. Nature 425, 926–933.

Dasen, J.S., Tice, B.C., Brenner-Morton, S., Jessell, T.M., 2005. A Hox regulatory network establishes motor neuron pool identity and target-muscle connectivity. Cell 123, 477–491.

Davis, A.P., Witte, D.P., Hsieh-Li, H.M., Potter, S.S., Capecchi, M.R., 1995. Absence of radius and ulna in mice lacking hoxa-11 and hoxd-11. Nature 375, 791–795.

Davis, N., Mor, E., Ashery-Padan, R., 2011. Roles for Dicer1 in the patterning and differentiation of the optic cup neuroepithelium. Development 138, 127–138.

De Navas, L., Foronda, D., Suzanne, M., Sánchez-Herrero, E., 2006a. A simple and efficient method to identify replacements of P-lacZ by P-Gal4 lines allows obtaining Gal4 insertions in the bithorax complex of Drosophila. Mech. Dev. 123, 860–867.

De Navas, L.F., Garaulet, D.L., Sánchez-Herrero, E., 2006b. The ultrabithorax Hox gene of Drosophila controls haltere size by regulating the Dpp pathway. Development 133, 4495–4506.

De Navas, L.F., Reed, H., Akam, M., Barrio, R., Alonso, C.R., Sánchez-Herrero, E., 2011. Integration of RNA processing and expression level control modulates the

function of the Drosophila Hox gene Ultrabithorax during adult development. Development 138, 107–116.

De Pontual, L., Yao, E., Callier, P., Faivre, L., Drouin, V., Cariou, S., Van Haeringen, A., Geneviève, D., Goldenberg, A., Oufadem, M., Manouvrier, S., Munnich, A., Vidigal, J.A., Vekemans, M., Lyonnet, S., Henrion-Caude, A., Ventura, A., Amiel, J., 2011. Germline deletion of the miR-17∼92 cluster causes skeletal and growth defects in humans. Nat. Genet. 43, 1026–1030.

Di Bonito, M., Narita, Y., Avallone, B., Sequino, L., Mancuso, M., Andolfi, G., Franzè, A.M., Puelles, L., Rijli, F.M., Studer, M., 2013. Assembly of the auditory circuitry by a Hox genetic network in the mouse brainstem. PLoS Genet. 9, e1003249.

Di Pietro, M., Lao-Sirieix, P., Boyle, S., Cassidy, A., Castillo, D., Saadi, A., Eskeland, R., Fitzgerald, R.C., 2012. Evidence for a functional role of epigenetically regulated midcluster HOXB genes in the development of Barrett esophagus. Proc. Natl. Acad. Sci. U.S.A. 109, 9077–9082.

Dill, H., Linder, B., Fehr, A., Fischer, U., 2012. Intronic miR-26b controls neuronal differentiation by repressing its host transcript, ctdsp2. Genes Dev. 26, 25–30.

Djuranovic, S., Nahvi, A., Green, R., 2012. miRNA-mediated gene silencing by translational repression followed by mRNA deadenylation and decay. Science 336, 237–240.

Dore, L.C., Amigo, J.D., Dos Santos, C.O., Zhang, Z., Gai, X., Tobias, J.W., Yu, D., Klein, A.M., Dorman, C., Wu, W., Hardison, R.C., Paw, B.H., Weiss, M.J., 2008. A GATA-1-regulated microRNA locus essential for erythropoiesis. Proc. Natl. Acad. Sci. U.S.A. 105, 3333–3338.

Duboule, D., Morata, G., 1994. Colinearity and functional hierarchy among genes of the homeotic complexes. Trends Genet. 10, 358–364.

Eulalio, A., Mano, M., Dal Ferro, M., Zentilin, L., Sinagra, G., Zacchigna, S., Giacca, M., 2012. Functional screening identifies miRNAs inducing cardiac regeneration. Nature 492, 376–381.

Fernandes, J., Celniker, S.E., Lewis, E.B., VijayRaghavan, K., 1994. Muscle development in the four-winged Drosophila and the role of the Ultrabithorax gene. Curr. Biol. 4, 957–964.

Fjose, A., McGinnis, W.J., Gehring, W.J., 1985. Isolation of a homoeo box-containing gene from the engrailed region of Drosophila and the spatial distribution of its transcripts. Nature 313, 284–289.

Freitas, R., Gómez-Marín, C., Wilson, J.M., Casares, F., Gómez-Skarmeta, J.L., 2012. Hoxd13 contribution to the evolution of vertebrate appendages. Dev. Cell 23, 1219–1229.

Galant, R., Walsh, C.M., Carroll, S.B., 2002. Hox repression of a target gene: extradenticle-independent, additive action through multiple monomer binding sites. Development 129, 3115–3126.

Gho, M., Bellaïche, Y., Schweisguth, F., 1999. Revisiting the Drosophila microchaete lineage: a novel intrinsically asymmetric cell division generates a glial cell. Development 126, 3573–3584.

Goff, D.J., Tabin, C.J., 1997. Analysis of Hoxd-13 and Hoxd-11 misexpression in chick limb buds reveals that Hox genes affect both bone condensation and growth. Development 124, 627–636.

Gross, S., Krause, Y., Wuelling, M., Vortkamp, A., 2012. Hoxa11 and Hoxd11 regulate chondrocyte differentiation upstream of Runx2 and Shox2 in mice. PLoS ONE 7, e43553.

Guillén, I., Mullor, J.L., Capdevila, J., Sánchez-Herrero, E., Morata, G., Guerrero, I., 1995. The function of engrailed and the specification of Drosophila wing pattern. Development 121, 3447–3456.

Guo, H., Ingolia, N.T., Weissman, J.S., Bartel, D.P., 2010. Mammalian microRNAs predominantly act to decrease target mRNA levels. Nature 466, 835–840.

Gutzwiller, L.M., Witt, L.M., Gresser, A.L., Burns, K.A., Cook, T.A., Gebelein, B., 2010. Proneural and abdominal Hox inputs synergize to promote sensory organ formation in the Drosophila abdomen. Dev. Biol. 348, 231–243.

Hagan, J.P., Piskounova, E., Gregory, R.I., 2009. Lin28 recruits the TUTase Zcchc11 to inhibit let-7 maturation in mouse embryonic stem cells. Nat. Struct. Mol. Biol. 16, 1021–1025.

Haramati, S., Chapnik, E., Sztainberg, Y., Eilam, R., Zwang, R., Gershoni, N., McGlinn, E., Heiser, P.W., Wills, A.-M., Wirguin, I., Rubin, L.L., Misawa, H., Tabin, C.J., Brown, R., Jr, Chen, A., Hornstein, E., 2010. miRNA malfunction causes spinal motor neuron disease. Proc. Natl. Acad. Sci. U.S.A. 107, 13111–13116.

Harding, K., Wedeen, C., McGinnis, W., Levine, M., 1985. Spatially regulated expression of homeotic genes in Drosophila. Science 229, 1236–1242.

Heitzler, P., Simpson, P., 1991. The choice of cell fate in the epidermis of Drosophila. Cell 64, 1083–1092.

Heo, I., Joo, C., Kim, Y.-K., Ha, M., Yoon, M.-J., Cho, J., Yeom, K.-H., Han, J., Kim, V.N., 2009. TUT4 in concert with Lin28 suppresses microRNA biogenesis through pre-microRNA uridylation. Cell 138, 696–708.

Herranz, H., Cohen, S.M., 2010. MicroRNAs and gene regulatory networks: managing the impact of noise in biological systems. Genes Dev. 24, 1339–1344.

Hersh, B.M., Nelson, C.E., Stoll, S.J., Norton, J.E., Albert, T.J., Carroll, S.B., 2007. The UBX-regulated network in the haltere imaginal disc of D. melanogaster. Dev. Biol. 302, 717–727.

Hilgers, V., Perry, M.W., Hendrix, D., Stark, A., Levine, M., Haley, B., 2011. Neural-specific elongation of 3' UTRs during Drosophila development. Proc. Natl. Acad. Sci. U.S.A. 108, 15864–15869.

Hornstein, E., Mansfield, J.H., Yekta, S., Hu, J.K.-H., Harfe, B.D., McManus, M.T., Baskerville, S., Bartel, D.P., Tabin, C.J., 2005. The microRNA miR-196 acts upstream of Hoxb8 and Shh in limb development. Nature 438, 671–674.

Hornstein, E., Shomron, N., 2006. Canalization of development by microRNAs. Nat. Genet. 38 Suppl, S20–24.

Huang, Y.-W.A., Ruiz, C.R., Eyler, E.C.H., Lin, K., Meffert, M.K., 2012. Dual regulation of miRNA biogenesis generates target specificity in neurotrophin-induced protein synthesis. Cell 148, 933–946.

Ingham, P.W., Martinez-Arias, A., 1986. The correct activation of Antennapedia and bithorax complex genes requires the fushi tarazu gene. Nature 324, 592–597.

Irvine, K.D., Helfand, S.L., Hogness, D.S., 1991. The large upstream control region of the Drosophila homeotic gene Ultrabithorax. Development 111, 407–424.

Jan, Y.N., Jan, L.Y., 1994. Neuronal cell fate specification in Drosophila. Curr. Opin. Neurobiol. 4, 8–13.

Jones, C.I., Grima, D.P., Waldron, J.A., Jones, S., Parker, H.N., Newbury, S.F., 2013. The 5'-3' exoribonuclease Pacman (Xrn1) regulates expression of the heat shock protein Hsp67Bc and the microRNA miR-277-3p in Drosophila wing imaginal discs. RNA Biol 10, 1345–1355.

Jung, H., Lacombe, J., Mazzoni, E.O., Liem, K.F., Jr, Grinstein, J., Mahony, S., Mukhopadhyay, D., Gifford, D.K., Young, R.A., Anderson, K.V., Wichterle, H., Dasen, J.S., 2010. Global control of motor neuron topography mediated by the repressive actions of a single hox gene. Neuron 67, 781–796.

Kaufman, T.C., Lewis, R., Wakimoto, B., 1980. Cytogenetic Analysis of Chromosome 3 in DROSOPHILA MELANOGASTER: The Homoeotic Gene Complex in Polytene Chromosome Interval 84a-B. Genetics 94, 115–133.

Kedde, M., Van Kouwenhove, M., Zwart, W., Oude Vrielink, J.A.F., Elkon, R., Agami, R., 2010. A Pumilio-induced RNA structure switch in p27-3' UTR controls miR-221 and miR-222 accessibility. Nat. Cell Biol. 12, 1014–1020.

Kertesz, M., Iovino, N., Unnerstall, U., Gaul, U., Segal, E., 2007. The role of site accessibility in microRNA target recognition. Nat. Genet. 39, 1278–1284.

Kim, H.H., Kuwano, Y., Srikantan, S., Lee, E.K., Martindale, J.L., Gorospe, M., 2009a. HuR recruits let-7/RISC to repress c-Myc expression. Genes Dev. 23, 1743–1748.

Kim, V.N., Han, J., Siomi, M.C., 2009b. Biogenesis of small RNAs in animals. Nat. Rev. Mol. Cell Biol. 10, 126–139.

Kmita, M., Tarchini, B., Zàkàny, J., Logan, M., Tabin, C.J., Duboule, D., 2005. Early developmental arrest of mammalian limbs lacking HoxA/HoxD gene function. Nature 435, 1113–1116.

Kornfeld, K., Saint, R.B., Beachy, P.A., Harte, P.J., Peattie, D.A., Hogness, D.S., 1989. Structure and expression of a family of Ultrabithorax mRNAs generated by alternative splicing and polyadenylation in Drosophila. Genes Dev. 3, 243–258.

Kredo-Russo, S., Mandelbaum, A.D., Ness, A., Alon, I., Lennox, K.A., Behlke, M.A., Hornstein, E., 2012. Pancreas-enriched miRNA refines endocrine cell differentiation. Development 139, 3021–3031.

Krol, J., Loedige, I., Filipowicz, W., 2010. The widespread regulation of microRNA biogenesis, function and decay. Nat. Rev. Genet. 11, 597–610.

Krumlauf, R., 1994. Hox genes in vertebrate development. Cell 78, 191–201.

Langmead, B., Trapnell, C., Pop, M., Salzberg, S.L., 2009. Ultrafast and memory-efficient alignment of short DNA sequences to the human genome. Genome Biol. 10, R25.

Laufer, E., Nelson, C.E., Johnson, R.L., Morgan, B.A., Tabin, C., 1994. Sonic hedgehog and Fgf-4 act through a signaling cascade and feedback loop to integrate growth and patterning of the developing limb bud. Cell 79, 993–1003.

Lecuit, T., Brook, W.J., Ng, M., Calleja, M., Sun, H., Cohen, S.M., 1996. Two distinct mechanisms for long-range patterning by Decapentaplegic in the Drosophila wing. Nature 381, 387–393.

Lemons, D., McGinnis, W., 2006. Genomic evolution of Hox gene clusters. Science 313, 1918–1922.

Lewis, E.B., 1978. A gene complex controlling segmentation in Drosophila. Nature 276, 565–570.

Li, X., Cassidy, J.J., Reinke, C.A., Fischboeck, S., Carthew, R.W., 2009. A microRNA imparts robustness against environmental fluctuation during development. Cell 137, 273–282.

Li, Y., Wang, F., Lee, J.-A., Gao, F.-B., 2006. MicroRNA-9a ensures the precise specification of sensory organ precursors in Drosophila. Genes Dev. 20, 2793–2805.

Li-Kroeger, D., Cook, T.A., Gebelein, B., 2012. Integration of an abdominal Hox complex with Pax2 yields cell-specific EGF secretion from Drosophila sensory precursor cells. Development 139, 1611–1619.

Liu, N., Landreh, M., Cao, K., Abe, M., Hendriks, G.-J., Kennerdell, J.R., Zhu, Y., Wang, L.-S., Bonini, N.M., 2012. The microRNA miR-34 modulates ageing and neurodegeneration in Drosophila. Nature 482, 519–523.

Logan, M., Simon, H.G., Tabin, C., 1998. Differential regulation of T-box and homeobox transcription factors suggests roles in controlling chick limb-type identity. Development 125, 2825–2835.

Lohmann, I., McGinnis, N., Bodmer, M., McGinnis, W., 2002. The Drosophila Hox gene deformed sculpts head morphology via direct regulation of the apoptosis activator reaper. Cell 110, 457–466.

Marin, E.C., Dry, K.E., Alaimo, D.R., Rudd, K.T., Cillo, A.R., Clenshaw, M.E., Negre, N., White, K.P., Truman, J.W., 2012. Ultrabithorax confers spatial identity in a context-specific manner in the Drosophila postembryonic ventral nervous system. Neural Dev 7, 31.

Marson, A., Levine, S.S., Cole, M.F., Frampton, G.M., Brambrink, T., Johnstone, S., Guenther, M.G., Johnston, W.K., Wernig, M., Newman, J., Calabrese, J.M., Dennis, L.M., Volkert, T.L., Gupta, S., Love, J., Hannett, N., Sharp, P.A., Bartel,

D.P., Jaenisch, R., Young, R.A., 2008. Connecting microRNA genes to the core transcriptional regulatory circuitry of embryonic stem cells. Cell 134, 521–533.

Martinez-Arias, A., Lawrence, P.A., 1985. Parasegments and compartments in the Drosophila embryo. Nature 313, 639–642.

McGinnis, W., Garber, R.L., Wirz, J., Kuroiwa, A., Gehring, W.J., 1984. A homologous protein-coding sequence in Drosophila homeotic genes and its conservation in other metazoans. Cell 37, 403–408.

McGlinn, E., Yekta, S., Mansfield, J.H., Soutschek, J., Bartel, D.P., Tabin, C.J., 2009. In ovo application of antagomiRs indicates a role for miR-196 in patterning the chick axial skeleton through Hox gene regulation. Proc. Natl. Acad. Sci. U.S.A. 106, 18610–18615.

McGuire, S.E., Le, P.T., Osborn, A.J., Matsumoto, K., Davis, R.L., 2003. Spatiotemporal rescue of memory dysfunction in Drosophila. Science 302, 1765–1768.

Meijer, H.A., Kong, Y.W., Lu, W.T., Wilczynska, A., Spriggs, R.V., Robinson, S.W., Godfrey, J.D., Willis, A.E., Bushell, M., 2013. Translational repression and eIF4A2 activity are critical for microRNA-mediated gene regulation. Science 340, 82–85.

Melton, C., Judson, R.L., Blelloch, R., 2010. Opposing microRNA families regulate self-renewal in mouse embryonic stem cells. Nature 463, 621–626.

Mendell, J.T., Olson, E.N., 2012. MicroRNAs in stress signaling and human disease. Cell 148, 1172–1187.

Miguel-Aliaga, I., Thor, S., 2004. Segment-specific prevention of pioneer neuron apoptosis by cell-autonomous, postmitotic Hox gene activity. Development 131, 6093–6105.

Miguez, A., Ducret, S., Di Meglio, T., Parras, C., Hmidan, H., Haton, C., Sekizar, S., Mannioui, A., Vidal, M., Kerever, A., Nyabi, O., Haigh, J., Zalc, B., Rijli, F.M., Thomas, J.-L., 2012. Opposing roles for Hoxa2 and Hoxb2 in hindbrain oligodendrocyte patterning. J. Neurosci. 32, 17172–17185.

Miles, W.O., Tschöp, K., Herr, A., Ji, J.-Y., Dyson, N.J., 2012. Pumilio facilitates miRNA regulation of the E2F3 oncogene. Genes Dev. 26, 356–368.

Millevoi, S., Vagner, S., 2010. Molecular mechanisms of eukaryotic pre-mRNA 3’ end processing regulation. Nucleic Acids Res. 38, 2757–2774.

Mohit, P., Makhijani, K., Madhavi, M.B., Bharathi, V., Lal, A., Sirdesai, G., Reddy, V.R., Ramesh, P., Kannan, R., Dhawan, J., Shashidhara, L.S., 2006. Modulation of AP and DV signaling pathways by the homeotic gene Ultrabithorax during haltere development in Drosophila. Dev. Biol. 291, 356–367.

Müller, J., Bienz, M., 1991. Long range repression conferring boundaries of Ultrabithorax expression in the Drosophila embryo. EMBO J. 10, 3147–3155.

Müller, J., Bienz, M., 1992. Sharp anterior boundary of homeotic gene expression conferred by the fushi tarazu protein. EMBO J. 11, 3653–3661.

Mukherji, S., Ebert, M.S., Zheng, G.X.Y., Tsang, J.S., Sharp, P.A., Van Oudenaarden, A., 2011. MicroRNAs can generate thresholds in target gene expression. Nat. Genet. 43, 854–859.

Muragaki, Y., Mundlos, S., Upton, J., Olsen, B.R., 1996. Altered growth and branching patterns in synpolydactyly caused by mutations in HOXD13. Science 272, 548–551.

Murata, Y., Wharton, R.P., 1995. Binding of pumilio to maternal hunchback mRNA is required for posterior patterning in Drosophila embryos. Cell 80, 747–756.

Nagaso, H., Murata, T., Day, N., Yokoyama, K.K., 2001. Simultaneous detection of RNA and protein by in situ hybridization and immunological staining. J. Histochem. Cytochem. 49, 1177–1182.

Nelson, C.E., Morgan, B.A., Burke, A.C., Laufer, E., DiMambro, E., Murtaugh, L.C., Gonzales, E., Tessarollo, L., Parada, L.F., Tabin, C., 1996. Analysis of Hox gene expression in the chick limb bud. Development 122, 1449–1466.

Neveu, P., Kye, M.J., Qi, S., Buchholz, D.E., Clegg, D.O., Sahin, M., Park, I.-H., Kim, K.-S., Daley, G.Q., Kornblum, H.I., Shraiman, B.I., Kosik, K.S., 2010. MicroRNA profiling reveals two distinct p53-related human pluripotent stem cell states. Cell Stem Cell 7, 671–681.

Niswander, L., Jeffrey, S., Martin, G.R., Tickle, C., 1994. A positive feedback loop coordinates growth and patterning in the vertebrate limb. Nature 371, 609–612.

Nottebohm, E., Usui, A., Therianos, S., Kimura, K., Dambly-Chaudière, C., Ghysen, A., 1994. The gene poxn controls different steps of the formation of chemosensory organs in Drosophila. Neuron 12, 25–34.

O'Connor, M.B., Binari, R., Perkins, L.A., Bender, W., 1988. Alternative RNA products from the Ultrabithorax domain of the bithorax complex. EMBO J. 7, 435–445.

Ohuchi, H., Nakagawa, T., Yamamoto, A., Araga, A., Ohata, T., Ishimaru, Y., Yoshioka, H., Kuwana, T., Nohno, T., Yamasaki, M., Itoh, N., Noji, S., 1997. The mesenchymal factor, FGF10, initiates and maintains the outgrowth of the chick limb bud through interaction with FGF8, an apical ectodermal factor. Development 124, 2235–2244.

Ohuchi, H., Takeuchi, J., Yoshioka, H., Ishimaru, Y., Ogura, K., Takahashi, N., Ogura, T., Noji, S., 1998. Correlation of wing-leg identity in ectopic FGF-induced chimeric limbs with the differential expression of chick Tbx5 and Tbx4. Development 125, 51–60.

Okamura, K., Hagen, J.W., Duan, H., Tyler, D.M., Lai, E.C., 2007. The mirtron pathway generates microRNA-class regulatory RNAs in Drosophila. Cell 130, 89–100.

Okamura, K., Liu, N., Lai, E.C., 2009. Distinct mechanisms for microRNA strand selection by Drosophila Argonautes. Mol. Cell 36, 431–444.

Okamura, K., Phillips, M.D., Tyler, D.M., Duan, H., Chou, Y., Lai, E.C., 2008. The regulatory activity of microRNA* species has substantial influence on microRNA and 3' UTR evolution. Nat. Struct. Mol. Biol. 15, 354–363.

Ooi, C.H., Oh, H.K., Wang, H.Z., Tan, A.L.K., Wu, J., Lee, M., Rha, S.Y., Chung, H.C., Virshup, D.M., Tan, P., 2011. A densely interconnected genome-wide network of microRNAs and oncogenic pathways revealed using gene expression signatures. PLoS Genet. 7, e1002415.

Ozsolak, F., Poling, L.L., Wang, Z., Liu, H., Liu, X.S., Roeder, R.G., Zhang, X., Song, J.S., Fisher, D.E., 2008. Chromatin structure analyses identify miRNA promoters. Genes Dev. 22, 3172–3183.

Pai, C.Y., Kuo, T.S., Jaw, T.J., Kurant, E., Chen, C.T., Bessarab, D.A., Salzberg, A., Sun, Y.H., 1998. The Homothorax homeoprotein activates the nuclear localization of another homeoprotein, extradenticle, and suppresses eye development in Drosophila. Genes Dev. 12, 435–446.

Pancratov, R., Peng, F., Smibert, P., Yang, J.-S., Olson, E.R., Guha-Gilford, C., Kapoor, A.J., Liang, F.-X., Lai, E.C., Flaherty, M.S., Dasgupta, R., 2013. The miR-310/13 cluster antagonizes β-catenin function in the regulation of germ and somatic cell differentiation in the Drosophila testis. Development 140, 2904–2916.

Pasquinelli, A.E., 2012. MicroRNAs and their targets: recognition, regulation and an emerging reciprocal relationship. Nat. Rev. Genet. 13, 271–282.

Pavlopoulos, A., Akam, M., 2011. Hox gene Ultrabithorax regulates distinct sets of target genes at successive stages of Drosophila haltere morphogenesis. Proc. Natl. Acad. Sci. U.S.A. 108, 2855–2860.

Pearson, J.C., Lemons, D., McGinnis, W., 2005. Modulating Hox gene functions during animal body patterning. Nat. Rev. Genet. 6, 893–904.

Peifer, M., Wieschaus, E., 1990. Mutations in the Drosophila gene extradenticle affect the way specific homeo domain proteins regulate segmental identity. Genes Dev. 4, 1209–1223.

Pencheva, N., Tavazoie, S.F., 2013. Control of metastatic progression by microRNA regulatory networks. Nat. Cell Biol. 15, 546–554.

Pirrotta, V., Chan, C.S., McCabe, D., Qian, S., 1995. Distinct parasegmental and imaginal enhancers and the establishment of the expression pattern of the Ubx gene. Genetics 141, 1439–1450.

Png, K.J., Halberg, N., Yoshida, M., Tavazoie, S.F., 2012. A microRNA regulon that mediates endothelial recruitment and metastasis by cancer cells. Nature 481, 190–194.

Poux, S., Kostic, C., Pirrotta, V., 1996. Hunchback-independent silencing of late Ubx enhancers by a Polycomb Group Response Element. EMBO J. 15, 4713–4722.

Proudfoot, N.J., 2011. Ending the message: poly(A) signals then and now. Genes Dev. 25, 1770–1782.

Qian, S., Capovilla, M., Pirrotta, V., 1991. The bx region enhancer, a distant cis-control element of the Drosophila Ubx gene and its regulation by hunchback and other segmentation genes. EMBO J. 10, 1415–1425.

Qian, S., Capovilla, M., Pirrotta, V., 1993. Molecular mechanisms of pattern formation by the BRE enhancer of the Ubx gene. EMBO J. 12, 3865–3877.

Raman, V., Martensen, S.A., Reisman, D., Evron, E., Odenwald, W.F., Jaffee, E., Marks, J., Sukumar, S., 2000. Compromised HOXA5 function can limit p53 expression in human breast tumours. Nature 405, 974–978.

Reed, H.C., Hoare, T., Thomsen, S., Weaver, T.A., White, R.A.H., Akam, M., Alonso, C.R., 2010. Alternative splicing modulates Ubx protein function in Drosophila melanogaster. Genetics 184, 745–758.

Reinitz, J., Levine, M., 1990. Control of the initiation of homeotic gene expression by the gap genes giant and tailless in Drosophila. Dev. Biol. 140, 57–72.

Riddle, R.D., Johnson, R.L., Laufer, E., Tabin, C., 1993. Sonic hedgehog mediates the polarizing activity of the ZPA. Cell 75, 1401–1416.

Rieckhof, G.E., Casares, F., Ryoo, H.D., Abu-Shaar, M., Mann, R.S., 1997. Nuclear translocation of extradenticle requires homothorax, which encodes an extradenticle-related homeodomain protein. Cell 91, 171–183.

Rivetti di Val Cervo, P., Lena, A.M., Nicoloso, M., Rossi, S., Mancini, M., Zhou, H., Saintigny, G., Dellambra, E., Odorisio, T., Mahé, C., Calin, G.A., Candi, E., Melino, G., 2012. p63-microRNA feedback in keratinocyte senescence. Proc. Natl. Acad. Sci. U.S.A. 109, 1133–1138.

Roch, F., Akam, M., 2000. Ultrabithorax and the control of cell morphology in Drosophila halteres. Development 127, 97–107.

Rodriguez-Esteban, C., Tsukui, T., Yonei, S., Magallon, J., Tamura, K., Izpisua Belmonte, J.C., 1999. The T-box genes Tbx4 and Tbx5 regulate limb outgrowth and identity. Nature 398, 814–818.

Rogulja-Ortmann, A., Renner, S., Technau, G.M., 2008. Antagonistic roles for Ultrabithorax and Antennapedia in regulating segment-specific apoptosis of differentiated motoneurons in the Drosophila embryonic central nervous system. Development 135, 3435–3445.

Ronshaugen, M., Biemar, F., Piel, J., Levine, M., Lai, E.C., 2005. The Drosophila microRNA iab-4 causes a dominant homeotic transformation of halteres to wings. Genes Dev. 19, 2947–2952.

Rozowski, M., Akam, M., 2002. Hox gene control of segment-specific bristle patterns in Drosophila. Genes Dev. 16, 1150–1162.

Ruby, J.G., Jan, C.H., Bartel, D.P., 2007a. Intronic microRNA precursors that bypass Drosha processing. Nature 448, 83–86.

Ruby, J.G., Stark, A., Johnston, W.K., Kellis, M., Bartel, D.P., Lai, E.C., 2007b. Evolution, biogenesis, expression, and target predictions of a substantially expanded set of Drosophila microRNAs. Genome Res. 17, 1850–1864.

Ryoo, H.D., Marty, T., Casares, F., Affolter, M., Mann, R.S., 1999. Regulation of Hox target genes by a DNA bound Homothorax/Hox/Extradenticle complex. Development 126, 5137–5148.

Sanicola, M., Sekelsky, J., Elson, S., Gelbart, W.M., 1995. Drawing a stripe in Drosophila imaginal disks: negative regulation of decapentaplegic and patched expression by engrailed. Genetics 139, 745–756.

Schuettengruber, B., Cavalli, G., 2009. Recruitment of polycomb group complexes and their role in the dynamic regulation of cell fate choice. Development 136, 3531–3542.

Schuettengruber, B., Martinez, A.-M., Iovino, N., Cavalli, G., 2011. Trithorax group proteins: switching genes on and keeping them active. Nat. Rev. Mol. Cell Biol. 12, 799–814.

Sekine, K., Ohuchi, H., Fujiwara, M., Yamasaki, M., Yoshizawa, T., Sato, T., Yagishita, N., Matsui, D., Koga, Y., Itoh, N., Kato, S., 1999. Fgf10 is essential for limb and lung formation. Nat. Genet. 21, 138–141.

Shroff, S., Joshi, M., Orenic, T.V., 2007. Differential Delta expression underlies the diversity of sensory organ patterns among the legs of the Drosophila adult. Mech. Dev. 124, 43–58.

Simakov, O., Marletaz, F., Cho, S.-J., Edsinger-Gonzales, E., Havlak, P., Hellsten, U., Kuo, D.-H., Larsson, T., Lv, J., Arendt, D., Savage, R., Osoegawa, K., De Jong, P., Grimwood, J., Chapman, J.A., Shapiro, H., Aerts, A., Otillar, R.P., Terry, A.Y., Boore, J.L., Grigoriev, I.V., Lindberg, D.R., Seaver, E.C., Weisblat, D.A., Putnam, N.H., Rokhsar, D.S., 2013. Insights into bilaterian evolution from three spiralian genomes. Nature 493, 526–531.

Simon, J., Chiang, A., Bender, W., Shimell, M.J., O'Connor, M., 1993. Elements of the Drosophila bithorax complex that mediate repression by Polycomb group products. Dev. Biol. 158, 131–144.

Simon, J., Peifer, M., Bender, W., O'Connor, M., 1990. Regulatory elements of the bithorax complex that control expression along the anterior-posterior axis. EMBO J. 9, 3945–3956.

Siomi, H., Siomi, M.C., 2010. Posttranscriptional regulation of microRNA biogenesis in animals. Mol. Cell 38, 323–332.

Slattery, M., Ma, L., Négre, N., White, K.P., Mann, R.S., 2011. Genome-wide tissue-specific occupancy of the Hox protein Ultrabithorax and Hox cofactor Homothorax in Drosophila. PLoS ONE 6, e14686.

Smibert, P., Miura, P., Westholm, J.O., Shenker, S., May, G., Duff, M.O., Zhang, D., Eads, B.D., Carlson, J., Brown, J.B., Eisman, R.C., Andrews, J., Kaufman, T., Cherbas, P., Celniker, S.E., Graveley, B.R., Lai, E.C., 2012. Global patterns of tissue-specific alternative polyadenylation in Drosophila. Cell Rep 1, 277–289.

Soshnikova, N., Duboule, D., 2009. Epigenetic temporal control of mouse Hox genes in vivo. Science 324, 1320–1323.

Stark, A., Bushati, N., Jan, C.H., Kheradpour, P., Hodges, E., Brennecke, J., Bartel, D.P., Cohen, S.M., Kellis, M., 2008. A single Hox locus in Drosophila produces functional microRNAs from opposite DNA strands. Genes Dev. 22, 8–13.

Struhl, G., 1983. Role of the esc+ gene product in ensuring the selective expression of segment-specific homeotic genes in Drosophila. J Embryol Exp Morphol 76, 297–331.

Struhl, G., White, R.A., 1985. Regulation of the Ultrabithorax gene of Drosophila by other bithorax complex genes. Cell 43, 507–519.

Suh, S.-S., Yoo, J.Y., Nuovo, G.J., Jeon, Y.-J., Kim, S., Lee, T.J., Kim, T., Bakàcs, A., Alder, H., Kaur, B., Aqeilan, R.I., Pichiorri, F., Croce, C.M., 2012. MicroRNAs/TP53 feedback circuitry in glioblastoma multiforme. Proc. Natl. Acad. Sci. U.S.A. 109, 5316–5321.

Sun, M., Song, C.-X., Huang, H., Frankenberger, C.A., Sankarasharma, D., Gomes, S., Chen, P., Chen, J., Chada, K.K., He, C., Rosner, M.R., 2013. HMGA2/TET1/HOXA9 signaling pathway regulates breast cancer growth and metastasis. Proc. Natl. Acad. Sci. U.S.A. 110, 9920–9925.

Suzuki, H.I., Arase, M., Matsuyama, H., Choi, Y.L., Ueno, T., Mano, H., Sugimoto, K., Miyazono, K., 2011. MCPIP1 ribonuclease antagonizes dicer and terminates microRNA biogenesis through precursor microRNA degradation. Mol. Cell 44, 424–436.

Takács-Vellai, K., Vellai, T., Chen, E.B., Zhang, Y., Guerry, F., Stern, M.J., Müller, F., 2007. Transcriptional control of Notch signaling by a HOX and a PBX/EXD protein during vulval development in C. elegans. Dev. Biol. 302, 661–669.

Takeuchi, J.K., Koshiba-Takeuchi, K., Matsumoto, K., Vogel-Höpker, A., Naitoh-Matsuo, M., Ogura, K., Takahashi, N., Yasuda, K., Ogura, T., 1999. Tbx5 and Tbx4 genes determine the wing/leg identity of limb buds. Nature 398, 810–814.

Tang, T., Kumar, S., Shen, Y., Lu, J., Wu, M.-L., Shi, S., Li, W.-H., Wu, C.-I., 2010. Adverse interactions between micro-RNAs and target genes from different species. Proc. Natl. Acad. Sci. U.S.A. 107, 12935–12940.

Thibault, S.T., Singer, M.A., Miyazaki, W.Y., Milash, B., Dompe, N.A., Singh, C.M., Buchholz, R., Demsky, M., Fawcett, R., Francis-Lang, H.L., Ryner, L., Cheung, L.M., Chong, A., Erickson, C., Fisher, W.W., Greer, K., Hartouni, S.R., Howie, E., Jakkula, L., Joo, D., Killpack, K., Laufer, A., Mazzotta, J., Smith, R.D., Stevens, L.M., Stuber, C., Tan, L.R., Ventura, R., Woo, A., Zakrajsek, I., Zhao, L., Chen, F., Swimmer, C., Kopczynski, C., Duyk, G., Winberg, M.L., Margolis, J., 2004. A complementary transposon tool kit for Drosophila melanogaster using P and piggyBac. Nat. Genet. 36, 283–287.

Thomsen, S., Azzam, G., Kaschula, R., Williams, L.S., Alonso, C.R., 2010. Developmental RNA processing of 3'UTRs in Hox mRNAs as a context-dependent mechanism modulating visibility to microRNAs. Development 137, 2951–2960.

Trabucchi, M., Briata, P., Garcia-Mayoral, M., Haase, A.D., Filipowicz, W., Ramos, A., Gherzi, R., Rosenfeld, M.G., 2009. The RNA-binding protein KSRP promotes the biogenesis of a subset of microRNAs. Nature 459, 1010–1014.

Trapnell, C., Williams, B.A., Pertea, G., Mortazavi, A., Kwan, G., Van Baren, M.J., Salzberg, S.L., Wold, B.J., Pachter, L., 2010. Transcript assembly and quantification by RNA-Seq reveals unannotated transcripts and isoform switching during cell differentiation. Nat. Biotechnol. 28, 511–515.

Tsang, J., Zhu, J., Van Oudenaarden, A., 2007. MicroRNA-mediated feedback and feedforward loops are recurrent network motifs in mammals. Mol. Cell 26, 753–767.

Tsurudome, K., Tsang, K., Liao, E.H., Ball, R., Penney, J., Yang, J.-S., Elazzouzi, F., He, T., Chishti, A., Lnenicka, G., Lai, E.C., Haghighi, A.P., 2010. The Drosophila miR-310 cluster negatively regulates synaptic strength at the neuromuscular junction. Neuron 68, 879–893.

Tyler, D.M., Okamura, K., Chung, W.-J., Hagen, J.W., Berezikov, E., Hannon, G.J., Lai, E.C., 2008. Functionally distinct regulatory RNAs generated by bidirectional transcription and processing of microRNA loci. Genes Dev. 22, 26–36.

Warren, R.W., Nagy, L., Selegue, J., Gates, J., Carroll, S., 1994. Evolution of homeotic gene regulation and function in flies and butterflies. Nature 372, 458–461.

Weatherbee, S.D., Halder, G., Kim, J., Hudson, A., Carroll, S., 1998. Ultrabithorax regulates genes at several levels of the wing-patterning hierarchy to shape the development of the Drosophila haltere. Genes Dev. 12, 1474–1482.

Weng, R., Cohen, S.M., 2012. Drosophila miR-124 regulates neuroblast proliferation through its target anachronism. Development 139, 1427–1434.

White, K., Grether, M.E., Abrams, J.M., Young, L., Farrell, K., Steller, H., 1994. Genetic control of programmed cell death in Drosophila. Science 264, 677–683.

White, R.A., Lehmann, R., 1986. A gap gene, hunchback, regulates the spatial expression of Ultrabithorax. Cell 47, 311–321.

White, R.A., Wilcox, M., 1985a. Distribution of Ultrabithorax proteins in Drosophila. EMBO J. 4, 2035–2043.

White, R.A.H., Wilcox, M., 1985b. Regulation of the distribution of Ultrabithorax proteins in Drosophila. Nature 318, 563–567.

Williams, A.H., Valdez, G., Moresi, V., Qi, X., McAnally, J., Elliott, J.L., Bassel-Duby, R., Sanes, J.R., Olson, E.N., 2009. MicroRNA-206 delays ALS progression and promotes regeneration of neuromuscular synapses in mice. Science 326, 1549–1554.

Winter, J., Jung, S., Keller, S., Gregory, R.I., Diederichs, S., 2009. Many roads to maturity: microRNA biogenesis pathways and their regulation. Nat. Cell Biol. 11, 228–234.

Wreden, C., Verrotti, A.C., Schisa, J.A., Lieberfarb, M.E., Strickland, S., 1997. Nanos and pumilio establish embryonic polarity in Drosophila by promoting posterior deadenylation of hunchback mRNA. Development 124, 3015–3023.

Wu, C.-I., Shen, Y., Tang, T., 2009. Evolution under canalization and the dual roles of microRNAs: a hypothesis. Genome Res. 19, 734–743.

Wu, H., Tao, J., Chen, P.J., Shahab, A., Ge, W., Hart, R.P., Ruan, X., Ruan, Y., Sun, Y.E., 2010. Genome-wide analysis reveals methyl-CpG-binding protein 2-dependent regulation of microRNAs in a mouse model of Rett syndrome. Proc. Natl. Acad. Sci. U.S.A. 107, 18161–18166.

Xiao, C., Calado, D.P., Galler, G., Thai, T.-H., Patterson, H.C., Wang, J., Rajewsky, N., Bender, T.P., Rajewsky, K., 2007. MiR-150 controls B cell differentiation by targeting the transcription factor c-Myb. Cell 131, 146–159.

Ye, B., Petritsch, C., Clark, I.E., Gavis, E.R., Jan, L.Y., Jan, Y.N., 2004. Nanos and Pumilio are essential for dendrite morphogenesis in Drosophila peripheral neurons. Curr. Biol. 14, 314–321.

Yin, V.P., Thomson, J.M., Thummel, R., Hyde, D.R., Hammond, S.M., Poss, K.D., 2008. Fgf-dependent depletion of microRNA-133 promotes appendage regeneration in zebrafish. Genes Dev. 22, 728–733.

Zecca, M., Basler, K., Struhl, G., 1995. Sequential organizing activities of engrailed, hedgehog and decapentaplegic in the Drosophila wing. Development 121, 2265–2278.

Zhang, C.C., Bienz, M., 1992. Segmental determination in Drosophila conferred by hunchback (hb), a repressor of the homeotic gene Ultrabithorax (Ubx). Proc. Natl. Acad. Sci. U.S.A. 89, 7511–7515.

Zhang, J.A., Mortazavi, A., Williams, B.A., Wold, B.J., Rothenberg, E.V., 2012. Dynamic transformations of genome-wide epigenetic marking and transcriptional control establish T cell identity. Cell 149, 467–482.

APPENDIX

Table.1 miRNAs detected in wing and haltere tissue sorted by haltere expression levels

miRNA	*Wing (FPKM)*	*Halt (FPKM)*
mir-92b-3p	6.85449E+14	1.69005E+15
ban-3p	1.68599E+15	1.66425E+15
mir-9a-5p	8.68295E+14	8.53126E+14
mir-9c-5p	1.07912E+15	6.66627E+14
mir-10-5p	8.51975E+14	3.69099E+14
mir-8-3p	2.68552E+14	3.33476E+14
mir-276a-3p	2.08262E+14	2.11529E+14
mir-184-5p	8.807E+14	1.69623E+14
mir-31a-5p	2.68522E+14	1.65984E+14
mir-995-3p	1.2629E+14	1.65643E+14
mir-279-3p	1.28337E+14	1.27708E+14
mir-92a-3p	4.74399E+13	1.24629E+14
mir-275-3p	3.68788E+13	1.10318E+14
mir-14-3p	5.13094E+13	8.50322E+13
mir-306-5p	1.05905E+14	7.81512E+13
mir-2b-2-3p	4.10627E+13	5.40464E+13
mir-2b-1-5p	4.01662E+13	5.31498E+13
mir-9b-5p	7.48633E+13	4.53331E+13
mir-317-3p	2.39531E+13	2.33439E+13
mir-1010-3p	2.86816E+13	2.03642E+13
mir-999-3p	2.24315E+13	1.92257E+13
let-7-5p	1.22196E+13	1.90082E+13
mir-996-3p	2.2178E+13	1.85779E+13
mir-10-3p	1.02806E+13	1.72938E+13
mir-986-5p	1.04342E+13	1.50951E+13
mir-13b-2-3p	3.62875E+13	1.39499E+13
mir-970-3p	6.58961E+12	1.27243E+13
mir-125-5p	1.59259E+13	1.25887E+13
mir-305-5p	4.49479E+13	1.09049E+13
mir-2a-2-3p	8.93578E+12	9.92864E+12
mir-100-5p	3.06268E+13	9.68793E+12
mir-2a-1-3p	9.17486E+12	9.5833E+12
mir-281-2-5p	2.99932E+12	8.33613E+12
mir-13b-1-3p	3.80195E+11	7.94185E+12
mir-282-5p	1.02026E+13	6.99556E+12
mir-1012-3p	2.15176E+12	5.1868E+12
mir-12-5p	1.88279E+12	4.59573E+12
mir-998-3p	4.4144E+12	3.99499E+12
mir-956-3p	1.13565E+12	3.54642E+12
mir-276b-3p	2.87258E+12	3.44522E+12

mir-312-3p	1.3518E+12	2.21546E+12
mir-286-3p	1.16554E+12	2.18497E+12
mir-375-3p	2.11219E+11	2.09342E+12
mir-982-5p	1.46439E+12	1.55405E+12
mir-278-3p	6.33658E+11	1.16405E+12
bft-5p	2.19774E+12	1.15437E+12
mir-965-3p	5.06927E+11	1.07018E+12
mir-306-3p	1.732E+12	8.44878E+11
mir-988-3p	5.91414E+11	8.26103E+11
mir-252-5p	1.26732E+11	6.66515E+11
mir-1-3p	1.90097E+12	6.38352E+11
mir-34-5p	7.54779E+11	6.26516E+11
mir-11-3p	2.55907E+11	6.25551E+11
mir-277-3p	1.79313E+11	6.24276E+11
mir-311-3p	2.11219E+11	5.63252E+11
mir-5-5p	2.39084E+11	3.58627E+11
mir-958-3p	3.80195E+11	3.00401E+11
mir-957-3p	84487800000	2.91013E+11
mir-1003-3p	3.37951E+11	2.34688E+11
mir-987-5p	2.88592E+11	2.3186E+11
mir-993-3p	89656600000	2.12519E+11
mir-190-5p	1.77595E+11	2.12127E+11
mir-927-5p	42243900000	2.06526E+11
mir-79-3p	2.95707E+11	1.68976E+11
mir-310-3p	84487800000	1.68976E+11
mir-316-5p	84487800000	1.68976E+11
mir-983-1-5p	2.11219E+11	1.40813E+11
mir-7-5p	2.39084E+11	1.39466E+11
mir-983-2-5p	1.26732E+11	1.1265E+11
mir-184-3p	1.27954E+11	99519400000
mir-33-5p	3.83861E+11	85302400000
mir-283-5p	0	85302400000
mir-1013-3p	0	71769500000
mir-304-5p	29885500000	66412300000
mir-281-2-3p	0	66412300000
mir-318-3p	84487800000	65712700000
mir-137-3p	0	65712700000
mir-2c-3p	1.19542E+11	59771100000
mir-966-5p	63976800000	56868200000
mir-1000-5p	0	56868200000
mir-6-3-3p	0	46937600000
mir-960-5p	0	46937600000
mir-984-5p	1.79313E+11	39847400000
mir-1006-3p	0	39847400000
mir-985-3p	84487800000	37550100000
mir-980-3p	42243900000	37550100000

mir-981-3p	42243900000	37550100000
mir-6-2-3p	0	37550100000
mir-124-3p	0	33206200000
mir-314-3p	63976800000	28434100000
mir-967-5p	0	28434100000
mir-13a-3p	0	28162600000
mir-281-1-5p	0	28162600000
mir-31b-5p	0	28162600000
mir-6-1-3p	0	28162600000
mir-281-1-3p	59771100000	19923700000
mir-308-3p	42243900000	18775100000
mir-964-5p	0	18775100000
mir-1005-3p	63976800000	14217100000
mir-210-3p	0	14217100000
mir-263b-5p	0	14217100000
mir-963-5p	0	9866390000
mir-1004-3p	0	9387530000
mir-1007-3p	0	9387530000
mir-313-3p	0	9387530000
mir-932-5p	0	9387530000
mir-972-3p	0	9387530000
mir-974-5p	0	9387530000
mir-iab-4-5p	0	9387530000
mir-2500-5p	0	7600210000
mir-284-3p	0	4441030000
mir-274-5p	0	3029440000
mir-2489-3p	1.26831E+11	0
mir-954-5p	63976800000	0
mir-1015-3p	42243900000	0
mir-276a-5p	29885500000	0

Table.2 miRNAs detected in wing and haltere tissue sorted by miRNA expression group association

miRNA	*Wing (FPKM)*	*Halt (FPKM)*	*Log Fold Change (H vs W)*	*Group*
ban-3p	1.68599E+15	1.66425E+15	-0.005636429	Average
bft-5p	2.19774E+12	1.15437E+12	-0.279631281	Average
let-7-5p	1.22196E+13	1.90082E+13	0.191884003	Average
mir-1003-3p	3.37951E+11	2.34688E+11	-0.158362852	Average
mir-1010-3p	2.86816E+13	2.03642E+13	-0.148736021	Average
mir-10-3p	1.02806E+13	1.72938E+13	0.22587197	Average
mir-125-5p	1.59259E+13	1.25887E+13	-0.1021231	Average
mir-14-3p	5.13094E+13	8.50322E+13	0.219386479	Average
mir-184-3p	1.27954E+11	99519400000	-0.109146118	Average
mir-190-5p	1.77595E+11	2.12127E+11	0.077165215	Average
mir-276a-3p	2.08262E+14	2.11529E+14	0.006759882	Average
mir-276b-3p	2.87258E+12	3.44522E+12	0.078944827	Average
mir-278-3p	6.33658E+11	1.16405E+12	0.264116713	Average
mir-279-3p	1.28337E+14	1.27708E+14	-0.002133779	Average
mir-282-5p	1.02026E+13	6.99556E+12	-0.163888374	Average
mir-286-3p	1.16554E+12	2.18497E+12	0.272918296	Average
mir-2a-1-3p	9.17486E+12	9.5833E+12	0.018915638	Average
mir-2a-2-3p	8.93578E+12	9.92864E+12	0.045757296	Average
mir-2b-1-5p	4.01662E+13	5.31498E+13	0.121640888	Average
mir-2b-2-3p	4.10627E+13	5.40464E+13	0.119319269	Average
mir-306-5p	1.05905E+14	7.81512E+13	-0.131980814	Average
mir-312-3p	1.3518E+12	2.21546E+12	0.214551471	Average
mir-317-3p	2.39531E+13	2.33439E+13	-0.011188313	Average
mir-318-3p	84487800000	65712700000	-0.10914469	Average
mir-31a-5p	2.68522E+14	1.65984E+14	-0.208913647	Average
mir-34-5p	7.54779E+11	6.26516E+11	-0.080887642	Average
mir-5-5p	2.39084E+11	3.58627E+11	0.17609247	Average
mir-7-5p	2.39084E+11	1.39466E+11	-0.234082168	Average
mir-79-3p	2.95707E+11	1.68976E+11	-0.24303658	Average
mir-8-3p	2.68552E+14	3.33476E+14	0.094036192	Average
mir-958-3p	3.80195E+11	3.00401E+11	-0.102305027	Average
mir-966-5p	63976800000	56868200000	-0.051153032	Average
mir-970-3p	6.58961E+12	1.27243E+13	0.285774188	Average
mir-980-3p	42243900000	37550100000	-0.051152908	Average
mir-981-3p	42243900000	37550100000	-0.051152908	Average
mir-982-5p	1.46439E+12	1.55405E+12	0.025808233	Average
mir-983-1-5p	2.11219E+11	1.40813E+11	-0.176090231	Average
mir-983-2-5p	1.26732E+11	1.1265E+11	-0.051155093	Average
mir-986-5p	1.04342E+13	1.50951E+13	0.160376838	Average
mir-987-5p	2.88592E+11	2.3186E+11	-0.095058456	Average
mir-988-3p	5.91414E+11	8.26103E+11	0.145142598	Average

mir-995-3p	1.2629E+14	1.65643E+14	0.117804124	Average
mir-996-3p	2.2178E+13	1.85779E+13	-0.076925758	Average
mir-998-3p	4.4144E+12	3.99499E+12	-0.043355987	Average
mir-999-3p	2.24315E+13	1.92257E+13	-0.066976155	Average
mir-9a-5p	8.68295E+14	8.53126E+14	-0.007654122	Average
mir-9b-5p	7.48633E+13	4.53331E+13	-0.217853549	Average
mir-9c-5p	1.07912E+15	6.66627E+14	-0.209186842	Average
mir-1012-3p	2.15176E+12	5.1868E+12	0.382105672	Halt Up
mir-11-3p	2.55907E+11	6.25551E+11	0.388180557	Halt Up
mir-12-5p	1.88279E+12	4.59573E+12	0.387552623	Halt Up
mir-13b-1-3p	3.80195E+11	7.94185E+12	1.319915279	Halt Up
mir-252-5p	1.26732E+11	6.66515E+11	0.720923639	Halt Up
mir-275-3p	3.68788E+13	1.10318E+14	0.475869599	Halt Up
mir-277-3p	1.79313E+11	6.24276E+11	0.541764862	Halt Up
mir-281-2-5p	2.99932E+12	8.33613E+12	0.443941675	Halt Up
mir-304-5p	29885500000	66412300000	0.346787995	Halt Up
mir-310-3p	84487800000	1.68976E+11	0.301031024	Halt Up
mir-311-3p	2.11219E+11	5.63252E+11	0.42596976	Halt Up
mir-316-5p	84487800000	1.68976E+11	0.301031024	Halt Up
mir-375-3p	2.11219E+11	2.09342E+12	0.996123387	Halt Up
mir-927-5p	42243900000	2.06526E+11	0.689210728	Halt Up
mir-92a-3p	4.74399E+13	1.24629E+14	0.419475345	Halt Up
mir-92b-3p	6.85449E+14	1.69005E+15	0.391924406	Halt Up
mir-956-3p	1.13565E+12	3.54642E+12	0.494545662	Halt Up
mir-957-3p	84487800000	2.91013E+11	0.537118388	Halt Up
mir-965-3p	5.06927E+11	1.07018E+12	0.324511407	Halt Up
mir-993-3p	89656600000	2.12519E+11	0.374815498	Halt Up
mir-1005-3p	63976800000	14217100000	-0.653211496	Halt Down
mir-100-5p	3.06268E+13	9.68793E+12	-0.49987063	Halt Down
mir-10-5p	8.51975E+14	3.69099E+14	-0.363283983	Halt Down
mir-13b-2-3p	3.62875E+13	1.39499E+13	-0.415185954	Halt Down
mir-1-3p	1.90097E+12	6.38352E+11	-0.47391504	Halt Down
mir-184-5p	8.807E+14	1.69623E+14	-0.715343256	Halt Down
mir-281-1-3p	59771100000	19923700000	-0.477121255	Halt Down
mir-2c-3p	1.19542E+11	59771100000	-0.301029269	Halt Down
mir-305-5p	4.49479E+13	1.09049E+13	-0.615087719	Halt Down
mir-306-3p	1.732E+12	8.44878E+11	-0.311753886	Halt Down
mir-308-3p	42243900000	18775100000	-0.352181747	Halt Down
mir-314-3p	63976800000	28434100000	-0.352183027	Halt Down
mir-33-5p	3.83861E+11	85302400000	-0.65321274	Halt Down
mir-984-5p	1.79313E+11	39847400000	-0.653211787	Halt Down
mir-985-3p	84487800000	37550100000	-0.352182904	Halt Down
mir-1000-5p	0	56868200000	NA	Halt Only
mir-1004-3p	0	9387530000	NA	Halt Only
mir-1006-3p	0	39847400000	NA	Halt Only
mir-1007-3p	0	9387530000	NA	Halt Only

mir-1013-3p	0	71769500000	NA	Halt Only
mir-124-3p	0	33206200000	NA	Halt Only
mir-137-3p	0	65712700000	NA	Halt Only
mir-13a-3p	0	28162600000	NA	Halt Only
mir-210-3p	0	14217100000	NA	Halt Only
mir-2500-5p	0	7600210000	NA	Halt Only
mir-263b-5p	0	14217100000	NA	Halt Only
mir-274-5p	0	3029440000	NA	Halt Only
mir-281-1-5p	0	28162600000	NA	Halt Only
mir-281-2-3p	0	66412300000	NA	Halt Only
mir-283-5p	0	85302400000	NA	Halt Only
mir-284-3p	0	4441030000	NA	Halt Only
mir-313-3p	0	9387530000	NA	Halt Only
mir-31b-5p	0	28162600000	NA	Halt Only
mir-6-1-3p	0	28162600000	NA	Halt Only
mir-6-2-3p	0	37550100000	NA	Halt Only
mir-6-3-3p	0	46937600000	NA	Halt Only
mir-932-5p	0	9387530000	NA	Halt Only
mir-960-5p	0	46937600000	NA	Halt Only
mir-963-5p	0	9866390000	NA	Halt Only
mir-964-5p	0	18775100000	NA	Halt Only
mir-967-5p	0	28434100000	NA	Halt Only
mir-972-3p	0	9387530000	NA	Halt Only
mir-974-5p	0	9387530000	NA	Halt Only
mir-iab-4-5p	0	9387530000	NA	Halt Only
mir-1015-3p	42243900000	0	NA	Wing Only
mir-2489-3p	1.26831E+11	0	NA	Wing Only
mir-276a-5p	29885500000	0	NA	Wing Only
mir-954-5p	63976800000	0	NA	Wing Only